

University of Southampton Research Repository ePrints Soton

Copyright © and Moral Rights for this thesis are retained by the author and/or other copyright owners. A copy can be downloaded for personal non-commercial research or study, without prior permission or charge. This thesis cannot be reproduced or quoted extensively from without first obtaining permission in writing from the copyright holder/s. The content must not be changed in any way or sold commercially in any format or medium without the formal permission of the copyright holders.

When referring to this work, full bibliographic details including the author, title, awarding institution and date of the thesis must be given e.g.

AUTHOR (year of submission) "Full thesis title", University of Southampton, name of the University School or Department, PhD Thesis, pagination

UNIVERSITY OF SOUTHAMPTON

FACULTY OF NATURAL AND ENVIRONMENTAL SCIENCES

School of Chemistry

Small molecule mimics of trans-proline: Synthesis and Applications

by

Boris Aillard

Thesis for the degree of Doctor of Philosophy

March 2014

UNIVERSITY OF SOUTHAMPTON

ABSTRACT

FACULTY OF NATURAL AND ENVIRONMENTAL SCIENCES SCHOOL OF CHEMISTRY

Doctor of Philosophy

SMALL MOLECULE MIMICS OF TRANS-PROLINE: SYNTHESIS AND APPLICATIONS

By Boris Aillard

Herein we detail the synthesis and application of small molecules of trans-proline mimics. A general introduction to the field of peptidomimetics and their uses in specific biological examples is provided; followed by a detailed review of the background and objectives of the project. The synthesis of *trans*-proline mimics using (–)-cytisine as a building block is disclosed. Its application is demonstrated by incorporation of (-)-cytisine derivatives in a specific anticancer peptide PRGPRP and determination of its anti-cancer activity. The synthesis and conformational analysis of a pyroglutamate based mimic, a trans-proline mimic designed to adopt a polyproline type II (PPII) helical conformation, is described. Incorporation of this mimic in the anti-cancer peptide PRGPRP and determination of its anti-cancer activity displays a useful application. To investigate the conformation of the pyroglutamic based mimic, synthesis and conformational analysis of its oligomers is detailed. Using circular dichroism (CD) spectroscopy, NMR and X-ray crystallographic structures, the PPII conformation of these oligomers are compared to the ideal PPII helices and known PPII mimics. A specific proteinligand interaction (SH3-peptide ligand) is discussed. Incorporation of the pyroglutamic based mimic in the peptide sequence and its binding properties are disclosed. As a result of these studies, a second generation pyroglutamate based mimic is currently under development in the group to further investigate conformational analysis and binding properties with SH3.

Contents

ABSTRACT	т	i
DECLARA	TION OF AUTHORSHIP	v
Acknowle	dgements	vi i
Definition	is and Abbreviations	ix
	oduction	
Aj Peptido	omimetic review	1
1.1 C	Considerations undertaken during peptide design	1
1.2 S	structural modification to improve peptide stability	2
1.2.1	Pseudopeptides	2
1.2.2	Reduced peptide bonds	3
1.2.3	Azapeptides	4
1.2.4	Retro-inverso peptides	5
1.2.5	Peptoids	6
1.3 lı	ncorporation of unnatural amino acids	7
1.3.1	D-amino acids	7
1.3.2	N-alkylated amino acids	7
1.3.3	C $lpha$ -tetrasubstituted $lpha$ -amino acids	9
1.3.4	β-Substituted α -amino acids	11
1.3.5	Proline mimics	11
1.3.6	β-amino acids	14
1.4 lı	ntroduction of global restrictions	17
1.4.1	Head to tail cyclisation	17
1.4.2	Side chain to Side chain cyclisation	17
1.4.3	Backbone to Side chain cyclisation	19
1.5 S	secondary structure peptidomimetics	20
1.5.1	α-helix peptidomimetics	20
1.5.2	β-sheet peptidomimetics	21
1.5.3	Reverse turn peptidomimetics	
1.5.4	Polyproline type II peptidomimetics	
	ional design and synthesis of small molecule trans-proline mimics	
applicatio	ns: Introduction to our project objectives	22
Cl Proi	iect background	23

1.6	5	PRGPRP	lead compound identification	23
2	1.6.1	Cytisi	ne 1.67 as a <i>trans</i> -proline mimic	27
-	1.6.2	Cytisi	ne 1.67 , functionalisation towards therapeutics	28
		5.2.1 uden gro	N-Functionalisation of cytisine 1.67 : An N–C migration developed by thoup 49	
	1.6	5.2.2	Pyridone functionalisation: Electrophilic aromatic bromination	30
		5.2.3 ect appr	Pyridone functionalisation: Electrophilic aromatic halogenation with a oach by Rouden <i>et al</i> ^{47b}	
	1.6	5.2.4	Pyridone functionalisation: Electrophilic aromatic nitration approach.	32
-	1.6.3	Cytisi	ne analogues	32
1.7	7	Protein-	Protein interactions involving proline rich motifs	36
-	1.7.1	. The p	olyproline type II (PPII) helix and its structural features	36
-	1.7.2	. PPII m	nimics known in the literature	38
	1.7	7.2.1	Spirolactam 1.99	39
	1.7	7.2.2	Sugar derived mimic 1.100	41
	1.7	7.2.3	Tricyclic Pro-Pro mimic 1.101	42
2	1.7.3	Pyrog	lutamate based mimic 1.125	45
-	1.7.4	Study	of protein-protein interactions using BioNMR	48
1.8	3	Summar	y of project objectives	53
1.0	•	Janina	y or project objectives	
2.			nalogues based on cytisine & clonogenic assay	
	PR	GPRP a	nalogues based on cytisine & clonogenic assay	55
2. 2.1	PR	Synthesi		55 55
2. 2.1	PR 2.1.1	Synthesi Clono	is of N-Ac-Pro-Arg(NO ₂)-Gly-Pro-Arg(NO ₂)-Pro-OMe 2.1	55 55
2.1 2.2 2.2	PR 2.1.1	Synthesi Clono *PRGPR	is of <i>N</i> -Ac-Pro-Arg(NO ₂)-Gly-Pro-Arg(NO ₂)-Pro-OMe 2.1 genic assay of <i>N</i> -Ac-Pro-Arg(NO ₂)-Gly-Pro-Arg(NO ₂)-Pro-OMe 2.1	55 55 58
2.1 2.2 2.2	PR 2.1.1	Synthesi Clono *PRGPR Synth	nalogues based on cytisine & clonogenic assay	55 58 60
2.1 2.2 2.2	PR 2.1.1 2.2.2.1 2.2.2.2	Synthesi Clono *PRGPR Synth	ris of <i>N</i> -Ac-Pro-Arg(NO ₂)-Gly-Pro-Arg(NO ₂)-Pro-OMe 2.1 genic assay of <i>N</i> -Ac-Pro-Arg(NO ₂)-Gly-Pro-Arg(NO ₂)-Pro-OMe 2.1	55 58 60 60
2.1 2.2 2.2 2.3	PR 2.1.1 2.2.2.1 2.2.2.2	Synthesi Clono *PRGPR Synth Clono PR*G*P	nalogues based on cytisine & clonogenic assay	55 58 60 60 65
2.1 2.2 2.2 2.3 2.3	PR 2.1.1 2.2.2.1 2.2.2.2	Synthesic Clono *PRGPR Synth Clono PR*G*P	nalogues based on cytisine & clonogenic assay	55 58 60 60 65 66
2.1 2.2 2.2 2.3	PR 2.1.1 2.2.2.1 2.2.2 3 2.3.1	Synthesi Clono *PRGPR Synth Clono PR*G*P Arom	nalogues based on cytisine & clonogenic assay	55 58 60 65 66 66
2.1 2.2 2.2 2.3 2.3	PR 2.1.1 2.2.2.1 2.2.2 3 2.3.1 2.3.2	Synthesi Clono *PRGPR Synth Clono PR*G*P Arom Arom	is of N-Ac-Pro-Arg(NO ₂)-Gly-Pro-Arg(NO ₂)-Pro-OMe 2.1	55 58 60 65 66 66
2.1 2.2 2.2 2.3 2.3	PR 2.1.1 2.2.2.1 2.2.2.2 3 2.3.1 2.3.2 2.3.3 2.3.4	Synthesic Clono *PRGPR Synth Clono PR*G*P Arom Arom Towa Synth	nalogues based on cytisine & clonogenic assay	55 55 60 60 66 66 67 69
2.1 2.2 2.2 2.3 2.3	PR 2.1.1 2.2.2.1 2.2.2 3 2.3.1 2.3.2 2.3.3 2.3.4 PR	Synthesic Clono *PRGPR Synth Clono PR*G*P Arom Arom Towa Synth	nalogues based on cytisine & clonogenic assay	55 55 60 66 66 67 69 70
2.1 2.2 2.3 2.3 3.	PR 2.1.1 2.2.2.1 2.2.2.3 2.3.1 2.3.2 2.3.3 2.3.4 PR	Synthesic Clono *PRGPR Synth Clono PR*G*P Arom Arom Towa Synth Synth Synth	nalogues based on cytisine & clonogenic assay	55 55 66 66 66 67 69 70 73
2.1 2.2 2.3 2.3 3. 3.	PR 2.1.1 2.2.2.1 2.3.2 2.3.3 2.3.4 PR	Synthesic Clono *PRGPR Synth Clono PR*G*P Arom Arom Towa Synth CGPRP b Synthesic Synthesic	is of <i>N</i> -Ac-Pro-Arg(NO ₂)-Gly-Pro-Arg(NO ₂)-Pro-OMe 2.1	55 55 66 66 66 67 69 70 73 73
2.1 2.2 2.3 2.3 3. 3.1 3.2	PR 2.1.1 2.2.2.1 2.3.2 2.3.3 2.3.4 PR	Synthesic Clono *PRGPR Synth Clono PR*G*P Arom Arom Towa Synth Synthesic Synthesic Clonoge	is of <i>N</i> -Ac-Pro-Arg(NO ₂)-Gly-Pro-Arg(NO ₂)-Pro-OMe 2.1	55 55 58 60 60 65 66 67 69 70 73 85 87

4.2	Conformational analysis	95
4.2.1	1 CD spectroscopy	95
4.2.2	2 NMR spectroscopy	97
4.2.3	3 X-ray crystallography	97
4.2.4	4 Discussion of previous PPII mimics	98
5. Bi	oNMR studies using 1.125 as <i>trans</i> -proline mimic	101
5.1	¹⁵ N–Heteronuclear single quantum correlation (HSQC) spectroscopy	101
5.2	Triple resonance experiments	101
5.2.1	1 HNCA experiment	101
5.2.2	2 HNCACB experiment	102
5.2.3	3 CBCA(CO)NH experiment	102
5.3	Sequence resonance assignment	104
5.4	Protein-ligand interaction studies	106
5.5	Synthesis of N-Ac-Arg-Pro-Leu-Pro-Val-Ala-Pro-Gly-NH ₂ 1.139 and its analogue	s 107
5.5.1	1 Solid phase synthesis	108
5.5.2	,	
	IO , 1.141 and 1.142	
5.6	NMR experimental setup	
5.7	Binding studies	
5.7.1	• •	
5.7.2		
6. Pr	roject perspective, current development and outlook	123
7. Ex	rperimental	129
7.1	General methods and starting materials	129
7.2	Compounds appearing in Chapter 2	130
7.3	Compounds appearing in Chapter 3	149
7.4	Compounds appearing in Chapter 4	176
7.5	Compounds appearing in Chapter 5	179
7.6	Bio-assays mammalian cell culture	187
7.7	BioNMR experiments	191
Append	ix	193
Referen	ces	282

DECLARATION OF AUTHORSHIP

I, Boris Aillard
declare that the thesis entitled
SMALL MOLECULE MIMICS OF <i>TRANS</i> -PROLINE: SYNTHESIS AND APPLICATIONS
and the work presented in the thesis are both my own, and have been generated by me as the result of my own original research. I confirm that:
• this work was done wholly or mainly while in candidature for a research degree at this University;
• where any part of this thesis has previously been submitted for a degree or any other qualification at this University or any other institution, this has been clearly stated;
• where I have consulted the published work of others, this is always clearly attributed;
 where I have quoted from the work of others, the source is always given. With the exception of such quotations, this thesis is entirely my own work;
I have acknowledged all main sources of help;
• where the thesis is based on work done by myself jointly with others, I have made clear exactly what was done by others and what I have contributed myself;
• none of this work has been published before submission,
Signed:
Date:

Acknowledgements

I would like firstly to thank Dr. Sally Bloodworth, Dr. Jeremy Blaydes and Prof. Jeremy Kilburn for giving me the opportunity to work with you for the past three years. I would also like to thank you all for encouraging me during my research and for giving me the freedom to grow as a research scientist.

I would like to express my gratitude to the Cancer and polio research fund and INTERREG for funding my PhD.

Thanks also to Prof. Peter Roach and Martin for their kindness with allowing me to use their HPLC. Many thanks to Will Mothersole in the Raja group for letting me make use of his high pressure reactor and also all the groups on level 3 for sharing chemicals, solvents or equipment when needed.

Many thanks to all the ex-members of the Kilburn Group, namely Emma, Will, Aleks and Biniam. Thank you Will for sharing great moments in the lab while listening to BBC radio 1 and of course the exciting cricket! The latter being an optimum way of integrating a French guy into the British culture.

I would like to thank Matt in the Blaydes group for all his contribution; none of these assays would have been possible without your help!

Many thanks to all the chemistry staff, especially Julie, Karl, Keith, Dr. Neil Wells, Dr. Graham Tizzard and Dr. Mark Light.

I would like to thank Dr. Patrick Duriez, Dr. Stuart Findlow and Dr. Joern Werner for all the work we undertook together. Thank you for your time, help and suggestions.

I sincerely thank my proofreaders Sally, Emma, Joern and both Jeremys for taking the time to spot errors and for providing suggestions and comments.

A very special thank you to Emma Packard for being a great source of support for the past three years and for giving me strength.

Thank you to all the friends I have made here in Southampton from biology, chemistry and the rugby club who made this adventure a special one.

Finally, I would like to thank my mum and sister for their support, encouragement and advice.

Definitions and Abbreviations

 $\begin{array}{lll} \text{Ac}_2\text{O} & \text{acetic anhydride} \\ \text{AcOH} & \text{acetic acid} \\ \text{Ala (A)} & \text{alanine} \\ \alpha & \text{alpha} \\ \text{aq.} & \text{aqueous} \\ \text{Arg (R)} & \text{arginine} \end{array}$

atm standard atmosphere

BF₃·Et₂O boron trifluoride diethyl etherate

β beta

Boc₂O di-*tert*-butyl dicarbonate

br broad

CAN cerium ammonium nitrate

cat. catalytic

CDK cyclin-dependant kinase CF_3CO_2Ag silver trifluoroacetate CH_2CI_2 dichloromethane CH_3CN acetonitrile Cs_2CO_3 cesium carbonate δ chemical shift (ppm)

Cys (C) cysteine

d.r. diastereomeric ratio

DCC *N,N'*-Dicyclohexylcarbodiimide

DDQ 2,3-dichloro-5,6-dicyano-1,4-benzoquinone

DFT density functional theory
DIBALH diisobutylaluminium hydride
DIPEA N, N-Diisopropylethylamine
DMAP 4-Dimethylaminopyridine

DMEM Dulbecco's Modified Eagle medium

DMF dimethyl formamide DMSO dimethyl sulfoxide

EDC 1-ethyl-3-(3-dimethylaminopropyl)carbodiimide

equiv. Molar equivalents

ESI electrospray ionisation

et al. et alia (Latin for 'and others')

ETDA ethylenediaminetetraacetic acid

 Et_2O diethyl ether Et_3N triethylamine Et_3SiH triethylsilane EtOAc ethyl acetate EtOH ethanol

FCS fœtal Calf serum

Fmoc 9-fluorenylmethoxycarbonyl

g gram

Glu (E) glutamic acid Gly (G) glycine

GST glutathione S-transferase

 $\begin{array}{ccc} \Delta & & \text{heat} \\ \text{h} & & \text{hour} \end{array}$

 $\begin{array}{ll} \text{H}_2\text{O}_2 & \text{hydrogen peroxyde} \\ \text{H}_2\text{S} & \text{hydrogen sulfide} \\ \text{H}_2\text{SO}_4 & \text{sulfuric acid} \end{array}$

HATU 1-[Bis(dimethylamino)methylene]-1*H*-1,2,3-triazolo[4,5-

b]pyridinium 3-oxid hexafluorophosphate

Ham F'12 Ham's Nutrient mixture

HBTU O-Benzotriazole-N, N, N', N'-tetramethyl-uronium-

hexafluorophosphate

HBSS Hank's balanced salt solution

HCI hydrochloric acid HCIO₄ perchloric acid HNO₃ nitric acid

HOBt hydroxybenzotriazole

HPLC high perforformance liquid chromatography

HRMS high resolution mass spectrometry

Hyp hydroxyproline

Hz hertz

IC₅₀ half maximal inhibitory concentration

IR infra-red

J coupling constant K₂CO₃ potassium carbonate KOH potassium hydroxide

λ lambda L litre

LC-MS liquid chromatography-mass spectrometry

LDA lithium diisopropylamide

Leu (L) leucine

LiBHEt₃ Super-hydride®, lithium triethylborohydride

LiCl lithium chloride

LiHMDS lithium bis(trimethylsilyl)amide

LiOH litium hydroxide

LRMS low resolution mass spectrometry
L-selectride® lithium tri-sec-butylborohydride

Lys (K) Lysine M molar

m.p melting point
MeOH methanol
min minute

NaBH₄ sodium borohydride
NaH sodium hydride
Nal naphthylalanine
NaN₃ sodium azide
NaNO₃ sodium nitrate
NaOH sodium hydroxide
NBS N-bromosuccinimide

ⁿBuLi n-butyllithium NH₃ ammonia

NH₄OH ammonium hydroxide NIS *N*-iodosuccinimide NMM *N*-methylmorpholine

NMR nuclear magnetic resonance nOe nuclear Overhauser effect

°C degrees Celsius

Orn ornithine

PBS phosphate buffer saline

P(ⁿBu)₃ tributylphosphine Pd(OH)₂ palladium hydroxide Pd/C palladium on carbon

Phe (F) phenylalanine PhSeCl diphenyl diselenide

PMBCl 4-methoxybenzyl chloride

PPh₃ triphenylphosphine ppm parts per million

π pi

PPTS pyridinium *p*-toluenesulfonate

Pro (P) proline

PTSA p-toluene sulfonic acid

Py pyridine

PyBop benzotriazol-1-yl-oxytripyrrolidinophosphonium hexafluorophosphate

PyBrop bromo-tris-pyrrolidino phosphoniumhexafluorophosphate

quant. quantitative

RT room temperature

sat. saturated
Ser (S) serine
SiO₂ silica

SOCl₂ thionyl chloride

TBAF tetra-*n*-butylammonium fluoride

^tBuOAc tert-butyl acetate ^tBuOH tert-butanol

^tBuOK tert butoxide, potassium

Tf₂O trifluoromethanesulfonic anhydride

TFA trifluoroacetic acid
TFAA trifluoroacetic anhydride

Tic tetrahydro-isoquinoline-3-carboxylic acid

TLC thin layer chromatography
TMSCl trimethylsilyl chloride
TMSCN trimethylsilyl cyanide

TMSOTf trimethylsilyl trifluoromethanesulfonate
TPSCl 2,4,6-triisopropylbenzenesulfonyl chloride

Trp (W) Tryptophan

TTBS tris-buffered saline and tween 20

Tyr (Y) tyrosine Val (V) valine

Xaa amino acid X

1. Introduction

The following introduction will be divided in two main parts; the first part giving a review on the general aspect of peptidomimetics and the second part introducing the specific project undertaken.

A] Peptidomimetic review

Peptides are generally used within medicinal chemistry for their ability to disrupt the binding of messenger molecules or enzymes with their substrates. However, they are not ideal due to inherent drawbacks such as a short biological half-life (cleavage by proteases) and poor membrane permeability, which limits their bioavailability. This has led to the development of peptidomimetics (replacement of peptide fragments with non-peptide fragments). Modern methods such as high-resolution crystallography have increased the accuracy of predicting the structural configuration of binding sites and so aid in the development of suitably related structures. The peptidomimetic strategy consists of altering the physico-chemical characteristics of a peptide without changing the biological activity. The designed peptidomimetics should show the same biological effects as the parent peptide but with increased biostability, bioavailability and often improved selectivity or potency.

1.1 Considerations undertaken during peptide design

Small peptides generally have high conformational flexibility due to the several conformations that each residue can adopt. The conformation of a peptide backbone is described by three torsion angles where ϕ is the angle defined by C(O)–N–C α –C(O); ψ the angle defined by N–C α –C(O)–N; ω the angle defined by C α –C(O)–N–C α and one side chain torsion angle, χ is defined by N–C α –C β –C γ (Figure 1.1).

Figure 1.1: Backbone and side chain torsional angles of peptides.⁶

Several techniques for the structural determination of biomolecules are well known including X-ray diffraction analysis on a single crystal, NMR spectroscopy, fluorescence and circular dichroism spectroscopy (CD). X-ray analysis gives the solid state conformation. However, we cannot correlate the solid state conformation is identical as the conformation adopted in solution or during the interactions with biological target.⁶ Moreover, NMR spectroscopy, fluorescence and CD spectroscopy have been shown to be powerful techniques, giving information about the peptide conformation in solution and its capability to interact with a target.⁶

For the development of peptidomimetics, the most significant parameters involved include the stereochemistry, charge and hydrophobicity. Overall, knowledge of the electronic, conformational and topochemical properties are essential. This firstly leads the design of a peptidomimetic to have a convenient fit to the binding site of the biological target and secondly to have the functional groups, polar and hydrophobic groups at defined positions to allow the appropriate interactions to take place. As detailed above, the main problem is the conformational flexibility of peptides thus, the introduction of conformational constraints into a peptide sequence is a very successful approach, which can be done by the incorporation of amino acids adopting a limited number of conformations or by cyclisation. The following sections (1.2, 1.3, 1.4 and 1.5) will discuss different approaches leading to peptidomimetics. This review highlights the modifications at the peptide backbone, the modifications at the side chains, the global restrictions and, finally secondary structure peptidomimetics.

1.2 Structural modification to improve peptide stability

As described above, peptidomimetics resemble native peptides or proteins but contain synthetic modifications designed to reduce metabolism and to optimise the biological activity. Peptides can be modified at the amino acid level, by rigidifying amino acid side chains or at the backbone of the peptide.

1.2.1 Pseudopeptides

Peptides can be modified by changing at least one of the peptide bonds with an isosteric or isoelectronic surrogate. These modifications can be classed into three main groups: a) the exchange of individuals groups, b) the extension of the backbone and c) the amide bond inversion (Figure 1.2). The most common isosters used are the reduced amides and

azapeptides (class 1), retro-inverso peptides (class 3) and peptoids (hybrid of class 1 and 3) (**Figure 1.2**). These surrogates will be presented in the next sections.

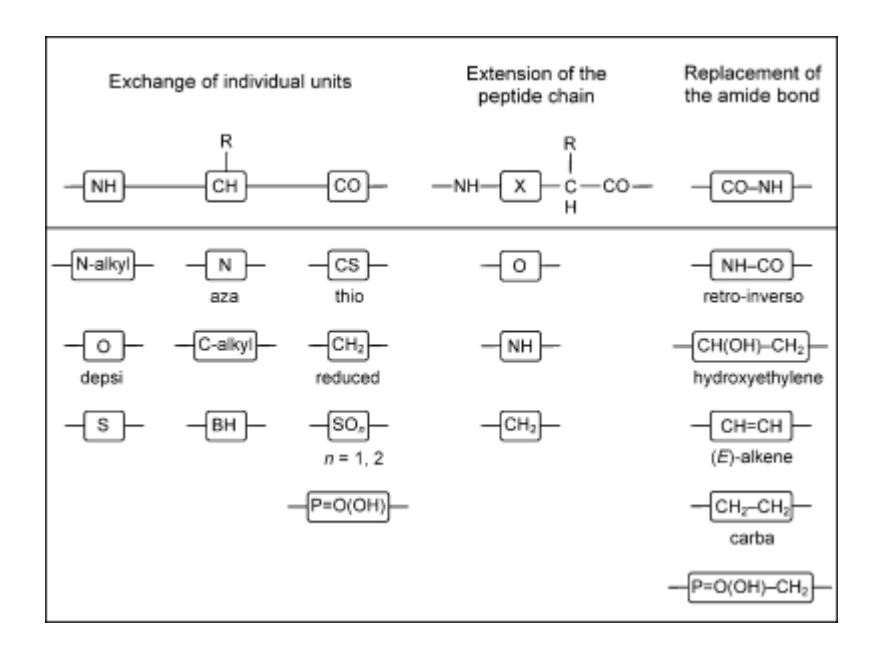


Figure 1.2: Three main classes of the common modifications to the peptide backbone (adapted from J. Gante, *Angewandte Chemie International Edition in English* **1994**, *33*, 1699-1720.).⁷

1.2.2 Reduced peptide bonds

The replacement of a peptide bond by a reduced peptide bond (CH₂-NH) often renders the peptides highly resistant towards enzymatic hydrolysis in the modified position. An example of this modification is found in the area of opioid peptides. H-Tyr–Tic Ψ [CH₂NH]Phe-Phe-OH (TIPP[Ψ]), for example, was synthesised and showed high stability against chemical and enzymatic degradation, slightly more potency and more selectivity to δ -receptors than the corresponding parent peptide (**Figure 1.3**).

Figure 1.3: Peptide backbone *vs* reduced amide surrogate.

1.2.3 Azapeptides

An interesting approach to peptide modification is the synthesis of azapeptides where the α -CH group of the backbone is replaced by a nitrogen atom and the side chain left untouched (**Figure 1.4**). This modification in a therapeutic peptide is exhibited in Atazanavir **1.5**, a highly active inhibitor of HIV protease. Generally, the synthesis of azapeptides is carried out from substituted hydrazines or hydrazides. The synthesis of **1.5** was undertaken from the advanced intermediates **1.1** and **1.2** giving the key intermediate **1.3**, which was reacted with two equivalents of the *N*-Moc protected *tert*-leucine **1.4** to give **1.5** (**Scheme 1.1**). 10

Figure 1.4: Peptide backbone vs azapeptide surrogate.

Reagents and conditions: a) Condensation, 85% then hydrolysis with HCl 12M, 95%; b) i) *N*-Moc-*tert*-Leu-OH **1.4**, EDC, HOBt, DIPEA; ii) H_2SO_4 , 71% over two steps.

Scheme 1.1: Synthesis of Atazanavir 1.5.10

1.2.4 Retro-inverso peptides

In retro-inverso modification peptidomimetics, the *N*- to *C*-terminus is reversed without changing the side chain positions. This does not lead to a more highly constrained peptide, but the main advantage over the native peptide is the higher *in vivo* stability as these mimetics are no longer substrates for proteases. Their disadvantage however is the inversion of charge at the termini. In fact, the positive charge located at the *N*-terminus is now replaced by a negative charge in the peptidomimetic and vice-versa for the *C*-terminus. This may be the cause of the low biological activity observed in several cases. In the synthesis of these peptidomimetics, p-amino acids are used instead of the natural properties (Figure 1.5). An evolution of this concept was developed, known as the partially modified retro-inverso (PMRI) peptide, where the retro-inversion is introduced into a normal sequence. The consequence of these PMRIs is that the retro-inversion and the normal portions are connected by a diamine and/or a diacid. The PMRI Tuftsin 1.7 is a good example of this modification where the two fragments are connected by a diacid (Figure 1.6). Tuftsin 1.6 is a immune system stimulator, which is completely degraded *in vivo* after 8 min while its PRMI peptidomimetic 1.7 showed less than 2% degradation in 50 min. The particular than the particular than the period of the properties of the period of the period of the period of the particular than the period of the pe

Figure 1.5: Peptide backbone vs retro-inverso surrogate.

$$H_2N$$
 H_2N
 H_2N

Figure 1.6: Tuftsin 1.6 and PMRI Tuftsin 1.7.11

Key to preparation of PMRI peptides is the synthesis of the *gem*-diaminoalkyl residue **1.11** and C-2 substituted malonyl residues **1.15** (Schemes **1.2** and **1.3**). Commonly, the Curtius and Hoffmann rearrangements are the methods used for preparation of the common isocyanate intermediate **1.10**. Then hydrolysis of **1.10** can form the *gem*-diaminoalkyl residue **1.11** (Scheme **1.2**).

$$PG \xrightarrow{R} CO_{2}H$$

$$PG \xrightarrow{R} N_{3} \xrightarrow{C} PG \xrightarrow{R} N_{4}CO_{2}H$$

$$PG \xrightarrow{R} PG \xrightarrow{R} N_{1.10}CO_{1.10}$$

$$PG \xrightarrow{R} N_{1.10}CO_{1.10}$$

$$PG \xrightarrow{R} N_{1.10}CO_{1.11}$$

$$PG \xrightarrow{R} N_{1.10}CO_{1.11}$$

Reagents and conditions: a) Curtius; b) Hoffmann; c) Δ; d) NaOBr.

Scheme 1.2: Synthesis of *gem*-diaminoalkyl residues **1.11** by the Curtius or Hoffmann rearrangement.

The preparation of malonyl derivatives **1.15** can be performed by the Knoevenagel reaction combined with reductive agents to yield intermediate **1.14**. Then, alcoholysis gives the desired C-2-substituted malonic acid monoester **1.15** (**Scheme 1.3**).

Reagents and conditions: a) NaCNBH₃; b) BzOH.

Scheme 1.3: Preparation of C-2-substituted malonyls **1.15** via a modified Knoevenagel reaction.

1.2.5 Peptoids

There is an interesting subgroup of pseudopeptides that contain *N*-alkylated glycines linked by peptide bonds. The α -CH groups are replaced by nitrogen atoms and the NH groups are substituted by CH₂ groups (**Figure 1.7**). Consequences of these modifications are firstly the loss of stereogenic α -CH groups being replaced by CH₂ groups and secondly introduction of the

side chain directly attached to the nitrogen atoms. The use of peptoid analogues have shown higher conformational flexibility compared to natural peptides and higher stability to proteases. A peptoid example is Ac-Nhtrp-Nharg-Nhtyr-NH $_2$ (where Nh indicates the peptoid homologue of the natural amino acid) which has shown a similar inhibition towards α -amylases compared with the natural peptide Ac-Trp-Arg-Tyr-OMe.

Figure 1.7: Peptide backbone vs peptoid surrogate.

1.3 Incorporation of unnatural amino acids

Several approaches have been investigated to prepare peptide analogues containing nonnatural amino acids. Reports indicate that peptide coupling with unnatural amino acids can be troublesome, with side reactions like racemisation occurring. The following sections will describe families of these unnatural amino acids.

1.3.1 D-amino acids

The main advantage of using D-amino acids in a sequence is that only a few enzymes can hydrolyse this peptide bond. Moreover, the conformation of the peptide involving D-residues is often changed which influences the receptor affinity and selectivity. A successful example is the DADLE analogue (H-Tyr-D-Ala-Gly-Phe-D-Leu-OH) being a selective enkephalin analogue (H-Tyr-Gly-Gly-Phe-Leu-OH) towards the δ -receptor. 13

1.3.2 N-alkylated amino acids

A very important modification of the peptide bond is *N*-alkylation and more specifically *N*-methylation which is used extensively.¹⁴ A large number of natural and synthetic biologically active peptides present *N*-methylated amino acids in their sequence. Generally, the use of *N*-methylated amino acids gives analogues improved pharmalogical properties such as stability, selectivity and bioavailability.¹⁴ These observed effects result from steric constraints introduced by the *N*-alkylated group. Flexibility of the backbone also affects the degree of rigidity of the side chain in the neighbouring group.⁵ Moreover, the substitution of NH groups

by *N*-alkyl groups eliminates some inter- and intramolecular hydrogen bonding.⁵ An example of an *N*-methylated peptide is cyclosporine A **1.16** isolated from *Trichoderma polysporum*, which contains seven *N*-methylated residues; It is used as an immunosuppressant after organ transplantations (**Figure 1.8**).¹⁵

Figure 1.8: Cyclosporin A ($R^1 = OH$; $R^2 = CH(CH_3)CH_2CH=CHCH_3$) 1.16.

Several *N*-alkyl amino acids are commercially available while many others can be synthesised (**Scheme 1.4**). ¹⁶ *N*-methylated amino acid **1.18** can be prepared by direct methylation of the protected amino acid **1.17**, or by a Mitsunobu reaction. ¹⁶

Reagents and conditions: a) NaH, Mel (PG = Boc, Cbz, Dpp); b) DEAD, PPh₃, MeOH (PG = arylsulfonyl).

Scheme 1.4: Syntheses of *N*-methylated amino acids **1.18**.

N-alkylated amino acids have proven useful for resisting enzymatic degradation without loss of biological activity. They have also been used extensively for structure-activity relationships (SAR) studies. The principle, called *N*-alkyl scan, consists of alkylating each backbone NH and evaluating the biological activity of the library of compounds synthesised. Thus, the most active peptide can be found and identified to be important for the interaction. For example, Sugano *et al.*¹⁷ prepared a series of analogues derived from H-Lys-Phe-Ile-Gly-Leu-Met-NH₂. The screening of analogues and biological assays undertaken on rabbit blood revealed that

substitution of Phe² and Leu⁵ showed a full depressor activity with a higher resistance to degradation. ^{17,5}

1.3.3 C α -tetrasubstituted α -amino acids

C α -tetrasubstituted α -amino acids have been investigated extensively in the last few years. ¹⁸ Common examples of α -alkyl α -amino acids are α -aminobutyric acid (Aib) **1.19** and isovaline (Iva) **1.20**. ⁵ These changes compared to natural amino acids give a conformational constraint which influences the chemical reactivity of the surrounding functional groups such as a reduced hydrolysis rate of an amide bond. Another approach to add even greater constraints is to prepare cyclic or heterocyclic C α -tetrasubstituted α -amino acids (**Figure 1.9**).

$$H_2N$$
 CO_2H H_2N CO_2H H_2N CO_2H CO_2H

Figure 1.9: α-Alkyl α-amino acid **1.19**, **1.20** and cyclic Cα-tetrasubstituted α-amino acids.⁵

The synthesis of C α -tetrasubstituted α -amino acids can be performed by the stereoselective alkylation of imidazolidinones (**Scheme 1.5**, **A**).¹⁹ In addition, α -methylamino acids can be synthesised by alkylation of Schiff bases derived from chiral amino acids and the Oppolzer's sultam (**Scheme 1.5**, **B**).¹⁹

Reagents: a) i) LDA ii) R¹-X; b) H⁺.

Scheme 1.5: Selected examples of the preparation of $C\alpha$ -tetrasubstituted α -amino acids **1.23** and **1.25**.

A successful example of the use of C α -tetrasubstituted α -amino acids is the modification of one glycine in the Leu-Enk sequence **1.26** which is an enkephalin. Enkephalin is a pentapeptide involved in the regulation of pain and nociception in the body. The synthesis of analogues **1.27**, **1.28** and **1.29** demonstrate that these analogues possess a β -turn conformation, which will be detailed in section 1.5.3, in solution with high activity exemplified by IC₅₀ values between 0.01 nM and 0.4 nM (**Figure 1.10**).²⁰

Figure 1.10: Structures of Leu-enkephalin 1.26 and three potent analogues 1.27, 1.28 and 1.29.

1.3.4 β -Substituted α -amino acids

In order to induce a particular conformational preference in side chains, analogues of natural amino acids alkylated at the β -carbon have often been used; for example including a methyl group incorporated into the side chain of Phe, Trp, and Tyr (**Figure 1.11**).⁵ Introduction of a methyl group into the side chains of phenylalanine or tryptophan for example, rigidifies the conformation of these residues and often results in higher biological stability and increased acitivity.²¹

$$H_2$$
N CO_2 H H_2 N CO_2 H H_2 N CO_2 H G -MePhe **1.30** β-MeTrp **1.31** β-MeTyr **1.32**

Figure 1.11: Selected examples of β-substituted α -amino acids.

1.3.5 Proline mimics

Proline is the only dialkylated amine among the 20 naturally occurring amino acids, thus it forms tertiary amides at the *N*-terminal side of the residue in a peptide chain or in proteins. The other 19 naturally occurring amino acids contain primary amines, which lead to secondary amides. Almost exclusively (>99.9%), secondary amides exist in the *trans* conformation due to the steric interactions between the two extended side chains. However, the *cis* conformation is much more favourable for an Xaa-Pro amide bond. *N*-alkylation reduces the steric advantage of the *trans* conformation; althought the *trans* conformation is still favoured energetically (**Scheme 1.6**). Raines *et al.*²² have shown that an electronic effect, an $n \rightarrow \pi^*$ interaction between the oxygen of the amide bond and the *C*-terminus carbonyl group, stabilises the *trans* conformer of prolyl amides (**Figure 1.12**).

$$cis$$
-rotamer $trans$ -rotamer

Scheme 1.6: *Xaa*-Pro isomerisation.

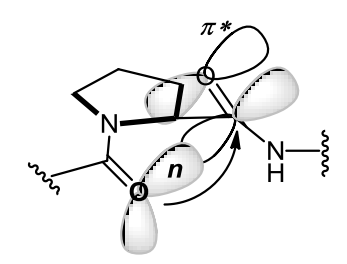


Figure 1.12: An $n \rightarrow \pi^*$ interaction contributes to the stability of the *trans*-Pro.²²

The cyclic structure of proline restricts the conformation of a peptide chain, influences the biological activity and stabilising properties of peptides containing prolines. ²³ Many natural proline derivatives have been found in proteins, antibiotics and cytotoxic peptides (**Figure 1.13, A**). ²⁴ Other proline derivatives have been synthesised by the introduction of alkyl chains, heteroatoms or halogens at different positions of the proline ring (**Figure 1.13, B, C**). ²⁴ The main difference among Azy **1.38**, Aze **1.39** and Pip **1.40** is the steric bulk of the side chain rather than the torsion angles (ϕ , ψ). Also, 4-F (fPro) **1.42** and 4-OH (Hyp) **1.41** substituted systems were found to be good mimetics in stabilising the collagen triple helix. ²⁵ The preference of the conformation was induced by pyrrolidine ring puckering of imino residues (**Figure 1.13, C**). ²⁶

Figure 1.13: Examples of natural prolines derivatives (**A**), unnatural proline derivatives (**B**) and mimics in stabilising the collagen triple helix (**C**).

In addition, conformationally constrained proline peptidomimetics have been designed by various strategies in order to lock the conformation of proline either *cis* or *trans*. A few examples of strategies are described below.

One of the strategies for conformationally defined peptidomimetics, is to use a linkage Y to tether the two amino acids. Forming a bicyclic lactam, the amide bond can be locked in the *cis* or *trans* conformation. An advantage of this strategy is that it affords *cis* as well as *trans* dipeptide mimics. The *cis* mimic is formed when Y is between the two α -carbons of both amino acids, while *trans* mimic is formed when Y is between α -carbon of Xaa and the δ -carbon of Pro as shown in **Figure 1.14**.

$$HO_2C$$
 NH_2
 HO_2C
 $trans$

Figure 1.14: Bicyclic lactam Xaa-Pro mimetics.

An ideal peptide bond surrogate is the olefinic moiety because of the similar geometrical disposition of substituents attached to either of these functional groups. Two alkene mimics of *trans*-Proline are the (E)-alkene **1.43** ^{2a} and the (Z)-fluoroalkene **1.44** (**Figure 1.15**). ^{2b}

Figure 1.15: Alkene trans-proline mimics.

A subclass of *trans*-proline mimics is those which adopt a polyproline type II (PPII) helix conformation. These are discussed in sections 1.7.1 and 1.7.2.

1.3.6 β-amino acids

There are two types of β -amino acids, the β^2 - or β^3 - versions (**Figure 1.16**). They have been used to construct peptidomimetics of β -amino acids occurring in natural peptide hormones, such as opioid peptides.⁵

Figure 1.16: β^2 - and β^3 -amino acids.

 β^3 - Derivatives can be prepared by direct Arndt-Eistert homologation of α -amino acids (**Scheme 1.7, A**). However, the best routes to prepare substituted β^3 -amino acids are via the functionalisation of intermediate **1.48** (**Scheme 1.7, B**) and the conjugate addition to α,β -unsaturated esters or imides in particular with chiral auxiliaries or chiral amines as nucleophiles (**Scheme 1.7, C**).

A PGNH
$$CO_2H$$
 A PGNH A PNH A PNH

Reagents: a) CH_2N_2 ; b) i) LDA, -78 °C, ii) R^1 -X (R^1 = Me, Bn, Bu, C_6H_{13}), 75-77% (>95% ds); c) i) 6 M HCl, ii) ion exchange, 62-69%.

Scheme 1.7: Different synthetic routes to prepare β^3 -amino acids.

There are various synthetic approaches to the preparation of β^2 - amino acids (**Scheme 1.8**).²⁷ One method includes the formation of the C2–C3 bond using aminoalkylating agents with chiral auxiliaries such as Evans oxazolidinones (**Scheme 1.8**, **A**). Xue *et al.*²⁸ for example described the synthesis of the enantiopure (R)- β^2 -homoaspartate derivative through stereoselective alkylation with *tert*-butyl bromoacetate. Another strategy is to form a C2–R bond via β -alkylations of chiral enolates derived from β -aminopropanoic acid (**Scheme 1.8**, **B**). Finally, an alternative to previous strategies is a diastereoselective protonation, hydrogenation or hydrogen- atom transfer of enols or enolates, forming the C2–H bond (**Scheme 1.8**, **C**).

Reagents: a) $(R^1 = H)$ i) PGN-CH₂⁺, ii) A* removal; b) $(R = CH_2-NPG, R^1 = H)$ i) R^2-X , ii) A* removal; c) $(R = CH_2-NPG)$ i) H^+ , ii) A* removal. * = stereogenic centre of controlled configuration.

Scheme 1.8: Various synthetic approaches to β^2 -amino acids.

The formation of single isomer β -amino acids described above required the use of chiral auxiliaries. Alternatively the C1–C2 bond can be formed enantioselectively by a stereoselective addition to the double bond of α,β -unsaturated carboxylic acid derivatives (**Scheme 1.9**).²⁷

Reagents and conditions: a) TMSCN, **1.58** (10 mol%), ⁱPrOH, toluene 70-96% (94-98% ee).

Scheme 1.9: Synthesis of β^2 -amino acis by C1–C2 bond formation.

Generally the substitution of α -amino acids by their β -isomers in biologically active peptides results in higher activity and enzymatic stability. An interesting example is the introduction of β^2 - or β^3 - amino acids in the native sequence of endomorphin-1, H-Tyr-Pro-Trp-Phe-NH₂, which gave varied affinity to μ -opioid receptor agonists. The replacement of β^2 -Pro and β^3 -Pro in the peptide sequence showed high affinity in the nanomolar range.

1.4 Introduction of global restrictions

Other than the amino acid modifications discussed, introduction of global restrictions into the peptide via cyclisation is another method for the preparation of active peptidomimetics. Generally, compared to the native peptide, these result in higher stability, more defined conformation and higher selectivity towards the target.⁵ Three connections have been developed for the preparation of cyclic analogues; the *N*- with the *C*-terminus (head-to-tail), the *C*- or *N*-terminus with one of the side chains (backbone/side chain) and the connection of two side chains not involved in the interaction with other proteins (side chain/side chain) (**Figure 1.17**).⁵

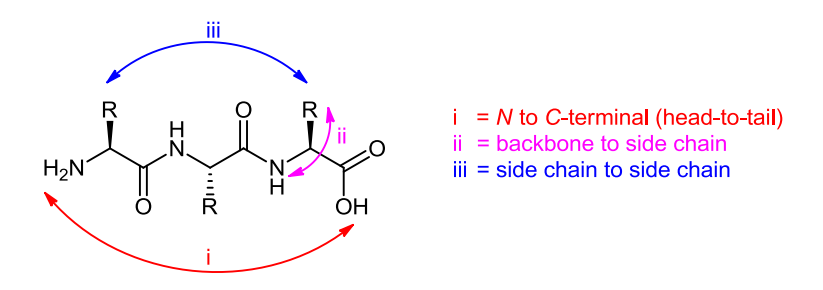


Figure 1.17: Three connections for the preparation of cyclic peptidomimetics.

1.4.1 Head to tail cyclisation

Most head to tail cyclic peptides are prepared via cyclisation of activated precursors in solution phase under standard peptide coupling conditions such as HBTU or HATU. An example of this type of cyclisation is reported by Strom *et al.*³⁰ where they found an improved anticancer potency by head to tail cyclisation of short linear heptapeptides containing a $\beta^{2,2}$ -amino acid: H-Lys-Lys-Trp- $\beta^{2,2}$ -Trp-Lys-Lys-NH₂, with an IC₅₀ of 22 μ M for the linear peptide and 10 μ M for the cyclic version against Ramos cancer cells.³⁰

1.4.2 Side chain to Side chain cyclisation

This cyclisation is the most common method to lock peptide chains into defined structures such as α -helices as detailed in section 1.5.1. Disulfide bridges are a key feature of many peptides and proteins and result in stabilising bioactive conformations. An example of this method is the cyclic enkephalin analogue DPDPE **1.59** which is active at the δ -opiate receptor (**Figure 1.18**).^{13,5}

HO

$$H_2N$$
 H_2N
 H_2N

Figure 1.18: Enkephalin analogue DPDPE 1.59.13

One covalent bridge can be a limiting factor as this linkage constrains only a section of the sequence. In order to avoid this problem, several covalent bridges can be incorporated into one sequence. A therapeutically relevant example is the modification of the human parathyroid hormone (hPTH). The introduction of three lactam bridges between i and i + 4 results in a highly constrained peptide which adopts a helical conformation, leading to a much more active compound than the native sequence (**Figure 1.19**).³¹

Figure 1.19: Peptidomimetic 1.60 of the hPTH stabilised by three lactam bridges.³¹

The stability of disulfide and lactam bridges have been shown to be efficient, however they are not always stable *in vivo* which has led to the development of a hydrocarbon linkage. A powerful strategy for this type of cyclisation is ring closing methatesis (RCM).⁵ A mimic of the minimal death domain BH3 of the pro-apoptotic subfamily of proteins illustrates the hydrocarbon cyclisation methodology. Insertion of the unnatural amino acids **1.61** and **1.62** followed by RCM forced the peptide sequence to adopt a helical conformation which improved its stability as well as its *in vitro* and *in vivo* activity (**Figure 1.20**).³²

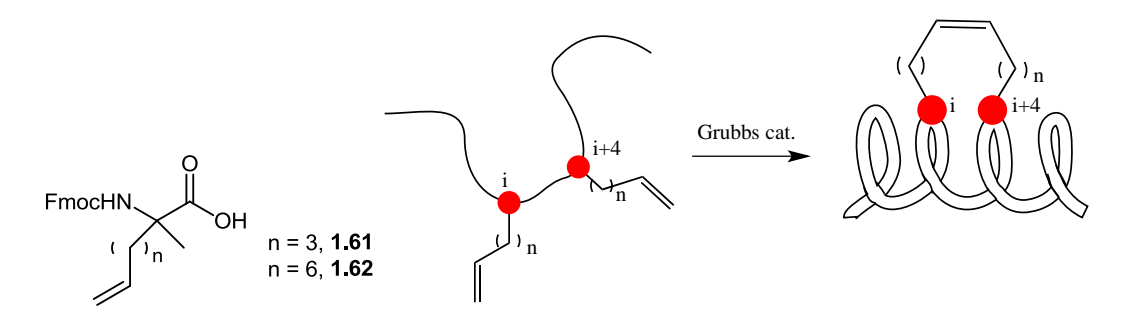


Figure 1.20: Unnatural amino acids **1.61** and **1.62**; helical conformation obtained by insertion of **1.61** or **1.62** followed by RCM into the peptide sequence (adapted from L. D. Walensky, A. L. Kung, I. Escher, T. J. Malia, S. Barbuto, R. D. Wright, G. Wagner, G. L. Verdine, S. J. Korsmeyer, *Science* **2004**, *305*, 1466-1470). ³²

1.4.3 Backbone to Side chain cyclisation

The final type of cyclisation is the linkage of the backbone and the side chain. A good example is the cyclic derivative **1.63**, Tyr-c[-p-Orn-2-Nal-p-Pro-NMe-Ala] of the β -casomorphin-5. β -casomorphins are peptides derived from the milk protein β -casein. Analogue **1.63** has proven to be highly selective for the μ -opioid receptor (IC₅₀ = 35 nM) (**Figure 1.21**). ³³

Figure 1.21: Cyclic β-casomorphin-5 derivative 1.63.³³

1.5 Secondary structure peptidomimetics

Well defined conformations are observed in proteins and polypeptides are known as secondary structures, defined by their torsion angles (ϕ, ψ) . The most abundant secondary structures are α -helices, β -sheets, reverse turns and polyproline type II (PPII) helices. The following sections (1.5.1, 1.5.2, 1.5.3 and 1.5.4) provide a brief overview of peptidomimetics of each type.

1.5.1 α-helix peptidomimetics

In an α -helix the torsion angle values are: $\varphi = -57^{\circ}$ and $\psi = -47^{\circ}$. The α -helical structure is stabilised by hydrogen bonding between the carbonyl oxygen at the i position and the carboxamide hydrogen at the i+3 and i+7 positions.³⁴ A good example of peptidomimetics adopting this helical structure was reported by Hamilton *et al.*³⁵ (**Figure 1.22**). Residues in these compounds present similar distances and angular relationships when compared with the side chains found in α -helices. To validate the design of α -helix mimicry by terphenyl derivatives, Hamilton *et al.*³⁵ focused on the interaction of calmodulin (CaM). This study revealed that the terphenyl derivatives **1.64** designed are the most potent CaM antagonists known to date, with an IC₅₀ of 800 nM.

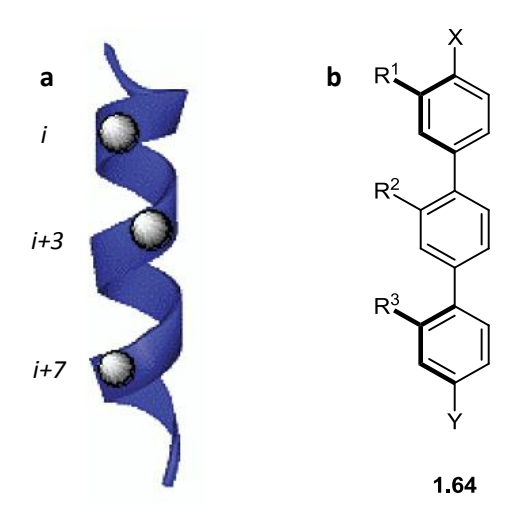


Figure 1.22: a) i, i + 3, i + 7 substituents of an α -helix; b) α -helix mimics (terphenyl scaffold **1.64**) by Hamilton *et al.*³⁵ (adapted from O. Kutzki, H. S. Park, J. T. Ernst, B. P. Orner, H. Yin, A. D. Hamilton, *Journal of the American Chemical Society* **2002**, *124*, 11838-11839).

1.5.2 β-sheet peptidomimetics

The β -sheet structure is based on a basic unit called a β -strand which is a single chain. A β -strand itself is not stable however when two strands come together via hydrogen bond linkage, a stable β -sheet conformation forms. The direction of the two strands defines two types of β -sheet structures, parallel and antiparallel (**Figure 1.23**). Nowick *et al.*³⁶ developed an artificial β -sheet mimetic based on cyclic fragments. The use of 2-methoxybenzoic acid amide and hydrazine derivatives allowed hydrogen bonds to form between the two chains. This was analogous to that found in an antiparallel β -sheet (**Figure 1.24**).

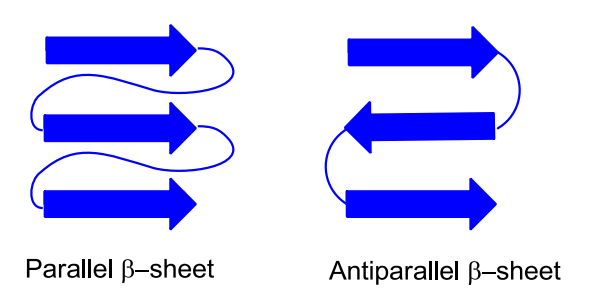


Figure 1.23: β-sheet structures

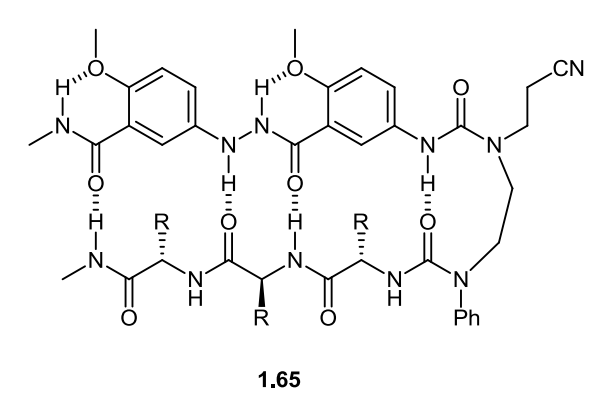


Figure 1.24: Artificial β-sheet mimetic **1.65** by Nowick *et al.*³⁶

1.5.3 Reverse turn peptidomimetics

The most common turn is called a β -turn. Here the distance between C α of residues i and i+3 is less than or equal to 7 Å (**Figure 1.25, A**). The turn can be stabilised by intramolecular hydrogen bonds or by chelation of a cation. β -Turn mimic development involves a rigid scaffold that orients the side chain residues in the same direction as the natural protein which would also give better solubility and resistance to enzymatic degradation.³⁷ A successful example of

the use of biologically active β -turn mimics was developed by Ellman *et al.*³⁷ They produced a large library of analogues (1152) derived from **1.66**, which were screened in binding assays against the fMLF receptor (**Figure 1.25**).

Figure 1.25: a) β -turn; b) replacement of the hydrogen bond between *i* and *i* +3 residues with a covalent linkage; c) β -turn mimic **1.66** by Ellman *et al*.³⁷

1.5.4 Polyproline type II peptidomimetics

Small peptidomimetics in this category will be reviewed in detail in the context of our specific project objectives (section 1.7.2).

B] Rational design and synthesis of small molecule *trans*-proline mimics, and their applications: Introduction to our project objectives

In the next section (1.6) we will discuss and introduce the synthesis and clonogenic assay of analogues of a functional (selective anti-cancer) proline-rich peptide, PRGPRP.

The synthesis of conformationally restricted proline-rich sequence mimics and analysis of their function in a specific protein-protein interaction (PPII helix-SH3 domain) will be also described (sections 1.7).

C] Project background

1.6 PRGPRP lead compound identification

Anti-cancer treatments have been developed to include surgery, radiopathy, chemotherapy, immunotherapy and hormone therapy⁴. Most cancers can be treated and some forced into remission, depending on the specific type, location and stage. Once diagnosed, cancer is usually treated with a combination of surgery, chemotherapy and radiotherapy. As research develops, treatments are becoming more specific for different varieties of cancer. There has been significant progress in the development of targeted therapy drugs that act specifically on detectable molecular abnormalities in certain tumors, and which minimise damage to normal cells. Surgery in combination with radiotherapy, for example has proven successful for some local tumors. Chemotherapy and immunotherapy have both been used successfully in the treatment of cancer with the latter having reduced side effects.⁴ Research is aimed at the discovery of new drugs, making modifications in the molecular structure and finding techniques to improve efficacy.³⁸ What has yet to be obtained is a selective treatment for a broad range of cancers with minimal side effects.

Cyclin-dependent kinase 4 (CDK4) is an enzyme that regulates cell division and causes cancer when mutated or over-expressed. Warenius *et al.*³⁹ found a new peptidic drug which may inhibit a protein-binding site in CDK4, based on collaboration with our group (vide infra),³⁹ which identified a sequence of amino acids in the CDK4 primary structure that may act as a binding site for a protein partner. The project detailed herein will involve modifying this peptide drug candidate using peptidomimetics in order to increase its drug-like characteristics, and potentially aid its progress through to drug discovery.

Cyclin-dependent kinases (CDKs) are a family of serine/threonine protein kinases. The CDKs play important roles in the regulation of cell division and form complexes with their activating partners (cyclins) to be active. 40 CDK/cyclin complexes can act as switches that regulate each of the cell cycle transitions through four distinct phases: G1 phase, S phase (synthesis), G2 phase (interphase) and M phase (mitosis). 41 In light of the strong link between CDKs and cancer these enzymes have been investigated as possible targets for cancer chemotherapies. 41 CDK4 is an important enzyme which has been implicated in the development of cancer cells. This enzyme, together with CDK2 and CDK6 are traditionally thought to be responsible for the hyper-phosphorylation of retinoblastoma protein (Rb). This hyper-phosphorylation is the signal to start cell division and allows transition of the cell from the G1 to the S phase (Figure 1.26). 42

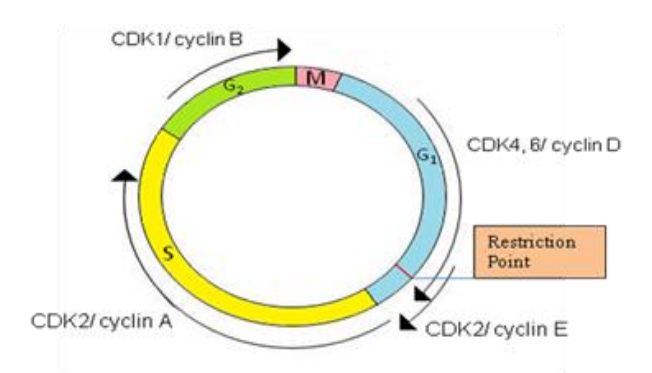


Figure 1.26: Cell cycle (Image taken from G. M. Cooper, E. R. Hausman, The Cell; A molecular approach: **2004**; Third Edition).⁴³

Warenius *et al.*⁴⁴ described a unique relationship between proteomic expression of CDK1 and CDK4 in human cancer cells. The over expression of CDK4 in cancer cell lines causes an increase in CDK1 protein levels but no increase in CDK4-dependent phosphorylation of Retinoblastoma (Rb) protein.⁴⁵ The crystal structure of CDK4 was not published at the time so a sequence homology model of the CDK protein family was calculated to produce a comparative model. *In silico* structural studies of CDK4 compared to CDK2 and CDK6, showed a kinase-independent functional site at the *C'*-terminus of CDK4, which was not shared by CDK6 or CDK2. This is a unique externalised water accessible loop with the amino acid sequence FPPRGPRPVQSV³⁹ (**Figure 1.27**). A hypothesis that the 12mer sequence constitutes a protein binding site which may account for the CDK4/CDK1 co-expression and may be susceptible to competitive inhibition, was developed.

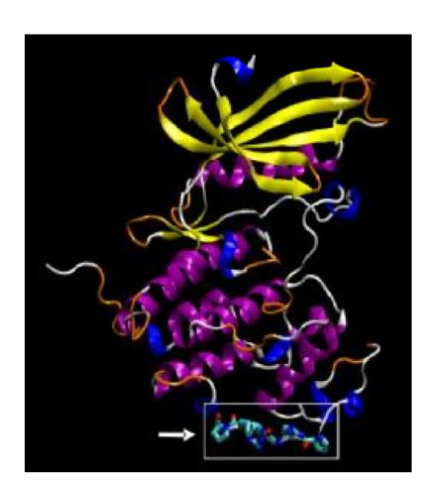


Figure 1.27: Computational structure of CDK4 (Image taken from J. Kilburn, J. Essex *et al.*³⁹).

The boxed region indicates the externalised position of FPPRGPRPVQSV.

Human bladder (RT112) cancer cells were tested with the synthetic 12mer sequence (1 mM) and it was found that 30-50% of the cells were dead within the first few days. Shorter peptide sequences of linear peptides derived from the 12mer were also exposed to RT112 bladder cancer cells and normal fibroblast cell lines (5 mM), the results are summarised in the Table 1.1 below.³⁹

Compound*	Dose	Human Bladder Cancer cells	Normal Diploid Fibroblasts
		Caricer cells	Tibioblasts
FPPRGPRPVQ	1.0 mM	+/-	++/-
PRGPRP	5.0 mM		+++++
PRGPR	5.0 mM		+++
RGPRP	5.0 mM	+/-	+++
RGPR	5.0 mM	+++	+++
PRRPGP	5.0 mM	+++	+++
PEGPRP	5.0 mM	+++	+++
PRGPEP	5.0 mM	+++	+++
PEGPEP	5.0 mM	+++	+++

Cell viability (+++ = same morphological appearance as untreated controls, --- = total morphological cell death

Table 1.1: *In-vitro* survival of RT112 Human Bladder Cancer and Normal Diploid Human Fibroblasts in response to treatment with small peptides.³⁹

This study revealed the hexapeptide PRGPRP to be the most selective and effective moiety, being non-toxic to normal fibroblasts but selectively killing RT112 bladder cancer cells (5 mM solution of peptide, **Figure 1.28**).³⁹

These assays also demonstrated that transposing one of the two arginines resulted in total loss of activity. Moreover, PEGPRP and PRGPEP (arginine substituted by glutamic acid) proved to be inactive towards RT112.

^{*} For all compounds the N-terminus is an acetyl group and C-terminus is a primary amide.

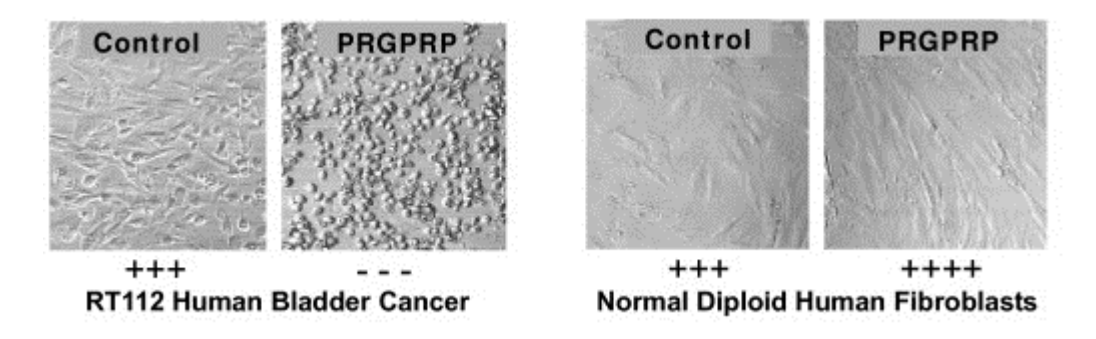


Figure 1.28: Photomicrographs illustrating *in-vitro* morphological appearances of RT112 human bladder cancer cells (left hand panels) and normal human fibroblasts (right hand panels) following exposure to 5.0 mM PRGPRP or control nonsense peptide (Image taken from H. Warenius, J. Kilburn, J. Essex, R. Maurer, J. Blaydes, U. Agarwala, L. Seabra, *Molecular Cancer* **2011**, *10*, 72.).³⁹

Recently, the first crystal structure data for CDK4 in complex with cyclin D1 was reported (**Figure 1.29**). ⁴⁶ This confirmed that the T-loop containing the 12mer sequence with the central hexamer PRGPRP is solvent accessible. These structural studies suggest that this sequence is a plausible candidate for competitive inhibition of CDK1/CDK4 co-expression. ⁴⁶

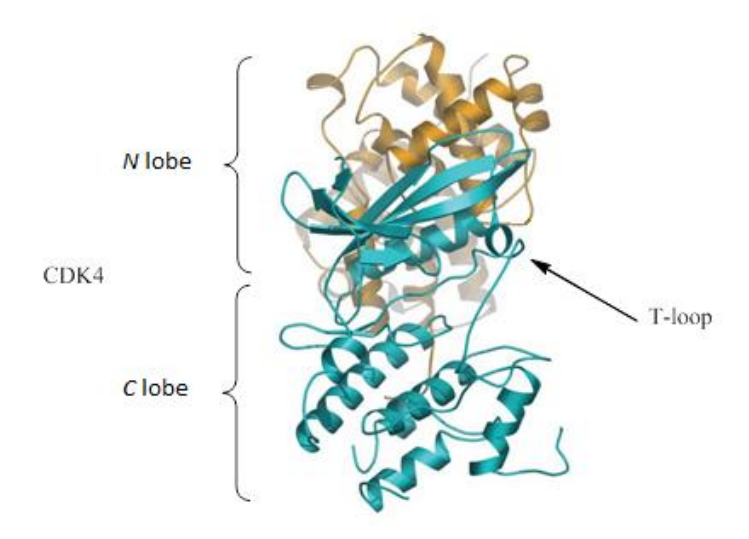


Figure 1.29: Ribbon diagram of the CDK4 (cyan)/cyclin D1 (orange) heterodimer. The *N*- and *C*-terminal lobes of the kinase are labelled as key secondary structural elements (Image taken from P. J. Day, A. Cleasby, I. J. Tickle, M. O'Reilly, J. E. Coyle, F. P. Holding, R. L. McMenamin, J. Yon, R. Chopra, C. Lengauer, H. Jhoti, *Proceedings of the National Academy of Sciences of the United States of America* **2009**, *106*, 4166-4170.).

1.6.1 Cytisine 1.67 as a *trans*-proline mimic

The first aspect of this project aims to produce peptidomimetics of PRGPRP based on the alkaloid cytisine **1.67** (**Figure 1.30**). This natural product can be extracted from *cytisus laburnum* seeds⁴⁷ and was first isolated in 1862. The absolute configuration (1R,5S) of the compound was established in 1961.⁴⁸

Figure 1.30: (-)-cytisine 1.67.

Crystallographic studies showed that only *trans*-proline occurs in the anti-cancer hexapeptide PRGPRP.⁴⁶ Using a combination of funtionalisation methods of cytisine **1.67**, a peptidomimetic can be synthesised with high resemblance to *trans*-L-proline. This mimic can be introduced in place of each of the natural *trans*-proline residues, in order to improve biological properties of the resulting full hexapeptide analogues.

Initial attempts at functionalisation of cytisine **1.67** will involve N–C aryl migration for stereoselective functionalisation of the 6α position (section 1.6.2), producing a stereocentre with the correct ι -stereochemistry to match that of the natural amino acid. The amide bond within the 2-pyridone ring locks the mimic into a *trans*-orientation. This produces a spatial configuration similar to natural *trans*-proline (**Figure 1.31**).

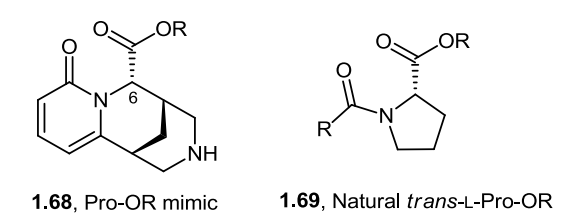


Figure 1.31: Comparative illustration of Pro-OR mimic 1.68 with natural trans-L-Pro-OR 1.69.

Functionalisation of the 9-position by regioselective nitration then reduction, should give the rigidified mimic Gly-Pro (**Figure 1.32**).⁴⁹

Figure 1.32: Comparative illustration of Gly-Pro-OR 1.70 with natural Gly-Pro-OR 1.71.

Modification of the 11-position could give the Arg-Pro mimic (**Figure 1.33**). An α -guanidyl side chain could be introduced via a Suzuki coupling or a Vilsmeier reaction which will be discussed in **Scheme 1.16** and **1.17**. The correct number of bonds represents the natural Arg fragment, but the presence of the aromatic ring increases the rigidity of the guanidine side chain.

Figure 1.33: Comparative illustration of Arg-Pro-OR mimic 1.72 with natural Arg-Pro-OR 1.73.

These hexapeptide analogues can be tested for efficacy in cell-based assays as illustrated previously in **Table 1.1** and **Figure 1.28**. A comparison can be established with Ac-PRGPRP-NH₂ as a control using the same method of detection.³⁹ Each mimic can be inserted independently, thus a small library can be synthesised to determine which structural modifications have most effect on activity.

1.6.2 Cytisine 1.67, functionalisation towards therapeutics

1.6.2.1 *N*-Functionalisation of cytisine 1.67: An N–C migration developed by the Rouden group⁴⁹

Cytisine **1.67** is a nicotinic agonist⁴⁹ and in order to synthesise new ligands for receptors of the central nervous system, Rouden *et al.*⁴⁹ developed methodology to structurally modify cytisine **1.67**. Highly regio- and diastereoselective functionalisation at the 6α -position was achieved

according to **Scheme 1.10**. (–)-*N*-Benzyl- 6α -propionyl-cytisine **1.75** was formed using LDA in the presence of excess LiCl, arising from an unusual acyl migration from nitrogen to carbon.

Reagents and conditions: a) Propionyl chloride, CH_2Cl_2 , Et_3N ; b) ⁿBuLi, DIPEA, LiCl, -20 °C, then THF, **1.67**, -78 °C, 30 min, then benzyl bromide, 3 h, 75% yield.

Scheme 1.10: N-C migration using LDA.⁴⁹

The proposed mechanism by Rouden *et al.*⁴⁹ for the migration involves a carbonyl-directed deprotonation at C-6. The resulting 6α -carbanion **1.74a** can undertake a nucleophilic attack on the acyl carbonyl carbon producing a strained 5-membered cyclic tetrahedral intermediate **1.74b**. The cage structure of acylated cytisine **1.74a** blocks the attack from the top face, accounting for the high stereoselectivity observed. Then, addition of an electrophile, here water, gives **1.74f** (Scheme **1.11**) via hemiaminal collapse.⁴⁹

Scheme 1.11: Mechanism for N–C acyl migration proposed by Rouden et al. 49

The nature of the *N*-acyl group was found to have a marked influence on the efficiency of *N*-acyl transfer. The intramolecular reaction of the carbanion formed on the adjacent position to the pyridone ring with different electrophiles is summarised in **Table 1.2**.

R^1	R ² Electrophile		Isolated yield of
ĸ	N.	Electrophile	1.77
OMe	Bn	BnBr	65 %
OMe	Н	H ₂ O	79 %
Et	Bn	BnBr	75 %
Et	Me	Mel	51 %
Et	Н	H ₂ O	70 %
^t Bu	Н	H ₂ O	57 %
ⁱ Pr	Н	H ₂ O	65 %

Table 1.2: N–C migration with a variety of migratory groups and electrophiles. 49

To conclude, this work demonstrated the possibility of diastereoselective intramolecular functionalisation of cytisine **1.67** on carbon 6. The key step involves a regiospecific carbonyl-directed deprotonation of cytisine using LDA followed by anion trapping with various electrophiles. Subsequent functionalisation on carbon 9 or 11 may give the Gly-Pro-OR mimic and the Arg-Pro-OR mimic respectively (**Figure 1.32** and **1.33**).

1.6.2.2 Pyridone functionalisation: Electrophilic aromatic bromination

In addition to *N*-functionalisation, and discovery of the described acyl migration, Rouden *et al.*⁴⁹ investigated pyridone ring functionalisation. Protection of the secondary amine by a nitroso group **1.78** was required to access C-9 halogenated derivatives **1.79** by electrophilic aromatic substitution according to **Scheme 1.12**.^{47b}

Reagents and conditions a) NaNO₂, HCl, quant.; b) NBS, DMF, 50% or CF₃COOAg, I₂, CH₂Cl₂, 50%.

Scheme 1.12: Synthesis of C-9 functionalised cytisine derivatives.

1.6.2.3 Pyridone functionalisation: Electrophilic aromatic halogenation with a direct approach by Rouden *et al*^{47b}

As shown previously, substitution at C-9 was undertaken with *N*-protected cytisine derivatives **1.78**. A one step procedure was also developed to obtain the C-9 substituted compound **1.80a** directly from cytisine **1.67**. This method utilised acetic acid to protonate the secondary amine, a source of halogen electrophile was then added to give the halogenated cytisine **1.80**. However, a mixture of three compounds was obtained; the mono C-9 and C-11 halogenated cytisine derivatives (**1.80a** & **1.80b**), and the bis-halogenated product **1.80c** (Scheme **1.13**). So

Reagents and conditions; a) NCS, AcOH/H₂O (3:2); b) NBS, AcOH/H₂O (3:2); c) ICl, AcOH.

Scheme 1.13: General scheme for the direct halogenation of (–)-cytisine 1.67.50

Halogen atom	1.80a	1.80b	1.80c
Cl	26	40	5
Br	27	27	5
I	Mixture of 1.80a	10	1
	and 1.80b		

Table 1.3: Isolated yield observed for halogenation on (–)-cytisine **1.67**. ⁵⁰

According to **Table 1.3**⁵⁰, bromination of cytisine gave a 1:1 ratio of the 9-bromo-cytisine and the 11-bromo-cytisine in rather poor yield. Chlorination gave the major 11-halogenated isomer (40% yield) and the 9-bromocytisine in 27% yield. Iodination did not give a pure 9-iodo isomer.

1.6.2.4 Pyridone functionalisation: Electrophilic aromatic nitration approach.

A second pyridone functionalisation reported by the Rouden group^{47b} involved direct nitration on **1.67** was undertaken to afford *N*-propionyl-9-nitrocytisine **1.81** and *N*-propionyl-11-cytisine **1.82** in 77% and 11% respectively (**Scheme 1.14**).

Reagents and conditions: a) HNO₃, H₂SO₄.

Scheme 1.14: Electrophilic aromatic nitration approach by Rouden *et al.*^{47b}

Many of the functionalisations were undertaken using *N*-protected cytisine derivatives and direct nitration of cytisine **1.67** has also been demonstrated.^{47b}

1.6.3 Cytisine analogues.

In this project our aim was to synthesise three different analogues of the anti-cancer hexapeptide PRGPRP. Our first target being *Pro-Arg-Gly-Pro-Arg-Pro 1.83 where *Pro indicates incorporation of the cytisine-based mimic as indicated in Figure 1.34.

Figure 1.34: *Pro-Arg-Gly-Pro-Arg-Pro-NH₂ 1.83.

We then envisaged accessing the second and third analogues by functionalisation of the pyridone ring at positions 6 and 9 (Pro-Arg-*Gly-*Pro-Arg-Pro, **1.84**), and at positions 6, 9 and 11 (Pro-Arg-Gly-Pro-*Arg-*Pro, **1.85**) respectively (**Figure 1.35**).

Figure 1.35: *N*-Ac-Pro-Arg-*Gly-*Pro-Arg-Pro-NH₂ **1.84** and *N*-Ac-Pro-Arg-Gly-Pro-*Arg-*Pro-NH₂ **1.85**.

For synthesis of *N*-Ac-Pro-Arg-*Gly-*Pro-Arg-Pro-NH₂ **1.84**, and following Rouden's method, ⁴⁹ the N–C migration will be used to introduce a benzyl ester functionality at the 6α -position to give **1.86**. Functionalisation of the pyridone ring will be undertaken by electrophilic aromatic nitration at the 9-position of functionalised cytisine **1.86**, followed by a Pd catalysed reduction, ⁴⁹ which will give mimic **1.87** representing the *Gly-*Pro dipeptide. Coupling onto this 9-amino group of **1.87** with Boc-Pro-Arg(NO₂)OH and then H.Arg(NO₂)Pro-OMe allows the formation of the hexapeptide mimic *N*-Ac-Pro-Arg-*Gly-*Pro-Arg-Pro-NH₂ **1.84** (Scheme **1.15**).

Reagents and conditions: a) i) benzylchloroformate, NEt₃, ii) LDA, –78 °C then water, iii) formic acid, formaldehyde; b) i) HNO₃, H₂SO₄, ii) H₂, Pd/C; iii) PMBCl; c) Boc-Pro-Arg(NO₂)OH, HOBt, DCC, DIPEA, DMF; d) i) CAN or DDQ ii) H.Arg(NO₂)Pro-OMe, HOBt, DCC, DIPEA, DMF, iii) TFA, iv) Ac₂O, v) NH₃, vi) H₂, Pd/C, AcOH.

Scheme 1.15: Synthetic approach for the construction of *N*-Ac-Pro-Arg-*Gly-*Pro-Arg-Pro-NH₂ **1.84**.

For preparation of the *N*-Ac-Pro-Arg-Gly-Pro-*Arg-*Pro-NH₂**1.85**, two different routes can be envisaged; intermediate **1.89** could be converted to aldehyde **1.90** under Vilsmeier conditions. Then introduction of the guanidine side chain could be carried out using pyrazole derivative **1.92** or **1.93** to afford intermediate **1.91**. Further peptide coupling reactions will then give access to the desired hexapeptide **1.85** (Scheme **1.16**).⁵¹

Reagents and conditions: a) i) ^tBuOH, H⁺, ii) Boc-Pro-OH, HOBt, DCC, DIPEA, DMF, iii) POCl₃, DMF; c) i) HCl, ii) Boc-Pro-Arg(NO₂)Gly-OH, HOBt, DCC, DIPEA, DMF, iii) HCl, iv) Ac₂O, v) TFA, vi) NH₃, vii) H₂, Pd/C, AcOH.

Scheme 1.16: Proposed synthesis of *N*-Ac-Pro-Arg-Gly-Pro-*Arg-*Pro-NH₂ **1.85** via a Vilsmeier reaction.

The second approach would be to undertake a Suzuki coupling with an α -amino borate **1.94** as the precursor. A Suzuki coupling reaction between **1.95** and **1.96** will then give an α -amine at the 11-position **1.97** and the N–C migration can be performed to afford intermediate **1.98** (Scheme **1.17**). ⁵²

Reagents and conditions: a) i) NIS, ii) Pd, base; b) i) LDA then H^+ , ii) N-methylation.

Scheme 1.17: Proposed synthesis of *Arg-*Pro mimic **1.98** via Suzuki coupling strategy.

In summary, the use of commercially available and cheap cytisine as a *trans*-proline building block will be useful to quickly access to a small library of PRGPRP analogues. However, because of the external position of the 12 mer FPPRGPRPVQSV, we postulated that protein-protein interactions could be involved in the biological mechanism of our lead compound PRGPRP.

An important class of protein-protein interactions contains proline rich motifs (PRMs). A common property of these PRMs is they adopt a polyproline type II helix (PPII helix). This will be discussed in greater detail in section 1.7.

Considering the hexapeptide PRGPRP is *trans*-proline rich, we will design a peptidomimetic building block which could adopt a PPII conformation. The design of this mimetic will be discussed in section 1.7.3, following introduction to the role of the PPII helix in protein-protein interactions below.

1.7 Protein-Protein interactions involving proline rich motifs

Protein-protein interactions are essential for cellular activity.⁵³ Low affinity protein-protein interactions (PPIs) between domains of proteins and solvent-exposed peptide sequences, play an essential role in intracellular signalling. An important class of PPIs comprise proline rich motifs (PRMs) that are specifically recognised by PRM-binding domains (PRDs).⁵⁴ Several of these PRMs-PRDs interactions are associated with cellular malfunction and cancer.⁵⁴

1.7.1 The polyproline type II (PPII) helix and its structural features

An interesting property of PRMs is that they preferentially form a left-handed polyproline type II (PPII) helix. One of the main known functional roles of PPII structure is to mediate protein interactions between the PPII helical peptide ligands and their recognition domains. This left handed helix has long been known to occur in the collagen triple-helix structures and shown to frequently occur in natural polypeptides and globular proteins. ^{54,55}

The name "PPII helix" does not imply that proline is mandatory for this structure. Actually, 46% of PPII helices in folded proteins contain no proline.⁵⁴ However, overall, proline has the highest occurrence in PPII helices. In comparison to other secondary structures in folded proteins, PPII helices (**Figure 1.36**) are the fourth most abundant regular secondary structures following α -helices, β -structures and 3-(10)-helices.⁵⁴

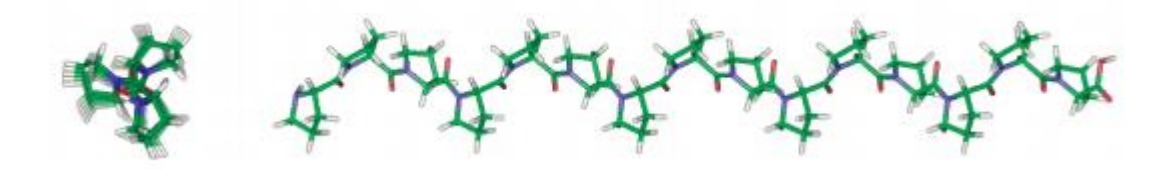


Figure 1.36: Representation of a 15-residue poly-L-proline. PPII helix contains all *trans*-residue forms. Two views are shown for clarity (Image taken from A. E. Counterman, D. E. Clemmer, *The Journal of Physical Chemistry B* **2004**, *108*, 4885-4898). ⁵⁶

The PPII conformation can be observed by CD (circular dichroism) spectroscopy, VCD (vibrational circular dichroism) and ROA (Raman optical activity). NMR spectroscopy has also been successfully used to determine this conformation. These methods are used to identify PPII helices as a predominant conformation in unfolded proteins and polypeptide chains.⁵⁷

One of the most sensitive techniques to determine secondary structure is CD spectroscopy which is a UV technique that measures the difference in absorption between left and right-handed circularly polarised light. The ideal CD spectrum for a PPII helix is illustrated in **Figure 1.37**. ⁵⁸

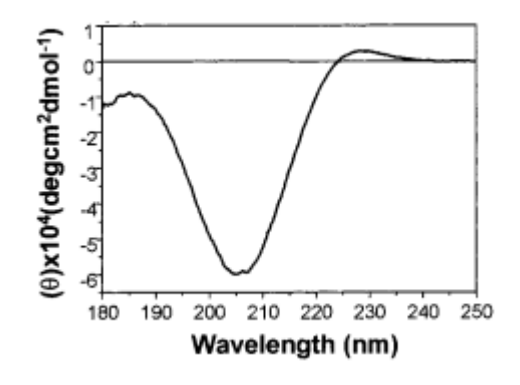
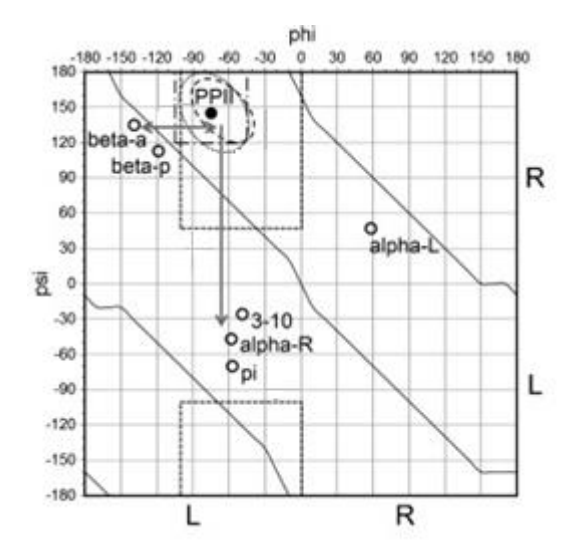


Figure 1.37: Circular dichroism spectrum of poly-*trans*-L-proline in 10 mM KPi, pH 6.9 at 2 °C (Image adapted from K. Ma, L.-s. Kan, K. Wang, *Biochemistry* **2001**, *40*, 3427-3438). ⁵⁸

A typical CD spectrum of PPII helix has a strong negative band at 206 nm and a weak positive band at 228 nm. The PPII helix has three residues per turn and ϕ (phi) and ψ (psi) angles centred around -75° and 145° as illustrated by the Ramachandran plot where comparison with other secondary structures is also shown (**Figure 1.38**). 55,59



Regions:

- R (right-handed conformation)
- L (left-handed conformation);
- beta-a (anti-parallel) and beta-p (parallel) β-structure;
- PPII, left handed PPII helix;
- 3-10, 3(10) helix;
- pi, π-helix;
- alpha-L, left handed α-helix;
- alpha-R, right handed α -helix.

Figure 1.38: Ramachandran plot representing the PPII helix and other regular periodic structures in proteins (Image adapted from A. A. Adzhubei, M. J. E. Sternberg, A. A. Makarov, *Journal of Molecular Biology* **2013**, 12, 2100-2132). 55

The main stabilising factor and hydrogen-bonding partner for the PPII conformation is water. The absence of intra- or inter-chain hydrogen bonds makes the PPII helix more flexible than α -helices and β -sheets.⁵⁴ The tendency of the PPII structure to form favourable contacts with water may be the reason why PPII helices within proteins are frequently solvent-exposed.⁵⁹

1.7.2 PPII mimics known in the literature.

Small molecule mimics of PPII are rare with distinction between the types which just stabilise the conformation by structures closely related to proline, and those which have totally different architecture. Attempts at stabilisation of PPII helices have been undertaken by replacing PRM-containing residues with conformationally restricted PPII mimetics. Only a few examples of PPII helix isoster have been described in the literature. These include a spirolactam **1.99**,⁶⁰ a functionalised sugar **1.100**⁶¹ and a vinyldiene bridged Pro-Pro mimic **1.101**⁶² (Figure **1.39**).

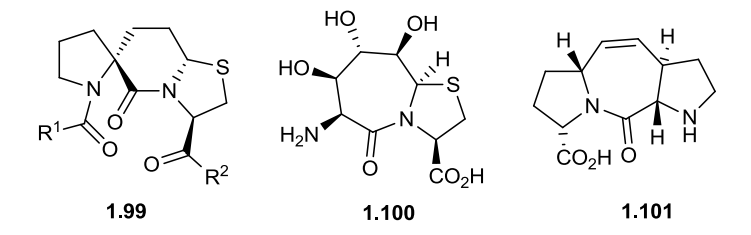


Figure 1.39: Various previously reported PPII mimetics.

1.7.2.1 Spirolactam 1.99

Witter et al.⁶⁰ described a highly constrained spirolactam *PP* (or PX) mimetic **1.99** of the PPII helix-forming PLPPLP sequence common to SH3 binding ligands. The strategy was to enhance binding at the central PLPPLP pocket with a conformationally constrained mimetic. The authors noticed that the bound conformation of the proline rich peptide PRPLPVAPG with the Src SH3 domain was different from a minimised unbound conformation of a PP-based fragment. They thought that the bound conformation could be "captured" in the constrained spirotricyclic systems (Figure 1.40). The synthetic route developed by Witter gave a mixture of diastereoisomers **1.99** (Scheme 1.18). Spirolactam **1.99** was generated from the commercially available Boc-proline **1.102**. Benzyl protection of the carboxylic acid followed by alkylation with allyl bromide gave the corresponding olefin **1.103**. Hydroboration/oxidation followed by Swern oxidation afforded aldehyde **1.104**. Hydrogenation of **1.104** and coupling with methyl ester cysteine gave **1.105**. Cyclisation to afford the desired spirolactam **1.99** was undertaken with EDCI. The overall yield was 36 % over eight steps. Direct replacement of the **PV** sequence with the tricyclic spirolactam **1.99** resulted in comparable binding affinities to reference peptides targeted for the SH3 domain of Lyn.⁶⁰

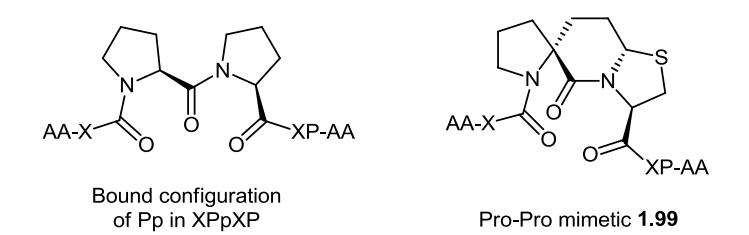


Figure 1.40: Constraining of the Pro-Pro consensus sequence (XPpXP) to mimic the bound conformation.

Reagents and conditions: a) Cs_2CO_3 , BnBr, 87%; b) LDA, allyl bromide, 65%; c) i) $BH_3 \cdot THF$, ii) KOH/H_2O_2 , 90%; d) Swern oxidation, 90%; e) H_2 , $Pd(OH)_2/C$, 90–94%; f) Cys-OMe, NaOH (aq.), 94%; g) EDCI, NMM, 85–90%.

Scheme 1.18: Synthesis of **1.99**. 60

More recently Jonhson $et~al.^{63}$ reported the synthesis and use of 5.6.5 spirotricyclic scaffolds for Pro-Pro-Pro-NH₂ peptidomimetics with the modulation of the dopamine receptor (**Figure 1.41**). Comparison of the torsion angles of **1.107** with those of a polyproline type II helix are illustrated in **Table 1.4**. Torsions angles determined by X-ray gave a relatively good PPII conformation on the Ramachadran plot where these torsions were ca. the optimal dihedral angles of the PPII helix. These results were consistent with the ones reported by Witter $et~al.^{60}$ on the use of the spirotricyclic scaffold as a potential mimic of PPII helix. No further conformational analysis were described for this mimic.

Figure 1.41: 5.6.5 spiro tricyclic lactam 1.107 designed to mimic the PPII helix.

System	Ф2	ψ ₂	Фз	ψ ₃
PPII helix	−75 (±15)°	145 (±15)°	−75 (±15)°	145 (±15)°
1.107a	-48.5	136.2	-64.3	160.5
1.107b	-50.0	148.4	-82.8	162.8

Table 1.4: Comparison of the torsion angles of **1.107a** and **1.107b** with those of a PPII helix determined from X-ray structure.⁶³

1.7.2.2 Sugar derived mimic 1.100

Tremmel and Geyer⁶¹ described the synthesis and structural analysis of a hexapeptide surrogate based on a trimer of scaffold of **1.100** displaying all characteristic features of the PPII helix. The bicyclic thiazolidinlactam **1.111** was obtained in a single step from the condensation of commercial ρ-γ-glucuronolactone **1.108** with the μ-cysteine methyl ester. The aminolysis of the lactone proceeded smoothly in a solvent mixture of water/pyridine (9:1) and the the bicylic scaffold **1.111** formed with excellent diastereoselectivity. Regioselective trifluoration of **1.111** at the α-hydroxy group position followed by azide exchange with retention of configuration followed by reduction and Boc-protection of the amino group gave the dipeptide mimic **1.100b** (**Scheme 1.19**). ^{61a} A trimer **1.112** derived from **1.100** was synthesised in order to resemble one full turn of the helix equivalent to two turns of the PPII helical amide backbone. On the other hand CD spectra of trimer **1.112** derived from **1.100** showed a strong minimum at 205 nm and the absence of the weak positive band at 228 nm. This suggests that the Ser-Pro dipeptide mimic **1.100** has singular propensity for PPII helices by NMR nevertheless CD spectroscopy did not show an ideal PPII helix conformation. ⁶¹

Reagents and conditions: a) L-Cys-OMe, H_2O/Py (9:1), 90%; b) Tf_2O , Py, CH_2Cl_2 , 89%; c) NaN_3 , DMF, 82%; d) i) H_2S , Py, H_2O , ii) Boc_2O , DIPEA, 78%.

Scheme 1.19: Synthesis of **1.100b**. 61

1.7.2.3 Tricyclic Pro-Pro mimic 1.101

Zaminer $et~al.^{62}$ designed and synthesised a tricyclic Pro-Pro mimic **1.101**. They envisioned that PPII conformation could be stabilised by a C_2 bridge between two consecutive proline residues. Their computational modelling revealed a vinyldiene bridge would adopt the desired conformation. Their synthetic approach is illustrated in **Scheme 1.20**.

Scheme 1.20: Retrosynthetic analysis of 1.101 described by Zaminer et al.⁶²

Conversion of pyroglutamic acid **1.116** to **1.117** was conducted by formation of the acyl chloride, then reduction with sodium borohydride, protection of the resulting alcohol with TPSCI and *N*-Boc protection. **1.117** was converted to the α,β -unsaturated **1.118** via α -selenation and oxidation-induced elimination using ozone. The vinyl group was introduced by 1,4-addition of a cuprate reagent to give the *trans*-pyrrolidone **1.119**. Reduction with Superhydride® gave the lactamol, which was subjected to a ionic hydrogenation to afford

1.120 in 65% over two steps. Cleavage of the silyl protecting group followed by Jones oxidation gave **1.114a** in 9% overall yield over 11 steps (**Scheme 1.21**).

Reagents and conditions: a) SOCl₂, EtOH, 99%; b) NaBH₄, LiCl, 73%; c) i) TPSCl, imidazole, 87%, ii) Boc₂O, DMAP, 89%; e) LiN(TMS)₂, PhSeCl, -78 °C, 78%; f) O₃, -78 °C, 78%; g) vinylMgBr, CuBr·SMe₂, TMSCl, -78 °C, 59%; h) LiBHEt₃, -78 °C; i) Et₃SiH, BF₃·OEt₂, -78 °C, 65% over 2 steps; j) TBAF, 89%; k) Jones reagent, acetone, RT, 2 h, 74%.

Scheme 1.21: Synthesis of fragment 1.114a.⁶²

The synthesis of fragment **1.115** began with the same starting material **1.116** (Scheme **1.22**). Intermediate **1.121** was prepared as mixture of diastereoisomers. **1.122** was then obtained by ionic allylation with allyl-TMS and $BF_3 \cdot Et_2O$. Ozonolysis of **1.122** gave **1.123** after reductive work-up. Elimination of the primary alcohol was undertaken by ozone oxidation of an intermediate o-nitrophenylselenide. Boc-removal gave a mixture of diastereoisomers which were then separated by flash column chromatograpy to afford the desired fragment **1.115a** in 15% yield overall (9 steps).

Reagents and conditions: a) $HClO_4$, tBuOAc , 72%; b) Boc_2O , DMAP, 84%; c) DIBALH, -78 oC , 93%; d) PPTS, 96%; e) $CH_2 = CHCH_2SiMe_3$, $BF_3 \cdot OEt_2$, -78 oC , 77%; f) O_3 , -78 oC , then $NaBH_4$, 87%; g) $(o-NO_2Ph)SeCN$, $P(^nBu)_3$, Py, 92%; h) O_3 , OOM; i) TMSOTf, OOM; i) OOM OOM0; i) OOM10; i) OOM10; i) OOM10; ii) OOM10; ii) OOM10; iii) OOM10; ii

Scheme 1.22: Synthesis of fragment 1.115a.62

The two advanced fragments described above (1.114a and 1.115a) were coupled to afford precursor 1.113a. Ring closing metathesis then gave the final tricyclic Pro-Pro mimic 1.101a (Scheme 1.23).

$$Boc$$
 CO_2H
 HN
 CO_2^tBu
 Boc
 CO_2^tBu
 CO_2^tBu

Reagents and conditions: a) PyBOP, DIPEA, 81%; b) 5 mol% Grubbs II, Δ, 91%.

Scheme 1.23: The final steps towards tricyclic Pro-Pro mimic 1.101a. 62

The authors⁶² demonstrated that this PPII mimetic **1.101** could be used in the area of protein-protein interactions using BioNMR. They prepared two peptides derived (**1.101**-WT and **1.101**-LL) from WT and LL with the substitution of two consecutive prolines by **1.101**. These peptides (WT and LL) are known to bind Fyn-SH3 domain which is a known domain to bind PPII motifs. The BioNMR study concluded that **1.101**-WT and **1.101**-LL showed a similar binding mode as the parent peptides WT and LL. They also determined binding constants (K_D) using ITC as illustrated in **Table 1.5**.

	WT	1.101 -WT	LL	1.101 -LL
K _D (μM)	18±5	62±13	8±2	27±4

Table 1.5: Results of the ITC measurements between peptide-ligands and Fyn-SH3.⁶² (solvent: phosphate buffer saline).

These values demonstrated a lower affinity of **1.101**-WT and **1.101**-LL in comparison to the parent peptides WT and LL, however it also demonstrated that the core motif of a PRD-binding peptide could be modified.⁶²

1.7.3 Pyroglutamate based mimic 1.125

As described above in sections 1.5.1, an important class of protein-protein interaction involves binding of a *trans*-proline rich sequence (PRM) with a recognition domain (PRD). It is well known that the PRM adopts a polyproline type II helix conformation.⁶⁴ Therefore, a mimetic of the *trans*-proline conformation found in the PPII helix would constitute a useful peptidomimetic building block for analogue synthesis of peptides involved in PRM-PRD type protein-protein interactions. To extend the scope of this project we aim to explore potential PPII mimics and their application. According to molecular dynamics simulations (AMBER and GROMOS 53A,) a residue is defined to be PPII if its dihedral angles fall within +/- 15° of the PPII geometry ($\phi = -75^{\circ}$ and $\psi = 145^{\circ}$).⁶⁴ Dr Bloodworth and Prof Whitby have designed motif **1.125** by DFT calculations to closely resemble the PPII helix conformation, with the backbone dihedral angles being within the range of theoretically determined PPII dihedral angles (**Figure 1.42**).

Figure 1.42: PPII helix indicating (a) optimal backbone dihedral angles and (b) the best candidate from DFT calculations of minimum energy conformers of small molecule candidates.

Our target, mimic **1.125a** could be synthesised from commercially available L-pyroglutamic acid **1.116** via literature methods (**Scheme 1.24**). In our retrosynthetic analysis, pyroglutamate based mimic **1.125a** could be obtained from **1.126a** via an intramolecular cyclisation. Alkene **1.127a** could be prepared from the corresponding aldehyde **1.128a** under Horner-Wadsworth-Emmons conditions. Aldehyde **1.128a** could be obtained from alcohol **1.129** using Dess-Martin oxidation. The Cbz protecting group could be introduced later in the synthesis, to aid the separation of diastereoisomers. Alcohol **1.130** could be obtained from the thiolactam **1.131** via an Eschenmoser coupling reaction. Thiolactam **1.131** could be prepared from the commercial starting material L-pyroglutamic acid **1.116**.

Scheme 1.24: Retrosynthetic approach of 1.125a

Esterification of **1.116**, followed by *N*-benzyl protection and treatment with Lawesson's reagent could afford the desired thiolactam **1.131**. In the forward synthesis, the first step described by Rapoport *et al.*⁶⁵ is the synthesis of the thiolactam **1.131** in 95% yield using Lawesson's reagent in (**Scheme 1.25**).

$$Y = \bigcap_{\substack{N \\ R^2}} CO_2R^1$$

1.132: R¹= ^tBu, R²=Bn, Y=O

1.131: R¹= ^tBu, R²= Bn, Y=S

Scheme 1.25: L-pyroglutamic derivative 1.132 and thiolactam 1.131.

Conditions of formation of the desired alkene **1.134** were optimised using triethylamine and triphenylphosphine. The distribution of product obtained is shown in **Table 1.6** by Rapoport et al.

Reactions conditions	1.131	1.137	1.132	1.134
Et ₃ N	15	10	15	30
Et ₃ N, 5 min, PPh ₃	15	/	nd	60
PPh ₃ , 5 min, Et ₃ N	2	2	5	85

Table 1.6: Optimisation of the sulphur contraction with 1.131.65

Thiolactam **1.131** was then subjected to a sulfide contraction with methylbromoacetate to yield olefin **1.134**. A closer look at this reaction revealed some mechanistic subtleties (**Scheme 1.26**). Isolation of thiolactam **1.137** suggested the formation of the intermediate ester **1.135**. Triethylamine abstracts a proton at C-4 of intermediate **1.133** instead of the desired proton abstraction from the methylene of the side chain. The isolation of further lactam **1.137** suggests also the presence of intermediate **1.136**, by hydrolysis of the latter on isolation.⁴⁵

Scheme 1.26: Revised mechanism for the alkene formation 1.134.65

According to the method of Rapoport *et al.*⁶⁵ reduction of the alkene **1.134**, results in *cis*: *trans* selectivity of 98 : 2 by catalytic hydrogenation. Then, reprotection with benzylchloroformate followed by reduction of the methyl ester affords **1.129** in good yield (**Scheme 1.27**). Scolastico

et al. 66 described the oxidation of **1.129** using Dess-Martin reagent to give the corresponding aldehyde. To form the second ring, a Horner-Emmons olefination followed by asymmetric double-bond reduction and lactam cyclisation were employed. The isolation of the two diastereoisomers **1.125a** and **1.138** has been described using flash column chromatography.

Reagents and conditions: a) i) H₂, Pd/C, ii) CbzCl, iii) LiAlH₄; b) Dess-Martin; c) i) Boc₂O, DMAP, ii) H₂, Pd/C.

Scheme 1.27: Preparation of bicyclic lactam 1.125a. 66

1.7.4 Study of protein-protein interactions using BioNMR

To validate the synthesis of pyroglutamic based mimic **1.125**, a specific protein-protein interaction of PRMs with Src-homology 3 (SH3) domain will be studied. They mediate protein-protein interactions involved in the subcellular localisation of proteins, cytoskeletal organisation and signal transduction. ⁶⁷ Several SH3 domain-mediated interactions have been described. ⁶⁸ The SH3 family binds peptides with the consensus sequence Pro-x-x-Pro. ^{68d} The proline-based motif adopts a PPII helix that is stabilised by hydrophobic interactions and sometimes by electrostatic interactions. SH3 domain-peptide ligand binding is studied by the combined use of phage display combinatorial libraries, NMR and X-ray crystallography. ⁶⁹ The SH3 domain will be employed for study of binding to our peptidomimetic ligand for several reasons. SH3 domains are small in size, only 60 amino acids, which provides them with very favourable spectroscopic properties for NMR analysis and have high stability (**Figure 1.43**).



Figure 1.43: 3D structure of Fyn SH3 wild-type domain (Image taken from PDB (1NYG)).

Morton *et al.*⁷⁰ have described the solution phase structure of the Fyn SH3 domain (**Figure 1.44**) and compared it with other known SH3 structures, in particular the structures of the Fyn-SH3 domain determined by X-ray crystallography.⁷¹ We have decided to work with Fyn-SH3 domains because of the known data and the high quality of this solution phase structure available at the PDB.⁷⁰ **Table 1.7** presents a list of Fyn-SH3 domain ligands with the corresponding K_D value for binding to given peptide sequences.

Name	Sequence	K _D (μM)	Technique* [¶]
"I"c+f' ⁷³	VSLARRPLPPLP	0.4	Fluo.*
"l"c+f ⁷⁴	VSLARRPLPPLPGGK	0.6	Fluo.*
"II"c+f ⁷⁴	KGGGAAPPLPPNPRL	1.7	Fluo.*
p85α2 ⁷⁵	PPRPLPVAP	4.4	Fluo.*
p85α2 ⁷⁷	KPRPPRPLPVA	10	Fluo.*
Nef ⁷⁵	TPPVPPRPM	12	Fluo.*
P2L ⁷⁶	PPRPLPVAPGSSKT	16	ITC*
Sos1-4 ⁷⁷	HSIAGPPVPPR	20	Fluo.*
"I"core ⁷⁴	RPLPPLPGGG	25	Fluo.*
3BP2 ⁷⁷	PPAYPPPPVP	34	Fluo.*
3PB1 ⁷⁷	RAPTMPPPLPP	34	Fluo.*
Sos1-3 ⁷⁷	PPESPPLLPPR	48	Fluo.*
FAK3A ⁷⁸	AAAARALPSIPKL	68	ITC*
p85α1 ⁷⁷	NERQPAPALPPKG	83	Fluo.*
"II"c ⁷⁴	KGGGAAPPLPPR	144	Fluo.*
Nef ⁷⁹	PVRPQVPLRPPMT	202	ITC*
p85p2 ⁷⁰	PPRPLPVA PGSSKT	50	NMR [¶]
p85p1 ⁷⁰	KKISPPTPKPRPPR	3000	NMR [¶]

Table 1.7: List of ligands for the Fyn SH3 domain. *Fluo and ITC meaning: Fluorescence and isothermal titration calorimetry. *NMR Conditions: 500 or 600 MHz NMR in phosphate buffer (pH 6.0).

Morton $et~al.^{70}$ described a study of the structural basis for the interaction of the SH3 domains of Fyn with ligands sequences. It has been suggested that residues 80-104 of the p85 α subunit of PI3' kinase interact with the SH3 domain $in~vivo.^{71}$ Two synthetic peptides spanning this sequence were constructed. The proline-rich p85p1 corresponds to residues 80-93 (KKISPPTPKPRPR) and p85p2 (PPRPLPVAPGSSKT) corresponds to residues 91-104. The NMR experiments conducted by Morton $et~al.^{70}$ to determine affinities of peptides with SH3 domains were quiet low ($K_D = 50~\mu M$) and intermolecular nOes were observed only for p85p2 (Table 1.8, Figure 1.44). This table shows the important amino acids of p85p2 that interact with Fyn-SH3 by nOes.

p85p2 atoms	Fyn SH3 atoms
Arg3 CβH, CγH	Trp51 C(2)H, N(1)H
Leu5 CαH	Trp51 N(1)H, C(7)H
Pro6 CδH	Trp51 N(1)H, C(7)H
Pro6 CγH	Tyr69 C(2, 6)H, C(3, 5)H
Ala8 CβH	Tyr23 C(2,6)H, Asn55 C CδH, Tyr69 C(2,6)H
Pro9 CδH	Tyr59 C(2,6)H

Table 1.8: Summary of the nOe peaks observed between the Fyn-SH3 domain and peptide p85p2.⁷⁰

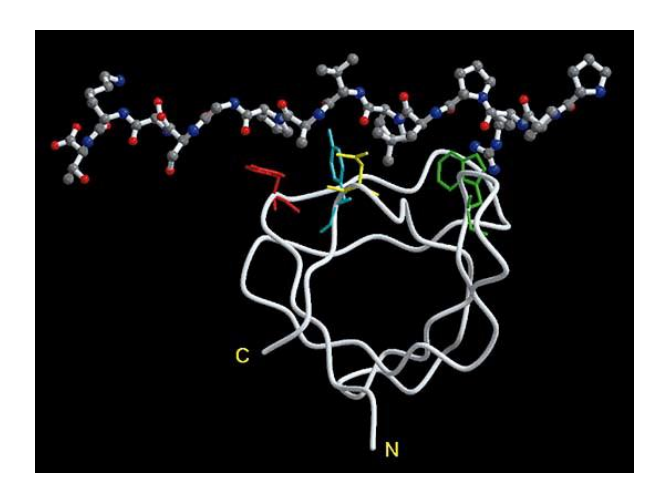


Figure 1.44: Structure of the Fyn-SH3-p85p2 complex (Image taken from C. J. Morton, D. J. R. Pugh, E. L. J. Brown, J. D. Kahmann, D. A. C. Renzoni, I. D. Campbell, *Structure* **1996**, *4*, 705-714). The protein is shown as a backbone worm, with residues displaying nOe crosspeaks with the peptide shown as sticks. They are Tyr91 (red), Tyr137 (cyan), Asn136 (yellow) and Trp119 (green).

p85p2 can be represented as: Pro-Pro-Arg-Pro-Leu-Pro-Val-Ala-Pro-Gly-Ser-Ser-Lys-Thr where coloured amino acids are the important ones for the binding with Fyn-SH3. This peptide sequence does adopt a PPII conformation. It was decided to reduce the size of this sequence to the following 8-mer: *N*-Ac-Arg-Pro-Leu-Pro-Val-Ala-Pro-Gly-NH₂ **1.139** which includes all of the key residues. The solubility of the 8mer might be an issue so the extra amino acid Gly will be

conserved. The project aims to replace an Xaa-Pro dipeptide by the constrained *trans*-proline mimic **1.125** (Figure **1.45**) being designed to adopt a PPII conformation.

Figure 1.45: Constrained trans-proline dipeptide mimic (1.125) and trans-proline Pro.

The synthesis of the parent 8mer will be undertaken using solid-phase synthesis. Using the same procedure of synthesis, another 3 analogues will be targeted with the sequence described as follows:

- N-Ac-Arg-Pro-Leu-Pro-Val-Ala-Pro-Gly-NH₂ (parent 8mer 1.139)
- *N*-Ac-Arg-Pro-Leu-Pro-Val-1.125-Gly-NH₂ (analogue 1.140)
- *N*-Ac-Arg-Pro-1.125-Val-Ala-Pro-Gly-NH₂ (analogue 1.141)
- *N*-Ac-**Arg**-Pro-**1.125**-Val-**1.125**-Gly-NH₂ (analogue **1.142**).

The affinity of interaction between the SH3 domain and the four synthetic peptides will be studied by BioNMR. Binding properties of peptides **1.139**, **1.140**, **1.141** and **1.142** will be then compared to results obtained by Morton *et al*.⁷⁰

It is a great advantage for the analysis of a protein by NMR, to introduce the NMR active stable isotopes ¹³C and ¹⁵N. With the introduction of these two spin active nuclei the spins in a protein are almost all connected by one-bond couplings, and this facilitates the structural assignment and the subsequent binding study. The preparation of proteins enriched with the two nuclei are accomplished by heterologous expression of the protein in micro-organisms grown in minimal growth medium where the carbon source is fully ¹³C labelled and the nitrogen source is fully ¹⁵N labelled.⁷⁰

1.8 Summary of project objectives

- 1. We aim to develop *trans*-proline mimics using cytisine **1.67** as building block. Synthesis and clonogenic assay of analogues of the functional peptide PRGPRP will be performed.
- 2. We aim to synthesise a pyroglutamate-derived constrained *trans*-proline mimic **1.125** which bears a PPII conformation. Synthesis and analysis of restricted sequence mimics will be investigated in a specific protein-protein interaction (PPII helix-SH3 domain binding) and in the functional peptide PRGPRP.

2. PRGPRP analogues based on cytisine & clonogenic assay

Solution phase synthesis is suitable for preparing peptides on a large scale. Our objectives included the preparation of the protected hexapeptide *N*-Ac-Pro-Arg(NO₂)-Gly-Pro-Arg(NO₂)-Pro-OMe **2.1**, this analogue will be used in the clonogenic assay as a positive control. Previous work in the group indicated *N*-Ac-Pro-Arg(NO₂)-Gly-Pro-Arg(NO₂)-Pro-OMe **2.1** may exhibit a similar, selective anticancer profile to *N*-Ac-Pro-Arg(H)-Gly-Pro-Arg(H)-Pro-NH₂ **2.2** (see chapter 1, PRGPRP). We also wished to verify this, confirming the suitability of *N*-Ac-Pro-Arg(NO₂)-Gly-Pro-Arg(NO₂)-Pro-OMe **2.1** as a positive control. Hexapeptide **2.1** was chosen for the assay since its synthesis by solution phase was achievable whereas its deprotected analogue **2.2** proved troublesome at the *C*-terminus (amidolysis) which we have confirmed and described herein. This chapter will detail the synthesis of **2.1**.

2.1 Synthesis of N-Ac-Pro-Arg(NO₂)-Gly-Pro-Arg(NO₂)-Pro-OMe 2.1

The hexapeptide **2.1** was synthesised accordingly to standard literature methods⁸⁰ and the most efficient route was found to be via coupling of two tripeptide fragments, **2.3a** and **2.4a**. This convergent method allows access to larger amounts of material overall than would be achieved by stepwise coupling. From commercially available *N*-Boc-L-Arg(NO₂)-OH **2.5**, H-Gly-OMe **2.6** and *N*-Boc-L-Pro-OH **2.7**, tripeptide **2.3a** was obtained in 29% yield over three steps. Following a similar procedure tripeptide **2.4a** was obtained in 19% yield over three steps (**Scheme 2.1**).

Chapter 2 PRGPRP analogues based on Cytisine & clonogenic assay

Reagents and conditions: a) HOBt (1.2 equiv.), DCC (1.0 equiv.), DIPEA (4.8 equiv.), DMF, RT, 16 h, 54 %; b) i) 20% TFA v/v in CH_2Cl_2 , ii) N-Boc-L-Pro-OH **2.7** (1.0 equiv.), HOBt (1.2 equiv.), DCC (1.0 equiv.), DIPEA (4.8 equiv.), DMF, RT, 16 h, 35% over 2 steps.

Reagents and conditions: a) HOBt (1.2 equiv.), DCC (1.0 equiv.), DIPEA (4.8 equiv.), DMF, RT, 16 h, 78%; b) i) 20% TFA v/v in CH_2Cl_2 , ii) N-Boc-L-Pro-OH **2.7** (1.0 equiv.), HOBt (1.2 equiv.), DCC (1.0 equiv.), DIPEA (4.8 equiv.), DMF, RT, 16 h, 36% over 2 steps.

Scheme 2.1: Synthesis of tripeptides 2.3a and 2.4a.

With the key intermediates in hand, we were in a position to undertake the coupling reaction to form hexapeptide **2.11**. This required deprotection of **2.4a** and hydrolysis of the methyl ester of **2.3a**.

Hydrolysis of the methyl ester of **2.3a** was undertaken using **1.0** equiv of **1** M aq. NaOH in ethanol, to provide tripeptide precursor **2.3b** which was used in the next step without further purification. Tripeptide, H.Pro-Arg(NO₂)-Pro-OMe, **2.4b** was synthesised from the *N*-Boc deprotection of **2.4a**. Compound **2.11**, *N*-Boc-Pro-Arg(NO₂)-Gly-Pro-Arg(NO₂)-Pro-OMe, was then synthesised via a coupling reaction between the tripeptide precursors **2.3b** and **2.4b** (Scheme **2.2**).

N-terminus modification of N-Boc-Pro-Arg(NO_2)-Gly-Pro-Arg(NO_2)-Pro-OMe **2.11** was undertaken by N-Boc deprotection of hexapeptide **2.11** using TFA in dichloromethane to give

the free *N*-terminus peptide in high yield. Following this, *N*-terminus acetylation, catalysed by DMAP using Ac_2O , afforded the acetylated compound **2.1** in 60% yield (**Scheme 2.2**).

Reagents and conditions: a) HOBt (1.2 equiv.), DCC (1.0 equiv.), DIPEA (4.8 equiv.), DMF, RT, 16 h, 40%; b) i) 20% TFA v/v in CH_2Cl_2 , ii) Ac_2O , DMAP, 80%.

Scheme 2.2: Synthesis of *N*-Ac-Pro-Arg(NO₂)-Gly-Pro-Arg(NO₂)-Pro-OMe **2.1**.

We then went on to target our lead compound N-Ac-Pro-Arg(H)-Gly-Pro-Arg(H)-Pro-NH₂ **2.2** as described previously by Warenius *et al.*³⁹ to undertake the biological assay. Two steps from **2.1** were required: the C-terminus amide formation and deprotection of the guanidine side chains.

Conversion of the methyl ester of **2.1** to the terminal amide was attempted via two different routes. The first included using a 7 M solution of ammonia in methanol for two hours at 0 $^{\circ}$ C. The reaction mixture was warmed to room temperature and stirred for 16 h. After concentration under reduced pressure the crude residue was obtained as a pale yellow oil.

The second method was based on the methodology of Ley *et al.*⁸¹ In their synthesis, magnesium nitride was used with a proton source (methanol, ethanol) to generate ammonia *in situ* (**Scheme 2.3**).

Chapter 2 PRGPRP analogues based on Cytisine & clonogenic assay

$$Mg_3N_2 + 6 \text{ MeOH} \longrightarrow 2 \text{ NH}_3 + Mg(OMe)_2$$

$$Q \longrightarrow Q \longrightarrow Q$$

$$R^1 = \text{alkyl, aryl, vinyl}$$

$$R^2 = \text{Me, Et, } ^t\text{Pr, } ^t\text{Bu}$$

Scheme 2.3: Preparation of primary amides using magnesium nitride by Ley et al.81

The crude materials from both experiments were precipitated using a mixture of MeOH and Et_2O . The ¹H NMR was encouraging showing the disappearance of the methyl singlet however very broad signals in DMSO- d_6 and MeOD- d_4 (possible hydrogen bonding with water in NMR solvents) were observed. Disappointingly the MS (ESI) results were inconclusive, no molecular ion was observed, and therefore we could not be fully certain that we formed the desired analogue **2.2**.

2.1.1 Clonogenic assay of N-Ac-Pro-Arg(NO₂)-Gly-Pro-Arg(NO₂)-Pro-OMe 2.1

Due to the inconclusive results previously described we reassessed our strategy in the hope that we could use hexapeptide **2.1** as the positive control in the assay rather than the capricious hexapeptide **2.2**. Compound **2.1** was successfully synthesised by solution phase peptide synthesis. Structural characterisation was confirmed by NMR, mass spectrometry and purity by HPLC. The clonogenic assay of **2.1** against RT112 bladder cancer and MRC5-hTERT fibroblast cells (evaluation of toxicity) was next carried out.

Both cells lines were grown in 500 μ L of tissue culture medium for the control experiment. For RT112 bladder cancer cells the culture medium used was Ham's F-12 medium and for MRC5-hTERT the culture medium used was DMEM. A solution containing **2.1** (2.1 mg/500 μ L) was prepared as described in section 7.7 at 5 mM. Plates were kept in an incubator at 37 °C, 5-10% CO₂ for 29 days (**Figure 2.1**).

The following images show the progress of the clonogenic assay over 29 days.

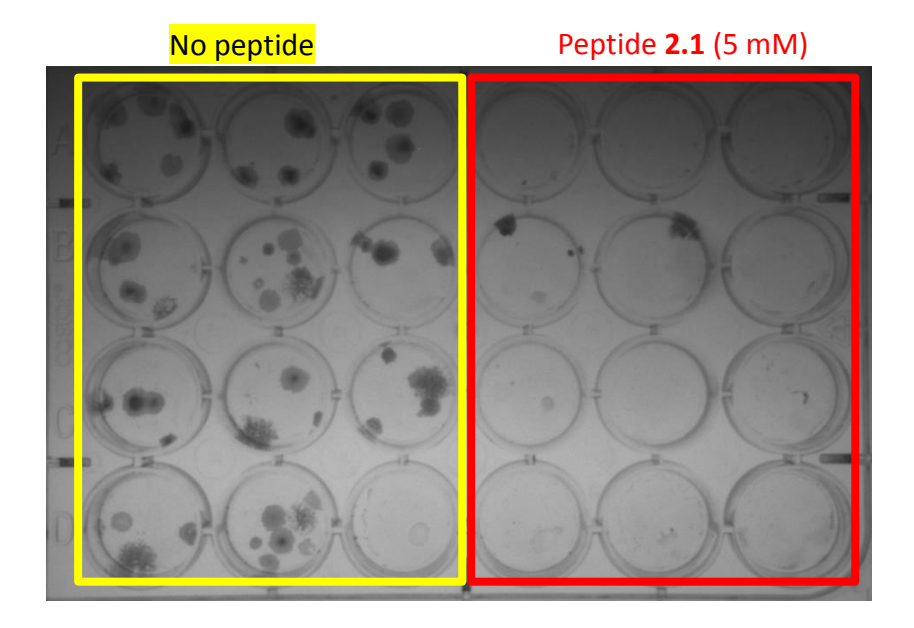


Figure 2.1: Pictures of colony formation of RT112 bladder cancer cells on day 29.

Bladder cells were trypsinised and seeded at 10 cells in each well dish of 24-well plate. The cells were allowed to grow in medium for the control experiment (500 μ L of final volume). The anticancer activity was studied when cells were exposed with a 5 mM solution of peptide **2.1**. Plates were kept at 37 °C in 5% CO₂ before staining with Giemsa's stain on day 29.

Morphological appearance of RT112 and MRC5-hTERT survival cells are illustrated in **Figures 2.2** and **2.3**.

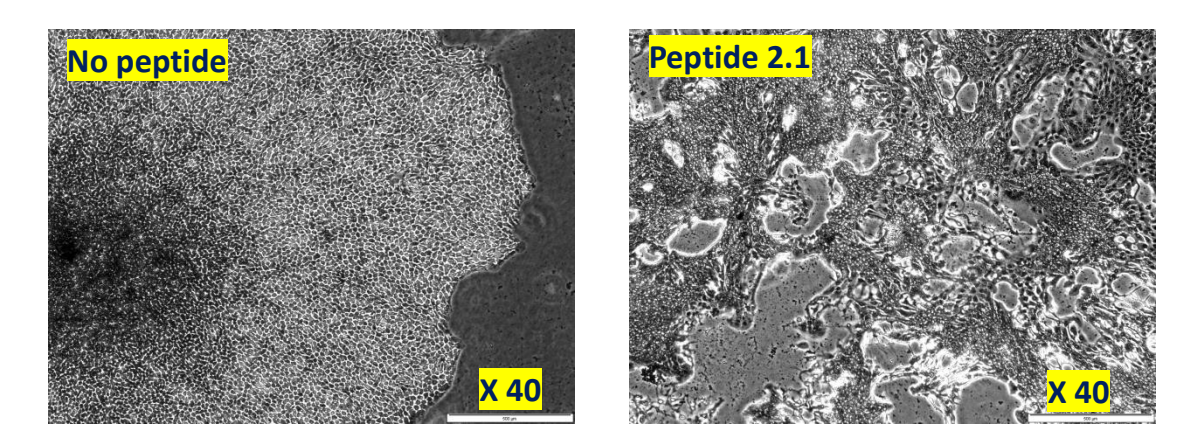
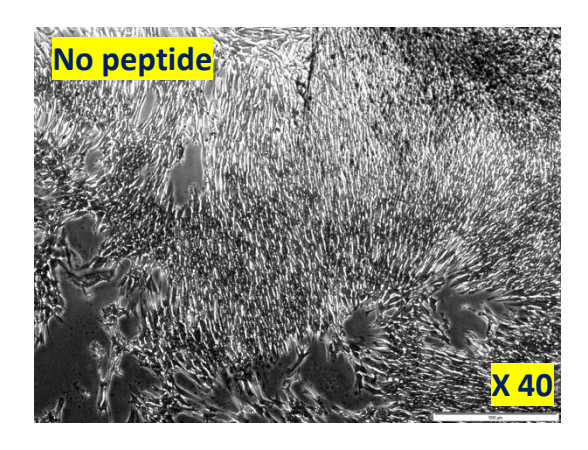


Figure 2.2: Morphological appearance of RT112 survival cells exposed to a 5 mM solution of synthetic peptide **2.1**, on day 29. Only two survival colonies were observed on day 29 which were, in fact, found to be debris of cells.



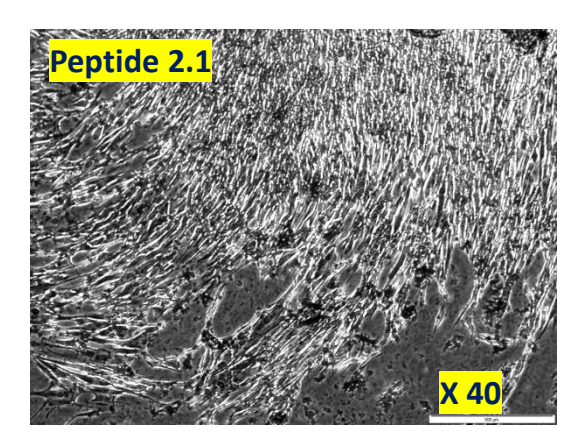


Figure 2.3: Morphological appearance of MRC5-hTERT survival cells exposed to a 5 mM solution of synthetic peptide **2.1**, on day 29. Normal fibroblasts were trypsinised and seeded at 250 cells in each well dish of 24-well plate. The cells were grown in DMEM medium for the control experiment (500 μ L of final volume). Plates were kept at 37 °C in 5% CO₂ before staining with Giemsa's stain on day 29.

The conclusion drawn from these assays are as follows. Peptide **2.1**, nitroprotected on the guanidine side chain and with a methyl ester at the *C*-terminus, showed excellent anticancer activity against RT112 bladder cancer cells (**Figures 2.1** and **2.2**). Only two survival colonies were observed which, under the microscope showed cell debris only (**Figure 2.2**). Also, peptide **2.1** did not kill normal fibroblast cell lines (**Figure 2.3**). Biological assays on human bladder cancer cells demonstrated excellent anticancer activity of **2.1** on RT112 without killing normal fibroblasts. These results were similar to those reported in the group and consistent with hexapeptide **2.2** reported by Warenius *et al.*³⁹ Protected hexapeptide **2.1** was thus selected to be our positive control peptide for the assay of peptidomimetic analogues of PRGPRP against RT112 and MRC5-hTERT cell lines.

2.2 *PRGPRP analogue 1.83 based on cytisine 1.67

2.2.1 Synthesis of 1.83

(–)-Cytisine **1.67** was extracted from *Cytisus laburnum* seeds using an NH_4OH (35% aq.), MeOH, and CH_2Cl_2 extraction and was obtained in 1.4% yield (w/w %).^{47b} The synthesis of *N*-methyl-6 α -carboxy-cytisine **2.14** was then undertaken following the methods developed by the Rouden group (**Scheme 2.4**).⁴⁹ Using benzyl

chloroformate and triethylamine, benzoylation of cytisine **1.67** gave *N*-benzoxycytisine **2.12** in 71% yield, without optimisation. The initial N–C migration reactions⁴⁹ were then undertaken on *N*-benzoxy-cytisine **2.12**. A 35% yield was obtained for 6α -benzoxy-cytisine **2.13**. Reductive methylation using formaldehyde and formic acid⁸² gave *N*-methyl- 6α -benzoxy-cytisine **1.86** in 83% yield. Hydrolysis of this compound, by catalytic hydrogenolysis in the presence of Pd/C, gave *N*-methyl- 6α -carboxycytisine **2.14** in 84% yield (**Scheme 2.4**).

Reagents and conditions: a) Et_3N , CH_2Cl_2 , benzylchloroformate, RT, 16 h, 71%; b) ⁿBuLi, DIPEA, LiCl, -20 °C, then THF, **2.12**, -78 °C, 4 h then H_2O , 35%; c) formaldehyde, formic acid, RT, 4 h, 83%; d) H_2 , Pd/C (10%), MeOH, 84%.

Scheme 2.4: Synthesis of *N*-methyl- 6α -carboxy-cytisine **2.14**.

The coupling reaction between *N*-methyl- 6α -carboxy-cytisine **2.14** and the dipeptide H.Arg(NO₂)Gly-OMe **2.8b** was optimised to afford **2.15** in 44% yield (**Scheme 2.5**).

Reagents and conditions: a) H.Arg(NO₂)Gly-OMe 2.8b, HBTU, DIPEA, DMF, 16 h, 44%.

Scheme 2.5: Optimised synthesis of **2.15**.

Dipeptide H.Arg(NO_2)-Gly-OMe **2.8b** was prepared using TFA in DCM from previously synthesised *N*-Boc-Arg(NO_2)-Gly-OMe **2.8**. To optimise the reaction; screening of peptide

coupling reagents was undertaken (**Table 2.1**). These included phosphonium reagents, uronium salts and carbodiimide reagents. Using PyBop the desired product **2.15** was obtained in 6% yield but the reaction was not complete after 2 days. Another attempt was undertaken using HOBt and DCC and the desired product **2.15** was isolated in 15% yield after 16 h. Three further attempts were undertaken using HBTU, HATU and PyBrop. After attempted purification by flash column chromatography none of **2.15** was isolated. However with HBTU and HATU, **2.15** was formed in 44% and 26% yield respectively. The carboxy group at position 6 on cytisine is sterically hindered. The presence of an extra alkyl group at $C\alpha$ significantly restricts the accessible conformational space in α,α -disubstituted amino acids; this forces the chain to bend in peptides containing these sterically hindered amino acids. This might explain the observed results.

Counting reagents	H Arg(NO)Chy OMa (aguiy)	2.15 Isolated	
Coupling reagents	H.Arg(NO₂)Gly-OMe (equiv.)	Yield (%)	
PyBop, DIPEA	1.5	6 ^a	
HOBt, DCC, DIPEA	1.1	15 ^b	
PyBrop, DIPEA	1.5	No reaction ^c	
HBTU, DIPEA	1.5	44 ^d	
HATU, DIPEA	1.5	26 ^e	

Reactions (a-e) were undertaken under argon atmosphere. Addition of the H.Arg(NO₂)Gly-OMe was performed at 0 $^{\circ}$ C. Then the reaction mixture was stirred at room temperature for 16 h. a,b,d,e Residual lost yield attributable to starting material recovery. c Lost yield attributable to byproducts.

Table 2.1: Screening of coupling reagents for the coupling reaction between 2.14 and 2.8b.

The next step was hydrolysis of the methyl ester on tripeptide mimic **2.15** using a solution of NaOH 1 M in ethanol; no racemisation was observed by 1 H NMR, the doublet (d, J = 7.0 Hz) observed at position 6 was still present. N-Deprotection of the tripeptide N-Boc-Pro-Arg(NO₂)-Pro-OMe **2.4a** was undertaken using a solution of TFA in $CH_{2}CI_{2}$ to give H.Pro-Arg(NO₂)-Pro-OMe **2.4b**. The coupling reaction of the two tripeptide derivatives **2.15b** and **2.4b** was then undertaken using HOBt and DCC (~100 mg). The first attempt gave one impure fraction which was isolated after flushing the column chromatography with MeOH and water. It was precipated using $CH_{2}CI_{2}$, MeOH and $Et_{2}O$. By 1 H NMR it was not possible to clearly identify the desired product. Moreover, the characteristic peak of the methyl ester (singlet) did not integrate correctly (**Scheme 2.6**). Another attempt was made successfully using PyBop as

Chapter 2 PRGPRP analogues based on cytisine & clonogenic assay

coupling reagent to facilitate the purification, compared to HOBt, DCC by column chromatography. The desired product **2.16** was isolated after column chromatography using $CH_2Cl_2/MeOH/NH_4OH$ (1% of 35% aq.) followed by reverse phase HPLC ($H_2O/CH_3CN/TFA$ (0.1%)) in 15% yield.

Reagents and conditions: a) NaOH 1 M in EtOH, RT, 16 h, quant.; b) H.Pro-Arg(NO₂)-Pro-OMe **2.4b**, HOBt, DCC, DIPEA, DMF; c) H.Pro-Arg(NO₂)-Pro-OMe **2.4b**, PyBop, DIPEA, DMF, 15%.

Scheme 2.6: Synthesis of **2.14**-Arg(NO₂)-Gly-Pro-Arg(NO₂)-Pro-OMe **2.16**.

C-Terminal amidolysis using ammonia in methanol described in section 2.1 was undertaken on **2.16**. Using a solution of ammonia in methanol, starting material was consumed after seven days (**Scheme 2.7**). Precipitation using a mixture of MeOH/Et₂O gave a pale yellow solid which was analysed by reverse phase HPLC (H_2O/CH_3CN) to evaluate the purity (**Figure 2.4**). These chromatograms confirmed the previous difficulties observed with hexapeptide **2.1** for this transformation.

Chapter 2 PRGPRP analogues based on Cytisine & clonogenic assay

Reagents and conditions: a) NH₃ in MeOH (7 M).

Scheme 2.7: Synthesis of 2.17.

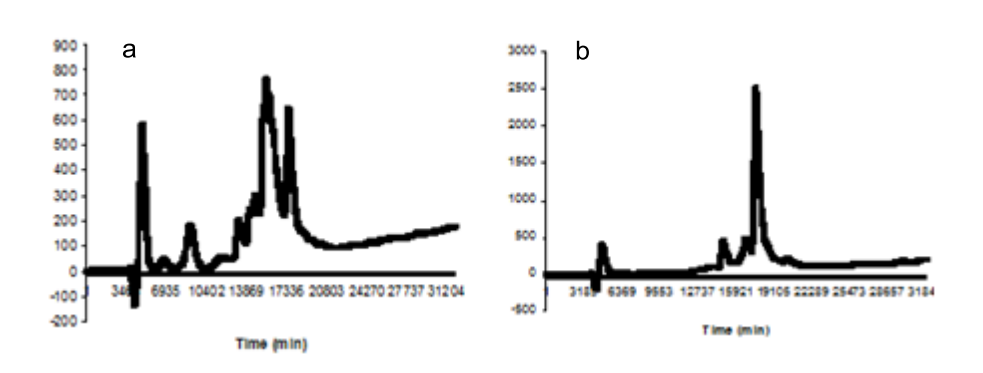


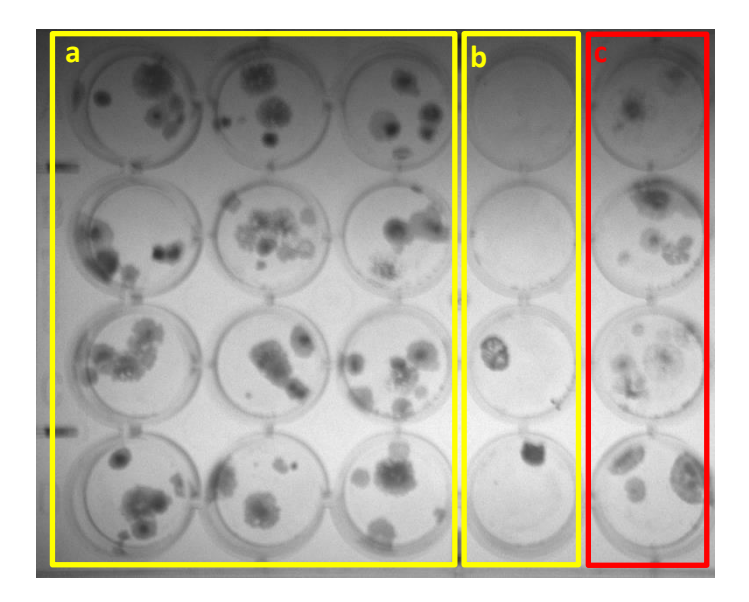
Figure 2.4: Chromatograms of: (a) the crude product **2.14**-Arg(NO₂)-Gly-Pro-Arg(NO₂)-Pro-NH₂ **2.17**, (b) fraction isolated suggesting desired peptide **2.17** by MS using RP-HPLC.

From the crude product mixture we managed to isolate one fraction by RP-HPLC confirmed by mass spectrometry to be the desired hexapeptide **2.17** (**Figure 2.4**). The conditions of elution were H_2O/CH_3CN with 1% NH_4OH (35% aq.) (0 \rightarrow 100%). The desired product **2.17** was obtained in 30% yield. The purity of intermediate **2.17** was evaluated around 80-85%. Hydrogenation of **2.17** was undertaken to cleave the nitro groups on the arginine side chains. Only 3 mg were isolated after precipitation. LCMS confirmed the formation of the desired peptide **1.83** but two undeterminated impurities were still present. Due to the poor yield, the purity obtained and to retain consistency with our positive control peptide **2.1**, we decided to expose the **2.14**-Arg(NO_2)-Gly-Pro-Arg(NO_2)-Pro-OMe **2.16** to RT112 bladder cancer cells.

2.2.2 Clonogenic assay of 2.14-Arg(NO₂)-Gly-Pro-Arg(NO₂)-Pro-OMe 2.16

Peptide **2.16** (53 mg) was prepared successfully using solution phase synthesis. The biological activities of **2.16** were investigated by clonogenic assay against RT112 bladder cancer cells in comparison to the positive control N-Ac-Pro-Arg(NO_2)-Gly-Pro-Arg(NO_2)-Pro-OMe **2.1**.

RT112 cells were grown in a tissue culture medium 500 μ L of final volume per well dish for the control experiment (without peptide). The cells were exposed to a 5 mM solution of *N*-Ac-Pro-Arg(NO₂)-Gly-Pro-Arg(NO₂)-Pro-OMe **2.1** as a positive control experiment and a 5 mM solution of **2.16** for determining anticancer activities for this analogue (**Figure 2.5**).



a) Control wells (no peptide); b) Positive control wells (compound 2.1, 5 mM); c) Compound 2.16 (5 mM).

Figure 2.5: Pictures of colony formation of RT112 bladder cancer cells on day 29. Bladder cells were trypsinised and seeded at 10 cells in each well dish of 24-well plate. The cells were allowed to grow in medium for control experiment (500 μ L of final volume). The anticancer activity was performed when cells were exposed with 5 mM of peptide **2.16**. Plates were kept at 37 °C in 5% CO₂ before staining with Giemsa's stain on day 29.

The conclusion of this assay is that RT112 bladder cancer cells treated with peptide **2.16** demonstrated that cancer colonies appeared after 29 days, which were comparable to the ones observed for the control experiment without peptide. This biological assay suggested that peptide **2.16** did not show any anticancer activity against RT112. (–)-Cytisine derivative **2.14** in

this case is not a suitable peptidomimetic. It could be related to the sterics/ability to bind to the target or the cell-permeability.

2.3 PR*G*PRP 1.84 and PRGP*R*P 1.85 analogues based on cytisine.

In order to prepare the other two analogues PR*G*PRP 1.84 and PRGP*R*P 1.85 (section 1.4.3) using cytisine as a building block further functionalisation of cytisine was developed including a functionalisation at the position C-9 to form a Gly-trans-Pro mimic and a further functionalisation at the position C-11 to afford a Arg-trans-Pro mimic. This work was carried out at an earlier stage (before assays results given in section 2.2.2) and before we were aware that cytisine was not a suitable peptidomimetic in this context.

2.3.1 Aromatic nitration: Standard Nitration Conditions (H₂SO₄, HNO₃)

Using acidic conditions for nitration of cytisine **1.67** described, by the Rouden group,^{47b} the C-9 nitro and C-11 nitro compounds **2.18** and **2.19** were prepared. After attempting this electrophilic nitration, only a 5% w/w yield was obtained. NMR analysis of the crude material also showed that the benzoyl ester had been hydrolysed, where the peaks representing the benzoyl group were missing (**Scheme 2.7**).

Reagents and conditions: a) H₂SO₄, HNO₃, 5%.

Scheme 2.7: Attempted synthesis of 9-nitro-*N*-methyl- 6α -carboxy-cytisine **2.18**.

In order to avoid the benzoyl deprotection encountered above, we decided to attempt the nitration via the formation of a nitronium ion using nitrate salts and trifluoroacetic anhydride.⁸³

2.3.2 Aromatic nitration: an Organic Approach

This procedure forms the required nitronium ion species in $situ^{83}$ allowing an electrophilic attack on the pyridone ring. The use of NH_4NO_3 has been shown to have short reaction time, alongside good yields. Reactions with excess of NH_4NO_3 and $(CF_3CO)_2O$ were undertaken to optimize the conditions of nitration and monitored by TLC (**Scheme 2.8**).

Reagents and conditions: a) NH₄NO₃, TFAA.

Scheme 2.8: Synthesis of 9-nitro-*N*-methyl- 6α -carboxy-cytisine **2.18**.

The best compromise to form the unique 9-nitro product **2.18** was to use 2.5 equivalents of NH_4NO_3 using the same ratio of TFAA (36%). The reaction was not completed using 2.5 equivalents, and at around 3 equivalents, a mixture of the 9-nitro-*N*-methyl-6 α -carboxy-cytisine **2.18** and 11-nitro-*N*-methyl-6 α -carboxy-cytisine **2.19** was obtained which could not be separated by flash chromatography. ¹H NMR analysis of these products **2.18** and **2.19** showed characteristic signals (**Table 2.2**). The product of nitration at the position C-9 was formed using 2.5 equivalents of NH_4NO_3 in 36% yield on a 300 mg scale of starting material **1.86**.

nitro-N-benzoxy-cytisine	¹ H NMR signals (CDCl ₃)
2.18: O ₂ N ₉ OBn	H ₁₀ : δ 8.32 (ppm) (d, $J = 7.9$ Hz) H ₁₁ : δ 6.11 (ppm) (d, $J = 7.9$ Hz)
2.19: 9 N N N N N N N N N N N N N N N N N N	H ₁₀ : δ 8.15 (ppm) (d, $J = 8.0 \text{ Hz}$) H ₉ : δ 6.41 (ppm) (d, $J = 8.0 \text{ Hz}$)

Table 2.2: NMR features of 9-nitro-benzoxy-cytisine **2.18** and 11-nitro-benzoxy-cytisine **2.19** based on literature precedents.^{47b}

Chapter 2 PRGPRP analogues based on Cytisine & clonogenic assay

Thinking that, in our hands, the unique 9-nitro compound **2.18** was only formed, hydrogenation of **2.18** was performed and gave surprisingly an inseparable mixture of product **2.14** and the desired 9-amino-*N*-carboxy-cytisine **1.89** (Scheme **2.9**). This showed that the 9-nitro product **2.18** was contaminated with **1.86**.

O₂N
$$\xrightarrow{O}$$
 OBn \xrightarrow{A} \xrightarrow{A}

Reagents and conditions: a) H₂, Pd/C, MeOH, 76%.

Scheme 2.9: Hydrogenation of 2.18 giving an unexpected mixture of 1.89 and 2.14 (ratio 1:1).

Since the reaction resulted in a mixture of **1.89** and **2.14**, and none of classical methods of purification were successful in the isolation of the desired 9-amino- 6α -carboxy cytisine **1.89** in its pure form, another method of nitration was performed using: HNO₃, Ac₂O.⁸⁴ The following **Table 2.3** summarises attempts made, using these conditions.

Reaction time	equiv. of HNO ₃	2.18 Isolated Yield (%)
30 min	3.0	Mixture of 2.18 and 2.19
30 min	1.2	6%
4 h	1.2	18%
> 4h	1.2	7%

Table 2.3: Attempted optimisation of nitration of 1.86 using HNO₃, Ac₂O.

Also, in each case, repeated column chromatography was necessary to obtain the desired product **2.18** in pure form. The conditions of purification were hexane/ethyl acetate (1:1) + 5% MeOH + 1% NH₄OH (37% aq.) then $CH_2Cl_2/MeOH$ (98:2). Column chromatography failed to separate 9-nitro **2.18** and 11-nitro **2.19**. Optimisation was then undertaken to obtain 9-nitro **2.18** compound only. The reaction proved to be highly troublesome. The best yield obtained was a poor 18% (**Table 2.3**). In order to drive the reaction to completion, we added an excess of HNO_3 , disappointingly the selectivity dropped with the formation of the 11-nitro adduct **2.19**.

At this stage it was crucial to obtain the 9-nitro **2.18** in its pure form prior to the hydrogenation since the free amino acid **1.89** (Scheme **2.9**) is impossible to purify via standard purification techniques due to its high polarity. 9-Amino compound **1.89** was obtained in 76% yield in its pure form prior to these conditions of nitration.

2.3.3 Towards the synthesis of 9-nitro-N-methyl-6 α-benzoxy-cytisine 2.18

At this stage, we had to reassess our route. Due to the poor yield and purity obtained or the synthesis of the 9-nitro-N-methyl-6 α -benzoxy-cytisine **2.18** described above, we thought that we could introduce the nitration as the first step as described by the Rouden group. Following purification we hoped that we could undertake the N–C migration to afford the desired 9-nitro product **2.18**. Following this procedure we managed to isolate **2.20a** in 69% yield after chromatographic separation (**Scheme 2.10**). Then, the N-benzoxy-9-nitro-cytisine **2.21** was obtained in 82% yield. The N–C migration using LDA at -78 °C was attempted, however only the starting material was recovered (**Scheme 2.11**).

Reagents and conditions: a) HNO₃, H₂SO₄, 88%.

Scheme 2.10: Direct nitration of cytisine **1.67** affording 9-nitro-cytisine **2.20a** by Rouden *et al.*^{47b}

A closer assessment of the electronics of the 9-nitro precursor showed that the migration would be challenging since the nitro group could cause chelation of the lithium ion reducing the possibility of deprotonation at the C6-position. Our postulation was supported with no desired product obtained under a slow addition at -78 °C for 16 h (**Scheme 2.11**).

Chapter 2 PRGPRP analogues based on Cytisine & clonogenic assay

$$O_2N$$
 O_2N
 O_2N

Reagents and conditions: a) Benzyl chloroformate, Et₃N, CH₂Cl₂, 81%; b) LDA, LiCl, -78 °C, 16 h then H₂O.

Scheme 2.11: Attempt to formation of cytisine derivative 2.22.

2.3.4 Synthesis of PR*G*PRP analogue 2.25

Once the dipeptide mimic **1.89** was in hand, our planned route involved protection of the acid functionality followed by coupling of the free C-9 amine to dipeptide **2.26**. Finally hydrolysis of the ester **2.24** and coupling with dipeptide **2.10b** should yield the desired protected hexapeptide analogue **2.25** (Scheme **2.12**).

Reagents and conditions: a) Esterification; b) N-Ac-Pro-Arg(NO_2)-OH **2.26**, PyBOP, DIPEA, DMF; c) hydrolysis then H.Arg(NO_2)-Pro-OMe **2.10b**.

Scheme 2.12: Proposed scheme for the formation of **2.25**.

We anticipated that a *p*-methoxybenzoate or *tert*-butyl ester could be a useful *C*-terminus protecting group regarding the orthogonality of protecting groups in the following steps. ^{85,86} Unfortunately, attempts at the protection of the acid functionality failed. These conditions were also attempted with heating however degradation of the compound was observed (**Scheme 2.13**).

Chapter 2 PRGPRP analogues based on cytisine & clonogenic assay

1.89

1.87:
$$R = PMB$$
2.27: $R = {}^{t}Bu$

Reagents and conditions: a) PMBCl, K₂CO₃, DMF; b) ^tBuOH, H₂SO₄, sieves.

Scheme 2.13: Attempted esterification of 1.89.

Since we could only obtain in a poor yield the functionalised C-9 cytisine derivative **1.89** and the culture cell assay with hexapeptide **2.16** using cytisine as a *trans*-proline mimic **2.14** was less fruitful than we had hoped, we decided to move onto the synthesis of the PPII mimic and its analogues.

3. PRGPRP based on pyroglutamate mimic 1.125 & clonogenic assay

3.1 Synthesis of pyroglutamate based mimic 1.125 and conformational analysis

As discussed in the introduction (section 1.7.3), we aimed to synthesise **1.125**, as a Xaa-*trans*-Pro mimic in which ϕ , ψ and ω dihedral angles are constrained to the ideal dihedral angles found in PPII conformation (**Figure 3.1**).

Figure 3.1: pyroglutamic based mimic 1.125.

Our synthesis began with commercial L-pyroglutamic acid **1.116**; esterification with perchloric acid in water (70%) in *tert*-butyl acetate gave the desired product ester **3.1a** in 89% yield without purification. This yield and spectroscopic data are comparable to those reported in the literature.⁸⁷ Benzylation using sodium hydride and benzylbromide afforded **1.132** in 79% yield. Thiolactam **1.131** was obtained from **1.132** using Lawesson's reagent which, following recrystallisation from chloroform/hexane, gave **1.131** in 92% yield (**Scheme 3.1**).⁸⁷

Reagents and conditions: a) HClO₄ aq., ^tBuOAc, 89%; b) BnBr, NaH, CH₂Cl₂, 79%; c) Lawesson's reagent, THF, 92%.

Scheme 3.1: Synthesis of thiolactam 1.131.

Rapoport *et al.*⁶⁵ described the formation of alkene **1.134** from thiolactam **1.131** with methyl bromoacetate, triphenylphosphine and triethylamine (**Scheme 3.2**). However several attempts at reproducing their conditions were unsuccessful with the starting material isolated following work-up. Interestingly in two separate reports Hussaini *et al.*⁸⁹ state that **1.134** is impossible to obtain using Rapoport conditions and they also observed the formation of **1.132**. A possible explanation is the hindered centre for the attack of triphenylphosphine.

Chapter 3 PRGPRP based on pyroglutamate mimic 1.125 & clonogenic assay

S
$$\longrightarrow$$
 $O_2^t Bu$ \longrightarrow $O_2^t Bu$ \longrightarrow $O_2^t Bu$ \bigcirc $O_2^t Bu$

Reagents and conditions: a) methylbromoacetate, PPh₃, Et₃N.

Scheme 3.2: Synthesis of 1.134 by Rapoport et al. 65

With our attempts at synthesising **1.134** being unsuccessful, another route was considered based on literature precedent (**Scheme 3.3**). As previously described in section 1.5.3, intramolecular cyclisation of **1.126a** could give the bicyclic lactam **1.125a**. Compound **1.126** could be obtained via a Horner-Wadswoth-Emmons reaction. Aldehyde **1.128a** could be formed via ozonolysis from the corresponding alkene **3.4a**. Alkene **3.4a** could be obtained from allylation of **3.3a** which is prepared from reduction of **3.2a**. As previously described in the first approach, L-pyroglutamic acid **1.116** will be used as the starting material.

Scheme 3.3: Retrosynthetic approach of 1.125a.

The synthesis of **1.122a** was described in the literature by Zaminer *et al.*⁶² (**Scheme 3.4**). Following the procedure above, **3.8a** was obtained in high yield (step a: 89%, step b: 70%). Reduction of **3.8a** using DIBALH afforded the desired compound **3.9a** however following purification the product was contaminated with unidentified byproducts. Also on scale up (~10 g) the formation of byproducts increased. Thus, reduction was undertaken with

Chapter 3 PRGPRP based on pyroglutamate mimic 1.125 & clonogenic assay

Superhydride® and **3.9a** was obtained in an excellent 96% yield. However, due to the hazards associated with quenching Superhydride® on a large scale, we decided to use L-Selectride in larger scale synthesis. The desired aminoalcohol was isolated and was immediately converted to the corresponding methyl ether **3.9a** in 76% yield over two steps (**Scheme 3.4**). 62

Reagents and conditions: a) HClO₄, tBuOAc , 89%; b) Boc₂O, DMAP, 70%; c) L-Selectride® 1M in THF, -78 ${}^\circ$ C, then MeOH, PTSA, 76% over two steps; e) BF₃·Et₂O, Allyl-TMS, -78 ${}^\circ$ C, 72%.

Scheme 3.4: Synthesis of 1.122a following the methods of Zaminer et al.⁶²

The syn allylation of pyroglutamic acid derivatives **3.5** have been described to proceed through an S_N1 —type intermediate. ^{90a} Commonly, addition of allytributylstannane or allyltrimethylsilane to N-acyliminium ions bearing an ester side chain were performed using a Lewis acid. These reactions lead predominantly to formation of the cis-isomer. The origin of the syn selectivity is believed to arise from activation of the allylsilane by the ester moiety thus delivering the reagent syn to the ester group (**Table 3.1** and **Scheme 3.5**). ^{90a}

Chapter 3 PRGPRP based on pyroglutamate mimic 1.125 & clonogenic assay

Entry	R ¹	R	R²	R³	R ⁴	Nu*	LA*	Yield	cis:trans
1	OMe	CO ₂ Me	Bn	/	/	Allyl-TMS	TiCl ₄	77%	4.5:1 ^{90b}
2	OAc	CBz	^t Bu	Cyclo	hexyl	Allyl- ^t Bu₃Sn	BF₃·Et₂O	70%	1.5 : 1 ^{90c}
3	OMe	Вос	Bn	/	/	Allyl-TMS	BF ₃ ·Et ₂ O	93%	4:1 ^{90d}
4	OMe	Вос	Bn	/	/	Allyl-TMS	TiCl ₄	95%	nd ^{90b}
5	ОН	Вос	Et	/	/	Allyl- ^t Bu₃Sn	BF₃·Et₂O	54%	2:1 ^{90e}
6	OEt	Вос	Et	/	/	Allyl-TMS	BF₃·Et₂O	79%	4:1 ⁹¹
7	ОН	Вос	^t Bu	/	/	Allyl- ^t Bu₃Sn	TMSOTf	70%	1.3:1 ^{90e}
8	OEt	Вос	^t Bu	/	/	Allyl-TMS	BF ₃ ·Et ₂ O	77%	3:1 ⁶²
9	OMe	Вос	Me	Ph	/	Allyl-TMS	BF ₃ ·Et ₂ O	77%	1:0 ^{90f}
10	OAc	Вос	Me	/	Ac	Allyl-TMS	BF₃·Et₂O	70%	3:1 ^{90g}

^{*}LA: Lewis acid and Nu: nucleophile.

Table 3.1: Various conditions for the allylation of pyroglutamic acid derivatives.

Entry 9 showed that absolute *syn* addition is induced by the substituent at the C-4 position, a phenyl group, which creates steric bulk. Reasonable *syn* selectivity was observed when R² is a benzyl group (entries 1 and 3). The only disadvantage with these examples is the possible orthogonality of protecting groups for the rest of the synthesis. Moderate selectivity and consistent yields were observed for entries 6, 8 and 10, which were undertaken using the same

conditions. For example the substitution of R^2 of entry 8 by a smaller group (entry 6) seems to give a slightly better selectivity for the *syn* addition. The three examples showing the use of allyltributylstannane as a nucleophile showed poor selectivity (entries 2, 5 and 7).

A final consideration in our synthesis will be separation of the diastereoisomers of **3.7**. Harris $et\ al.^{90e}$ described the separation of the cis and trans isomers using classic column chromatography after Boc removal when $R^2 = {}^tBu$, but disclose that they were not able to separate diastereoisomers after Boc removal when $R^2 = Et$.

Based on these observations, we decided to react **3.9** with allyl-TMS in the presence of $BF_3 \cdot Et_2O$ at -78 °C to give the protected 5-allylpyrrolidine **1.122a** in 72% yield. The *cis/trans* ratio by NMR was ca. 3 : 1 which is consistent with literature precedent (entry 8) (**Scheme 3.4**).

The *cis*-arrangement relies on the facial preference with which an allylsilane attacks the cyclic iminium species **3.10a** gerenated by the BF₃ catalysed OMe-elimination from aminal **3.9a** (**Scheme 3.5**). This mechanism would involve the formation of a BF₃ complex with the ester in which the fluoride would acquire sufficient nucleophilicity to attack the trimethylsilyl group and facilitate allyl transfer to the iminium ion.

MeO
$$CO_2$$
'Bu O' Bu O' Bu

Scheme 3.5: Cis-selective allylation. 91

Disappointingly, we were unable to separate the two diastereoisomers at this stage. However, Boc-deprotection afforded the *cis*-(**3.11a**) and *trans*-alkene (**3.12a**) which were successfully separated using flash column chromatography as described above (**Scheme 3.6**).

Scheme 3.6: N-Boc deprotection to afford 3.11a (48%*) and 3.12a (24%*). *Isolated yield

Chapter 3 PRGPRP based on pyroglutamate mimic 1.125 & clonogenic assay

In an attempt to avoid protection and deprotection of the amino group in order to isolate the *cis*-isomer **3.11**, we repeated the synthesis instead with a Cbz protecting group. Starting from L-pyroglutamic acid **1.116**, esterification and *N*-protection were undertaken in 89% and 61% yield respectively without optimisation. Reduction with L-Selectride (76%) followed by allylation gave **3.15** in 78% yield. Again the two diastereoisomers were inseparable (**Scheme 3.7**).

1.116

d

$$CO_2^tBu$$
 CO_2^tBu
 CO_2^tBu

Reagents and conditions: a) HClO₄, tBuOAc , 89%; b) CBzCl, NaH, 61%; c) L-Selectride® 1M in THF then MeOH, PTSA, 76% over two steps; d) BF₃·Et₂O, Allyl-TMS, -78 ${}^{\circ}C$, 78%.

Scheme 3.7: Synthesis of 3.15.

We therefore reverted to our previous synthesis using *N*-Boc-protection, deprotection to isolate the desired *cis* isomer **3.11** then reprotection with Cbz. The choice of Cbz protecting group ensures orthogonality with the *C*-terminus ester. With the mechanism of the formation of **1.122** in mind, we also decided to swap to the methyl ester in an attempt to enhance the selectivity for the *cis* isomer (**Scheme 3.8**).

Chapter 3 PRGPRP based on pyroglutamate mimic 1.125 & clonogenic assay

Reagents and conditions: a) MeOH, Dowex®, reflux, 96%; b) Boc_2O , DMAP, 82%; c) L-Selectride® 1M in THF then MeOH, 52% over two steps; d) $BF_3 \cdot Et_2O$, Allyl-TMS, -78 °C, 77%; e) TFA (20% v/v) in CH_2Cl_2 , 65%.

Scheme 3.8: Synthesis of 3.11b and 3.12b.

From L-pyroglutamic acid **1.116**, esterification was undertaken using MeOH catalysed by Dowex® (96%) followed by *N*-Boc protection to afford **3.8b** in 82% yield. Reduction of the lactam carbonyl **3.8b** was undertaken with L-Selectride, followed by etherification to obtain **3.9b** in 52% yield. The yield was slightly lower than that observed with *tert*-butyl ester **3.9a**. Several attempts at reduction using DIBALH were undertaken but the same range of yields was obtained. Purification of **3.9b** with L-Selectride proved less challenging than with DIBALH so we used the former as the reducing agent for this step. Allylation with allyl-TMS gave **1.122b** in 77% yield and *N*-Boc deprotection was undertaken using TFA. The two diastereoisomers were separated by flash column chromatography in a ratio of 5:1 (*cis*: *trans*) (**Scheme 3.8**).

Following the method of Scolastico *et al.*, 66 reprotection of the free amine with benzyl carbamate was performed with NaH in the presence of CbzCl to afford **3.4b** in 87% yield (**Scheme 3.9**). Ozonolysis of **3.4b** gave the corresponding aldehyde **1.128b** in good yield (96%). The phosphonate **3.13** was also prepared in three steps from glyoxylic acid monohydrate following the method of by Ben *et al.* 92 (**Scheme 3.10**). Glyoxylic acid **3.14** and benzyl carbamate **3.15** gave 2-(benzyloxycarbonyl)-2-hydroxyacetic acid **3.16** in 50% yield. **3.16** was then converted into **3.17** using a mixture of methanol and PTSA in 82% yield. Using the Arbusov reaction, phosphonate **3.13** was formed in 66% yield after precipitation. The aldehyde **1.128b** was treated with phosphonate **3.13** and potassium *tert*-butoxide to give **1.127b** as a mixture of *E/Z* isomers (ratio = 1:3) in 79% yield (**Scheme 3.9**). Boc protection of the amine was

Chapter 3 PRGPRP based on pyroglutamate mimic 1.125 & clonogenic assay

undertaken using Boc₂O catalysed by DMAP, compound **1.126b** was formed in 71% yield. Reduction of **1.126b** with hydrogen, catalysed by palladium on carbon, gave a mixture of compounds after filtration. Following flash column chromatography, the two diastereoisomers **1.125b** (67%) and **1.138b** (23%) were isolated with a ratio of 3:1 respectively. Scolastico *et al.* ⁶⁶ undertook the reduction and cyclisation by heating reflux in MeOH in two steps. In our case the cyclic products **1.125b** and **1.138b** were obtained without reflux (**Scheme 3.9**).

Reagents and conditions: a) CbzCl, NaH, THF, 87%; b) O_3 , PPh₃, MeOH:CH₂Cl₂(1:1), -78 °C, 96%; c) ^tBuOK, CH₂Cl₂, -78 °C, 79%; d) Boc₂O, DMAP, CH₃CN, 71%; e) H₂, Pd/C, 90%.

Scheme 3.9: Synthesis of **1.125b** and **1.138b**.

Reagents and conditions: a) Et₂O, 50%; b) MeOH, PTSA, 82%; c) PCl₃, P(OEt)₃, toluene, 70 °C, 66%.

Scheme 3.10: Synthesis of phosphonate 3.13.92

We next developed a method of asymmetric hydrogenation of **1.127b**, in order to optimise the formation of the desired diastereoisomer **1.125b**.

Rhodium-catalysed hydrogenation is well suited to the enantioselective reduction of α - and β -dehydroamino acid derivatives and enamides. These reductions are largely dependent on the chiral ligands and substrates used. Generally, electron-rich and rigid ligands, such as DuPhos, BenzP* and others, give high selectivity. 93

Hruby *et al.*^{93a} described the reduction of the E/Z mixture of **3.18** under high-pressure hydrogenation with rhodium catalysts **3.21** and **3.22**. The (R,R)-**3.22** catalyst gave **3.20** and the (S,S)-**3.21** catalyst afforded **3.19**. However, the authors do not discuss the mechanism pathway of the reaction (**Scheme 3.11**).

MeO₂C OEt 3.19

MeO₂C OEt
$$\frac{1}{N}$$
 NeO₂C OEt $\frac{1}{N}$ NeO₂C OEt $\frac{1}{N}$ NeO₂C OEt $\frac{1}{N}$ OET $\frac{$

Reagents and conditions: a) H_2 (5 bar), (S,S)-Rh(COD)[DUPHOS-Et]OTf **3.21**, MeOH, 99%, b) H_2 (5 bar), (R,R)-Rh[DUPHOS-Et]OTf **3.22**, MeOH, 99%.

Scheme 3.11: Asymmetric hydrogenation of 3.18 by Hruby et al. 93a

Separately, the mechanism of the asymmetric hydrogenation using a similar rhodium catalyst $([Rh-((R,R)-BenzP^*(nbd)]BF_4))$ has been recently investigated. Thus, based on this mechanism, one can deduce that the asymmetric hydrogenation described by Hruby *et al.* Could follow a similar pathway (Scheme 3.12). The mechanism begins when the solvated complex 3.23 is hydrogenated to 3.25 via intermediate 3.24. Reaction of 3.25 with 3.18 gives intermediate 3.28. The non-chelating catalyst-substrate complex 3.26 is also hydrogenated affording intermediate 3.28 via 3.27. The hydrogenation of the chelating catalyst-substrate complex 3.29 requires a much higher activation energy compared to 3.26, therefore the unsaturated

pathway does not occur. Then coordination of the double bond of **3.28** to the rhodium allows the formation of the chelated intermediate **3.30**. Finally, the migratory insertion produces intermediate **3.31** which is then subjected to reductive elimination to generate **3.20** with the desired absolute configuration (**Scheme 3.12**).

Scheme 3.12: Reaction pathway of the asymmetric hydrogenation of **3.18** catalysed by the **3.22** by analogy to the asymmetric hydrogenation with Rh-(R,R)-BenzP* complex by Inamoto *et al.* ^{93b} Ligand structures have been simplified for intermediates **3.24-3.31**.

In our case, the desired absolute configuration required the use of **3.22** as a catalyst. Several attempts were undertaken on **1.126b** and **1.127b** under high pressure (7 bar) using (*R*,*R*)-**3.22** with a large amount of starting material being obtained on each occasion. We found this to be due to the catalyst **3.22** being extremely air sensitive. A glove bag was used to weigh the catalyst, and dry and degassed solvent was also used. The desired product **3.32** was then obtained in 90% yield. However the reduction of diprotected amine **1.126b** under these conditions gave only the starting material **1.126b**. The alkene **1.126b** is very hindered due to the presence of protecting groups, which probably made the formation of the complex with the rhodium impossible (**Scheme 3.13**).

Chapter 3 PRGPRP based on pyroglutamate mimic 1.125 & clonogenic assay

Reagents and conditions: a) H₂ (7 bar), (R,R)-Rh[DUPHOS-Et]OTf 3.22, MeOH, 90%.

Scheme 3.13: Asymmetric hydrogenation of **1.127b**.

Intramolecular cyclisation gave **3.34** in good yield using classical hydrogenation conditions (72%). Boc-protection of the amine **3.32** followed by hydrogenation gave **1.125b** in 98% yield. The optimised synthesis of **1.125b** was performed in 12 steps with an overall yield of 10% (**Scheme 3.14**).

Reagents and conditions: a) Boc₂O, DMAP, 97%; b) H₂, Pd/C, 98%; c) H₂, Pd/C, 72%.

Scheme 3.14: Intramolecular lactam cyclisation under hydrogenation conditions to afford **3.34** and **1.125b**.

Conformational analysis of **3.34** and **1.138b** was undertaken using nOe experiments. Under non-asymmetric hydrogenation conditions, lactams **1.125b** and **1.138b** were isolated after an intramolecular cyclisation. Irradiation of H-3 gave a 2.5% correlation to H-6 and 0.6% correlation to H₉ confirming the stereochemistry to be as depicted in **1.138b**. For lactam **3.34** the irradiation of H-3 did not show any correlation with H-6 and H-9, as expected (**Figure 3.2**).

The (3R,6S,9S) absolute configuration is inferred from the configuration of the enantiopure starting ι -pyroglutamic acid **1.116**.

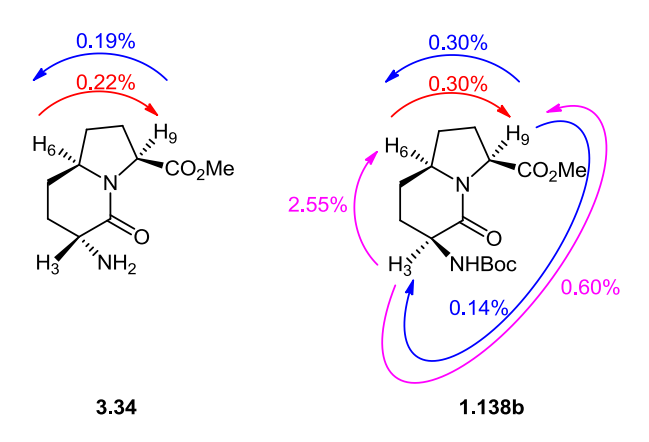
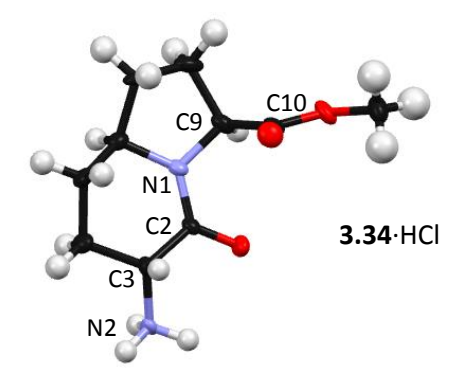


Figure 3.2: nOe experiments of lactams 3.34 and 1.125b (CDCl₃, 400 MHz).

In addition, X-ray structure of **3.34**·HCl (co-crystallised with dimer **4.1**, see section 4.2.3) was obtained and confirmed the absolute conformation of **3.34** (see Appendix). These data also allow us to determine the torsion angles of **3.34** and compare them to the ideal torsions angles of the PPII geometry (**Figure 3.3**). Values of the torsions angles obtained for **3.34** matched nicely the optimal values of the ideal PPII geometry which suggest strongly the PPII conformation of **3.34**.



	ф (C2-N1-C9-C10)	ψ (N2–C3–C2–N1)	ω (C3–C2–N1–C9)
PPII helix	–75 (±15)°	145 (±15)°	180 (±15)°
Predicted torsion angles (DFT)	– 69	144°	175°
3.34 ·HCl angles by X-ray	–59°	150°	167°

Figure 3.3: X-ray structure and comparison of the torsion angles of **3.34** with those of a PPII helix.⁵⁹

3.2 Synthesis of PR*G*PRP analogue using 1.125 as a Gly-Pro mimic

To prepare an analogue of the lead compound PR-1.125-RP, mimic 1.125 was used as a replacement of the Gly-Pro dipeptide 1.71 (Figure 3.4).

$$H_{N}$$
 CO_2H H_{N} CO_2H NH_2 NH_2 $NATURE 1.125$

Figure 3.4: Use of pyroglutamate mimic 1.125 as a replacement for the Gly-Pro dipeptide 1.71.

Our proposed strategy involved first reacting the dipeptide H.Arg(NO₂)Pro-OMe **2.10b** with **1.125c** and then coupling of the resulting 'tetrapeptide' **3.35** to *N*-Ac-Pro-Arg(NO₂)-ONa (Scheme **3.15**).

Reagents and conditions: a) i) LiOH 1M in THF, ii) H.Arg(NO₂)Pro-OMe, HBTU, DIPEA, DMF; b) i) TFA in CH_2Cl_2 (20% v/v), ii) N-Ac-Pro-Arg(NO₂)-ONa, HBTU, DIPEA, DMF.

Scheme 3.15: Our proposed route to prepare N-Ac-PR(NO₂)-1.125-R(NO₂)P-OMe 3.36.

Firstly hydrolysis of the methyl ester of **1.125b** was undertaken using a solution of 1M lithium hydroxide followed by coupling with H.Arg(NO₂)Pro-OMe **2.10b** using HBTU as a coupling reagent. Under these conditions, no racemisation was observed at C-9. The H-9 signal appeared to be a doublet (${}^{3}J_{H9-H8} = 9.5$ Hz), however when racemisation intentionally was induced using LiOH 2 M in dioxane, a doublet-doublet (${}^{3}J_{H9'-H8} = 9.6$ Hz and ${}^{3}J_{H9'-H8'} = 10.1$ Hz) was observed. This result was consistent with the method described by Lubell *et al.* ⁹⁴ Intermediate **3.35** was obtained in 85% yield over two steps. *N*-deprotection of **3.35** was undertaken using a solution of TFA in DCM. Unfortunately, the coupling reaction between the deprotected amine **3.35b** and the salt *N*-Ac-Pro-Arg(NO₂)-ONa failed (**Scheme 3.16**). Most of the starting material **3.35b** was recovered.

Chapter 3 PRGPRP based on pyroglutamate mimic 1.125 & clonogenic assay

To investigate this further, we decided to use commercial *N*-Boc-Arginine **2.5** and *N*-Ac-Proline **3.38** in two successive reactions with HBTU as coupling reagent (**Scheme 3.17**). Intermediate **3.37** was obtained in 53% yield thus proving the use of HBTU as a coupling reagent was not the problem in the reaction. Deprotection and coupling with commercial *N*-Boc-proline gave **3.36** in 85% yield. The failed coupling could thus be related to the use of the sodium salt of the dipeptide *N*-Ac-Pro-Arg(NO₂)-ONa. To confirm this postulation, dipeptide *N*-Ac-Pro-Arg(NO₂)-ONa was treated with 1M HCl until the solution was at pH 5 to give *N*-Ac-Pro-Arg(NO₂)-OH. The reaction with **3.35** was repeated using the same conditions (HBTU, DIPEA, DMF) and this gave the desired analogue **3.36** (46% yield) (**Scheme 3.17**).

Reagents and conditions: a) i) LiOH 1 N in THF, ii) H.Arg(NO₂)-Pro-OMe **2.10b**, HBTU, DIPEA, DMF, 85%; b) i) TFA in CH₂Cl₂ (20% v/v), ii) N-Ac-Pro-Arg(NO₂)ONa, HBTU, DIPEA, DMF.

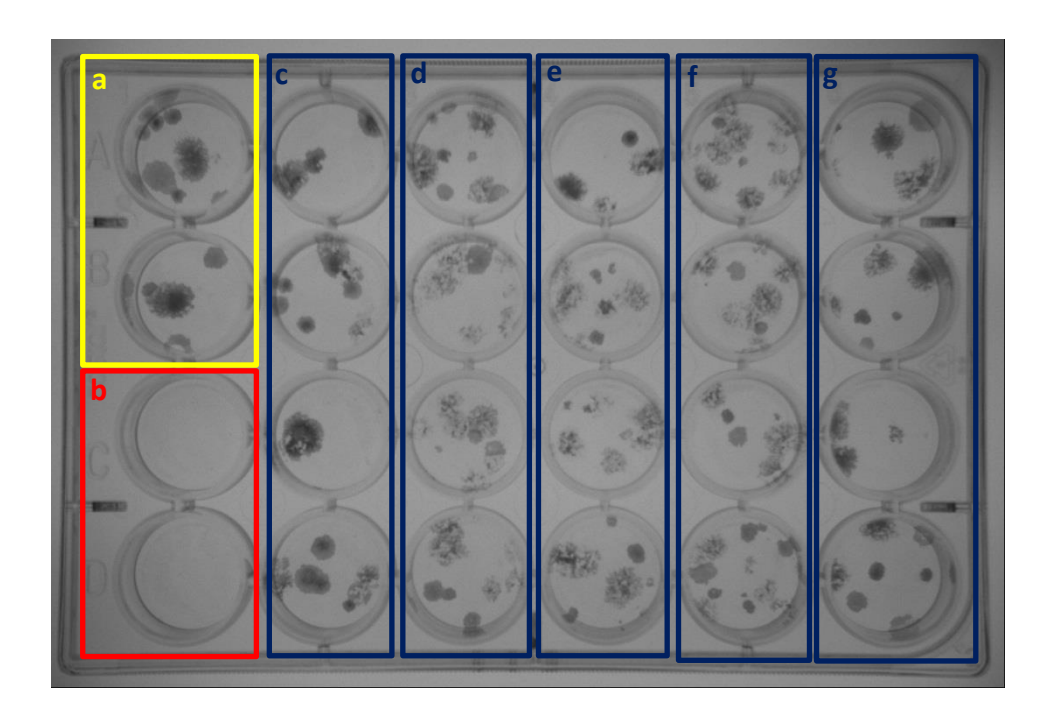
Scheme 3.16: Synthesis of 3.36.

Reagents and conditions: a) *N*-Boc-Arg(NO₂)-OH **2.5**, HBTU, DIPEA, DMF, 53%; b) *N*-Ac-Pro-OH **3.38**, HBTU, DIPEA, DMF, 85%; c) *N*-Ac-Pro-Arg(NO₂)-OH, HBTU, DIPEA, DMF, 46%.

Scheme 3.17: Synthesis of the Boc protected analogue N-Ac-Pro-Arg-1.125-Arg-Pro-OMe 3.36.

3.3 Clonogenic assay of N-Ac-PR(NO₂)-1.125-R(NO₂)P-OMe 3.36

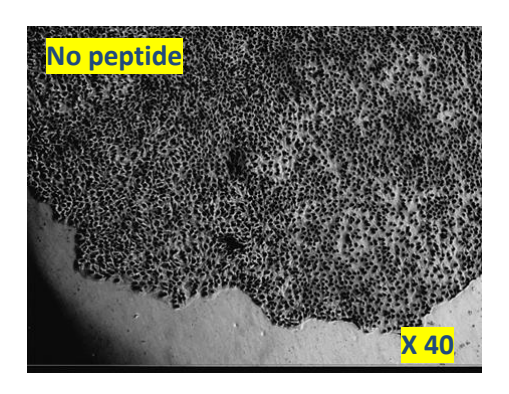
The anticancer activity of **3.36**, containing nitro protecting groups on both guanidine side chains and a methyl ester at the *C*-terminus, was investigated by clonogenic assay. These assays demonstrated that peptide **3.36** had an effect on the size and the shape of survival cancer cell colonies (**Figure 3.5**). However on comparison to the control peptide **2.1** where complete cell death is observed at 5 mM, it seemed that survival cancer colonies were in the process of dying where cell debris were present. At lower concentration of peptide **3.36** (**Figures 3.7**, **3.8**, **3.9** and **3.10**) the same effect was observed up to 1.0 mM. At 5 and 4 mM exposure of peptide **3.36** on MRC5-hTERT showed a toxic effect (**Figures 3.14** and **3.15**). At lower doses (from 3 mM to 1 mM) of peptide **3.36** normal fibroblasts were not killed anymore (**Figures 3.16**, **3.17** and **3.18**).



a) Control wells (no peptide); b) Positive control wells (compound **2.1**, 5mM); c) Compound **3.36** (5 mM); d) Compound **3.36** (4 mM); e) Compound **3.36** (3 mM); f) Compound **3.36** (2 mM); g) Compound **3.36** (1 mM).

Figure 3.5: Images of the formation of colonies of RT112 bladder cancer cells on day 31. Bladder cells were trypsinised and seeded at 10 cells in each well dish of a 24-well plate. The cells were allowed to grow in the medium for control experiment (500 μ L of final volume). The anticancer activity was studied when cells were exposed with several concentrations (5 to 1 mM) of peptide **3.36**. The plates were kept at 37 °C in 5% CO₂ before staining with Giemsa's stain on day 31.

Chapter 3 PRGPRP based on pyroglutamate mimic 1.125 & clonogenic assay



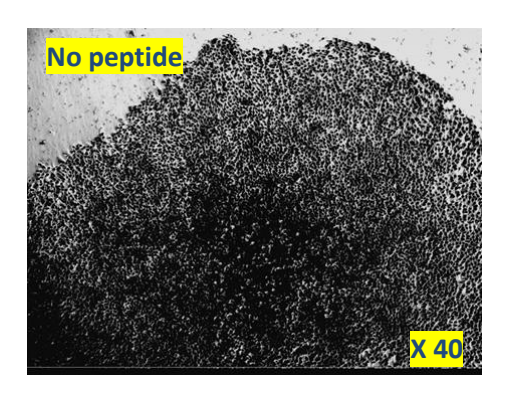
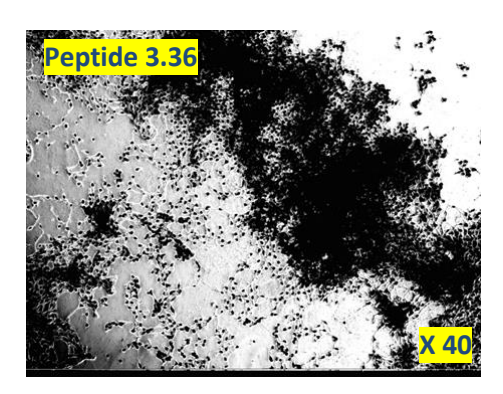


Figure 3.6: Morphological appearance of RT112 cells on day 31.



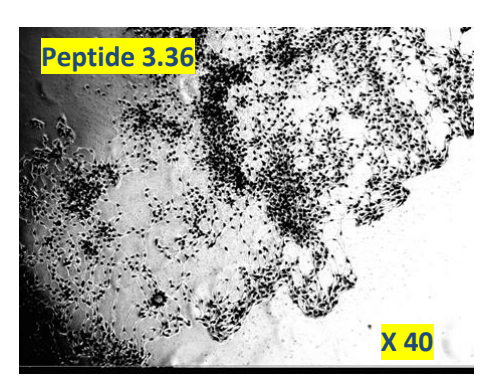
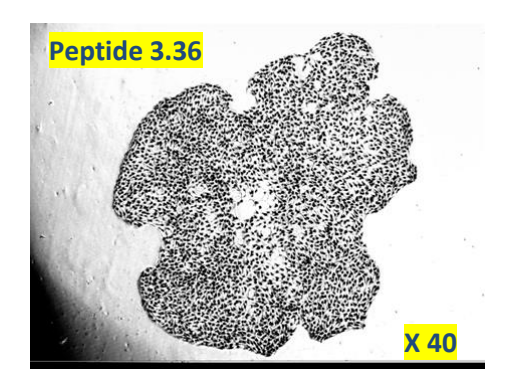


Figure 3.7: Morphological appearance of RT112 cells exposure to 5 mM of synthetic peptide **3.36** on day 31. Peptide **3.36** induced almost completed cell death of the bladder cancer cells after one month. This was compared to peptide **2.1** as a positive control.

Images of RT112 survival cancer cells exposed to **3.36** at lower concentration are presented in the next figures.



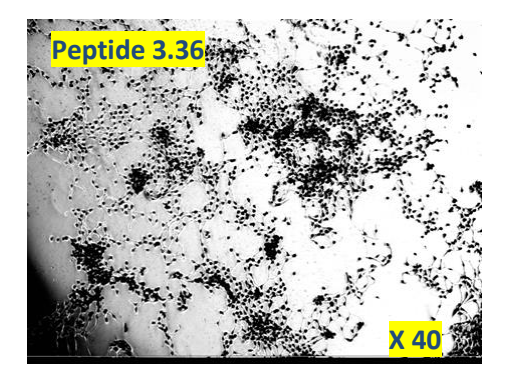
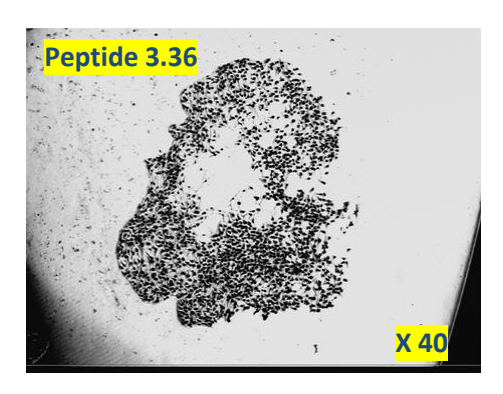


Figure 3.8: Morphological appearance of RT112 cells exposure to 4 mM of synthetic peptide **3.36** on day 31.



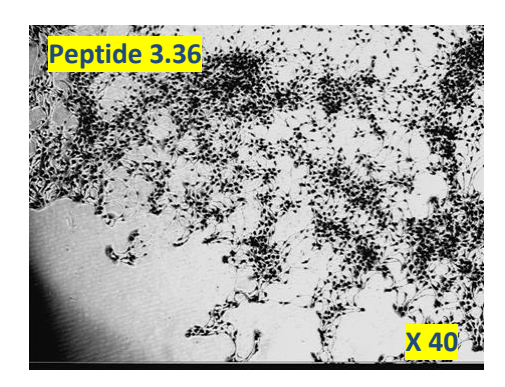
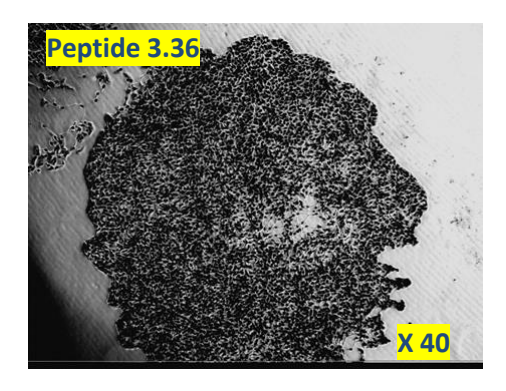


Figure 3.9: Morphological appearance of RT112 cells exposure to 3 mM of synthetic peptide **3.36** on day 31.



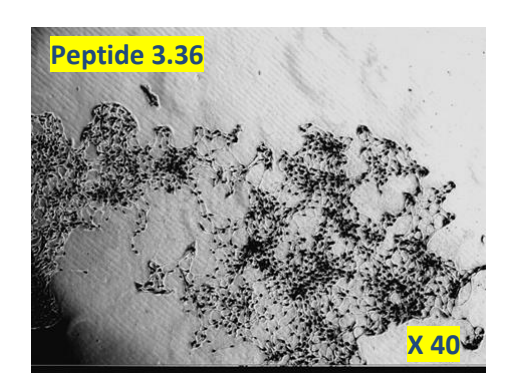
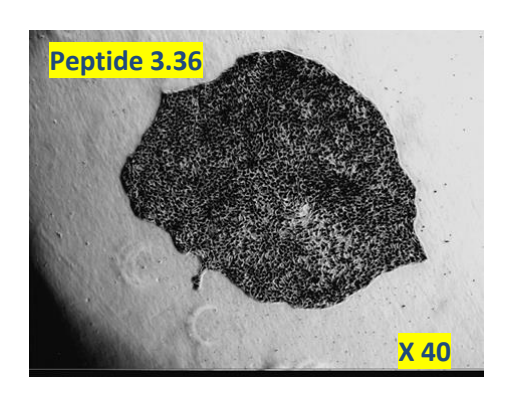


Figure 3.10: Morphological appearance of RT112 cells exposure to 2 mM of synthetic peptide **3.36** on day 31.



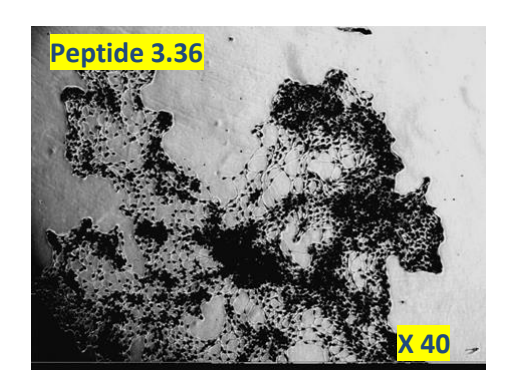
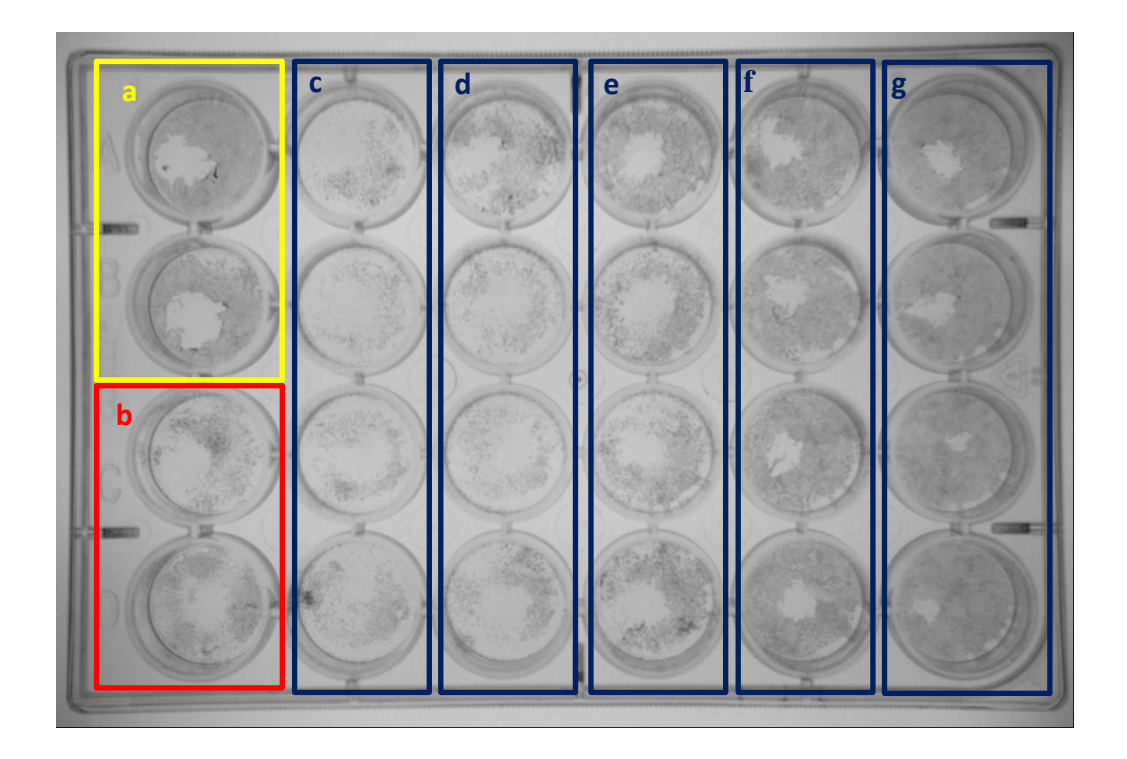


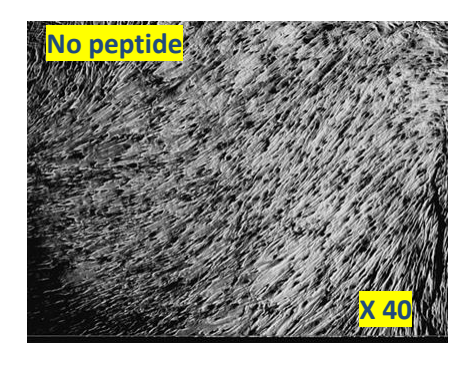
Figure 3.11: Morphological appearance of RT112 cells exposure to 1 mM of synthetic peptide **3.36** on day 31.

To investigate the toxicity of peptide **3.36**, clonogenic assays were undertaken against MRC5-hTERT.



a) Control wells (no peptide); b) Positive control wells (compound **2.1**, 5 mM); c) Compound **3.36** (5 mM); d) Compound **3.36** (4 mM); e) Compound **3.36** (3 mM); f) Compound **3.36** (2 mM); g) Compound **3.36** (1 mM).

Figure 3.12: Morphological appearance of MRC5-hTERT cells exposure to synthetic peptide **3.36** at different concentrations (5 to 1 mM) on day 31. Normal fibroblasts were trypsinised and seeded at 250 cells in each well dish of a 24-well plate. The cells were allowed to grow in DMEM medium for the control experiment (500 μ L of final volume). The plates were kept at 37 °C in 5% CO₂ before staining with Giemsa's stain on day 31.



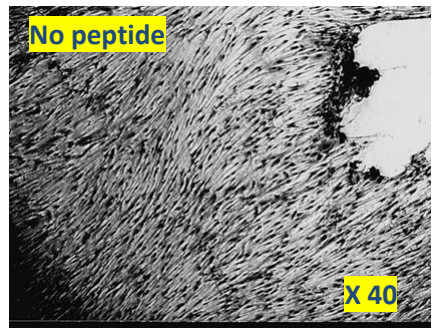
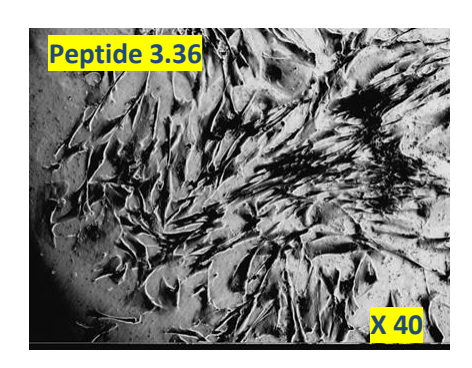


Figure 3.13: Morphological appearance of MRC5-hTERT cells on day 31.



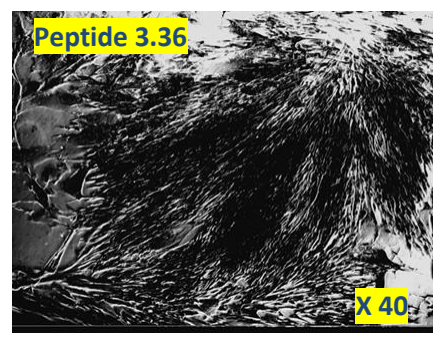
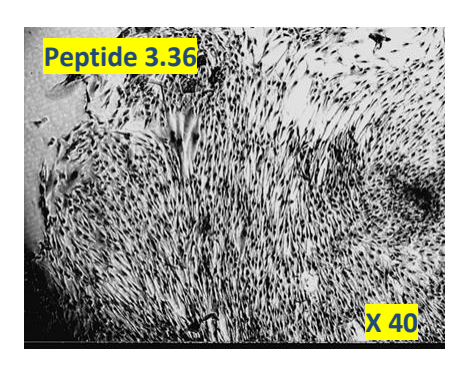


Figure 3.14: Morphological appearance of MRC5-hTERT cells exposure to 5 mM of synthetic peptide **3.36** on day 31.



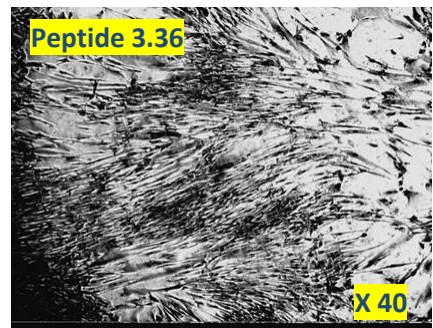
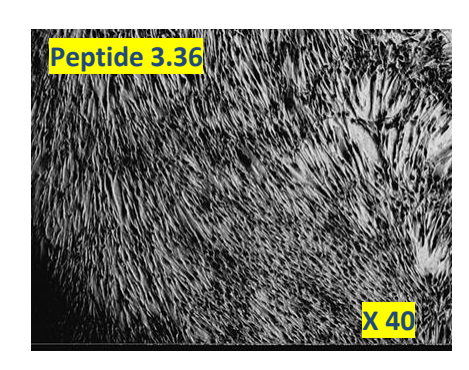


Figure 3.15: Morphological appearance of MRC5-hTERT cells exposure to 4 mM of synthetic peptide **3.36** on day 31.



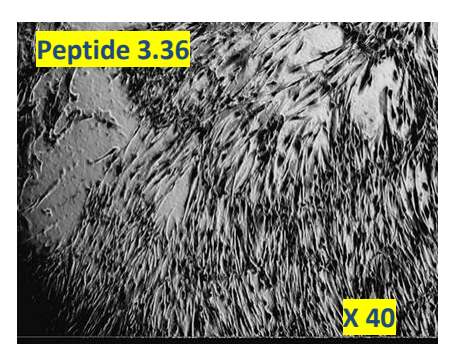
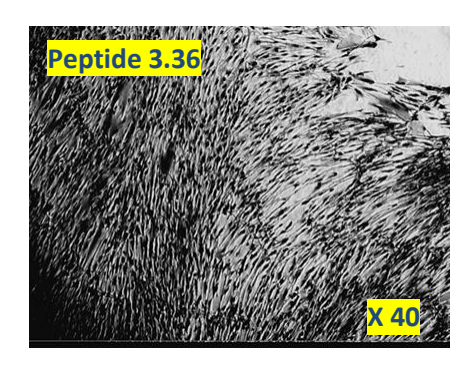


Figure 3.16: Morphological appearance of MRC5-hTERT cells exposure to 3 mM of synthetic peptide **3.36** on day 31.



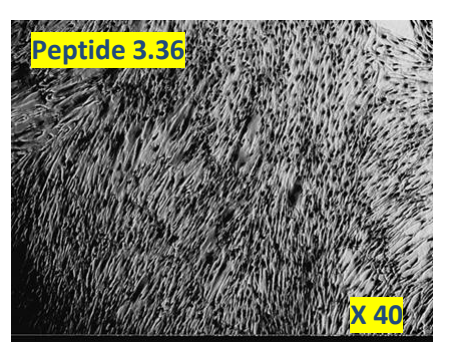
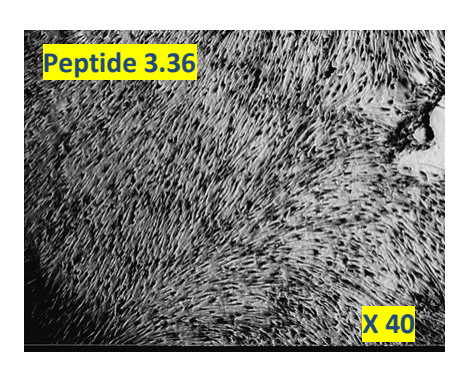


Figure 3.17: Morphological appearance of MRC5-hTERT cells exposure to 2 mM of synthetic peptide **3.36** on day 31.



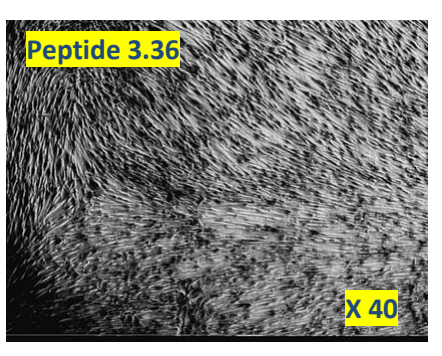


Figure 3.18: Morphological appearance of MRC5-hTERT cells exposure to 1 mM of synthetic peptide **3.36** on day 31.

In summary, we* have designed by DFT calculation pyroglutamate based mimic **1.125**. The synthesis of this *trans*-proline mimic was performed in twelve steps with an overall yield of 10%. A conformational analysis was undertaken using nOe experiments confirming the relative stereochemistry of mimic **3.34**. The absolute configuration was inferred from the configuration of enantiopure starting L-pyroglutamic acid. In addition, X-ray structure of **3.34**·HCl also confirmed the absolute configuration of **3.34**.

Clonogenic assays incorporating mimic **1.125** as a replacement of a Gly-Pro dipeptide **1.71** in the functional peptide PRGPRP was performed on RT112 and MRC5-hTERT cell lines. These assays demonstrated that the anticancer activity was not as good as the control peptide *N*-Ac-Pro-Arg(NO₂)-Gly-Pro-Arg(NO₂)-Pro-OMe **2.1**. Peptide **3.36** containing mimic **1.125** had an effect on the size and shape of the survival cancer colonies but complete cell death was not observed. The toxicity of **3.36** was investigated on normal fibroblasts MRC5-hTERT and it was found that the peptide was not toxic in a concentration of between 3 mM and 1 mM. This was comparable to the results observed with the control peptide **2.1**.

^{*} done by Dr. Bloodworth and Prof. Whitby

4. Oligomers of 1.125

As described previously (chapter 3), pyroglutamic mimic **1.125** was designed by DFT calculations to adopt a PPII conformation. A PPII helix has three residues per turn and ω , ψ and φ angles centred around 180°, 145° and –75° respectively. Mimic **1.125** represents a two residue motif Xaa-*trans*-Pro (**Figure 4.1**).

Figure 4.1: Mimic 1.125 representing Xaa-trans-Pro dipeptide.

To investigate the conformation of mimic **1.125**, we aimed to synthesise short oligomers of **1.125** and study their conformation in comparison to PPII helices.

4.1 Synthesis of dimer 4.1, trimer 4.2 and tetramer 4.3

Starting from pyroglutamic based mimic **1.125b**, prepared following the procedure described in chapter 3, dimer **4.1** was obtained by subjecting half the material to an *N*-deprotection using TFA to afford intermediate **4.4**, while the reminder of **1.125b** was converted to the free acid **1.125c**, without racemisation using LiOH 1 N in THF. The coupling of the two intermediates gave the desired dimer **4.1** in 81% yield overall (**Scheme 4.1**).

Reagents and conditions: a) TFA (20% v/v) in CH_2Cl_2 , RT, 16 h, quant.; b) LiOH 1N in THF, RT, 1 h, quant.; c) HOBt, EDC, DIPEA, DMF, 16 h, 81% over 3 steps.

Scheme 4.1: Synthesis of dimer **4.1**.

Chapter 4 Oligomers of 1.125

Preparation of trimer **4.2** was initially attempted by methyl ester hydrolysis of dimer **4.1**, which gave the free acid **4.5** quantitatively followed by a coupling reaction with intermediate **4.4** using the conditions previously described. However, this did not yield the desired trimer **4.2**. We were unsure as to why this reaction failed but it might be due to carboxylic acid not being activated under these conditions because of recovery of the starting material **4.5** (Scheme **4.2**).

Reagents and conditions: a) EDC, HOBt, DIPEA, DMF, RT, 16 h.

Scheme 4.2: Initial attempts at the synthesis of trimer **4.2**.

N-deprotection was performed on dimer **4.1** to afford intermediate **4.6** which was then reacted with intermediate **1.125c** under the same conditions previously described. Trimer **4.2** was obtained in good yield (73%) after column chromatography (**Scheme 4.3**).

Reagents and conditions: a) HOBt, EDC, DIPEA, DMF, RT, 16 h, 73%.

Scheme 4.3: Synthesis of trimer **4.2**.

Tetramer **4.3** was prepared following the same procedure and was obtained in 15% over three steps (**Scheme 4.4**). The yield was significantly lower than the shorter oligomers, perhaps due to the steric hindrance introduced by folded conformations.

Reagents and conditions: a) TFA (20% v/v) in CH_2CI_2 , RT, 16 h; b) 1N LiOH in THF; c) HOBt, EDC, DIPEA, DMF, RT, 16 h, 15% over three steps.

Scheme 4.4: Synthesis of tetramer **4.3**.

4.2 Conformational analysis

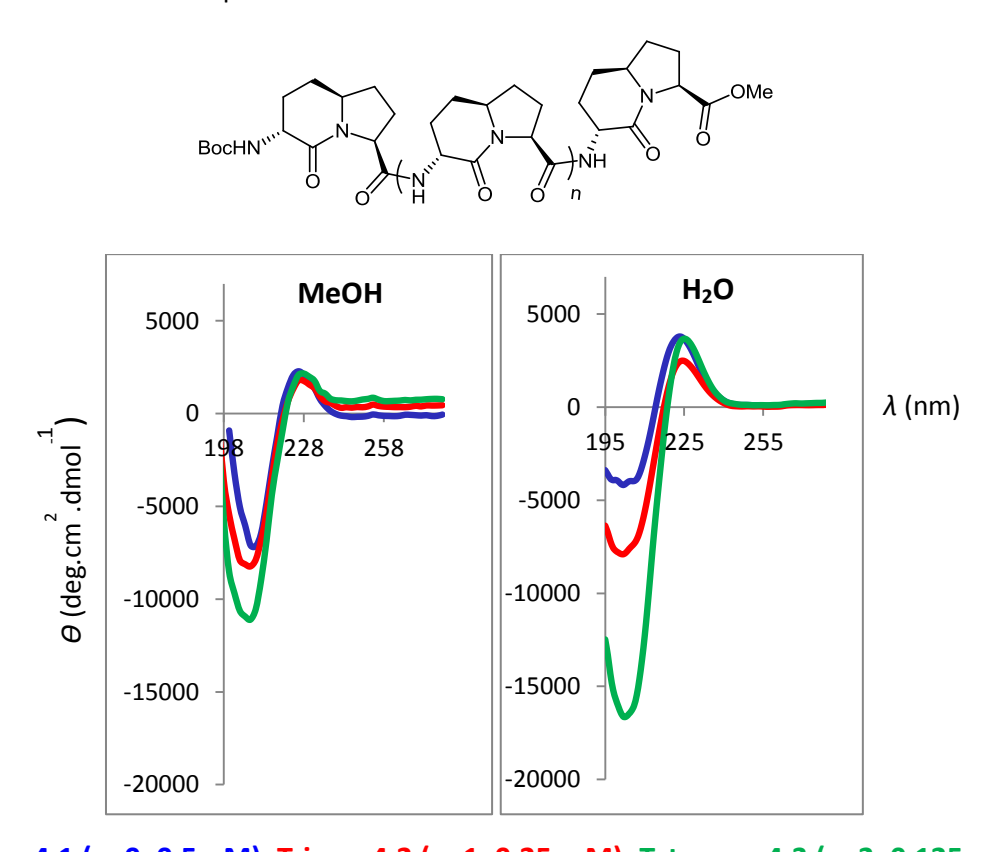
4.2.1 CD spectroscopy

With short oligomers (4 to 8 residue peptide chain mimics) in hand, conformational analysis was undertaken. One of the most popular techniques to determine spatial arrangement of chiral molecules, protein conformations, peptides and more specifically PPII helix conformation is circular dichroism spectroscopy. Oligomers based on proline adopt extended conformations in solutions called PPI and PPII helices. PPI helices (right-handed) are favoured in more hydrophobic environments such as aliphatics alcohols and PPII helices (left-handed) in water. The CD spectrum of PPII helices is characterised by a strong negative band at 206 nm, an $\pi \rightarrow \pi^*$ transition, and a weak positive band at 226 nm corresponding to the $n \rightarrow \pi^*$

Chapter 4 Oligomers of 1.125

transition characteristic of the *trans* conformation (see section 1.2). For PPI helices, a medium negative band at 199 nm, a strong positive band at 215 nm and a weak negative band at 232 nm are observed.^{57,58,95}

Solutions of oligomers **4.1**, **4.2** and **4.3** were prepared in methanol and water, and the CD spectra were recorded (**Figure 4.2**). The CD spectrum of **4.1**, **4.2** and **4.3** (**Figure 4.2**) in MeOH at 23 °C shows a strong negative band at 208 nm and a weak positive band at 228 nm. In water, a strong band at 206 nm and a weak positive band at 226 nm are observed. The CD spectra recorded in methanol and water of oligomers **4.1**, **4.2** and **4.3** suggested that they adopted a PPII helix conformation in both solvents. We also observed that the intensity of the CD signal increased as a function of chain length. We know that from literature precedents it is a phenomenon which could be observed until it reaches a maximal intensity depending upon the peptide monomer sequence and solvent conditions. ^{95b,95c}



Dimer 4.1 (n=0, 0.5mM), Trimer 4.2 (n=1, 0.25 mM), Tetramer 4.3 (n=2, 0.125

Figure 4.2: Circular dichroism data for oligomers in MeOH and H_2O (23 $^{\circ}C$). The data has been normalised for concentration and the number of amide groups.

Also few experiments were recorded with dimer **4.1** and trimer **4.2** at lower concentration (c = 0.125 mM, see Appendix). CD spectra were similar, independent of concentration indicating the absence of intermolecular association.

4.2.2 NMR spectroscopy

There are several NMR parameters characteristics of a PPII helical structure.⁵⁸ These parameters are summarised below (**Table 4.1**).

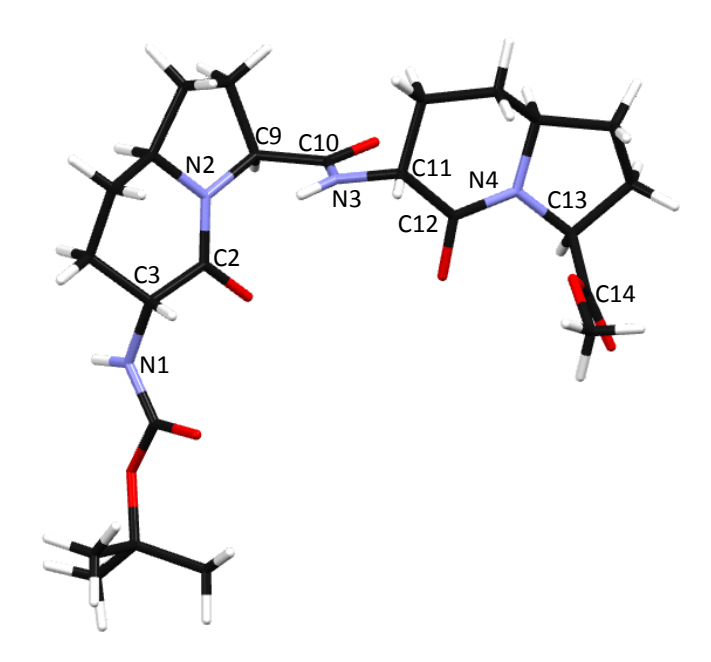
NMR parameters	Oligomers 4.1, 4.2, 4.3
NH chemical shift difference (ppm)	< 0.3 ppm
$^{3}J_{\alpha N}$ coupling constants	7.6-7.7 Hz
nOe NN(i,i+1)	No

Table 4.1: NMR parameters found in PPII helices.

The narrow NH chemical shift range is consistent with solvent-exposed NH that is not involved in hydrogen bonding. Torsion angles (ψ and φ) are essential parameters for defining the backbone conformation of a polypeptide chain. Angles about the N(3)–C(3) bonds are characterised by the³ $J_{\alpha N}$ coupling constants of 7.6–7.7 Hz. Using the Karplus equation { $J(\varphi)$ = Acos²(φ) + Bcos(φ) + C }, φ can be determined (–87°/–88°) and strongly suggest the presence of PPII conformation (φ = –75 (±15)°) in solution. Also the lack of nOe NH-NH indicates that oligomers are extended structures such as PPII helices.

4.2.3 X-ray crystallography

Only good quality co-crystals with monomer **3.34**·HCl were obtained for dimer **4.1** (see Appendix). Torsions angles were determined and are highlighted in **Figure 4.3**. Torsions angles of the two bicyclic lactams observed for dimer **4.1** are very close to the optimal dihedral angles of the PPII helix geometry (ϕ_1 , ϕ_3 , ψ_1 , ψ_3 , ω_1 , ω_3). However as expected on the solid state, torsions angles (ϕ_2 , ψ_2 , ω_2) observed for the new amide bond are not controlled by our mimic structure and so are very different to the optimal values.

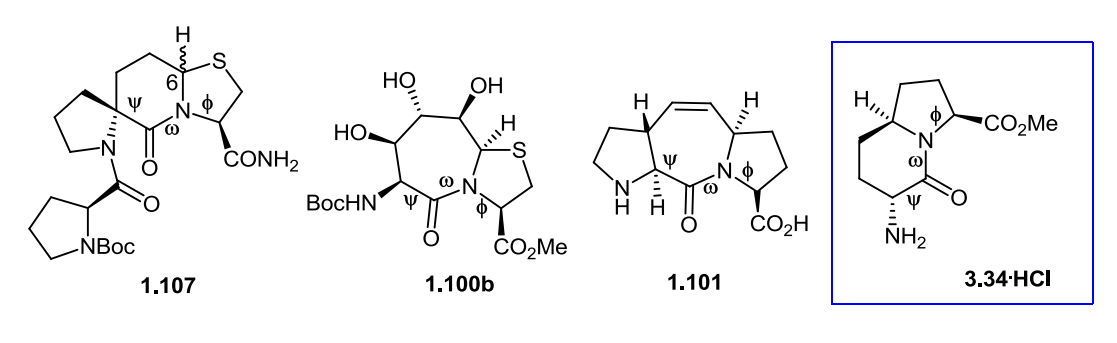


	Dimer 4.1	PPII helix ³⁹
φ ₁ (C2–N2–C9–C10)	-71°	−75 (±15)°
φ ₂ (N2–C9–C10–N3)	−25°	−75 (±15)°
φ ₃ (N3–C11–C12–N4)	−63.5°	−75 (±15)°
ψ ₁ (N1–C3–C2–N2)	149°	145 (±15)°
ψ ₂ (C10–N3–C11–C12)	-60°	145 (±15)°
ψ ₃ (N3–C11–C12–N4)	142°	145 (±15)°
ω ₁ (C3–C2–N2–C9)	179°	180 (±15)°
ω ₂ (C9–C10–N3–C11)	–168°	180 (±15)°
ω ₃ (C11–C12–N4–C13)	170°	180 (±15)°

Figure 4.3: X-ray structure and comparison of the torsion angles of dimer **4.1** with those of a PPII helix determined by X-ray structure. $(\phi_1, \psi_1, \omega_1)$ and $(\phi_3, \psi_3, \omega_3)$ are constrained within the bicyclic monomer. Torsion angles $(\phi_2, \psi_2, \omega_2)$ are unconstrained.

4.2.4 Discussion of previous PPII mimics

As described in chapter 1, only a few examples of PPII mimetics are described in the literature and include spirolactam **1.107**,⁶⁰ sugar derived mimic **1.100**⁶¹ and tryclyclic Pro-Pro mimic **1.101**.⁶² A comparison of the X-ray data based on torsions angles of these mimics is shown in **Table 4.2**.



Mimics	ф		ψ		ω	
1.107 $(6 = R)^{60}$	-64°		136°		nd	
1.107 (6 = S) ⁶⁰	-83°		148°		nd	
*1.100b ⁶¹	−55°		175°		179°	
1.101 ⁶²	nd		nd		nd	
3.34 ·HCl	–59°		150°		167°	
Dimer 4.1	-71°	-63.5°	149°	142°	179°	170°
PPII helix ⁵⁶	-75 (±15)°		145 (±15)°		180 (±15)°	

nd: non determined; * determined ourselves from supporting information data.

Table 4.2: Comparison of torsion angles of PPII mimics and an ideal PPII helix.

Based on the torsion angles determined by crystal structures, we can conclude that our mimic $\bf 3.34 \cdot HCl$ has close torsion angle values to that of sugar $\bf 1.100b$, except for the ψ angle. Spirolactam $\bf 1.107$ has torsion angles in good agreement with the ideal PPII helix however, the ω was not disclosed in their report. The crystal structure of mimic $\bf 1.101$ is not published to our knowledge. The solid state structure of mimic $\bf 3.34 \cdot HCl$ has a very good match with the ideal PPII helix.

Conformational analysis of peptidomimetic **1.107** and **1.101** using CD spectroscopy was not described in the literature. However, a CD spectrum of trimer **1.112** derived from sugar **1.100** showed a strong minimum at 205 nM ($\pi \rightarrow \pi^*$) and the absence of a weak positive band at 228 nm ($n \rightarrow \pi^*$). The features of the ideal PPII helix were not in good agreement. Oligomers derived from mimic **1.125** showed these specific characteristics in MeOH and water, confirming the PPII conformation in solution.

Chapter 4 Oligomers of 1.125

Tremmel *et al.*⁶¹ described undertaking the conformational analysis using NMR. They found that for the trimer **1.112** derived from **1.100**, the NH chemical shift difference was narrow (~0.15 ppm) and had ${}^3J_{\alpha N}$ coupling constants of 8.4–8.6 Hz. This resulted in φ being ca. –95°*. In comparison the data in solution that we obtained are closer to the ideal PPII helix (φ = –75°). None of these analyses have been undertaken for peptidomimetics **1.107** and **1.101**, simply by the fact that oligomers derived from these mimetics were not prepared.

The CD spectroscopic data, NMR studies and X-ray crystallographic data for dimer **4.1** strongly support the conclusion that oligomers derived from motif **1.125** adopt a PPII helix conformation. An application of pyroglutamate mimic **1.125** will be investigated in a specific protein-protein interaction in chapter 5.

^{*} In the paper, ${}^3J_{\alpha N}$ were found to be about 7.6–7.8 Hz. However in the supporting information, trimer **1.112** derived from **1.100** had ${}^3J_{\alpha N}=8.4$ –8.6 Hz. Based on the supporting information values we determined the torsion angle φ to be around –95°.

In order to investigate pyroglutamate based mimic 1.125 as an Xaa-trans-Pro mimic, we aimed to study a specific protein-protein interaction of PRMs with SH3 domains. Morton et al. 70 identified a 14 amino acid peptide residues 91-104 (p85p2) of the p85 α regulatory subunit of human phosphoinositide 3-kinase (PI-3-kinase) (http://www.uniprot.org/uniprot/P27986), that interacts with the SH3 domain of human Fyn kinase (Fyn-SH3) (http://www.uniprot.org/uniprot/P06241). We aimed to prepare a panel of peptides analogues of p85p2 incorporating our mimic 1.125 and study its interaction with Fyn-SH3 using NMR. A series of titration of Fyn-SH3 with the peptide analogues were carried out and chemical shift perturbation experiments of isotope labelled Fyn-SH3 were measured to obtain binding constants and identify interaction surfaces. The following sections include a brief introduction to the method and assignment of the ¹⁵N/¹³C labelled Fyn-SH3 domain as well as the protein-ligand interaction studies.

5.1 ¹⁵N-Heteronuclear single quantum correlation (HSQC) spectroscopy

An ¹⁵N–HSQC spectrum⁹⁶ shows the correlation between nitrogens attached to an hydrogen in the protein. By scalar coupling, magnetisation is transferred along N–H bonds. The spectrum gives rise to a resonance for each N–H bond present. Every backbone N–H gives a unique peak corresponding to a particular amino acid and its environment (**Figure 5.6**, section 5.3).⁹⁶

5.2 Triple resonance experiments

If a ¹³C and –¹⁵N labelled protein is available, magnetisation can be transferred between ¹H, ¹⁵N and ¹³C nuclei using a suite of triple resonance experiments that allow rapid sequential assignment of the resonances of the backbone atoms in a protein.⁹⁶ The principle of these experiments and the protein assignment is detailed below.

5.2.1 HNCA experiment

In an HNCA experiment the magnetisation of the amide hydrogen of an amino acid residue is transferred to the amide nitrogen. Then the magnetisation is transferred to the C_{α} of the

amino acid itself as well as the C_{α} of the previous residue. It is then transferred back to the same amide hydrogen for detection. The two $C\alpha$ resonances of a single amide then allow connecting the signals of the sequential residues in the amino acids sequence and hence assignment of the entire protein backbone (**Figure 5.1**).

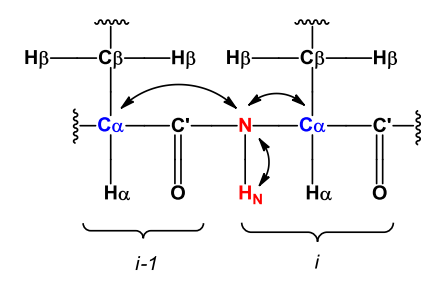


Figure 5.1: Schematic representation of magnetisation transfer during an HNCA experiment. 96

5.2.2 HNCACB experiment

The principle of the HNCACB experiment extends the HNCA transfers to C_{β} . The result is four peaks at an amide hydrogen frequency, the C_{α} and C_{β} of the amino acid residue (*i*) and the previous amino acid residue (*i*-1). The nature of the transfer pathway means that C_{β} signals are of opposite phase to the C_{α} resonances aiding the identification of C_{β} resonances and hence the assignment process (**Figure 5.2**).

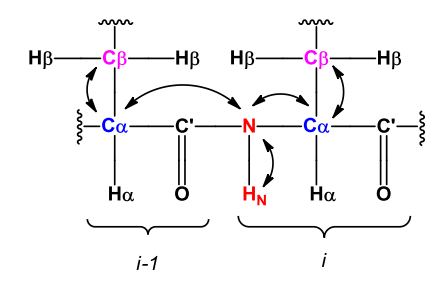


Figure 5.2: Schematic representation of magnetisation transfer during an HNCACB experiment.⁹⁶

5.2.3 CBCA(CO)NH experiment

In the CBCA(CO)NH experiment, magnetisation is transferred to the aliphatic protons to C_{β} and C_{α} atoms whose chemical shifts are recorded. The magnetisation is then transferred to the

amide nitrogen of the preceding amino acid via the carbonyl and to the amide hydrogen. (Figure 5.3). 96

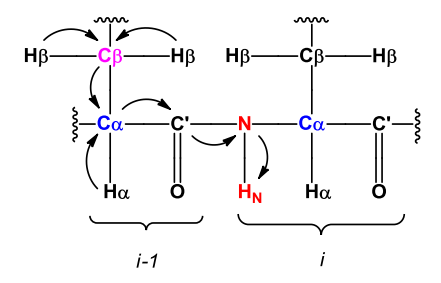


Figure 5.3: Schematic representation of magnetisation transfer during an CBCA(CO)NH experiment. 96

In a HNCACB experiment a strong correlation is observed between each NH group and $C\alpha$ and $C\beta$ in its own residue strongly and a weak correlation with the preceding residue. While CBCA(CO)NH only correlates the NH group to the preceding $C\alpha$ and $C\beta$ chemical shifts. A combination of the above experiments is used to link the N-H groups in a long peptide sequence (Figure 5.4).⁹⁶

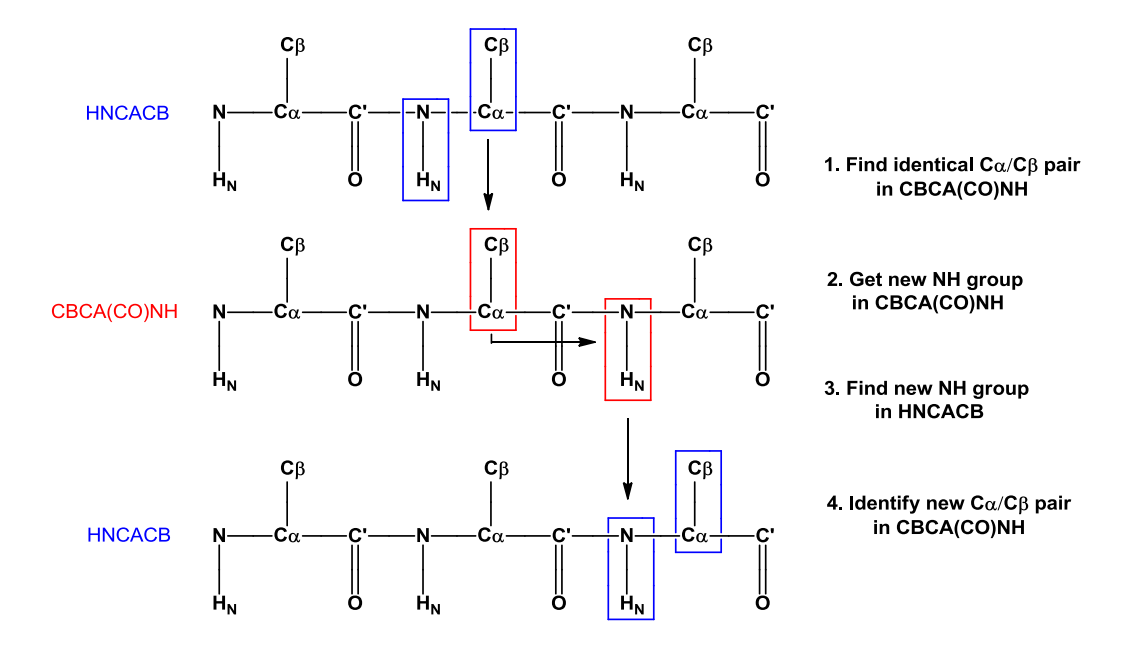


Figure 5.4: Schematic representation of the method of assignment. 96

5.3 Sequence resonance assignment

The complete assignment of the protein was undertaken using standard triple resonance experiments with a $^{13}\text{C}/^{15}\text{N}$ double labelled human Fyn-SH3 protein as described below (**Figure 5.6**). A representative sample of $^{1}\text{H}-^{13}\text{C}$ sections of the HNCACB spectrum ordered according to the amino acid sequence are shown in **Figure 5.5**. Selective strips taken from a NHCACB spectrum of the Fyn-SH3 domain are depicted. Sequential connectivities are marked by lines for C_{α} (black) and C_{β} (red) resonances. An example of the sequential assignment is described in **Figure 5.5**.

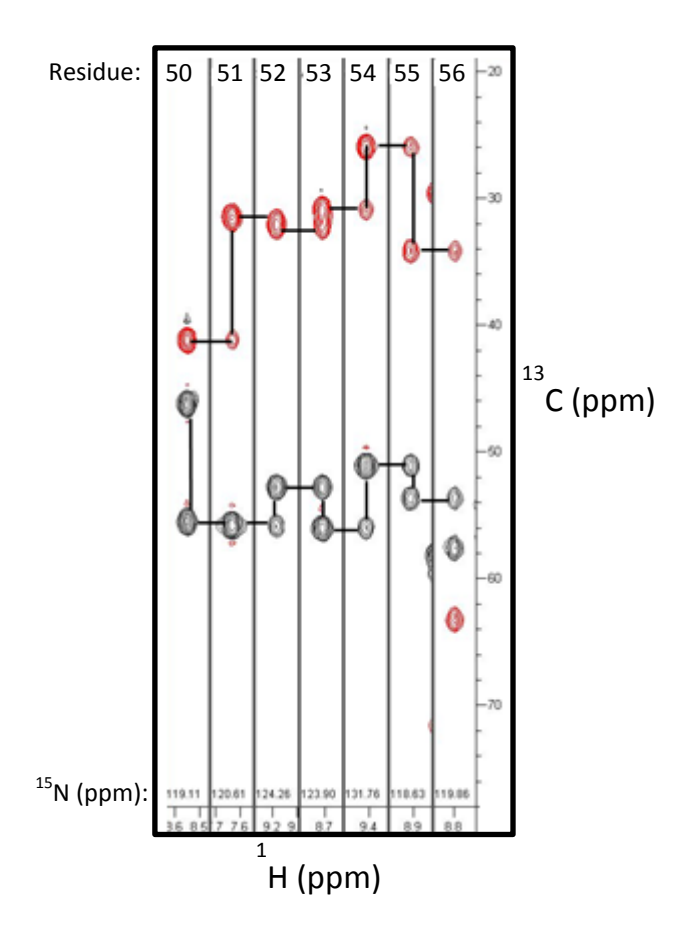


Figure 5.5: A representative series of two dimensional ${}^{1}H^{-13}C$ sections of the 3D NHCACB experiment of given ${}^{15}N$ position indicated by the ${}^{15}N$ chemical shift. Shown are strips extracted at the amide chemical shifts of Fyn residues 50-56 as indicated. Sequential connectivities are indicated by lines.

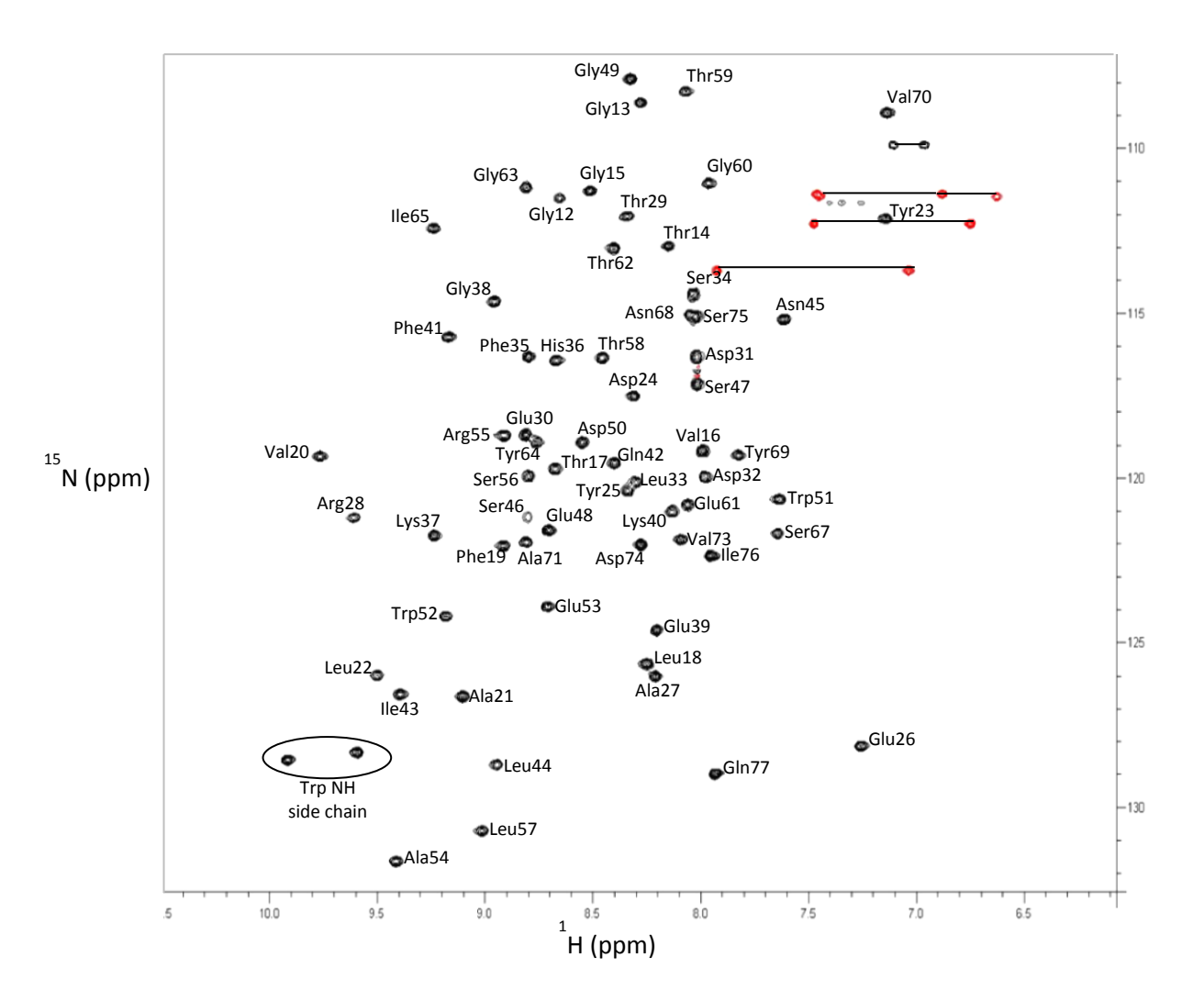


Figure 5.6: ${}^{1}\text{H}-{}^{15}\text{N}$ HSQC spectrum of the ${}^{15}\text{N}$ labelled Fyn SH3. Each correlation represents an NMR signal from the ${}^{1}\text{H}-{}^{15}\text{N}$ atom pair from one of the amino acid residues in the protein. Each resonance is labelled with its assigned amino acid. NH₂ groups are connected by drawing lines (4 pairs in red in one in black) arising from Asn68, Asn45, Gln42, Arg55 and Gln77 NH₂ side chains.

To investigate any problem of solubility of the peptides in phosphate buffer $^{15}N/^{13}C$ HSQC of Fyn-SH3 was also recorded in phosphate buffer with 10% DMSO- d_6 . Similar spectrum was obtained proving that the protein was stable with 10% DMSO- d_6 .

5.4 Protein-ligand interaction studies

For the analysis of protein-ligand interactions 2D ¹H–¹⁵N HSQC spectroscopy is well suited. This is due to the fact that the backbone N–H chemical shifts are highly sensitive to their local environment, thus a slight change can easily be observed with a change in chemical shift. Chemical shifts of signals in HSQC change when the corresponding amino acid is in proximity to the bound ligand. Information on the binding site, the affinity and kinetics of the interaction are then obtained. Thus, the ligand binding site can be localised on the protein.

The simplest protein ligand equilibrium may be described by the presence of the free protein and ligand, P, L and their complex PL that associate with a rate k_{on} and dissociate k_{off} :

In this case the dissociation constant K_D is the ratio of k_{off} and k_{on} . A peculiar and immensely powerful feature of NMR is that the kinetics of the reaction is related to chemical shift difference of the free and ligand bound signals. As a consequence using NMR it is in principle possible to obtain kinetic information from an equilibrium measurement. Assuming that the rate of association is diffusion controlled, there are two distinct regimes of observing the interaction. Slow exchange occurs when the k_{off} rate of the ligand is smaller than the chemical shift difference ($k_{off} << \Delta \delta$). In this case a titration of ligand leads to a gradual disappearance of the free protein signal and simultaneously reappearing at the resonance of the signal of the complex. If however the rate of dissociation is much faster, the chemical shift difference of the free and bound signal is $k_{off} >> \Delta \delta$, where the reaction is said to be in fast exchange leading to signals gradually moving from the free to bound resonance. Finally, the intermediate exchange occurs when $k_{off} \sim \Delta \delta$ which leads to broadening of the resonances.

In the current study, the interaction was by and large in the fast exchange regime allowing the dissociation constant (K_D) to be extracted using the equation 1:

$$\frac{\Delta}{\Delta \max} = \frac{(K_D + [L] + [P]) - \sqrt{(K_D + [L] + [P])^2 - 4[P][L]}}{2[P]} (1)$$

where Δ represents the difference of the measured shift at any maximum (Δ max) ligand concentration and the shift of the free protein. [L] and [P] are the ligand and protein concentrations respectively

Finally, the chemical shift perturbations observed for hydrogen ($\Delta\delta_H$) and nitrogen ($\Delta\delta_N$) atoms in the amide bond are combined into a single parameter using the following weighting:⁹⁶

$$\Delta \delta_{\text{H,N}} = \sqrt{(\Delta \delta_{\text{H}})^2 + 1/6 (\Delta \delta_{\text{N}})^2}$$

where $\Delta\delta_{H,N}$ represents the overall N–H chemical shift perturbations.

In favourable cases plotting N–H chemical shift perturbation in ligand saturation for each amino acid allows the identification of a ligand binding site.

5.5 Synthesis of *N*-Ac-Arg-Pro-Leu-Pro-Val-Ala-Pro-Gly-NH₂ 1.139 and its analogues

As described in section 1.5.4, Morton *et al.*⁷⁰ described a study of the structural basis for the interaction of the SH3 domains of Fyn with ligands sequences. The synthetic peptide p85p2 (PPRPLPVAPGSSKT) was identified to bind the Fyn-SH3 domain ($K_D = 50 \,\mu\text{M}$). **Table 5.1** shows the important amino acids (blue colour) of p85p2 that interact with Fyn SH3, determined by nOe.

Fyn SH3 atoms	p85p2 atoms	Analogues		5
		1.141	1.140	1.142
Trp51	Arg3			
Trp51	Leu5	1.125		1.125
Trp51	Pro6	1.123		1.123
Tyr69	Pro6			
Tyr23, Asn55, Tyr69	Ala8	_	1.125	1.125
Tyr69	Pro9		1.123	1.123

Table 5.1: Summary of the nOe correlations observed between the Fyn SH3 domain and peptide p85p2.⁷⁰

We aimed to synthesise a series of analogues derived from p85p2 incorporating our pyroglutamate based mimic **1.125** in the peptide sequence. A binding study with Fyn-SH3 can then show if a disruption in the binding or a positive interaction is obtained with mimic **1.125** incorporated in the sequence. Following this, fragments **Leu-Pro** and **Ala-Pro**, which are known to be involved in binding, will be replaced by the constrained Xaa-*trans*-proline mimic **1.125** synthesised in our group (**Figure 5.7**).

Figure 5.7: Constrained Xaa-trans-proline mimic 1.125.

The following parent 8mer and its analogues were synthesised (section 5.5.1):

- N-Ac-Arg-Pro-Leu-Pro-Val-Ala-Pro-Gly-NH₂ (Parent 8mer 1.139)
- N-Ac-Arg-Pro-Leu-Pro-Val-1.125-Gly-NH₂ (analogue 1.140)
- N-Ac-Arg-Pro-1.125-Val-Ala-Pro-Gly-NH₂ (analogue 1.141)
- *N*-Ac-**Arg**-Pro-**1.125**-Val-**1.125**-Gly-NH₂ (analogue **1.142**).

The affinity of interaction between the SH3 domain and the four synthetic peptides will be studied by BioNMR. Binding properties of peptides **1.139**, **1.140**, **1.141** and **1.142** will be then compared to results obtained by Morton *et al*. 50

5.5.1 Solid phase synthesis

Since the development of SPPS, peptide preparation on a small to medium scale has been often undertaken on solid support. One of the primary advantages of solid phase methodology was to overcome the technical difficulties associated with solubility and purification of growing peptide chains in solution. ^{96c} In order to obtain a series of RPLPVAPG peptides we developed a solid phase approach using the Fmoc-based methodology.

Linear peptides were synthesised using manual solid phase techniques employing the Fmoc protection strategy. All of the amino acids used in the synthesis of these compounds were Fmoc-L-amino acids building blocks.

The *Rink amide resin* (**Figure 5.8**) was used as a solid support in order to yield a C-terminus amide (CO-NH₂).

Figure 5.8: Structure of the Rink amide resin. 96c

To monitor the amide bond formation or Fmoc-deprotection at each step, two colour tests were used:

The *Kaiser test* is a useful method to determine the presence of '*N*-free' amino group. Using this test we were able to monitor coupling reactions and deprotection steps. Ninhydrin reacts with the primary free amine giving a blue chromophore. For the amide bond coupling, completion of the reaction was also monitored using the Kaiser test, when the beads were colourless the primary free amine was consumed. Using the same principle, the Chloranil test was used to follow coupling reactions with secondary amines such as proline residues. In the presence of a fully deprotected free secondary amino group the resin beads turned deep blue in colour, indicating a positive result. On completion of the coupling reaction on the secondary amino group, a pale yellow solution/colourless beads were obtained.

Amide coupling was conducted using DIC and HOBt or HBTU in the presence of DIPEA in DMF. N-terminus acetylation of the peptides was undertaken using acetic anhydride. Cleavage of the peptide from the resin and removal of side chain protecting group (Pbf) was then undertaken using a mixture of TFA/TIS/H₂O (96:2:2). The crude residue was then purified by precipitation using a mixture of DCM/MeOH and Et₂O.

5.5.2 Synthesis of *N*-Ac-Arg-Pro-Leu-Pro-Val-Ala-Pro-Gly-NH₂ 1.139 and its analogues 1.140, 1.141 and 1.142.

The Rink amide resin was first treated with a solution of 20 % piperidine in DMF to obtain the free *N*-terminus of the solid support. Fmoc-L-amino acids were activated as above, except in the case of Fmoc-L-Arg(Pbf)-OH which was activated using HBTU in the presence of DIPEA in DMF. This activation with HBTU is often recommended for difficult couplings, such as the branched side chain of arginine. The deprotection and coupling steps were repeated for each amino acid coupled to the sequence. The resin beads were subjected to a stepwise assembly of Fmoc-L-Gly-OH, Fmoc-L-Pro-OH, Fmoc-L-Ala-OH, Fmoc-L-Val-OH, Fmoc-L-Pro-OH, Fmoc-L-Leu-OH, Fmoc-L-Pro-OH and Fmoc-Arg(Pbf)-OH. *N*-terminus of the peptide was treated with a 50% solution of acetic anhydride in pyridine. The peptide residue was cleaved from the solid support using a mixture of TFA/TIS/H₂O, which also deprotects Pbf protecting group. Precipitation of the peptide was undertaken using a mixture of DCM/MeOH with Et₂O (Scheme 5.1).

Reagents and conditions: a) 20% piperidine/DMF; b) Fmoc-AA-OH (5.0 equiv.), DIC (3.0 equiv.), HOBt (3.0 equiv.), DIPEA (3.0 equiv.), DMF or HBTU (5.0 equiv.), DIPEA (3.0 equiv.), DMF; c) 20% piperidine/DMF then $Ac_2O/pyridine$ (3.0 equiv.); d) TFA/TIS/H₂O (96:2:2), 45%.

Scheme 5.1: Synthesis of *N*-Ac-Arg(H)-Pro-Leu-Pro-Val-Ala-Pro-Gly-NH₂ **1.139**.

Pyroglutamate mimic **1.125b** was converted to the Fmoc protected carboxylic acid **1.125d** in 71% yield (Figure 5.9).

Chapter 5 BioNMR studies using 1.125 as trans-proline mimic

Reagents and conditions: a) i) LiOH 1M in THF, quant., ii) TFA (20%) in CH_2Cl_2 , quant.; b) Fmoc-OSu, sat. aq. NaCO₃, dioxane, 71%.

Scheme 5.9: Synthesis of Fmoc protected pyroglutamate mimic **1.125d**.

In a similar procedure, analogues **1.140**, **1.141** and **1.142** were successfully synthesised by solid phase support in 40%, 48%, 41% yield respectively.

5.6 NMR experimental setup

Dr. Duriez has undertaken the expression and purification of the labelled Fyn SH3 domain. NMR spectra of the isotopically labelled SH3 domain were collected at 25 $^{\circ}$ C with a 600 MHz four-channel Varian INOVA NMR spectrometer equipped with a 5 mm triple resonance z-gradient cold probe. Resonance assignments of the free protein and peptide bound form of the backbone 15 N and H-N nuclei were obtained by a combination of 2D 1 H- 15 N-HSQC, as well as HNCA, HNCACB and CBCA(CO)NH spectra. The NMR experiments were conducted on a 0.1 mM protein solution of potassium phosphate buffer (10 mM, pH 6.0), 5% D₂O and 10% DMSO- d_6 and to enhance the solubility of peptides analogues while not affecting the protein and the interactions. Identical HSQC of Fyn-SH3 was observed with or without DMSO- d_6 .

NMR data were processed with NMRPipe, applying sine function, zero filling and phasing prior to Fourier Transformation and analysed with NMRView.

The localisation of the peptide binding site was obtained by nine 2D $^{1}H^{-15}N$ -HSQC spectra at a concentration ratio of peptide: protein of 0:1, 0.25:1, 0.5:1, 0.75:1, 1:1, 2:1, 4:1, 8:1, 12:1 and 20:1.

For the titration experiments, protein concentrations were kept constant while increasing the concentration of ligand. Upon peptide addition, the chemical shift perturbation was calculated by weighting 1HN and ^{15}N chemical shift differences using the formula described in section 5.4. The equilibrium binding constant (K_D) was obtained for residues in fast exchange by fitting K_D to the fractional shift (Δ/Δ max) using equation 1.96

5.7 Binding studies

5.7.1 Parent peptide **1.139**

Ligand binding induces chemical shift perturbations at the binding site of the protein. Using N-H protein assignment, the binding site can be mapped to the protein sequence.

Morton *et al.*⁷⁰ described the NMR study of Fyn-SH3 with p85p2 (PPRPLPVAPGSSKT). They identified contacts by nOe experiments of the SH3 domain-p85p2 complex for residues Tyr23, Tyr69, Asn68 and Trp51. They also determined contacts between the leucine residue of p85p2 and the following SH3 residues: Gly49, Asp50, Trp51, Pro66, Ser47, Asn68 and Trp69.

¹⁵N $^{-1}$ H HSQC (solvent: phosphate buffer + 10% DMSO- d_6) were recorded for our peptide **1.139** at different peptide : protein ratios (as previously up to 12 : 1) (**Figures 5.10** and **5.11**).

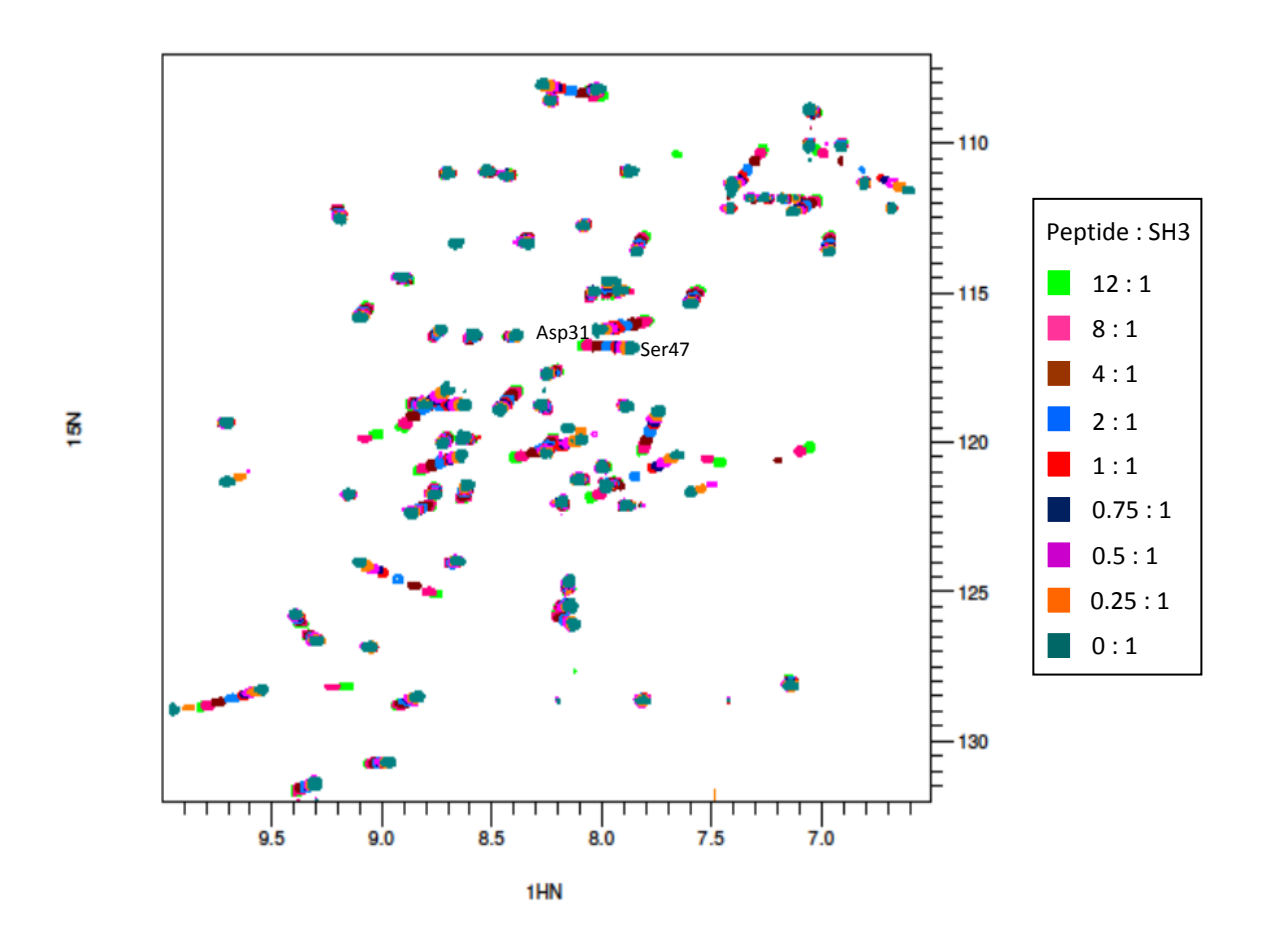


Figure 5.10: Overlay of nine 2D-¹H-¹⁵N-HSQC spectra obtained for the titration of SH3 with peptide **1.139** with increasing concentration of **1.139**.

Chapter 5 BioNMR studies using **1.125** as trans-proline mimic

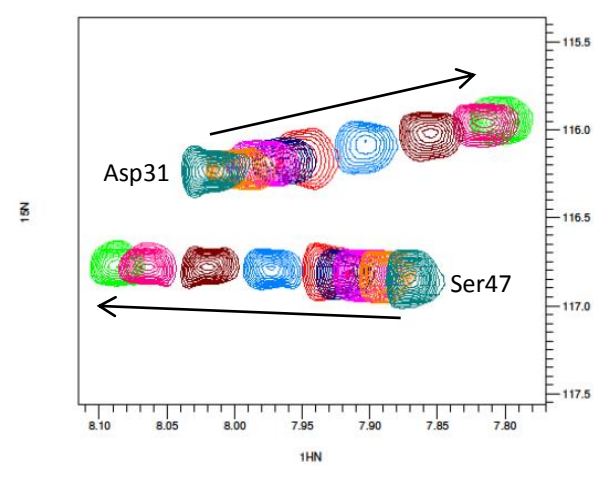


Figure 5.11: The gradual shift of the protein resonances with increasing ligand concentration indicated by arrows for residues Asp31 and Ser47.

The effects combined with only small changes in the line widths indicate that the reaction is generally well described by the fast exchange regime. There are eight residues that show significant perturbations while most signals show no or very small perturbations consistent with a defined binding site. It is also worth noting that most of the perturbations follow a straight line indicating that the association follows a simple equilibrium involving only free and bound protein.

We were able to plot a histogram showing the ${}^{1}H^{-15}N$ chemical shift perturbations for each residue of the SH3 domain (**Figure 5.12**). In order to visualise the binding site, amino acids showing chemical shift perturbations larger than 0.2 ppm were selected to be involved in the binding.

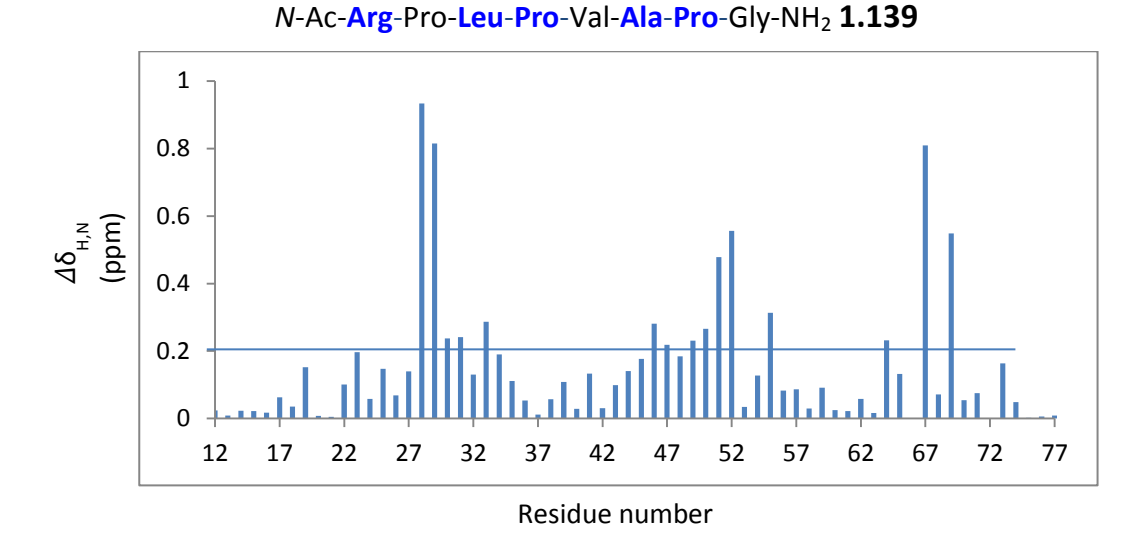


Figure 5.12: ¹H–¹⁵N chemical shift perturbations for each residue of the SH3 domain. Prolines residues lack an amide hydrogen and are not shown.

The greatest differences in the pattern of chemical shift changes in the fast exchange occurred for residues Tyr23, Asp31, Gly49, Asp50, Trp51, Trp52, Ser47, and Tyr69. These changes matched the previous study conducted by Morton *et al.*⁷⁰ Binding curves were determined by plotting the fractional shift (Δ/Δ_{max}) against ligand concentration (molar excess of peptide over protein). Two examples of Asp31 and Ser47 are shown in **Figure 5.13** while the complete data set is found in appendix 5.6.1. The small fractional shift changes at high ligand concentration indicated that the protein is saturated with ligand and hence binding curves could be derived by fitting equation **1** relating chemical shift to the peptide: protein ratio (see section 5.6).

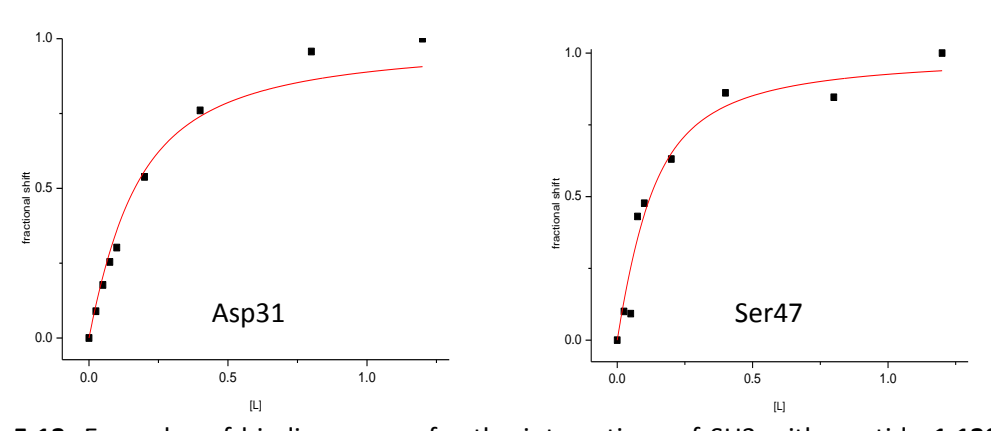


Figure 5.13: Examples of binding curves for the interactions of SH3 with peptide **1.139**. The change in chemical shift at different protein : peptide ratios (see appendix for full binding data).

The K_D was also determined for each residue above the 0.2 ppm cut-off and is shown in **Table 5.2**. Apart from Gly49, Ser47 and Trp51 the fitted K_D are remarkably homogeneous yielding an average K_D of 120 μ M. For Gly49, Ser47 and Trp51 the average K_D is 41 μ M.

Residues	K _D (μM)
Tyr23	123
Trp52	120
Asp31	125
Gly49	11
Tyr69	124
Ser47	71
Asp50	112
Trp51	42

Table 5.2: Residues with $\Delta\delta$ >0.2 ppm in chemical shift changes with K_D values determination for analogue **1.139**. (Curve fitting was carried out using Origin 8.6).

A 3D representation shows the residues involved in binding are located in the same region of the protein described by Morton *et al.*⁷⁰ Moreover, Morton *et al.*⁷⁰ determined the K_D of the 14mer (PPRPLPVAPGSSKT) with Fyn-SH3 to be 50 μ M; as compared to our parent 8-mer **1.139** (**Figure 5.14**).

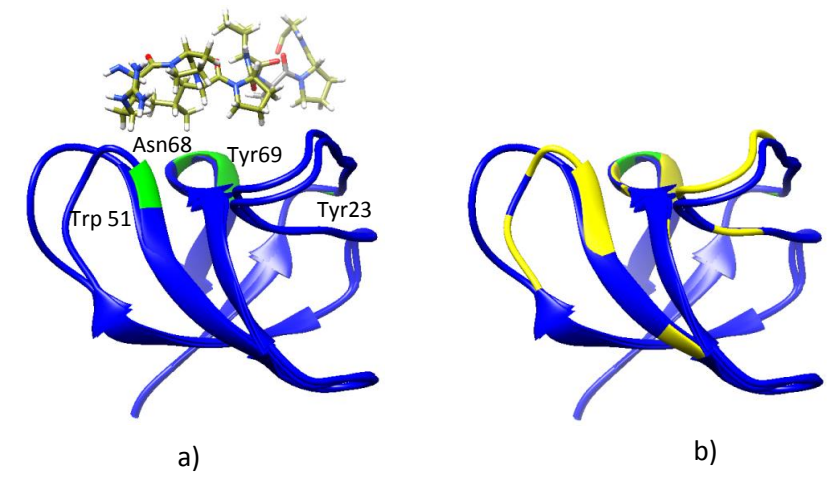


Figure 5.14: Backbone representation of the overlay of the X-ray structure of the free human Fyn-SH3 (pdb entry 1NYF) with the average NMR structure of the protein in complex with p85p2 peptide (pdb entry 1AZG), the peptide is shown in a stick representation. Residues in the SH3 domain are coloured according to the interaction of the ligands. a) Residues that show nOes between SH3 domain and peptide p85p2 by Morton *et al.*⁷⁰ are coloured in green; b) Residues that show chemical shift perturbations induced by binding to peptide 1.139 are shown in yellow. (Figure produced by UCSF Chimera software).

The difference in the K_D values between Morton *et al.*⁷⁰ study and ours is strongly due two parameters: the length of the peptide-ligand (8 residues in peptide **1.139** instead of 14 residues for Morton *et al.*⁷⁰) and the addition of DMSO- d_6 which might play a role on the binding property. In addition, in terms of energy ($\Delta G = -RT \ln(K_D)$), it means than the difference in energy between the two different peptide ligands is about 1.6 kJ.mol⁻¹. Considering that a hydrogen bond can vary from very weak (1-2 kJ.mol⁻¹) to very strong (~150 kJ.mol⁻¹), we can conclude that it is not a big difference between p85p2 and our parent peptide **1.139**.

5.7.2 Binding studies with analogues 1.140, 1.141 and 1.142

Following the same procedure, titration with analogue **1.140** was recorded using $^{15}N-^{1}H$ HSQC (solvent: phosphate buffer + 10% DMSO- d_6) (see Appendix).

The effects combined with only small changes in the line widths indicate that the reaction is generally well described by the fast exchange regime. The chemical shift perturbation versus residue number is represented in **Figure 5.15**. The perturbations with analogue **1.140** were similar to the parent peptide **1.139** localised in the following residues: Glu30, Trp51, Ser47, Ser67, Gly49, Asp50, Trp52 and Tyr69. Binding curves were plotted for residues involved in fast exchange and K_D was measured to be about 300 μM (**Table 5.3**).

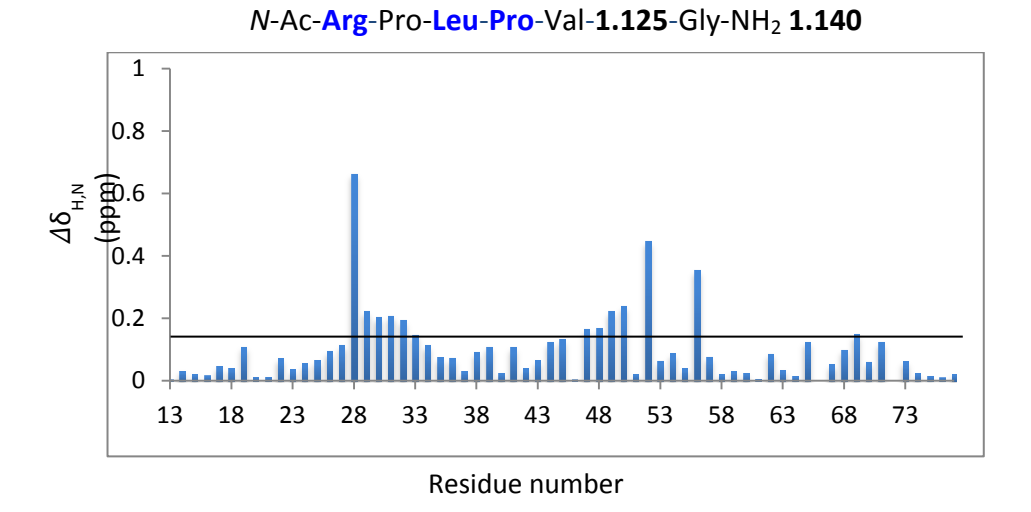


Figure 5.15: Histogram of the amide chemical shift perturbation upon *N*-Ac-**Arg**-Pro-**Leu-Pro**-Val-**1.125**-Gly-NH₂ **1.140** binding.

Residues	K _D (μM)
Glu30	203
Asp31	563
Asp32	13
Ser47	153
Asn48	410
Gly49	515
Asp50	326
Trp52	364
Tyr69	293

Table 5.3: Residues with with $\Delta\delta$ >0.17 ppm in chemical shift changes with K_D values determination for analogue **1.140**. (Curve fitting was carried out with Origin 8.6).

Analogue **1.140** showed a similar binding mode as the parent peptide **1.139** (**Figure 5.16**). K_D values obtained with analogue **1.140** showed a slightly lower affinity with Fyn-SH3 (K_D ca. 360 μ M) in comparison to parent peptide **1.139** (K_D ca. 120 μ M) apart for residue Asp32. Incorporation of mimic **1.125**, as an Ala-*trans*-Pro mimic, in the selective peptide does not disrupt the binding interaction. However a reduction of affinity with analogue **1.140** was observed and we can postulate that the incorporation of mimic **1.125** could affect firstly the side chains configuration, secondly the flexibility of the peptide-ligand and thirdly the hydratation of the peptide-ligand compared to parent peptide **1.139**. These three parameters

could affect individually or together the difference in affinity between parent peptide **1.139** and peptide **1.140** with Fyn-SH3.

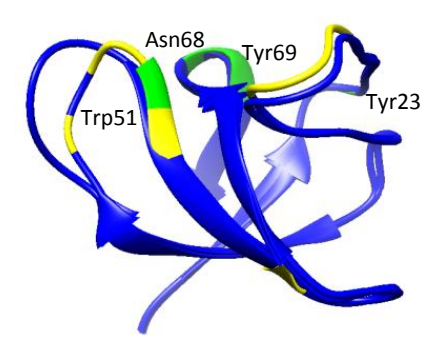


Figure 5.16: Backbone representation of the overlay of the X-ray structure of the free human Fyn-SH3 (**pdb entry 1NYF**) with the average NMR structure of the protein in complex with p85p2 peptide (**pdb entry 1AZG**). Residues in the SH3 domain are coloured according to the interaction of the ligands. Residues that show nOes between SH3 domain and peptide p85p2 by Morton *et al.*⁷⁰ are coloured in green; residues that show chemical shift perturbations induced by binding to peptide **1.140** are shown in yellow. (Figure produced by UCSF Chimera software).

Morton *et al.*⁷⁰ described the study of two synthetic peptides: p85p2 (PPRPLPVAPGSSKT) and p85p3 (PPRPTPVAPGSSKT). The only difference is the substitution of the leucine residue by the threonine as highlighted in blue. This replacement into the sequence resulted in approximately a fivefold decrease in affinity of p85p3 peptide for the Fyn-SH3 domain. This result suggested that the interaction between this position of the peptide and the SH3 module contributed significantly to the affinity of binding.

The synthesis of analogues **1.141** and **1.142** involved the replacement of the leucine residue in the selected peptide: *N*-Ac-Arg-Pro-1.125-Val-Ala-Pro-Gly-NH₂ (analogue 1.141).

N-Ac-**Arg**-Pro-**1.125**-Val-**1.125**-Gly-NH₂ (analogue **1.142**).

Titrations were recorded for both peptides with the Fyn-SH3 domain (see Appendix). Histograms of the amide chemical shift perturbation *versus* residue number are illustrated below (**Figures 5.17** and **5.18**).

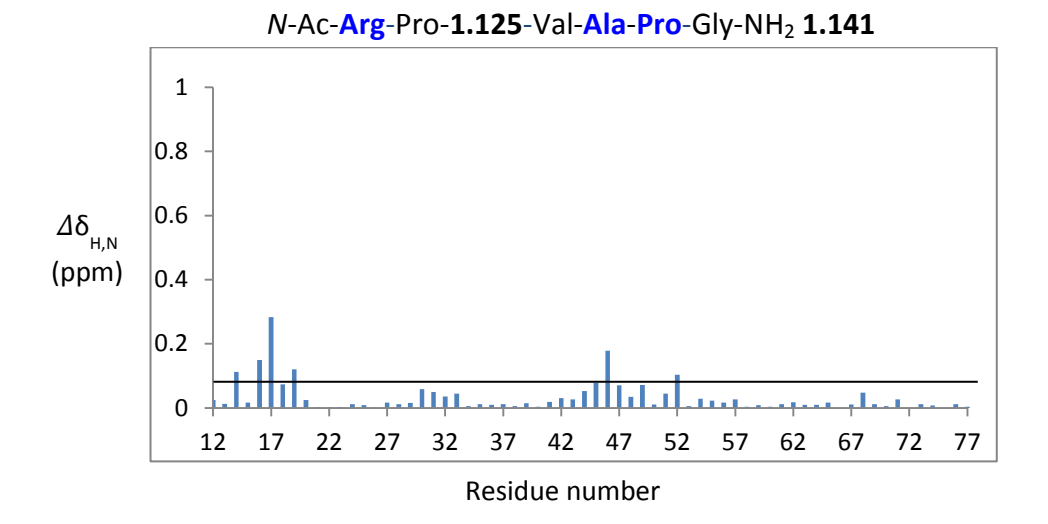


Figure 5.17: Histograms of the amide chemical shift perturbation upon binding, with analogue **1.141**.

The perturbations observed for analogue **1.141** were very weak in comparison to the others. The greatest differences in the pattern of chemical shift changes occurred for the residues Val16, Thr17, Asn45 and Ser47 where the binding constant K_D was determined (**Table 5.4**).

Residues	K _D (μM)
Val16	970
Thr17	731
Asn45	665
Ser47	771
Trp52	851

Table 5.4: Residues with with $\Delta\delta$ >0.1 ppm in chemical shift changes with K_D values determination for analogue **1.141**. (Curve fitting was carried out with Origin 8.6).

In comparison to the previous binding studies of peptides **1.139** and **1.140** with Fyn-SH3, affinity of analogue **1.141** was about an order of magnitude lower than the parent peptide. It also showed that the regions of the SH3 domain involved in binding were different as the residues were also different. A possible new binding site might be present in this case.

Binding analysis for analogue **1.142** showed a very weak affinity in comparison to parent 8mer **1.139** and analogue **1.140** (Figure 5.18). Tables 5.4 and 5.5 describe the corresponding K_D measured. For analogues **1.141** and **1.142**, the K_D determination is less accurate than for the

parent peptide **1.139** or analogue **1.140** because of the small chemical shift perturbations and shows increased variation between individual amino acids.

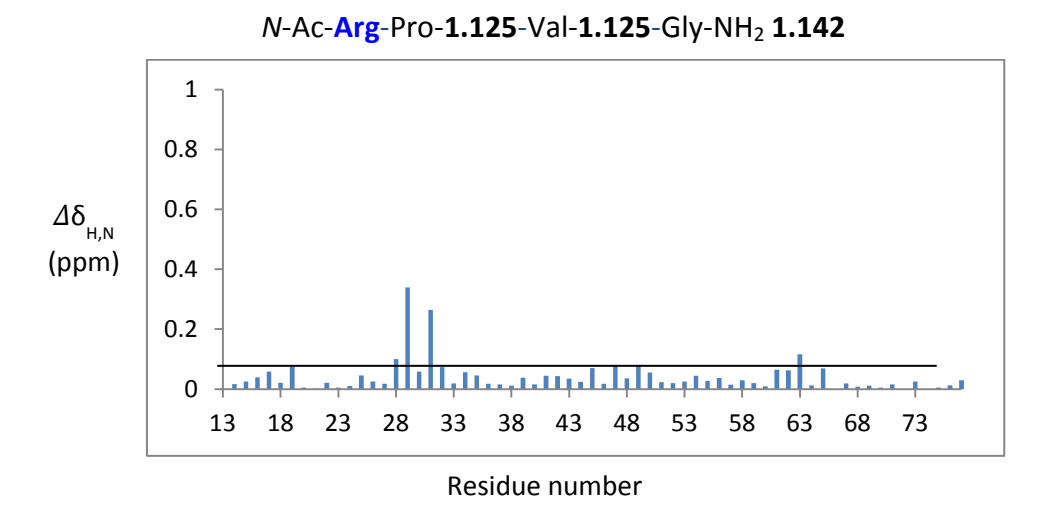


Figure 5.18: Histograms of the amide chemical shift perturbation upon binding, with analogue **1.142**.

Residues	K _D (μM)
Phe19	429
Asp31	149
Asp32	142
Ser47	681
Gly49	741
Gly63	579
lle65	910

Table 5.5: Residues with $\Delta\delta$ >0.075 ppm in chemical shift changes with K_D values determination for analogue **1.142**. (Curve fitting was carried out on Origin 8.6).

As observed for peptide **1.141**, binding studies with peptide **1.142** showed a very weak affinity. The SH3 ligand-binding site could not be clearly identified as perturbations are very small and the affected residues do not show a consistent pattern of perturbations (**Figure 5.19**).

Chapter 5 BioNMR studies using **1.125** as trans-proline mimic

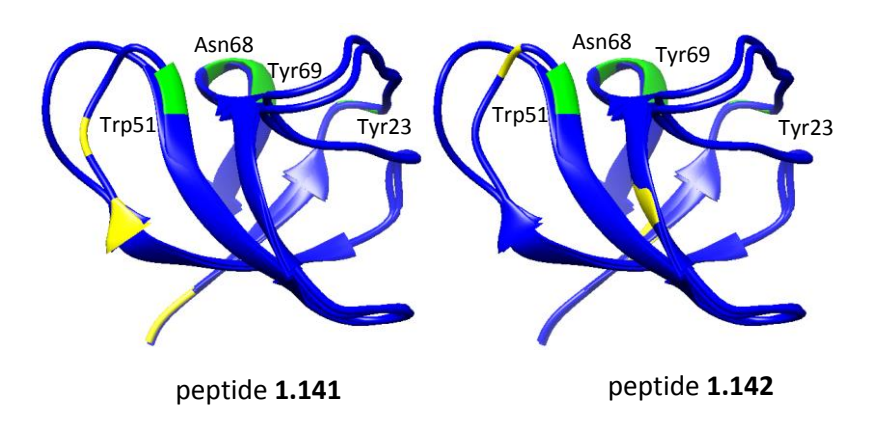


Figure 5.19: Backbone representation of the overlay of the X-ray structure of the free human Fyn-SH3 (pdb entry 1NYF) with the average NMR structure of the protein in complex with p85p2 peptide (pdb entry 1AZG). Residues in the SH3 domain are coloured according to the interaction of the ligands. Residues that show nOes between SH3 domain and p85p2 by Morton *et al.*⁷⁰ are coloured in green; residues that show chemical shift perturbations induced by binding to peptide 1.141 or 1.142 are shown in yellow. (Figure produced by UCSF Chimera software).

The collective NMR studies clearly demonstrate that the pyroglutamate based mimic **1.125** developed in our group could be used as a *trans*-proline mimic without disrupting the SH3-ligand binding interaction (example with analogue **1.140**). However, the loss of the leucine residue from the parent peptide **1.139** showed a strong decrease in binding affinity. This was consistent with the previous observations by Morton *et al.*⁷⁰ suggesting that the interaction between this residue of the peptide and SH3 domain is significant.

They⁷⁰ also demonstrated that the single replacement of the leucine residue of peptide p85p2 by a threonine residue giving peptide p85p3 showed a five-fold decrease in the binding affinity. Upon the hypothesis that the side chain of the leucine residue is an important factor in the binding affinity, we next targeted a second-generation *trans*-proline mimetic **5.1** where the specific alkyl chain could mimic the desired leucine residue (**Figure 5.20**).

Figure 5.20: Second generation mimic 5.1.

6. Project perspective, current development and outlook

As highlighted in chapter 2, we confirmed that peptide N-Ac-Pro-Arg(NO₂)-Gly-Pro-Arg(NO₂)-Pro-OMe **2.1** showed excellent anticancer activity against RT112 cell line, without killing normal fibroblasts MRC5-hTERT. This activity was similar to that reported by Warenius $et\ al.^{39}$ with peptide N-Ac-Pro-Arg(H)-Gly-Pro-Arg(H)-Pro-NH₂ **2.2**. We decided to use N-Ac-Pro-Arg(NO₂)-Gly-Pro-Arg(NO₂)-Pro-OMe **2.1** as a positive control due to challenges faced when preparing peptide **2.2** in solution phase.

In order to improve the biostability of the lead compound *N*-Ac-Pro-Arg(H)-Gly-Pro-Arg(H)-Pro-NH₂ **2.2**, we went on to develop peptidomimetics of *trans*-proline. Using a combination of functionalisation methods of cytisine **1.67** at position 6 and 9, peptidomimetics of *trans*-proline **1.68** were prepared (**Figure 6.1**). The first analogue *PRGPRP **2.16** with the incorporation of cytisine derivative, was synthesised and tested on RT112 cell line. It was found that survival cancer cells were present after 29 days, thus **2.16** proved inactive. In parallel, the development of a Gly-*trans*-Pro mimic **1.70** was investigated (**Figure 6.1**). After several attempts at optimising the key nitration step, a route using Ac₂O and HNO₃ was found to give a reasonable selectivity and good purity to afford **1.70**, albeit in very poor yield. After the clonogenic assays observed for peptide *PRGPRP **2.16**, we concluded that the cytisine building block was not a suitable mimic.

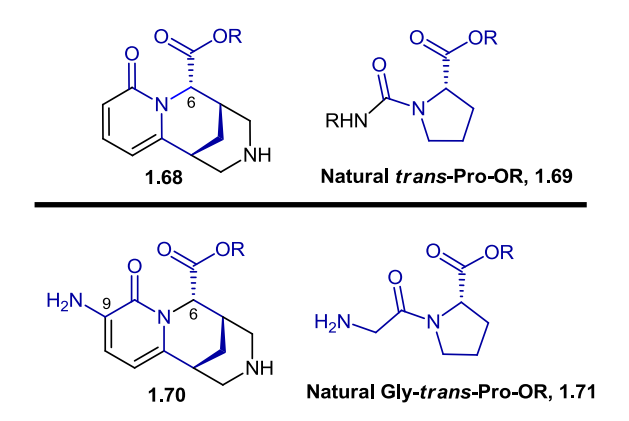


Figure 6.1: Synthesis of *trans*-proline mimics 1.70 and 1.68 based on (–)-cytisine.

The PRGPRP sequence is proline rich, a common property of proline rich motifs is that they adopt a PPII helix conformation. Based on the optimal dihedral angles of the PPII helix

conformation ($\phi = -75^{\circ}$, $\psi = 145^{\circ}$), pyroglutamate based mimic **1.125** was designed and prepared in 10% overall yield over twelve steps (**Figure 6.2**).

Figure 6.2: Pyroglutamate based mimic 1.125.

PR*G*PRP analogue **3.36** based on pyroglutamate mimic **1.125** was synthesised and tested on both RT112 and MRC5-hTERT cell lines. We observed apparent survival cells after 31 days following the cells exposure to **3.36** at varying concentrations (1 mM to 5 mM). We observed that cells had a different shape when compared to the control cells, which appeared to be debris of cells. The toxicity of **3.36** against MRC5-hTERT was comparable to the positive control **2.1**, meaning that the use of pyroglutamate mimic **3.36** in the PRGPRP sequence was a good example of the remaining activity without being toxic between 3 and 1 mM.

Since pyroglutamate based mimic **1.125** is a dipeptide mimic, we prepared oligomers derived from **1.125** to study their conformation and compare them with that of the PPII helix (**Figure 6.3**). Using CD spectroscopy, X-ray and NMR, we found that our oligomers adopted an 'ideal' PPII helix conformation; these positive results further validated our design and synthesis of **1.125**.

Figure 6.3: Oligomers derived from 1.125.

To investigate the potential of mimic **1.125**, study of a specific protein-protein interaction was undertaken. It is known that SH3 domains bind PPII motifs, and Morton *et al.*⁷⁰ identified a peptide p85p2. A series of analogues derived from p85p2 were prepared incorporating mimic **1.125** and binding studies were undertaken. The studies revealed that analogue **1.140** was interacting with the protein in the same mode as the control peptide **1.139** but with a slightly

Chapter 6 Project perspective, current development and outlook

lower binding affinity. Morton's study also showed that the loss of the leucine residue in the peptide ligand caused a fivefold decrease in the binding affinity. Binding studies with analogues **1.141** and **1.142**, where the leucine is deliberately replaced by our mimic dipeptide in the sequence also showed a very weak binding affinity, consistent with the previous observations reported by Morton *et al.*⁷⁰ We assumed that the leucine side chain might play an important role in the binding affinity. We therefore decided to target a second-generation mimic **6.1** (**Scheme 6.1**). This dipeptide could mimic any side chain of the Xaa residue in a Xaa*trans*-Pro mimic. Our retrosynthetic approach involved accessing the final mimic from precursor **6.2** via ring closing metathesis. The precusor **6.2** could be obtained by coupling of the advanced fragments **6.3** and **6.4** (**Scheme 6.1**).

Scheme 6.1: Retrosynthetic approach of **6.1**.

Fragments **6.3** and **6.4** were previously described in the literature. Fragment **6.3** was prepared following the synthesis developed by Zaminer *et al.*⁶² from commercially available L-pyroglutamic acid **1.116**. Allylation was performed to give a 3 : 1 ratio of diastereoisomers **1.122a** which was directly subjected to ozonolysis to give **1.123** after reductive work-up. Elimination of the OH functionality of **1.123** was undertaken through ozone oxidation of an intermediate *o*-nitrophenylselenide. Boc deprotection with TMSOTf allowed the isolation of the pure *cis*-isomer **1.115**. Following this route, we prepared the advanced intermediate **1.115** in 15% yield overall (**Scheme 6.2**).

Chapter 6 Project perspective, current development and outlook

Reagents and conditions: a) $HClO_4$, tBuOAc , RT, 15 h, quant.; b) Boc_2O , DMAP, MeCN, RT, 15 h, 84%; c) i) L-Selectride®, CH_2Cl_2 , -78 oC , 2 h, ii) PTSA, MeOH, RT, 15 h, 86% over two steps; e) Allyl-TMS, $BF_3 \cdot Et_2O$, CH_2Cl_2 , -78 oC , 30 min, 79%; f) O_3 , -78 oC , then $NaBH_4$, CH_2Cl_2 /MeOH, RT, 12 h, 70%; g) $(o-NO_2Ph)SeCN$, $P(^nBu)_3$, Py, THF, RT, 30 min, 94%; h) O_3 , CH_2Cl_2 , Δ , 30 min, 90%; i) TMSOTf, CH_2Cl_2 , O oC , 5, min, then chromatographic separation of diastereoisomers.

Scheme 6.2: Synthesis of 1.115.

Retrosynthetic analysis of **6.4** indicated that fragment **6.4** could be prepared from commercially available aspartic acid **6.5** following Lugtenberg synthesis.⁹⁷ Vinylglycine **6.8** could also be obtained using an intermediate selenide **6.7** via the same route. Then Angelo's auxiliary could be installed by direct installation of the benzamino acid **6.8** under PTSA catalysis. Alkylation of **6.9** developed by Berkowitz *et al.*⁹⁸ for varying alkyl chains could give **6.10** in very good yields (65–80%) and very good diastereoselectivity (82% to 96% de). Then hydrolysis would afford **6.4** and regenerate Angelo's auxiliary. Following Lugtenberg's synthesis, we prepared the vinylglycine intermediate **6.8** in 42% yield overall (**Scheme 6.3**).

Chapter 6 Project perspective, current development and outlook

Reagents and conditions: a) NMM, CICO₂Et, NaBH₄, H₂O, 76%; b) (o-NO₂Ph)SeCN, P(n Bu)₃, THF, 80%; c) O₃, then TFA, then BzCl, 70%; d) PTSA, Angelo's auxiliary, Dean stark; e) LDA, n BuLi, HMPA, -78 $^{\circ}$ C, then R-X; f) KO t Bu, H₂O, dioxane.

Scheme 6.3: Planned synthesis of 6.4 based on alkylation method by Berkowitz et al. 98

Advanced intermediate **1.115** following Zaminer's method and vinylglycine intermediate **6.8** following Lugtenberg⁹⁷ methods were prepared. Future work will involve synthesis of the second generation pyroglutamate based mimic **6.1** from intermediates **1.115** and **6.4**, followed by the synthesis of analogues derived from p85p2 using this new mimic **6.1**. This will allow us to investigate binding studies with the SH3 domain and determine the potential of this mimic in this specific protein-ligand interaction (**Figure 6.4**).

Chapter 6 Project perspective, current development and outlook

Figure 6.4: Proposed analogues of p85p2 with incorporation of mimic 6.1

7. Experimental

7.1 General methods and starting materials

Reactions were carried out in solvents of commercial grade unless otherwise stated. Reactions requiring dry conditions were conducted in flame dried glassware, under argon and with distilled solvents. THF was distilled under argon from benzophenone and sodium. CH2Cl2, Et3N, MeCN, MeOH, piperidine and Ac₂O were distilled from calcium hydride. All chemicals were used as received. Thin layer chromatography (TLC) was performed using aluminium sheets precoated with silica gel 60 F₂₅₄ (Merck). Column chromatography was carried out on silica gel SI 60 (40-63 micron, MERCK). Melting points were determined with open capillary tubes using a Gallenkamp Electrothermal Melting point Apparatus. Compounds analysed were obtained from concentrating under vacuum unless crystallisation systems are stated. Some melting points of novel compounds were not obtained due to instability whilst storing. Optical rotations were measured on an Optical Activity POLAAR 2001. Compounds analysed were purified by column chromatography. NMR spectra were recorded on a Bruker 300 or 400 MHz spectrometer as stated. ¹H chemical shifts are reported in ppm values, with reference to residual solvent. The following abbreviations have been used to assign multiplicity; s = singlet, d = doublet, t = triplet, m = multiplet. Coupling constants, J, are measured in Hertz (Hz). Each assignment has been labelled 'Hn' with reference to its labelled proton only, and does not represent standard IUPAC numbering. ¹³C signals (100 or 75 MHz) have been assigned by their chemical shift referenced to solvent, and have been reported as s, d, t, q, depending on the number of directly attached protons (0, 1, 2, 3 respectively). Where possible each assignment has been labelled 'Cn' with reference to its labelled carbon determined by DEPT experiments. Infrared (IR) spectra were obtained using a PerkinElmer Spectrum One FT6IR Spectrometer. Absorptions are given in wave numbers (cm⁻¹). Low resolution Mass spectra (LRMS) were obtained from a Waters 2700 sample manager ESI+ in methanol. High resolution accurate mass measurements were carried out at 10,000 resolutions on a Bruker Apex III FT-ICR mass spectrometer.

In the absence of conclusive purity information from ¹³C NMR (compounds **1.139**, **1.140**, **1.141** and **1.142** exhibiting multiple rotamers) LCMS data is provided (appendix).

7.2 Compounds appearing in Chapter 2

N-Boc-Arg(NO₂)-Gly-OMe 2.8

To a stirred solution of N-Boc-Arg(NO₂)-OH **2.5** (3.35 g, 10.5 mmol) in DMF (20 mL), was added 1-hydroxybenzotriazole (3.15 g, of ~90% [undried] material, 21.0 mmol) followed by dicyclohexylcarbodiimide (2.16 g, 10.5 mmol). The mixture was stirred at room temperature for 15 min before cooling to 0 °C and addition of a solution of HCl.Gly-OMe **2.6** (1.32 g, 10.5 mmol) and DIPEA (7.3 mL, 42.0 mmol) in DMF (25 mL) dropwise. The mixture was now stirred at 0 °C for 1 h before warming to room temperature and stirring overnight. The mixture was filtered and washed with DMF (20 mL) before concentration of the filtrate under vacuum. The residue obtained was taken into EtOAc (250 mL) and washed with ice-cold saturated aqueous solution of NaHCO₃ (50 mL), ice cold H₂O (10 mL), ice-cold aqueous citric acid solution (1 M, 50 mL), and ice-cold H₂O (10 mL). The aqueous extracts were each re-extracted with EtOAc (5 x 70 mL). The combined organic extracts were dried over MgSO₄ and concentrated under vacuum. Purification by column chromatography (SiO₂ eluted with EtOAc/hexane/MeOH (3:6:1)) gave the title compound as a white solid (2.23 g, 54%).

m.p: 56-58 °C (CH₂Cl₂/Et₂O).

¹H NMR (DMSO- d_6 , 300 MHz): δ (ppm) 8.24 (1H, t, J = 6.0 Hz, H-3), 6.90 (1H, d, J = 8.0 Hz, H-8), 3.94 (1H, m, H-4), 3.82-3.85 (2H, 2 x d, J = 6.0 Hz, H-2, two doublets from rotamers), 3.62 (3H, s, H-1), 3.13 (2H, apparent d, J = 6.0 Hz, H-7), 1.62-1.51 (4H, m, H-5, H-6), 1.38 (9H, s, H-9). There are 3 x N-H protons of the arginine side chain missing from the ¹H-spectrum.

¹³C NMR (DMSO- d_6 , 75 MHz): δ (ppm) 172.5 (s), 170.2 (s), 159.7 (s), 155.3 (s), 78.1 (s), 53.7 (d), 51.7 (q), 29.2 (t), 28.2 (q). 3 x C(t) are missing from the spectrum because of solvents overlapping.

IR (cm⁻¹): 3304, 2976, 1743, 1628, 1524, 1366, 1248, 1158.

 $[\alpha]_D^{24}$ -7.0 (c 0.25, MeOH).

LRMS (ESI): $m/z = 413 [M+Na]^{+}$.

HRMS (ESI): Calculated for $C_{14}H_{26}N_6NaO_7$ 413.1755, found 413.1761.

N-Boc-Pro-Arg(NO₂)-Gly-OMe 2.3a

N-Boc-Arg(NO2)-Gly-OMe 2.8 (1.82 g, 4.7 mmol) was treated with TFA (50 mL of a 20% v/v solution in CH₂Cl₂) at room temperature and the mixture stirred overnight. CH₂Cl₂ was removed under vacuum and the residue washed with toluene (3 x 60 mL), removal of the azetrope with TFA was made under vacuum each time. The crude oil was washed alternately with EtOAc (11 x 30 mL in total) and MeOH (11 x 30 mL in total) until a white solid of consistent weight was obtained, TFA.Arg(NO2)-Gly-OMe 2.8b. To a stirred solution of N-Boc-Pro-OH 2.7 (1.0 g, 4.7 mmol) in DMF (15 mL), was added 1-hydroxybenzotriazole (1.26 g, of ~90% [undried] material, 9.3 mmol) followed by dicyclohexylcarbodiimide (0.96 g, 4.7 mmol). The mixture was stirred at room temperature for 15 min before cooling to 0 °C and addition of a solution of TFA.Arg(NO₂)-Gly-OMe 2.8b prepared above (4.7 mmol) and DIPEA (8 mL, 47.0 mmol) in DMF (15 mL) dropwise. The mixture was now stirred at 0 °C for 1 h before warming to room temperature and stirring overnight. The mixture was filtered and washed with DMF (15 mL) before concentration of the filtrate under vacuum. The residue obtained was taken into 100 mL of EtOAc, and washed with ice-cold saturated aqueous solution of NaHCO₃ (11.5 mL), ice cold H₂O (4.8 mL), ice-cold aqueous 1 M solution of citric acid (11.5 mL), and ice-cold H_2O (4.8 mL). The aqueous extracts were each re-extracted with EtOAc (4 x 60 mL). The combined organic extracts were dried over MgSO₄ and concentrated under vacuum. Purification by column chromatography (SiO₂ eluted with EtOAc/hexane (2:3) \rightarrow EtOAc/hexane/MeOH (3:6:1)) gave the title compound as a white solid (0.80 g, 35%).

m.p: 64-66 °C (CH₂Cl₂/Et₂O).

¹H NMR (DMSO- d_6 , 300 MHz): δ (ppm) 8.56 (1H, broad s, NH), 8.09 (1H, broad s, NH), 4.51 (1H, m, H-4), 4.30 (1H, m, H-9), 4.20-4.08 (2H, m, H-2), 3.61 (3H, s, H-1), 3.29-3.22 (2H, m, H-12), 3.16 (2H, d, J = 6.0 Hz, H-7), 2.08-1.62 (6H, m, H-11, H-10, H-5), 1.61-1.45 (2H, m, H-6), 1.38 and 1.31 (9H, 2 x s, H-13, there are two singlets from rotamers). There are 3 x N-H protons of the arginine side chain missing from the ¹H-spectrum.

¹³C NMR (100 MHz, DMSO- d_6): δ (ppm) 173.3 (s), 172.9 (s), 171.0 (s), 160.2 (s), 154.3 (s), 79.4 (s), 60.3 (d), 52.7 (d), 52.6 (q), 47.4 (t), 41.4 (t), 41.2 (t), 31.9 (t), 30.6 (t), 28.9 (q), 24.9 (t), 23.9 (t). Additional peaks arise from rotomers at 154.8 (s), 79.7 (s), 47.6 (t), 30.4 (t), 30.1 (t) and 29.0 (q).

IR (cm⁻¹): 3294, 2971, 1739, 1654, 1395, 1257.

 $[\alpha]_D^{24}$ –59.0 (c 0.25, MeOH).

LRMS (ESI): $m/z = 510 [M+Na]^{+}$.

HRMS (ESI): Calculated for C₁₉H₃₃N₇NaO₈ 510.2283, found 510.2278.

N-Boc-Arg(NO₂)-Pro-OMe 2.10

To a stirred solution of N-Boc-Arg(NO₂)OH **2.5** (0.60 g, 1.8 mmol) in DMF (5 mL), was added 1-hydroxybenzotriazole (0.54 g, of ~90% [undried] material, 3.6 mmol) followed by dicyclohexylcarbodiimide (0.37 g, 1.8 mmol). The mixture was stirred at room temperature for 15 min before cooling to 0 °C and addition of a solution of HCl.Pro-OMe **2.9** (0.30 g, 1.8 mmol) and DIPEA (1.25 mL, 18.0 mmol) in DMF (5 mL) dropwise. The mixture was now stirred at 0 °C for 1 h before warming to room temperature and stirring overnight. The mixture was filtered, washed with DMF (10 mL) before concentration of the filtrate under vacuum. The residue obtained was taken into 50 mL of EtOAc, and washed with an ice-cold aqueous saturated solution of NaHCO₃ (7 mL), 5 mL ice cold H₂O (5 mL), an aqueous solution of ice-cold citric acid (1 M, 7 mL), and 5 mL of ice-cold H₂O. The aqueous extracts were each re-extracted with

EtOAc (4 x 50 mL). The combined organic extracts were dried over MgSO₄ and concentrated under vacuum. Purification by column chromatography (SiO₂ eluted with EtOAc/hexane (2:3) \rightarrow EtOAc/hexane/MeOH (3:6:1)) gave the title compound as a white solid (0.60 g, 78%).

m.p: 54-56 °C (CH₂Cl₂/Et₂O).

¹H NMR (DMSO- d_6 , 300 MHz): δ (ppm) 8.49 (1H, broad s, NH), 7.92 (2H, broad s, NH), 6.99 (1H, d, J = 7.7 Hz, H-10), 4.32 (1H, dd, J = 5.0, 9.0 Hz, H-2), 4.18 (1H, m, H-6), 3.68-3.45 (2H, m, H-5), 3.59 (3H, s, H-1), 3.13 (2H, apparent d, J = 6.0 Hz, H-9), 2.16 (1H, m, H-3), 1.92 (2H, apparent pentet, J = 8.0 Hz, H-4), 1.81 (2H, tt, J = 8.0, 6.0 Hz, H-8), 1.43-1.64 (2H, m, H-7), 1.36 (9H, m, H-11). There is one N-H proton missing from ¹H spectrum.

¹³C NMR (DMSO- d_6 , 75 MHz): δ (ppm) 172.3 (s), 170.5 (s), 159.3 (s), 155.3 (s), 78.0 (s), 58.4 (d), 51.7 (q), 51.5 (d), 46.4 (t), 28.5 (t), 28.1 (q), 27.9 (t), 24.6 (t). 2 x C(t) are missing from ¹H spectrum due to signals overlapping.

IR (cm⁻¹): 3295, 2973, 1740, 1622, 1533, 1434, 1355, 1247.

 $[\alpha]_{D}^{24}$ -64.2 (c 0.25, MeOH).

LRMS (ESI): $m/z = 453 [M+Na]^+$, 883 $[2M+Na]^+$.

HRMS (ESI): Calculated for $C_{17}H_{30}N_6NaO_7$ 453.2068, found 453.2070.

N-Boc-Pro-Arg(NO₂)-Pro-OMe 2.4a

N-Boc-Arg(NO₂)-Pro-OMe **2.10** (0.39 g, 0.96 mmol) was treated with TFA (10 mL of a 20% v/v solution in CH_2Cl_2) at room temperature and the mixture stirred overnight. CH_2Cl_2 was removed under vacuum and the residue washed with toluene (3 x 60 mL), removal of the azetrope with TFA was made under vacuum each time. The crude oil was washed alternately with EtOAc (11 x 30 mL in total) and MeOH (11 x 30 mL in total) until a white solid of consistent

weight was obtained TFA.Arg(NO₂)-Pro-OMe **2.10b**. To a stirred solution of *N*-Boc-Pro-OH **2.7** (0.21 g, 0.96 mmol) in 2.5 mL DMF, was added 1-hydroxybenzotriazole (0.13 g, of ~90% [undried] material, 1.92 mmol) followed by dicyclohexylcarbodiimide (0.20 g, 0.96 mmol). The mixture was stirred at room temperature for 15 min before cooling to 0 °C and addition of a solution of TFA.Arg(NO₂)-Pro-OMe **2.10b** prepared above (0.96 mmol) and DIPEA (0.70 mL, 3.84 mmol) in 2.5 mL DMF, dropwise. The mixture was now stirred at 0 °C for 1 h before warming to room temperature and stirring overnight. The mixture was now filtered, washing with 15 mL DMF before concentration of the filtrate under vacuum. The residue obtained was taken into 50 mL of EtOAc, and washed with 5 mL of an ice-cold aqueous saturated solution of NaHCO₃, 2.5 mL of ice cold H₂O, 5 mL of an ice-cold aqueous 1 M solution of citric acid, and 2.5 mL of ice-cold H₂O. The aqueous extracts were each re-extracted with EtOAc (4 x 30 mL). The combined organic extracts were dried over MgSO₄ and concentrated under vacuum. Purification by column chromatography (SiO₂ eluted with EtOAc/hexane (2:3) \rightarrow EtOAc/hexane/MeOH (3:6:1)) gave the title compound as a white solid (0.18 g, 36%).

m.p: 69-72 °C (CH₂Cl₂/Et₂O).

¹H NMR (DMSO- d_6 , 300 MHz): δ (ppm) 8.56 (1H, broad s, NH), 8.09 (1H, broad s, H-10), 4.51 (1H, m, H-6), 4.29 (1H, dd, J = 5.0, 9.0 Hz, H-2), 4.13 (1H, m, H-11), 3.73-3.62 (2H, m, H-5), 3.61 (3H, s, H-1), 3.29-3.22 (2H, m, H-14), 3.21-3.10 (2H, m, H-9), 2.18-1.55 (12H, m, H-3, H-4, H-7, H-8, H-12, H-13), 1.38 and 1.31 (9H, 2 x s, H-15, there are two singlets from rotamers). There are 2 x N-H protons of the arginine side chain missing from the ¹H-spectrum.

¹³C NMR (DMSO- d_6 , 75 MHz): δ (ppm) 173.1 (s), 170.9 (s), 160.3 (s), 154.5 (s), 154.2 (s), 79.3 (s), 60.2 (d), 59.4 (d), 52.7 (q), 50.7 (d), 47.4 (t), 41.3 (t), 31.9 (t), 30.7 (t), 29.5 (t), 29.2 (t), 28.9 (q), 25.6 (t), 24.8 (t), 24.0 (t). Additional peaks arise from rotamers at 173.3 (s), 170.8 (s), 79.5 (s), 60.1 (d), 47.6 (t), 31.8 (t) and 29.0 (q).

IR (cm⁻¹): 3294, 1736, 1624, 1395, 1245.

 $[\alpha]_D^{24}$ –103.4 (c 0.25, MeOH).

LRMS (ESI): $m/z = 550 [M+Na]^{+}$.

HRMS (ESI): Calculated for C₂₂H₃₇N₇NaO₈ 550.2596, found 550.2587

• N-Boc-Pro-Arg(NO₂)-Gly-Pro-Arg(NO₂)-Pro-OMe 2.11

To a stirred solution of N-Boc-Pro-Arg(NO₂)-Gly-OMe **2.3a** (0.13 g, 0.27 mmol) in EtOH (1.5 mL) was added NaOH (0.28 mL of a 1 M aqueous solution). The solution was stirred at room temperature overnight and then concentrated in vacuo to yield crude N-Boc-Pro-Arg(NO₂)-Gly-O $^{-}$ Na $^{+}$ **2.3b** which was not purified further.

N-Boc-Pro-Arg(NO₂)-Pro-OMe **2.4a** (0.14 g, 0.27 mmol) was treated with TFA (5 mL of a 20% v/v solution in CH_2Cl_2) at room temperature and the mixture stirred overnight. CH_2Cl_2 was removed under vacuum and the residue washed with toluene (3 x 30 mL), removal of the azetrope with TFA was made under vacuum each time. The crude oil was washed alternately with EtOAc (11 x 30 mL in total) and MeOH (11 x 30 mL in total) until a white solid of consistent weight was obtained TFA.H-Pro-Arg(NO₂)-Pro-OMe 2.4b. To a stirred solution of N-Boc-Pro-Arg(NO₂)-Gly-O⁻Na⁺ **2.3b** (0.14 g, 0.27 mmol) in 1.5 mL DMF, was added 1hydroxybenzotriazole (0.07 g, of ~90% [undried] material, 0.53 mmol) followed by dicyclohexylcarbodiimide (0.055 g, 0.27 mmol). The mixture was stirred at room temperature for 15 min before cooling to 0 °C and addition of a solution of TFA.H-Pro-Arg(NO2)-Pro-OMe 2.4b prepared above (0.27 mmol) and DIPEA (0.19 mL, 1.10 mmol) in 1.5 mL DMF, dropwise. The mixture was now stirred at 0 °C for 1 h before warming to room temperature and stirring overnight. The mixture was now filtered, washing with 10 mL DMF before concentration of the filtrate under vacuum. The residue obtained was taken into 30 mL of EtOAc, and washed with 5 mL of an ice-cold saturated aqueous solution of NaHCO₃, 2.5 mL of ice cold H₂O, 5 mL of an ice-cold aqueous solution of citric acid (1 M), and 2.5 mL of ice-cold H₂O. The aqueous extracts were each re-extracted with EtOAc (4 x 30 mL). The combined organic extracts were dried over MgSO₄ and concentrated under vacuum. Purification by column chromatography (SiO₂ eluted with MeOH/CH₂Cl₂ (5:95) \rightarrow MeOH/CH₂Cl₂ (10:90)) gave the title compound as a white solid (95 mg, 40%).

m.p.: 82-83 °C (CH_2CI_2/Et_2O).

¹H NMR (DMSO- d_6 , 300 MHz): δ (ppm) 8.52 (1H, broad s, NH), 8.42 (1H, d, J = 8.0 Hz, NH), 8.12 (1H, d, J = 8.0 Hz, NH), 7.94-7.97 (5H, broad s, NH), 4.55-3.86 (7H, m, H-2, H-6, H-7, H-8, H-12, H-16), 3.63 (3H, s, H-20), 3.70-3.15 (10H, m, H-5, H-23, H-11, H-15, H-19), 2.20-1.50 (20H, m, H-3, H-4, H-21, H-22, H-9, H-10, H-13, H-14, H-17, H-18), 1.37 and 1.31 (9H, 2 x s, H-1, there are two singlets from rotamers). There is 1 x N-H protons of the arginine side chain missing from the 1 H-spectrum.

¹³C NMR (DMSO- d_6 , 75 MHz): δ (ppm) 173.3 (s), 173.1 (s), 172.9 (s), 172.4 (s), 172.3 (s), 170.7 (s), 167.7 (s), 167.6 (s), 160.2 (s), 77.3 (s), 60.1 (d), 59.4 (d), 52.8 (d), 52.6 (q), 52.4 (d), 50.8 (d), 47.3 (t), 46.8 (t), 42.1 (t), 41.2 (t), 41.1 (t), 41.0 (t), 40.2 (t), 38.5 (t), 36.9 (t), 33.3 (t), 30.1 (t), 29.4 (t), 29.1 (t), 28.9 (q), 25.5 (t), 25.1 (t), 23.9 (t). There is an extra peak arising from rotamers at 77.5 (s).

IR (cm⁻¹): 3294, 2955, 1742, 1624, 1401, 1252, 1159.

 $[\alpha]_{D}^{24}$ -67.6 (c 0.25, MeOH).

LRMS (ESI): $m/z = 905 [M+Na]^{+}$.

HRMS (ESI): Calculated for $C_{35}H_{58}N_{14}NaO_{13}$ 905.4200, found 905.4216.

• N-Ac-Pro-Arg(NO₂)-Gly-Pro-Arg(NO₂)-Pro-OMe 2.1

The *N*-Boc-protected peptide **2.11** (0.882 g, 1.0 mmol) was treated with 20% v/v TFA in CH_2Cl_2 (3.0 mmol) at 0 °C. The solution was stirred at room temperature overnight. All solvents were removed by toluene azeotrope under vacuum and the desired product TFA.Pro-Arg(NO₂)Gly-Pro-Arg(NO₂)-Pro-OMe **2.11b** was precipitated from CH_2Cl_2 (1 mL), MeOH (1 mL) and Et_2O (10 mL). To a stirred solution peptide of TFA.Pro-Arg(NO₂)-Gly-Pro-Arg(NO₂)-Pro-OMe **2.11b** (1.0 mmol) in DMF (5 mL) was added triethylamine (0.42 mL, 3.0 mmol), DMAP (61 mg, 0.05 mmol), and then acetic anhydride (0.28 mL, 3.0 mmol) at 0 °C. The reaction mixture was

warmed to room temperature and stirred overnight. All solvents were removed under reduced pressure. The crude residue was washed with CH_2Cl_2 (3 x 10 mL) and cold H_2O (10 mL), and purified by column chromatography (SiO₂ eluted with $CH_2Cl_2/MeOH$ (93:7)). The title product **2.1** was precipitated from CH_2Cl_2 (2 mL), MeOH (2 mL) and Et_2O (15 mL) (0.66 g, 80%).

m.p: 65-67 °C (CH₂Cl₂/Et₂O).

¹H NMR (400 MHz, DMSO- d_6): δ (ppm) 11.14 (1H, broad s, NH), 9.36 (1H, broad s, NH), 8.41 (1H, d, J = 8.0 Hz, NH), 8.24 (1H, d, J = 8.0 Hz, NH), 8.10 (1H, d, J = 8.0 Hz, NH), 8.01 (1H, t, J = 4.0 Hz, NH), 7.83 (1H, t, J = 4.0 Hz, NH), 4.53-3.91 (7H, m, H-2, H-6, H-7, H-8, H-12, H-16), 3.59 (3H, s, H-20), 3.70-3.13 (10H, m, H-5, H-23, H-11, H-15, H-19), 1.97 (3H, s, H-1), 2.03-1.47 (20H, m, H-3, H-4, H-21, H-22, H-9, H-10, H-13, H-14, H-17, H-18). There are 2 x N-H protons missing from 1 H-spectrum.

¹³C NMR (100 MHz, DMSO- d_6): 172.3 (s), 172.0 (s), 171.4 (s), 169.8 (s), 168.6 (s), 166.7 (s), 159.3 (s), 158.3 (s), 158.0 (s), 59.3 (d), 59.2 (d), 58.5 (d), 52.0 (d), 51.7 (q), 50.0 (d), 47.6 (t), 46.8 (t), 46.5 (t), 46.3 (t), 45.9 (t), 41.3 (t), 31.8 (t), 29.4 (t), 29.2 (t), 28.6 (t), 28.2 (t), 24.7 (t), 24.4 (t), 24.2 (t), 22.5 (t), 22.3 (q), 22.0 (t). Additional peaks arise from rotamers at 172.2 (s), 171.5 (s), 169.8 (s), 168.8 (s), 166.8 (s), 52.3 (d), 50.2 (d), 46.5 (t), 29.1 (t) and 22.1 (t) ppm.

IR (cm⁻¹): 3293, 2956, 1740, 1619, 1532, 1433, 1255, 1095.

 $[\alpha]_{D}^{24}$ -76.4 (c 0.25, MeOH).

LRMS (ESI): $m/z = 847 [M+Na]^+$, 825 $[M+H]^+$.

HRMS (ESI): Calculated for $C_{32}H_{53}N_{14}O_{12}$ 825.3962, found 825.3975.

HPLC-MS (ESI): $825.3975 [(M + H)^{+}, 100\%]$.

• (-)-(1*R*,5*S*)-1,2,3,4,5,6-Hexahydro-1,5-methanopyrido-[1,2-a][1,5]diazocin-8-one, (-)-Cytisine 1.67

Powdered cytisus seeds (Laburnum anagyroides, Vilmorin, 500 g) in mixed suspension of CH₂Cl₂ (700 mL), MeOH (400 mL) and NH₄OH (aq. 35% w/v, 75 mL) were stirred for 3 days at

room temperature, and then filtered. The solids were washed with 800 mL CH_2Cl_2 and the filtrate was treated with HCl (3N) until pH 1. The aqueous layer was recovered, basified with NH₄OH (aq. 35% w/v) and extracted with CH_2Cl_2 (10 x 200 mL). The combined organic layers were dried over MgSO₄, and then concentrated under vacuum. The solid was extracted with minimal acetone (40 mL) and concentrated to give the title compound as a yellow solid (7.13 g, 1.4%).

m.p.: 153-154 °C (acetone).

¹H NMR (CDCl₃, 300 MHz): δ (ppm) 7.26 (1H, dd, J = 8.9, 6.7 Hz, H-10), 6.39 (1H, dd, J = 8.9, 1.3 Hz, H-9), 5.88 (1H, dd, J = 6.7, 1.3 Hz, H-11), 4.10 (1H, d, J = 15.4 Hz, H-6), 3.86 (1H, ddd, J = 15.4, 6.7, 0.9 Hz, H-6), 3.07 (1H, dd, J = 12.4, 1.3 Hz, H-4), 3.04 (1H, dd, J = 12.1, 2.4 Hz, H-2), 2.99 (2H, broad d, J = 12.3 Hz, H-2, H-4), 2.86 (1H, broad s, H-1), 2.31 (1H, broad s, H-5), 1.94 (2H, t, J = 3.2 Hz, H-13), 1.51 (broad s, 1H, H-3).

¹³C NMR (CDCl₃, 75 MHz): δ (ppm) 163.7 (s, C8), 151.0 (s, C12), 138.8 (d, C10), 116.8 (d, C9), 105.0 (d, C11), 53.9 (t, C4), 52.9 (t, C2), 49.7 (t, C6), 35.6 (d, C1), 27.7 (d, C5), 26.3 (t, C13).

IR (cm⁻¹): 3313, 2929, 1646, 1571.

 $[\alpha]_D^{22}$ -76.0 (c 1.0, CHCl₃).

LRMS (ESI): $m/z = 213 [M+Na]^{+}$.

HRMS (ESI): Calculated for C₁₁H₁₅N₂O 191.1184, found 191.1181 [M+H][†].

Data according to literature. 47b

• N-benzoxy-cytisine 2.12

To a stirred mixture of cytisine **1.67** (3.35 g, 17.6 mmol) and Et_3N (5.8 mL, 44.0 mmol) in CH_2Cl_2 (80 mL) was added benzyl chloroformate (7.4 mL, 35.2 mmol) dropwise over 15 min at 0 °C. After stirring overnight at room temperature, the solvent was evaporated under vacuum and the crude product was taken into ethyl acetate (2 x 75 mL), and the precipitate was removed

by filtration. Removal of solvent from the filtrate under reduced pressure was undertaken and the crude residue was purified by column chromatography (SiO₂ eluted with CH₂Cl₂/MeOH (97:3)) to give the title compound as a pale yellow solid (4.06 g, 71%).

m.p.: 116-118 °C (CH₂Cl₂/Et₂O).

¹**H NMR** (CDCl₃, 300 MHz): δ (ppm) 7.41-7.09 (6H, m, H-10, H-17, H-18, H-19), 6.44 (1H, d, J = 9.1 Hz, H-9), 6.06 (1H, m, H-11), 5.12-4.83 (2H, m, H-15), 4.43-4.22 (2H, m, H-4, H-2), 4.16 (1H, d, J = 15.8 Hz, H-6), 3.86 (1H, dd, J = 15.8, 6.6 Hz, H-6), 3.21-2.95 (3H, m, H-1, H-4, H-2), 2.48 (1H, m, H-5), 2.12-1.91 (2H, m, H-13).

¹³C NMR (CDCl₃, 75 MHz): δ (ppm) 163.3 (s, C8), 155.3 (s, C14), 148.8 (s, C12), 139.0 (d, C10), 136.3 (s, C16), 128.5 (d, C18), 128.0 (d, C17), 127.8 (d, C19), 117.4 (d, C9), 105.6 (d, C11), 67.4 (t, C15), 51.1 (t, C6), 50.1 (t, C4), 49.0 (t, C2), 34.5 (d, C1), 27.2 (d, C5), 25.9 (t, C13).

IR (cm⁻¹): 3051, 2932, 2863, 1695, 1650, 1564, 1427, 1231, 1119, 841.

 $[\alpha]_D^{24}$ -105.8 (c 1.0, CHCl₃).

LRMS (**ESI**): $m/z = 342 [M+NH_4]^+$.

HRMS (ESI): Calculated for $C_{19}H_{21}N_2O_3$ 325.1552, found 325.1554 $[M+H]^{\dagger}$.

• 6α-benzoxy-cytisine 2.13

To a mixture of lithium chloride (5.29 g, 12.5 mmol) and diisopropylamine (3.5 mL, 25.0 mmol) was added n-butyllithium (2.5 M solution in hexanes, 10.0 mL, 25.0 mmol) dropwise over 25 min at -20 °C under nitrogen. After stirring for 15 min, 30 mL of dry THF was added and the temperature was cooled to -78 °C. A solution of *N*-benzoxy-cytisine **2.12** (4.06 g, 12.5 mmol) in 60 mL THF was added dropwise over 30 min to the LDA solution at -78 °C. After stirring for 3.5 h at -78 °C, the reaction was quenched with saturated ammonium chloride solution (2 mL) and then basified with ammonium hydroxide (aq. 35% w/v, 20 mL). Extraction of the aqueous

phase was carried out with CH_2CI_2 (6 x 50 mL), and the combined organic layers were dried over MgSO₄, filtered and concentrated under vacuum. The residue was purified by column chromatography (SiO₂ eluted with $CH_2CI_2/MeOH$ (95:5)) to give the title compound as a pale yellow solid (1.43 g, 35%).

m.p.: 177-179 °C (CH₂Cl₂/Et₂O).

¹H NMR (CDCl₃, 300 MHz): δ (ppm) 7.49-7.29 (6H, m, H-10, H-17, H-18, H-19), 6.51 (1H, d, J = 9.1 Hz, H-9), 6.06 (1H, d, J = 7.0 Hz, H-11), 5.42-5.22 (2H, m, H-15), 4.91 (1H, d, J = 7.0 Hz, H-6), 3.18-3.00 (2H, m, H-4, H-2), 2.95 (1H, m, H3), 2.86-2.75 (2H, m, H-4, H-2), 2.52 (1H, m, H-1), 2.19-1.90 (3H, m, H-13, H-5).

¹³C NMR (CDCl₃, 75 MHz): δ (ppm) 169.9 (s, C14), 163.4 (s, C8), 150.3 (s, C12), 139.5 (d, C10), 135.4 (s, C16), 128.5 (d, C18), 128.5, (d, C19), 128.4 (d, C17), 117.4, (d, C9), 105.5 (d, C11), 67.3 (t, C15), 60.6 (d, C6), 52.4 (t, C2), 49.0 (t, C4), 35.3 (d, C1), 29.5 (d, C5), 26.8 (t, C13).

IR (cm⁻¹): 3034, 2943, 2856, 1737, 1645, 1539, 1246, 1175.

 $[\alpha]_{D}^{24}$ -3.5 (c 1.0, CHCl₃).

LRMS (ESI): $m/z = 347 [M+Na]^{+}$.

HRMS (ESI): Calculated for C₁₉H₂₁N₂O₃ 325.1552, found 325.1550 [M+H][†].

• N-methyl-6α-benzoxy-cytisine 1.86

To a mixture of formic acid (0.55 mL, 11.8 mmol), formaldehyde (37%, 0.43 mL, 5.3 mmol) and 10 mL $_2$ O at 45 $^{\circ}$ C was added 6 $_4$ -benzoxy-cytisine **2.13** (1.42 g, 4.4 mmol). The mixture was then heated to 65 $^{\circ}$ C, and stirred for 4 h. The solution was then basified to pH 10 with 2 mL NH $_4$ OH (aq. 35% w/v). The aqueous phase was then extracted with CH $_2$ Cl $_2$ (4 x 50 mL). The combined organic extracts were then dried over MgSO $_4$. After evaporation of the solvent

under vacuum, the residue was purified by column chromatography (SiO_2 eluted with $CH_2Cl_2/MeOH$ (93:7)) to give the title compound as a white solid (1.24 g, 83%).

m.p.: 65-67 °C (CH₂Cl₂/Et₂O).

¹**H NMR** (CDCl₃, 300 MHz): δ (ppm) 7.53-7.28 (6H, m, H-10, H-17, H-18, H-19), 6.45 (1H, d, J = 8.6 Hz, H-9), 6.05 (1H, d, J = 7.8 Hz, H-11), 5.30 (2H, s, H-15), 4.90 (1H, d, J = 6.6 Hz, H-6), 3.14-2.91 (2H, m, H-4, H-2), 2.71 (1H, m, H-4), 2.51-1.75 (2H, m, H-13, H-5), 2.32 (1H, m, H-2), 2.18 (1H, m, H-1), 1.84-1.96 (3H, m, H-20), 1.64-1.80 (1H, m, H-13).

¹³C NMR (CDCl₃, 75 MHz): δ (ppm) 163.1 (s, C14), 162.1 (s, C8), 147.8 (s, C12), 139.5 (d, C10), 135.5 (s, C16), 129.0 (d, C17), 128.6 (d, C19), 128.6 (d, C18), 118.0 (d, C9), 106.1 (d, C11), 67.3 (t, C16), 60.9 (t, C2), 59.9 (d, C6), 57.0 (t, C4), 47.5 (q, C20), 46.3 (d, C1), 33.6 (d, C5), 27.2 (t, C13).

IR (cm⁻¹): 3436, 3047, 2943, 2788, 1757, 1726, 1657, 1574, 1547, 1164, 1064.

 $[\alpha]_D^{24}$ -7.2 (c 1.0, CHCl₃).

LRMS (ESI): m/z= 339 [M+H]⁺, 699 [2M+Na]⁺.

HRMS (ESI): Calculated for $C_{40}H_{44}N_4O_6Na$ 699.3159, found 699.3172 $[2M+Na]^+$.

• (1R,5S,6S)-benzyl 3-methyl-9-nitro-8-oxo-2,3,4,5,6,8-hexahydro-1H-1,5-methanopyrido[1,2-a][1,5]diazocine-6-carboxylate 2.18, 9-nitro-N-methyl-6 α -benzoxy-cytisine 2.18

$$O_2N$$
 O_2N
 O_2N
 O_2N
 O_3
 O_4
 O_5
 O_5
 O_5
 O_7
 O_7

A mixture of HNO_3 (0.22 mL, 2.56 mmol) and acetic anhydride (3 mL) was added dropwise at 0 $^{\circ}$ C to a stirred solution of *N*-methyl-6 α -benzoxy-cytisine **1.86** (720 mg, 2.13 mmol) in acetic anhydride (4 mL). The resulting mixture was allowed to warm to room temperature and was stirred for 4 h. The mixture was poured onto ice (10 g) and was extracted with CH_2Cl_2 (3 x 50 mL). The combined organic extracts were washed with brine, dried over MgSO₄ and

concentrated under reduced pressure. Purification by two successive column chromatography (SiO_2 eluted with EtOAc/hexane (1:1) + 5% MeOH + 1% NH₄OH (aq. 35% w/v) and CH₂Cl₂/MeOH (98:2)) gave the title compound as a yellow solid (146 mg, 18%).

m.p.: 63-65 °C (CH₂Cl₂/hexane).

¹H NMR (CDCl₃, 300 MHz): δ (ppm) 8.37 (1H, d, J = 7.9 Hz, H-10), 7.53-7.21 (5H, m, H-17, H-18, H-19), 6.18 (1H, d, J = 7.9 Hz, H-11), 5.35 (1H, d, J = 9.4 Hz, H-15), 5.10 (1H, d, J = 9.4 Hz, H-15), 4.98 (1H, d, J = 6.8 Hz, H-6), 3.16-2.92 (2H, m, H-4, H-2), 2.72 (1H, m, H-4), 2.33 (1H, d, J = 10.2 Hz, H-2), 2.10-1.65 (7H, m, H-20, H-5, H-13, H-1).

¹³C NMR (CDCl₃, 75 MHz): δ (ppm) 168.9 (s, C14), 160.4 (s, C8), 155.4 (s, C12), 138.6 (d, C10), 135.4 (s, C16), 134.9 (s, C9), 129.2 (d, C19), 128.5 (2 x d, C17, C18), 103.2 (d, C11), 67.5 (t, C15), 61.5 (t, C2), 60.7 (d, C6), 57.4 (t, C4), 45.4 (q, C20), 36.6 (d, C1), 30.1 (d, C5), 26.0 (t, C13).

IR (cm⁻¹): 2940, 2787, 1729, 1658, 1545, 1302, 1277, 1440, 1155.

 $[\alpha]_D^{22}$ -324.1 (c 0.5, CHCl₃).

LRMS (ESI): m/z= 384 [M+H]⁺, 407 [M+Na]⁺.

HRMS (ESI): Calculated for $C_{20}H_{22}N_3O_5$ 384.1554, found 384.1557.

• (1*R*,5*S*,6*S*)-9-amino-3-methyl-8-oxo-2,3,4,5,6,8-hexahydro-1*H*-1,5-methanopyrido[1,2-a][1,5]diazocine-6-carboxylic acid 1.89

$$H_2N$$
 9
 8
 N
 10
 12
 13
 3
 15

A mixture of *N*-methyl-9-nitro-6 α -benzoxy-cytisine **2.18** (100 mg, 0.26 mmol), Pd/C (10%, 20 mg) and 10 mL MeOH, under nitrogen, was purged with H₂. The reaction was left to stir for 3 h under H₂ (1 atm.), before filtering, and concentrating under vacuum, to give the title compound as a light yellow solid (52 mg, 76%).

m.p.: 202-204 °C (CH₂Cl₂/Et₂O).

¹**H NMR** (DMSO- d_6 , 300 MHz): δ (ppm) 6.43 (1H, d, J = 7.2 Hz, H-10), 5.90 (1H, d, J = 7.2 Hz, H-11), 4.70 (1H, d, J = 7.2 Hz, H-6), 3.77 (1H, broad s, NH), 2.91(1H, m, H-1), 2.77 (1H, m, H-4), 2.68 (1H, m, H-2), 2.55 (1H, m, H-5), 2.20 (1H, m, H-4), 2.09 (1H, m, H-2), 2.00 (3H, s, H-15), 1.80-1.65 (2H, m, H-13). There are two protons of carboxylic acid and amino group missing from the ¹H-spectrum.

¹³C NMR (DMSO-*d*₆, 75 MHz): δ (ppm) 169.8 (s, C14), 157.7 (s, C8), 136.4 (s, C12), 135.7 (s, C9), 110.5 (d, C11), 104.0 (d, C10), 61.5 (t, C2), 60.9 (d, C6), 57.6 (t, C4), 45.4 (q, C15), 33.8 (d, C1), 29.51 (d, C5), 26.2 (t, C13).

IR (cm⁻¹): 3304, 2941, 1642, 1587, 1536, 1469, 1359, 1283, 1198.

 $[\alpha]_D^{22}$ –14.5 (c 0.5, MeOH).

LRMS (ESI): $m/z = 264 [M+H]^+$, 327 $[M+Na+CH_3CN]^+$, 549 $[2M+Na]^+$.

HRMS (ESI): Calculated for $C_{13}H_{18}N_3O_3$ 264.1343, found 264.1347.

• (1*R*,5*S*)-9-nitro-3,4,5,6-tetrahydro-1*H*-1,5-methanopyrido[1,2-a][1,5]diazocin-8(2*H*)-one 2.20

To a solution of (–)-cytisine **1.67** (1.0 g, 5.26 mmol) in concentrated H_2SO_4 (1.5 mL), at 0 °C, was added concentrated HNO_3 (1.2 mL, 19.0 mmol) dropwise. The resulting mixture was stirred for 5 h at room temperature, cooled to 0 °C and quenched by addition of NH_4OH (aq. 35 % w/v, 3 mL) until a basic pH (10). Following extraction with CH_2CI_2 (40 mL), the combined organic layers were dried over $MgSO_{4}$, and concentrated under reduced pressure. The residue was dissolved in HCl (37%, 2.5 mL) and the mixture was refluxed for 15 min, cooled, quenched with water (3 mL) then NH_4OH (aq. 35% w/v, 3 mL). The residue was extracted with CH_2CI_2 (3 x 25 mL). The combined organic extracts were washed with brine (10 mL), dried over $MgSO_4$ and concentrated under reduced pressure. Purification by column chromatography (SiO_2 eluted with NH_4OH (aq.35% w/v)/ $MeOH/CH_2CI_2$ (1:5:94)) gave the title compound as a yellow solid (0.85 g, 69%).

m.p.: 211 $^{\circ}$ C (CH₂Cl₂/Et₂O).

¹H NMR (CDCl₃, 300 MHz): δ (ppm) 8.35 (1H, d, J = 8.1 Hz, H-10), 6.12 (1H, d, J = 8.1 Hz, H-11), 4.22 (1H, d, J = 16.5 Hz, H-6), 4.00 (1H, dd, J = 16.5, 6.5 Hz, H-6), 3.16-2.98 (5H, m, H-4, H-1, H-2), 2.42 (1H, broad s, H-2), 1.98 (2H, broad s, H-13), 1.54 (1H, broad s, H-3).

¹³C NMR (CDCl₃, 75 MHz): δ (ppm) 160.6 (s, C8), 155.2 (s, C12), 137.8 (d, C10), 134.4 (s, C9), 102.9 (d, C11), 53.2 (t, C2), 52.8 (t, C4), 51.0 (t, C6), 36.5 (d, C1), 27.4 (d, C5), 25.6 (t, C13).

IR (cm⁻¹): 3324, 3063, 2914, 1678, 1549, 1462, 1309.

 $[\alpha]_D^{22}$ -66.1 (c 1.0, CHCl₃).

LRMS (ESI): $m/z = 236 [M+H]^+$, 493 $[2M+Na]^+$.

Data according to literature. 47b

• (1*R*,5*R*)-benzyl 9-nitro-8-oxo-4,5,6,8-tetrahydro-1*H*-1,5-methanopyrido[1,2-a][1,5]diazocine-3(2*H*)-carboxylate 2.21

$$O_2N$$
 9
 10
 13
 13
 3
 14
 0
 15
 16
 18

To a mixture of **2.20** (200 mg, 0.85 mmol) and NEt₃ (0.24 mL, 1.72 mmol) in CH_2Cl_2 (10 mL), was added benzylchloroformate (0.3 mL, 2.12 mmol) dropwise at 0 °C. The resulting mixture was stirred overnight. Solvents were removed under reduced pressure. Purification by column chromatography (SiO₂ eluted with MeOH/CH₂Cl₂ (2:98)) gave the title compound as a yellow solid (255 mg, 81%).

m.p: 172-175 °C (CH₂Cl₂/Et₂O).

¹H NMR (CDCl₃, 300 MHz): δ (ppm) 8.22 (1H, m, H-10), 7.36-7.11 (5H, m, H-17, H-18, H-19), 6.14 (1H, m, H-11), 5.05 (2H, apparent d, J = 12.1 Hz, H-15), 4.90 (1H, m, H-6), 4.40-4.06 (2H, m, H-4, H-2), 3.95 (1H, dd, J = 16.2, 6.4 Hz, H-6), 3.17 (3H, broad s, H-1, H-4, H-2), 2.55 (1H, broad s, H-5), 2.01 (2H, m, H-13).

¹³C NMR (CDCl₃, 75 MHz): δ (ppm) 157.6 (s, C8), 154.8 (s, C14), 139.1 (s, C12), 137.9 (s, C16), 135.9 (d, C10), 135.0 (s, C9), 128.5 (d, C18), 128.3 (d, C17), 128.0 (d, C19), 103.4 (d, C11), 67.7 (t, C15), 50.3 (t, C6), 50.2 (t, C4), 50.0 (t, C2), 35.4 (d, C1), 26.8 (d, C5), 25.2 (t, C13).

IR (cm⁻¹): 3067, 2941, 1680, 1543, 1421, 1273, 1221, 1083.

 $[\alpha]_D^{24}$ -335.6 (c 0.5, CH₂Cl₂).

LRMS (ESI): $m/z = 370 [M+H]^+$, 761 $[2M+Na]^+$.

HRMS (ESI): Calculated for $C_{19}H_{19}N_3NaO_5$ 392.1217, found 392.1220.

• (1*R*,5*S*,6*S*)-3-methyl-8-oxo-2,3,4,5,6,8-hexahydro-1*H*-1,5-methanopyrido[1,2-a][1,5]diazocine-6-carboxylic acid 2.14

A mixture of N-methyl-6 α -benzoxy-cytisine **1.86** (1.9 g, 5.6 mmol), Pd/C (10%, 100 mg) and 10 mL MeOH, under nitrogen, was purged with H₂. The reaction was left to stir overnight under H₂ (1 atm.), before filtering, and concentrating under vacuum, to give the title compound as a light yellow solid (1.12 g, 84%).

m.p.: 140-142 °C (MeOH/diethylether).

¹H NMR (MeOD- d_4 , 300 MHz): δ (ppm) 7.38 (1H, dd, J = 9.0, 6.8 Hz, H-10), 6.36 (1H, d, J = 9.0 Hz, H-9), 6.26 (1H, d, J = 6.8 Hz, H-11), 4.74 (1H, d, J = 8.3 Hz, H-6), 3.47 (1H, d, J = 12.0 Hz, H-2), 3.35 (1H, m, H-4), 3.30 (1H, m, H-4), 3.26 (1H, m, H-2), 3.08 (1H, m, H-1), 2.84 (1H, m, H-5), 2.69-2.61 (3H, m, H-15), 2.09-1.86 (2H, m, H-13). There is one proton (OH) missing from ¹H spectum.

¹³C NMR (DMSO-*d*₆, 100 MHz): δ (ppm) 171.2 (s, C14), 162. 5 (s, C8), 148.3 (s, C12), 138.2 (d, C10), 116.8 (d, C9), 104.8 (d, C11), 61.3 (t, C2), 59.2 (d, C6), 57.3 (t, C4), 44. 3 (q, C15), 33.7 (d, C1), 28.2 (d, C5), 24.3 (t, C13).

IR (cm⁻¹): 3472, 2937, 1649, 1569, 1543, 1359, 1139, 799.

 $[\alpha]_{D}^{24}$ -4.2 (c 1.0, MeOH).

LRMS (ESI): $m/z = 312 [M+CH₃CN+Na]^+$, 519 $[2M+Na]^+$.

HRMS (ESI): Calculated for C₁₃H₁₆N₂O₃Na 271.1053, found 271.1058.

• Methyl 2-((*S*)-2-((1*R*,5*S*,6*S*)-3-methyl-8-oxo-2,3,4,5,6,8-hexahydro-1*H*-1,5 methanopyrido[1,2-a] [1,5]diazocine-6-carboxamido)-5-(3-nitroguanidino)pentanamido)acetate 2.15

To a mixture of **2.14** (300 mg, 1.20 mmol) and HBTU (631 mg, 1.81 mmol) in DMF (5 mL) stirred for 1 hour, was added dropwise at room temperature, a solution of H.Arg(NO₂)Gly-OMe **2.8b** (810 mg, 1.81 mmol) and DIPEA (2 mL, 12 mmol) in DMF (5 mL). The resulting mixture was stirred overnight. The mixture was concentrated under vacuum. Purification by column chromatography (SiO₂ eluted with MeOH/CH₂Cl₂/NH₄OH (aq.35% w/v) (6:93:0.1)) gave the title compound as a white solid (277 mg, 44%).

m.p: 155-157 °C (CH₂Cl₂/Et₂O).

¹H NMR (DMSO- d_6 , 300 MHz): δ (ppm) 8.60 (1H, broad s, NH), 8.40 (1H, m, NH), 7.39 (1H, dd, J = 8.7, 7.2 Hz, H-10), 6.25 (1H, d, J = 7.9 Hz, H-9), 6.18 (1H, d, J = 6.4 Hz, H-11), 4.69 (1H, d, J = 6.4 Hz, H-6), 4.31 (1H, d, J = 6.4 Hz, H-17), 3.84 (2H, d, J = 5.7 Hz, H-23), 3.61 (3H, s, H-25), 3.23-3.12 (2H, m, H-20), 3.17 (2H, d, J = 5.0 Hz, H-4), 3.04 (1H, broad s, H-2), 2.85 (1H, d, J = 8.7 Hz, H-1), 2.67 (1H, d, J = 12.4 Hz, H-4), 2.56 (1H, m, H-2), 2.22 (1H, d, J = 9.0 Hz, H-5), 1.98 (3H, broad s, H-15), 1.83-1.46 (6H, m, H-13, H-18, H-19). There are 3 x N-H protons of the arginine side chain missing from the ¹H-spectrum.

¹³C NMR (DMSO-*d*₆, 100 MHz): δ (ppm) 174.5 (s, C21), 171.9 (s, C14), 166.1 (s, C24), 161.1 (s, C8), 153.9 (s, C26), 142.1 (s, C12), 129.7 (d, C10), 117.9 (d, C9), 108.6 (d, C11), 62.9 (t, C2), 59.2 (d, C6), 54.7 (t, C4), 54.0 (d, C17), 52.8 (q, C25), 46.4 (q, C15), 42.0 (t, C23), 41.9 (t, C20), 37.1

(d, C1), 32.3 (d, C5), 30.4 (t, C18), 27.3 (t, C13), 26.5 (t, C19). Additional peaks arise from rotamers at 171.7 and 42.0.

IR (cm⁻¹): 3275, 2941, 2790, 1745, 1647, 1540, 1434, 1254, 1205, 1142.

 $[\alpha]_{D}^{24}$ -99.4 (c 0.5, MeOH).

LRMS (ESI): $m/z = 521 [M+H]^{+}$.

HRMS (ESI): Calculated for $C_{22}H_{33}N_8O_7$ 521.2467, found 521.2459.

Cytisine-Arg(NO₂)-Gly-Pro-Arg(NO₂)-Pro-OMe 2.16

To a stirred solution of **2.14**-Arg(NO₂)Gly-OMe **2.15** (200 mg, 0.38 mmol) in EtOH (3.0 mL) was added NaOH (0.40 mL of an aqueous 1 M solution). The solution was stirred at room temperature overnight and then concentrated in vacuo to yield crude **2.14**-Arg(NO₂)Gly-O⁻Na⁺ **2.15b** which was not purified further.

N-Boc-Pro-Arg(NO₂)-Pro-OMe **2.4a** (200 mg, 0.38 mmol) was treated with trifluoroacetic acid (5 mL of a 20% v/v solution in CH₂Cl₂) at room temperature and the mixture stirred overnight. CH₂Cl₂ was removed under vacuum and the residue washed with toluene (3 x 30 mL), removal of the azetrope with TFA was made under vacuum each time. The crude oil was washed alternately with EtOAc (5 x 10 mL in total) and MeOH (5 x 10 mL in total) until a white solid of consistent weight was obtained TFA.H-Pro-Arg(NO₂)-Pro-OMe **2.4b**. To a stirred solution of **2.14**-Arg(NO₂)-Gly-O Na⁺ **2.15b** (0.38 mmol) in 3.5 mL DMF, was added PyBop (400 mg, 0.77 mmol). The mixture was stirred at room temperature for 1 h before cooling to 0 °C and addition of a solution of TFA.H-Pro-Arg(NO₂)-Pro-OMe **2.4b** prepared above (0.38 mmol) and DIPEA (0.77 mL, 3.85 mmol) in 3.5 mL DMF, dropwise. The mixture was now stirred at 0 °C for 1 h before warming to room temperature and stirring overnight. The mixture was

concentrated under reduced pressure. Purification by column chromatography (SiO_2 eluted with MeOH/CH₂Cl₂ (7:93)) gave a white solid (134 mg). Purification by reverse-phase HPLC (H₂O/CH₃CN 0-100%) gave the title compound as a white solid (53 mg, 15 %).

m.p: 172-175 °C (CH₂Cl₂/MeOH/Et₂O).

¹H NMR (DMSO- d_6 , 400 MHz): δ (ppm) 8.63-7.59 (9H, m, NH), 7.37 (1H, dd, J = 9.0, 6.8 Hz, H-10), 6.24 (1H, d, J = 9.0 Hz, H-9), 6.16 (1H, d, J = 6.8 Hz, H-11), 4.78 (1H, d, J = 6.6 Hz, H-6), 4.58-4.23 (4H, m, H-31, H-29, H-40, H-17), 4.03-3.34 (7H, m, H-26, H-37, H-23, H-4), 3.60 (3H, s, H-42), 3.24-3.09 (4H, m, H-20, H-34), 3.05 (1H, m, H-2), 2.85 (1H, m, H-1), 2.73-2.52 (2H, m, H-5, H-4), 2.36-1.39 (22H, m, H-15, H-2, H-28, H-39, H-13, H-27, H-38, H-32, H-18, H-19, H-33).

¹³C NMR (DMSO- d_6 , 100 MHz): δ (ppm) 172.2 (s), 171.4 (s), 169.8 (s), 166.7 (s), 162.6 (s), 159.3 (s), 152.1 (s), 139.2 (s, C10), 116.2 (s, C9), 104.6 (s, C11), 61.3 (d), 59.2 (d), 58.5 (d), 57.3 (d), 51.7 (q), 50.2 (d), 49.9 (d), 48.6 (t), 46.8 (d), 46.4 (t), 45.8 (t), 45.4 (q), 41.3 (t), 34.8 (d), 30.1 (t), 29.7 (t), 29.1 (t), 28.5 (t), 28.1 (t), 25.9 (t), 25.9 (t), 25.7 (t), 24.6 (t), 24.2 (t). There are 1 x (t) and 2 x (d) missing from spectrum due to solvents overlapping. Additional peaks arise from rotamers at 171.4 (s), 169.7 (s), 166.8 (s), 58.6 (d), 31.8 (d).

IR (cm⁻¹): 3292, 2949, 2359, 1740, 1625, 1538, 1435, 1255, 1096, 1026, 841.

 $[\alpha]_D^{24}$ -101.9 (c 0.6, MeOH).

HRMS (ESI): Calculated for $C_{38}H_{57}N_{15}O_{12}$ 916.4384, found 916.4374

HPLC-MS: $916.4 [(M+H)^{+}, 100\%]$.

7.3 Compounds appearing in Chapter 3

(S)-tert-Butyl 5-oxopyrrolidine-2-carboxylate 3.1a

To a stirred solution of L-pyroglutamic acid **1.116** (9.0 g, 69.7 mmol) in *tert*-butylacetate (130 mL) was added $HClO_4$ (70% in aq., 4.7 mL, 76.7 mmol) dropwise at room temperature. The resulting mixture was stirred for 24 h. Then, it was carefully poured into a aqueous saturated solution of $NaHCO_3$ and extracted with CH_2Cl_2 (3 x 100 mL). The combined organic layers were dried over $MgSO_4$ and concentrated under reduced pressure to give **3.1a** (11.5 g, 89%) as a white solid without further purification.

m.p.: 97-98 °C (CH₂Cl₂/Et₂O).

¹**H NMR** (CDCl₃, 300 MHz): δ (ppm) 6.25 (1H, broad s, H-1), 4.14 (1H, m, H-5), 2.55-2.30 (3H, m, H-3, H-4), 2.19 (1H, m, H-4), 1.48 (9H, s, H-8).

¹³C NMR (CDCl₃, 75 MHz): δ (ppm) 177.9 (s, C2), 170.9 (s, C6), 82.5 (s, C7), 56.2 (d, C5), 29.3 (t, C3), 27.9 (q, C8), 24.8 (t, C4).

IR (cm⁻¹): 3257, 2969, 1731, 1697, 1678, 1226, 1143, 1104.

 $[\alpha]_{D}^{22}$ 10.3 (c 1.0, MeOH).

LRMS (ESI): $m/z = 249 [M+Na+CH₃CN]^{+}$, 393 $[2M+Na]^{+}$.

HRMS (ESI): calculated for $C_9H_{15}NO_3Na$ 208.0944 found 208.0944.

Data according to literature. 62

• *tert*-Butyl (2S)-1-benzylpyroglutamate 1.132

To a suspension of NaH (60% in mineral oil, $1.56 \, \text{g}$, $40.5 \, \text{mmol}$) in dry CH_2Cl_2 (10 mL) was added a solution of **3.1a** (5.0 g, 27.0 mmol) in CH_2Cl_2 dropwise. Then, BnBr (6.5 mL, 54.0 mmol) was added to the mixture at room temperature. The resulting mixture was stirred overnight at room temperature. Then, the solution was washed with water (15 mL) and extracted with CH_2Cl_2 (3 x 15 mL). The combined organic layers were dried over MgSO₄ and concentrated under reduced pressure. Purification by column chromatography (SiO₂ eluted with hexane/EtOAc (3:2)) gave the title compound as a colourless oil (5.83 g, 79%).

m.p.: 62-63 °C (EtOAc/Et₂O).

¹H NMR (CDCl₃, 300 MHz) δ (ppm) 7.40-7.20 (5H, m, H-10, H-11, H-12), 5.06 (1H, d, J = 14.8 Hz, H-8), 3.96 (1H, d, J = 14.8 Hz, H-8), 3.83 (1H, dd, J = 3.4, 9.0 Hz, H-4), 2.52 (1H, m, H-2), 2.37 (1H, m, H-2), 2.20 (1H, m, H-3), 2.04 (1H, m, H-3), 1.44 (9H, s, H-7).

¹³C NMR (CDCl₃, 75 MHz): δ (ppm) 175.6 (s, C1), 171.3 (s, C5), 136.3 (s, C9), 129.1, 128.9 and 128.1 (d, C10, C11, C12), 82.6 (s, C6), 59.9 (d, C4), 45.9 (t, C8), 30.0 (t, C2), 28.3 (q, C7), 23.3 (t, C3).

 $[\alpha]_D^{22}$ 35.1 (c 1.0, CHCl₃).

IR (cm⁻¹): 2977, 2935, 1716, 1675, 1301, 1144.

LRMS (ESI): $m/z = 339 [M+CH₃CN+Na]^+, 573 [2M+Na]^+.$

Data according to literature. 65

• (S)-tert-Butyl 1-benzyl-5-thioxopyrrolidine-2-carboxylate 1.131

To a solution of **1.132** (5.83 g, 21.2 mmol) in dry THF (30 mL) was added Lawesson's reagent (8.57 g, 21.2 mmol,) at room temperature. The mixture was stirred overnight. THF was evaporated and the residue was taken up in EtOAc (30 mL), washed with saturated aqueous solutions of NaHCO₃ (3 x 20 mL) and NaCl (2 x 20 mL). The aqueous layer was back extracted with EtOAc (3 x 35 mL). The combined organic layers were dried over MgSO₄ and concentrated

under reduced pressure. Recrystallisation from CHCl₃/hexane gave **1.131** (5.65 g, 92%) as a white solid.

m.p.: 78-79 $^{\circ}$ C (CHCl₃/hexane).

¹**H NMR** (CDCl₃, 300 MHz) δ (ppm) 7.40-7.20 (5H, m, H-10, H-11, H-12), 5.81 (1H, d, J = 14.6 Hz, H-8), 4.27 (1H, d, J = 14.6 Hz, H-8), 4.14 (1H, dd, J = 3.4, 9.2 Hz, H-4), 3.05-3.20 (2H, m, H-2), 2.35-2.10 (2H, m, H-3), 1.44 (9H, s, H-7).

¹³C NMR (CDCl₃, 75 MHz): δ (ppm) 203.6 (s, C1), 169.2 (s, C5), 134.7 (s, C9), 128.8, 128.7 (2 x d, C10, C11), 128.2 (d, C12), 82.9 (s, C6), 66.3 (d, C4), 50.4 (t, C8), 43.4 (t, C2), 27.8 (q, C7), 24.8 (t, C3).

IR (cm⁻¹): 2980, 2933, 1726, 1468, 1226, 1147.

 $[\alpha]_D^{20}$ 195.2 (c 1.85, CHCl₃).

Data according to literature. 65

• (S)-Di-tert-butyl 5-oxopyrrolidine-1,2-dicarboxylate 3.8a

(*S*)-tert-Butyl 5-oxopyrrolidine-2-carboxylate **3.1a** (5.0 g, 27.0 mmol) was dissolved in CH_3CN (100 mL) and the mixture was cooled to 0 °C. DMAP (0.33 g, 2.7 mmol) was added to the stirred mixture, followed by a solution of Boc_2O (8.85 g, 41.0 mmol) in CH_3CN (30 mL). The resulting mixture was stirred at 0 °C for 2 h and overnight at room temperature. The solvents were removed under reduced pressure. Purification by column chromatography (SiO_2 eluted with Et_2O /petroleum ether (40:60)) gave **3.8a** as dark orange oil (5.4 g, 70%).

¹**H NMR** (CDCl₃, 300 MHz) δ (ppm) 4.46 (1H, dd, J = 9.4, 2.6 Hz, H-4), 2.64-2.38 (2H, m, H-2), 2.27 (1H, m, H-3), 1.99 (1H, m, H-3), 1.49-1.47 (18H, 2 x s, H-7, H-10).

¹³C NMR (CDCl₃, 75 MHz): δ (ppm) 173.5 (s, C1), 170.3 (s, C5), 149.3 (s, C8), 83.3 (s, C6), 82.2 (s, C9), 59.6 (d, C4), 31.1 (t, C2), 27.9 (2 x q, C7, C10), 21.6 (t, C3).

 $[\alpha]_{D}^{20}$ -36.0 (c 0.9, CHCl₃).

IR (cm⁻¹): 2982, 1793, 1743, 1712, 1366, 1289, 1221, 1155.

LRMS (ESI): $m/z = 349 [M+CH₃CN+Na]^+$, 593 $[2M+Na]^+$.

Data according to literature. 62

• (2S)-Di-tert-butyl 5-methoxypyrrolidine-1,2-dicarboxylate 3.9a

(*S*)-Di-*tert*-butyl 5-oxopyrrolidine-1,2-dicarboxylate **3.8a** (2.0 g, 6.27 mmol) was dissolved in dry THF (10 mL) under an argon atmosphere. Superhydride® (9.40 mL, 9.40 mmol, 1 M in THF) was added dropwise at -78 °C. The resulting mixture was stirred for 2 h at -78 °C. NaHCO₃ saturated aqueous solution (10 mL) was slowly added and the mixture was allowed to warm to 0 °C. H₂O₂ (35% in water, 39 drops) was added and the reaction was stirred at 0 °C for 20 min. The organic solvent was removed and the aqueous residue was extracted with CH₂Cl₂ (3 x 25 mL). The combined organic extracts were dried over MgSO₄ and concentrated under reduced pressure to give (2*S*)-Di-*tert*-butyl 5-hydroxypyrrolidine-1,2-dicarboxylate as a clear oil (929 mg, 93% yield) which was not further purified. (2*S*)-Di-*tert*-butyl 5-hydroxypyrrolidine-1,2-dicarboxylate (6.27 mmol) was dissolved in MeOH (20 mL) under an argon atmosphere. PTSA (110 mg, 0.63 mmol) was then added to the solution and the resulting mixture was stirred overnight. NaHCO₃ saturated aqueous solution (20 mL) was added and solvents were removed under reduced pressure. The residue was extracted with Et₂O (3 x 20 mL). The combined organic extracts were dried over MgSO₄ and concentrated under reduced pressure to give **3.9a** as a clear oil (1.6 g, 76%) which was not further purified (*d. r* = 2:1).

¹H NMR (CDCl₃, 300 MHz) δ (ppm) 5.20 (0.66H, dd, J = 9.9, 4.8 Hz, H-2), 5.05 (0.33H, dd, J = 5.6, 4.5 Hz, H-2), 4.07 (1H, m, H-5), 3.29 (3H, m, H-1), 2.40-1.60 (4H, m, H-3, H-4), 1.37 (18H, 2 x s, H-11, H-8).

¹³C NMR (CDCl₃, 75 MHz): δ (ppm) 171.6 and 171.4 (s, C6), 154.3, 154.1 and 153.7 (s, C9), 89.2, 89.1, 88.3, 88.2 (d, C2), 80.7 and 80.5 and 80.0 (s, C7, C10), 60.0 and 59.8 (d, C5), 55.9, 55.7,

55.0, 54.8 (q, C1), 32.8, 32.0, 30.9, 29.7 (t, C3), 28.1, 28.0, 27.9, 27.8, 27.7 (q, C8, C11), 26.9, 26.8 (t, C4). Additional peaks arise from rotamers and diastereoisomers.

IR (cm⁻¹): 2975, 2950, 1740, 1705, 1456, 1366, 1216, 1149, 1084.

LRMS (ESI): $m/z = 365 [M+CH_3CN+Na]^+$.

Data according to literature. 99

(2S)-Di-tert-butyl 5-allylpyrrolidine-1,2-dicarboxylate 1.122a

To a solution of **3.9a** (0.17 g, 0.56 mmol) in CH_2Cl_2 (17 mL) at -78 °C under an argon atmosphere, $BF_3 \cdot Et_2O$ (0.07 mL, 0.56 mmol) was added dropwise. The mixture was stirred for 20 min, then allyl-TMS (0.21 mL, 0.7 mmol) was added slowly. The resulting mixture was stirred for 3 h at -78 °C. H_2O (17 mL) was added and the mixture was allowed to warm to room temperature. The aqueous layer was extracted with CH_2Cl_2 (3 x 15 mL). The combined organic extracts were dried over $MgSO_4$ and concentrated under reduced pressure. Purification by column chromatography (SiO₂ eluted with hexane/EtOAc (92:8)) gave **1.122a** as a clear oil (*d.r* = 3 : 1) (0.125 g, 72%).

¹H NMR (CDCl₃, 300 MHz) δ (ppm) 5.76 (1H, m, H-2), 5.10-4.95 (2H, m, H-1), 4.20-3.70 (2H, m, H-4, H-7), 2.80-2.40 (1H, m, H-3), 2.20-1.65 (5H, m, H-3, H-5, H-6), 1.46-1.41 (18H, 2 x s, H-10, H-13). Additional peaks arise from rotamers and diastereoisomers.

¹³C NMR (CDCl₃, 75 MHz): δ (ppm) 172.4, 172.2, 172.1 (s, C8), 154.3, 153.8 (s, C11), 135.5, 135.2 (d, C2), 117.0, 116.7 (t, C1), 80.8 (s, C9), 79.5 (s, C12), 60.8 (d, C7), 58.1 (d, C4), 39.1 and 38.2 (t, C3), 29.4, 28.8, 28.4, 28.3, 27.9, 26.6 (t, C5; q, C13; q, C10, t, C6). Additional peaks due to rotamers and diastereoisomers at 153.7 (s, C11), 135.1 (d, C2), 117.1 (t, C1), 80.7 (s, C9), 79.7 (s, C12), 60.6 (d, C7), 57.5 (d, C4), 39.0 and 38.1 (t, C3).

IR (cm⁻¹): 3070, 2977, 2950, 1738, 1693, 1389, 1366, 1152.

LRMS (ESI): $m/z = 375 [M+Na+CH₃CN]^{+} (100%).$

• (S)-1-benzyl 2-tert-butyl 5-oxopyrrolidine-1,2-dicarboxylate 3.13

To a solution of **3.1a** (2.0 g, 10.8 mmol) in dry THF (10 mL) under an argon atmosphere, was added in portions sodium hydride (60% in mineral oil, 0.79 g, 20.5 mmol). The resulting mixture was stirred for 30 min at room temperature. Then, benzyl chloroformate (20.5 mL, 20.5 mmol) was added dropwise at room temperature. The mixture was stirred for 48 h. Solvents were removed under reduced pressure, the residue was then treated with the aqueous citric acid solution (10%, 10 mL). The aqueous layer was extracted with EtOAc (3 x 15 mL). The combined organic extracts were dried over MgSO₄ and concentrated under reduced pressure. Purification by column chromatography (SiO₂ eluted with hexane/EtOAc (75:25)) gave **3.13** as a clear oil (2.1 g, 61%).

¹H NMR (CDCl₃, 300 MHz) δ (ppm) 7.45-7.31 (5H, m, H-11, H-12, H-13), 5.27 (2H, d, J = 5.3 Hz, H-9), 4.55 (1H, dd, J = 9.4, 2.6 Hz, H-4), 2.71-2.37 (2H, m, H-2), 2.33 (1H, m, H-3), 2.04 (1H, m, H-3), 1.39 (9H, s, H-7).

¹³C NMR (CDCl₃, 100 MHz): δ (ppm) 173.1 (s, C1), 170.0 (s, C5), 150.9 (s, C8), 135.0 (s, C10), 128.5 and 128.2 (2 x d, C11, C12), 128.1 (d, C13), 82.5 (s, C6), 68.2 (t, C9), 59.3 (d, C4), 31.0 (t, C2), 27.7 (q, C7), 21.8 (t, C3).

IR (cm⁻¹): 2978, 1789, 1752, 1728, 1381, 1286, 1257, 1227, 1152, 1039.

 $[\alpha]_D^{20}$ -37.4 (c 4.5, CH₂Cl₂).

LRMS (ESI): $m/z = 383 [M+CH_3CN+Na]^+$, 661 $[2M+Na]^+$.

(2S)-1-benzyl 2-tert-butyl 5-methoxypyrrolidine-1,2-dicarboxylate 3.14

To a solution of **3.13** (2.0 g, 6.3 mmol) in dry THF (20 mL) under an argon atmosphere, was added L-Selectride (1 M, 9.4 mL, 9.4 mmol) at -78 °C. The resulting mixture was stirred at -78 °C for 2 h. Then, NaHCO₃ saturated solution was added and the solution was allowed to warm to 0 °C. H₂O₂ (35%, 1 mL) was added and the solution was then stirred for 20 min. The aqueous layer was extracted with CH₂Cl₂ (3 x 25 mL). The combined organic extracts were dried over MgSO₄ and concentrated under reduced pressure. The residue was dissolved in MeOH (30 mL) and PTSA (110 mg, 0.63 mmol) was added and the mixture was stirred overnight. Aqueous saturated solution of NaHCO₃ (30 mL) was added and the solvents were removed under reduced pressure. The aqueous layer was extracted with diethyl ether (3 x 30 mL). The combined organic extracts were dried over MgSO₄ and concentrated under reduced pressure. Purification by column chromatography (SiO₂ eluted with petroleum ether/Et₂O (70:30)) gave **3.14** as a clear oil (1.6 g, 76% yield over 2 steps).

¹**H NMR** (CDCl₃, 300 MHz) δ (ppm) 7.45-7.30 (5H, m, H-12, H-13, H-14), 5.38-5.05 (3H, m, H-10, H-2), 4.24 (1H, m, H-5), 3.47-3.26 (3H, 4 x s, H-1), 2.50-1.60 (4H, m, H-3, H-4), 1.47-1.32 (9H, 2 x d, H-8).

¹³C NMR (CDCl₃, 100 MHz): δ (ppm) 171.4, 171.3, 171.2 (s, C6), 155.3, 155.0, 154.9, 154.7 (s, C9), 136.3, 136.2 (s, C11), 128.5, 128.4, 128.3, 127.6, 127.5, 127.4 (d, C12, C13, C14), 89.9, 89.1, 88.5 (d, C2), 81.3, 81.1 (s, C7), 67.4, 67.3, 67.2 (t, C10), 60.2, 60.0 (d, C5), 56.3, 55.4, 55.0 (q, C1), 32.8, 32.2, 30.7, 29.9 (t, C3), 28.2, 27.9, 27.9, 27.8, 27.7 (q, C8), 27.0, 26.9 (t, C4). Additionnal peaks arise from rotamers and diastereoisomers.

IR (cm⁻¹): 2980, 1794, 1722, 1369, 1299, 1258, 1225, 1149, 1028, 732, 697.

LRMS (ESI): $m/z = 358 [M+Na]^{+}$.

Benzyl 2-tert-butyl 5-allylpyrrolidine-1,2-dicarboxylate 3.15

To a solution of **3.14** (1.5 g, 4.48 mmol) in CH_2Cl_2 (10 mL) under an argon atmosphere was added allyl-TMS (1.83 mL, 11.20 mmol) followed by $BF_3 \cdot Et_2O$ (1.14 mL, 8.96 mmol) at -78 °C. The resulting mixture was stirred for 1 h at -78 °C. H_2O (3 mL) was then added followed by addition of aqueous saturated solution $NaHCO_3$ (5 mL). The aqueous layer was extracted with CH_2Cl_2 (3 x 20 mL). The combined organic extracts were dried over $MgSO_4$ and concentrated under reduced pressure. Purification by column chromatography (SiO_2 eluted with petroleum ether/ Et_2O (65:35)) gave **3.15** as a mixture of diastereoisomers (1.2 g, 78%).

¹**H NMR** (CDCl₃, 300 MHz): δ (ppm) 7.37-7.30 (5H, m, H-14, H-15, H-16), 5.78 (1H, m, H-2), 5.20-5.01 (4H, m, H-12, H-1), 4.25 (1H, m, H-7), 4.02 (1H, m, H-4), 2.90-1.60 (6H, m, H-3, H-5, H-6), 1.47-1.33 (9H, 2 x d, H-10).

¹³C NMR (CDCl₃, 100 MHz): δ (ppm) 172.0, 171.9, 171.7 (s, C8), 154.8, 157.7, 154.3, 154.2 (s, C11), 136.7, 136.6, 136.5 (s, C13), 135.2, 134.9, 137.7 (d, C2), 128.4, 128.3, 127.8, 126.9 (d, C14, C15, C16), 117.4, 117.3, 116.9 (t, C1), 81.1 (s, C9), 66.9, 66.8, 66.7 (t, C12), 61.1, 60.7, 60.6 (d, C7), 58.7, 58.0, 57.4 (d, C4), 38.9, 38.1, 37.9 (t, C3), 29.3, 28.9, 28.8 (t, C5), 27.9, 27.8, 27.7, 26.7 (t, C6; q, C10). Additional peaks arise from rotamers and diastereoisomers.

IR (cm⁻¹): 3050, 1738, 1702, 1498, 1405, 1349, 1214, 1151, 1103.

LRMS (ESI): $m/z = 368 [M+Na]^+$, 409 $[M+CH_3CN+Na]^+$.

Data according to literature. 66

(S)-Methyl 5-oxopyrrolidine-2-carboxylate 3.1b

A solution of L-pyroglutamic acid **1.116** (4.3 g, 33.3 mmol) in MeOH (50 mL) with Dowex® (small spatula) was heated at reflux for 16 h. The mixture was filtered and the filtrate was concentrated under reduced pressure to give **3.1b** (4.96 g, 96%) as a light yellow oil without further purification.

¹**H NMR** (CDCl₃, 300 MHz): δ (ppm) 6.89 (1H, broad s, NH), 4.26 (1H, dd, J = 8.5, 5.0 Hz, H-4), 3.76 (3H, s, H-6), 2.49-2.10 (4H, m, H-2, H-3).

¹³C NMR (CDCl₃, 100 MHz): δ (ppm) 178.3 (s, C1), 172.5 (s, C5), 55.4 (d, C4), 52.5 (q, C6), 29.2 (t, C2), 24.7 (t, C3).

IR (cm⁻¹): 3259, 1732, 1678, 1378, 1226, 1142, 1104, 1002, 848, 759, 702, 662, 629.

 $[\alpha]_{D}^{24}$ -7.5 (c 1.0, CH₂Cl₂).

LRMS (ESI): $m/z = 207 [M+Na+CH_3CN]^+$.

Data according to literature. 102

• (S)-1-tert-Butyl 2-methyl 5-oxopyrrolidine-1,2-dicarboxylate 3.8b

To a stirred solution of **3.1b** (4.5 g, 31.6 mmol) in CH_3CN (50 mL) was added DMAP (0.4 g, 3.16 mmol) and cooled to 0 °C. A solution of Boc_2O (10.4 g, 47.4 mmol) in CH_3CN (30 mL) was then added slowly. The resulting mixture was warmed to room temperature and stirred overnight. The solvents were removed under reduced pressure. Purification by column chromatography (SiO_2 eluted with EtOAc/hexane (4:6)) gave **3.8b** (6.27 g, 82%) as white crystals.

m.p: 68-70 °C (Et₂O/hexane).

¹**H NMR** (CDCl₃, 300 MHz): δ (ppm) 4.62 (1H, dd, J = 9.5, 3.2 Hz, H-4), 3.78 (3H, s, H-6), 2.64 (1H, dt, J = 17.4, 10.0 Hz, H-2), 2.49 (1H, ddd, J = 17.5, 10.0, 3.0 Hz, H-3), 2.32 (1 H, apparent dq, J = 13.1, 10.0 Hz, H-3), 2.04 (1H, ddd, J = 9.4, 6.4, 3.4 Hz, H-2), 1.49 (9H, s, H-9).

¹³C NMR (CDCl₃, 100 MHz): δ (ppm) 173.1 (s, C1), 171.8 (s, C5), 149.3 (s, C7), 83.6 (s, C8), 58.8 (d, C4), 52.5 (q, C6), 31.1 (t, C2), 27.8 (q, C9), 21.5 (t, C3).

IR (cm⁻¹): 2981, 1790, 1755, 1737, 1700, 1310, 1142.

 $[\alpha]_{D}^{24} - 31.9$ (c 1.0, CH₂Cl₂).

LRMS (ESI): $m/z = 509 [2M+Na]^{+}$.

HRMS (ESI): Calculated for C₁₁H₁₇NO₅Na 266.0999, found 266.0994.

Data according to literature. 103

(2S)-1-tert-Butyl 2-methyl 5-methoxypyrrolidine-1,2-dicarboxylate 3.9b

To a stirred solution of **3.8b** (1.1 g, 4.5 mmol) in dry THF (10 mL) under an argon atmosphere, was added L-Selectride® (6.8 mL, 6.8 mmol, 1 M in THF) at -78 °C dropwise. The resulting mixture was stirred at -78 °C for 2 h. Then, a saturated aqueous solution of NaHCO₃ (10 mL) was added and the reaction mixture was allowed to warm to 0 °C followed by the addition of Et₂O (10 mL). The aqueous layer was extracted with CH₂Cl₂ (3 x 15 mL). The combined organic extracts were dried over MgSO₄ and concentrated under reduced pressure. The residue was dissolved in MeOH (15 mL) and PTSA (79 mg, 0.45 mmol) was added and the mixture was stirred overnight. A saturated aqueous solution of NaHCO₃ (15 mL) was added and the solvents were removed under reduced pressure. The aqueous layer was extracted with diethyl ether (3 x 25 mL). The combined organic extracts were dried over MgSO₄ and concentrated under reduced pressure. Purification by column chromatography (SiO₂ eluted with Et₂O/petroleum ether (3:7)) gave **3.9b** as a clear oil (0.61 g, 52% yield over 2 steps) as a mixture of diastereoisomers (*d.r* = 1.75 : 1).

¹H NMR (DMSO- d_6 , 400 MHz, 100 °C): δ (ppm) 5.15 (1H, dd, J = 5.5, 2.5 Hz, H-2), 4.24 (1H, apparent t, J = 10.1 Hz, H-5), 3.67 and 3.66 (3H, 2 x s, H-7), 3.31 and 3.28 (3H, 2 x s, H-1), 2.28 (1H, m, H-3), 2.00-1.75 (3H, m, H-3, H-4), 1.40 (9H, s, H-10).

¹³C NMR (DMSO- d_6 , 100 MHz, 80 °C): δ (ppm) 172.1 (s, C1), 152.8 (s, C8), 88.1 (d, C2), 79.3 (s, C9), 58.7 (d, C5), 54.7 (q, C1), 54.0 (q, C7), 31.3 (t, C3), 27.5 (q, C10), 25.6 (t, C4). Additionnal peaks arise from rotamers and diastereoisomers at 153.0, 88.5 and 27.1.

IR (cm⁻¹): 2977, 1740, 1704, 1365, 1149, 1084.

LRMS (ESI): $m/z = 323 [M+Na+CH_3CN]^+$.

Data according to literature. 104

(2S)-1-tert-Butyl 2-methyl 5-allylpyrrolidine-1,2-dicarboxylate 1.122b

To a stirred solution of **3.9b** (2.87 g, 11.1 mmol) in CH_2Cl_2 (20 mL) under an argon atmosphere was added allyl-TMS (4.6 mL, 27.7 mmol) followed by the dropwise addition of $BF_3 \cdot Et_2O$ (2.8 mL, 22.2 mmol) at -78 °C. After 1 h, H_2O (3 mL) was then added followed by a saturated aqueous solution of $NaHCO_3$ (10 mL). The aqueous layer was extracted with CH_2Cl_2 (3 x 20 mL). The combined organic extracts were dried over $MgSO_4$ and concentrated under reduced pressure. Purification by column chromatography (SiO_2 eluted with petroleum ether/ Et_2O (9:1)) gave **1.122b** as a mixture of diastereoisomers (2.29 g, 77%) as a colourless oil as a mixture of diastereosiomers (d.r = 4.5 : 1).

¹H NMR (DMSO- d_6 , 400 MHz, 100 °C): δ (ppm) 5.80 (1H, m, H-2), 5.04 (2H, m, H-1), 4.21 (1H, apparent t, J = 8.1 Hz, H-7), 3.89-3.85 (0.3H, m, H-4), 3.83 (0.7H, tdd, J = 8.0, 4.0, 4.0 Hz, H-4), 3.66 (3H, s, H-9), 2.55 (1H, m, H-3), 2.30-2.13 (2H, m, H-3, H-5), 2.03-1.76 (2H, m, H-6), 1.71 (1H, m, H-5), 1.39 (9H, s, H-12).

¹³C NMR (DMSO- d_6 , 100 MHz, 80 °C): δ (ppm) 172.6 (s, C8), 152.7 (s, C10), 135.1 (d, C2), 116.1 (t, C1), 78.6 (s, C11), 59.3 (d, C7), 57.3 (d, C4), 51.1 (q, C9), 37.8 (t, C3), 28.3 (2 x t, C5, C6), 27.6 (q, C12). Additional peaks arise from rotamers and diastereoisomers at 134.8, 116.6, 56.8.

IR (cm⁻¹): 2975, 1749, 1695, 1387, 1365, 1256, 1163, 1124.

LRMS (ESI): $m/z = 333 [M+Na+CH_3CN]^{+}$.

HRMS (ESI): Calculated for C₁₄H₂₃NO₄Na 292.1519, found 292.1515.

• (2S)-Methyl 5-allylpyrrolidine-2-carboxylate 3.11b and 3.12b

1.122b (2.2 g, 8.2 mmol) was dissolved in a solution of TFA in CH_2Cl_2 (20% v/v, 15 mL). The mixture was stirred at room temperature for 1 h. The solvent was removed under reduced pressure. The residue was washed with toluene (3 x 15 mL) and removal of the azetrope with TFA was made under vacuum each time. Then, the residue was diluted in EtOAc (15 mL), washed with an aqueous saturated solution of NaHCO₃ (10 mL) and brine (10 mL). The organic extracts were dried over MgSO₄ and concentrated under reduced pressure. Purification by column chromatography (SiO₂ eluted with petroleum ether/Et₂O (1:1)) gave **3.11b** (*Cis*-diastereoisomer, 751 mg, 54%) and **3.12b** (*Trans*-diasteroisomer, 147 mg, 11%).

3.11b (*Cis*):

¹H NMR (CDCl₃, 300 MHz): δ (ppm) 5.82 (1H, m, H-2), 5.13 (1H, dd, J = 17.0, 1.5 Hz, H-1), 5.07 (1H, d, J = 10.1 Hz, H-1), 3.82 (1H, dd, J = 8.9, 5.8 Hz, H-7), 3.74 (3H, s, H-9), 3.19 (1H, m, H-4), 2.66 (1H, broad s, H-10), 2.37-2.19 (2H, m, H-3), 2.12 (1H, m, H-6), 1.98-1.85 (2H, m, H-6, H-5), 1.38 (1H, m, H-5).

¹³C NMR (CDCl₃, 100 MHz): δ (ppm) 175.4 (s, C8), 135.5 (d, C2), 166.8 (t, C1), 59.8 (d, C7), 59.1 (d, C4), 52.1 (q, C9), 39.9 (t, C3), 30.9 (t, C5), 30.0 (t, C6).

IR (cm⁻¹): 2953, 1734, 1640, 1434, 1336, 1204, 1173, 1120, 995, 914.

 $[\alpha]_D^{22}$ -52.2 (c 1.25, CHCl₃).

HRMS (ESI): Calculated for C₉H₁₆NO₂ 170.1176, found 170.1178.

nOe experiments (CDCl₃, 400 mHz):

3.12b (*Trans*):

¹H NMR (CDCl₃, 300 MHz): δ (ppm) 5.78 (1H, m, H-2), 5.06 (1H, dd, J = 17.3, 1.4 Hz, H-1), 5.01 (1H, d, J = 10.2 Hz, H-1), 3.84 (1H, dd, J = 8.1, 5.6 Hz, H-7), 3.69 (3H, s, H-9), 3.28 (1H, m, H-4), 2.69 (1H, broad s, NH), 2.22-2.15 (3H, m, H-3, H-6), 1.92-1.80 (2H, m, H-6, H-5), 1.43 (1H, m, H-5).

¹³C NMR (CDCl₃, 100 MHz): δ (ppm) 175.9 (s, C8), 135.7 (d, C2), 166.3 (t, C1), 58.8 (d, C7), 57.5 (d, C4), 51.7 (q, C9), 40.5 (t, C3), 30.6 (t, C5), 29.2 (t, C6).

IR (cm⁻¹): 2953, 1733, 1640, 1434, 1332, 1206, 1129, 996, 912.

 $[\alpha]_{D}^{22}$ -70.2 (c 1.25, CHCl₃).

LRMS (ESI): $m/z = 170 [M+H]^{+}$.

Data according to literature. 105

• (2S,5R)-1-Benzyl 2-methyl 5-allylpyrrolidine-1,2-dicarboxylate 3.4b

To a solution of **3.11b** (0.2 g, 1.18 mmol) in dry THF (5 mL) under an argon atmosphere was added in portions sodium hydride (60% in mineral oil, 50 mg, 1.42 mmol). The resulting mixture was stirred for 30 min at room temperature. Then, benzyl chloroformate (0.21 mL, 1.78 mmol) was added dropwise to the mixture at room temperature. The mixture was stirred for 24 h at room temperature. Solvents were removed under reduced pressure and the residue

was then treated with an aqueous solution of citric acid (aq. 10%, 5 mL). The aqueous layer was extracted with EtOAc (3 x 10 mL). The combined organic extracts were dried over MgSO₄ and concentrated under reduced pressure. Purification by column chromatography (SiO₂ eluted with petroleum ether/Et₂O (75:25)) gave **3.4b** as a clear oil (0.31 g, 87%).

¹H NMR (DMSO- d_6 , 400 MHz, 100 °C): δ (ppm) 7.42-7.26 (5 H, m, H-13, H-14, H-15), 5.51 (1H, ddt, J = 17.2, 10.1, 7.1 Hz, H-2), 5.10 (1H, d, J = 10.1 Hz, H-1), 5.09 (2H, s, H-11), 5.03 (1H, d, J = 17.1 Hz, H-1), 4.35 (1H, dd, J = 8.1, 6.6 Hz, H-7), 3.95 (1H, tdd, J = 10.6, 5.2, 2.7 Hz, H-4), 3.63 (3H, s, H-9), 2.60 (1H, m, H-3), 2.28-2.14 (2H, m, H-3, H-5), 2.05-1.87 (2H, m, H-6, H-5), 1.73 (1H, m, H-6).

¹³C NMR (DMSO- d_6 , 100 MHz, 80 °C): δ (ppm) 172.3 (s, C8), 153.8 (s, C10), 136.4 (s, C12), 134.8 (d, C2), 127.9, 127.3 and 126.9 (3 x d, C13, C14, C15), 116.4 (t, C1), 65.8 (t, C11), 59.3 (d, C7), 57.7 (d, C4), 51.2 (q, C9), 37.7 (t, C3), 28.3 (t, C5), 27.6 (t, C6).

IR (cm⁻¹): 2976, 1738, 1702, 1405, 1350, 1215, 1155, 1103.

 $[\alpha]_D^{22}$ -18.1 (c 0.9, CHCl₃).

LRMS (ESI): $m/z = 326 [M+Na]^{+}$.

HRMS (ESI): Calculated for $C_{17}H_{21}NO_4Na$ 326.1363, found 326.1361.

Data according to literature. 106

• (25,5R)-1-Benzyl 2-methyl 5-(2-oxoethyl)pyrrolidine-1,2-dicarboxylate 1.128b

3.4b (900 mg, 2.97 mmol) was dissolved in 10 mL of MeOH/CH₂Cl₂ (1 : 1). The solution was treated with O_3 at -78 °C until a blue solution appeared. Then O_3 was bubbled through the solution (20 min). Triphenylphosphine (875 mg, 3.27 mmol) was added and the mixture was stirred for 30 min. The solution was concentrated under reduced pressure. A mixture of pentane/Et₂O (1 : 1, 15 mL) was used to precipitate PPh₃O. The mixture was filtered and the

filtrate was concentrated under reduced pressure. Purification by column chromatography (SiO₂ eluted with hexane/EtOAc (7:3)) gave **1.128b** as a clear oil (870 mg, 96%).

¹**H NMR** (DMSO- d_6 , 400 MHz, 100 °C): δ (ppm) 9.72 (1H, s, H-1), 7.40-7.28 (5H, m, H-12, H-13, H-14), 5.11 (1H, d, J = 12.6 Hz, H-10), 5.04 (1H, d, J = 12.6 Hz, H-10), 4.38 (1H, dd, J = 8.1, 6.1 Hz, H-6), 4.33 (1H, dtd, J = 7.3, 4.8, 2.5 Hz, H-3), 3.63 (3H, s, H-8), 2.89 (1H, ddd, J = 16.2, 5.1, 2.0 Hz, H-2), 2.63 (1H, ddd, J = 16.5, 7.5, 1.8 Hz, H-2), 2.25 (1H, dddd, J = 13.6, 6.6, 4.5, 3.0 Hz, H-5), 2.16 (1H, dddd, J = 12.6, 10.1, 5.1, 2.5 Hz, H-4), 1.70 (1H, dddd, J = 13.6, 6.6, 4.5, 3.0 Hz, H-5).

¹³C NMR (DMSO- d_6 , 400 MHz, 80 °C): δ (ppm) 200.9 (d, C1), 172.3 (s, C7), 153.2 (s, C9), 136.2 (s, C11), 127.9 (d, C13), 127.4 (d, C12), 126.9 (d, C14), 65.9 (t, C10), 59.2 (d, C6), 53.4 (q, C8), 51.4 (d, C3), 47.8 (t, C2), 29.8 (t, C4), 27.7 (t, C5).

IR (cm⁻¹): 3449, 2953, 1743, 1699, 1407, 1349, 1202, 1175, 1116, 1026, 1001, 918, 770, 746, 698.

 $[\alpha]_{D}^{22}$ 23.6 (*c* 1.0, MeOH).

HRMS (ESI): Calculated for $C_{16}H_{19}NO_5Na$ 328.1161, found 328.1158.

• (25,5R)-1-Benzyl 2-methyl 5-((E)-3(((benzyloxy)carbonl)amino)-4-methoxy-4-oxobut-2-en-1-yl)pyrrolidine-1,2-dicarboxylate 1.127b

To a solution of **1.128b** (460 mg, 1.52 mmol) in CH_2Cl_2 (20 mL) was added **3.13** (710 mg, 2.13 mmol). The solution was cooled to -78 °C and stirred for 30 min. Then, potassium *tert*-butoxide (204 mg, 1.82 mmol) in CH_2Cl_2 (5 mL) was added to the solution. The resulting mixture was stirred for 5 h. The mixture was allowed to warm to room temperature and a

solution of phosphate buffer (pH 6, 10 mL) was added to neutralise. The aqueous layer was extracted with CH_2CI_2 (3 x 25 mL). The combined organic extracts were dried over MgSO₄ and concentrated under reduced pressure. Purification by column chromatography (SiO₂ eluted with EtOAc/hexane/NH₄OH (aq.35% w/v) (40:60:1)) gave **1.127b** as a clear oil (610 mg, 79%) as a mixture of diastereoiosomers (d.r = 3:1).

¹H NMR (DMSO- d_6 , 400 MHz, 100 °C) δ (ppm) 8.34 (1H, broad s, NH), 7.44-7.27 (10H, m, H-1, H-2, H-3, H-21, H-23), 6.54 (1H, t, J = 7.3 Hz, H-10), 5.16-5.00 (4H, m, H-5, H-19, H-5), 4.35 (1H, apparent t, J = 6.6 Hz, H-15), 4.06 (1H, m, H-12), 3.66 (3H, s, H-17), 3.63 (3H, s, H-9), 2.65 (1H, m, H-11), 2.49 (1H, m, H-11), 2.20 (1H, m, H-13), 2.03-1.85 (2H, m, H-13, H-14), 1.67 (1H, m, H-14).

¹³C NMR (DMSO- d_6 , 100 MHz, 80 °C): δ (ppm) 172.4 (s, C16), 164.3 (s, C8), 154.0 and 153.5 (2 x s, C6, C18), 136.4 and 136.3 (2 x s, C20, C4), 132.8 (s, C7), 128.2, 127.9, 127.9, 127.4, 127.3, 127.1, 126.9 (7 x d, C23, C3, C10, C1, C22, C2, C21), 65.9 and 65.5 (2 x t, C5, C19), 59.4 (d, C15), 57.1 (d, C12), 51.9 and 51.3 (2 x q, C17, C9), 31.6 (t, C11), 28.9 (t, C13), 27.7 (t, C14).

IR (cm⁻¹): 3350, 3100, 2985, 1730, 1490, 1380, 750.

LRMS (ESI): $m/z = 533 [M+Na]^{+}$.

HRMS (ESI): Calculated for $C_{27}H_{30}N_2O_8Na$ 533.1900, found 533.1899.

• 1.126b

To a solution of **1.127b** (0.4 g, 0.78 mmol) in dry THF (5 mL) was added DMAP (10 mg, 0.078 mmol). At 0 $^{\circ}$ C, a solution of Boc₂O (0.34 g, 1.57 mmol) in THF was added to the mixture. The resulting mixture was stirred for 1 h at rt. H₂O (5 mL) followed by NaHCO₃ (5 mL) saturated solution were added. The aqueous layer was extracted with EtOAc (3 x 15 mL). The combined organic extracts were dried over MgSO₄ and concentrate under reduced pressure. Purification

by column chromatography (SiO₂ eluted with hexane/EtOAc (30 %)) gave **1.126b** as a mixture of diastereoisomers (d.r = 3:1) as a colourless oil (338 mg, 71 %).

¹H NMR (CDCl₃, 300 MHz) (mixture of conformers): δ (ppm) 7.35-7.10 (10H, m, H-26, H-25,H-24, H-16, H-17, H-18), 7.00-6.65 (1H, m, H-5), 5.20-4.80 (4H, m, H-22, H-14), 3.24 (1H, m, H-10), 3.98 (1H, m, H-7), 3.65-3.41 (6H, m, H-12, H-19), 2.70-1.40 (6H, m, H-6, H-8, H-9), 1.34 (9H, s, H-1).

¹³C NMR (CDCl₃, 100 MHz) (mixture of conformers) : δ (ppm) 172.5 (s, C11), 163.5 (s, C20), 154.3 (s, C13), 153.7 (s, C21), 151.5 (s, C3), 149.6 (d, C5), 138.5 (s, C15), 134.9 (s, C23), 129.6 (s, C4), 128.1, 128.0, 127.8, 127.7, 127.6, 127.3 (6 x d, C26, C25, C24, C16, C17, C18), 83.1 (s, C2), 68.0 (t, C22), 66.6 (t, C14), 59.5 (d, C10), 57.2, (d, C7), 51.9 and 51.8 (2 x q, C12, C19), 31.6 (t, C6), 29.8 (t, C8), 28.9 (t, C9), 27.4 (q, C1). Additional peaks arise from rotamers and diastereoisomers at 172.4, 163.4, 138.2, 134.8, 129.8, 116.6, 83.2, 68.1, 66.8, 59.9, 56.5, 32.5, and 28.5.

LRMS (ESI): 633 [M+Na]⁺ (100 %).

HRMS (ESI): Calculated for $C_{32}H_{38}N_2O_{10}Na$ 633.2419, found 633.2409.

• (2*S*,5*S*)-1-Benzyl 2-methyl 5-((*R*)-3-(((benzyloxy)carbonyl)amino)-4-methoxy-4-oxobutyl)pyrrolidine-1,2-dicarboxylate 3.32

To a stirred solution of **1.127b** (1.0 g, 1.96 mmol) in dry methanol (10 mL) was added (R,R)-Rh(DUPHOS-Et)OTf (10 mg, 0.014 mmol), under argon, then purged with 7 bar of H₂ five times. The reaction mixture was stirred 24 h under 7 bar of H₂ and concentrated under reduced pressure. Purification by column chromatography (SiO₂ eluted with petroleum ether/Et₂O (25:75)) gave the title compound **3.32** as a colourless oil (900 mg, 90 %).

¹H NMR (DMSO- d_6 , 400 MHz, 80 °C): δ (ppm) 7.47 (1H, broad s, NH), 7.39-7.24 (10H, m, H-16, H-17, H-18, H-22, H-23, H-24), 5.12-5.00 (4H, m, H-14, H-20), 4.34 (1H, apparent t, J = 7.6 Hz x 3, H-8), 4.04 (1H, m, H-2), 3.87 (1H, m, H-5), 3.62 (3H, s, H-12), 3.60 (3H, s, H-10), 2.21 (1H, m, H-4), 2.00-1.60 (6H, m, H-4, H-6, H-3, H-7), 1.51 (1H, m, H-6).

¹³C NMR (DMSO- d_6 , 100 MHz, 80 °C) δ (ppm) 172.5 (s, C9), 172.29 (s, C11), 155.7 (s, C19), 153.6 (s, C13), 136.7 (s, C15), 136.5 (s, C21), 127.9, 127.4, 127.3, 127.2, 127.2, 126.9 (6 x d, C17, C22, C16, C24, C18, C23), 65.8 (t, C14), 65.2 (t, C20), 59.2 (d, C2), 57.9 (d, C5), 53.9 (d, C8), 51.3 (2 x q, C12, C10), 30.2 (t, C7), 28.9 (t, C6), 27.5 (2 x t, C3, C4).

IR (cm⁻¹): 3324, 2952, 1699, 1501, 1409, 1349, 1203, 1173, 1111, 1045, 771, 739, 697.

 $[\alpha]_{D}^{24}$ 9.9 (*c* 0.5, MeOH).

LRMS (ESI): $m/z = 535 [M+Na]^{+}$.

HRMS (ESI): $C_{27}H_{32}N_2O_8Na$ calculated 535.2051, found 535.2057.

• 3.33

To a solution of **3.32** (1.0 g, 2.0 mmol) in acetonitrile (10 mL) was added DMAP (26 mg, 0.2 mmol). Then a solution of Boc_2O (0.64 g, 3.0 mmol) in acetonitrile (5 mL) was added dropwise at 0 °C. The reaction mixture was stirred overnight at RT and concentrated under reduced pressure. Purification by column chromatography (SiO₂ eluted with petroleum ether/Et₂O (4:6)) gave the title compound as a colourless oil (1.2 g, 97%).

¹**H NMR** (CDCl₃, 400 MHz): δ (ppm) 7.43-7.28 (10 H, m, H-16, H-17, H-18, H-22, H-23, H-24), 5.31-5.01 (4H, m, H-20, H-14), 4.94 (1H, m, H-8), 4.37 (1H, m, H-2), 3.94 (1H, m, H-5), 3.79-3.53 (6H, 2 x s, H-12, H-10), 2.28-1.42 (6H, m, H-3, H-4, H-7), 2.26-1.80 (2H, m, H-6), 1.45 (9H, s, H-27).

¹³C NMR (CDCl₃, 400 MHz): δ (ppm) 173.2 (s, C11), 170.8 (s, C9), 153.8 (2 x s, C19, C13), 151.3 (s, C25), 136.6 (s, C15), 135.3 (s, C21), 128.5, 128.4, 128.3, 127.9, 127.8, 127.6 (6 x d, C22, C23, C24, C16, C17, C18), 83.7 (s, C26), 68.8 (t, C20), 67.2 (t, C14), 60.0 (d, C2), 59.8 (d, C8), 58.5 (d, C5), 52.2 (2 x q, C10, C12), 30.3 (t, C4), 29.3 (t, C6), 29.1 (t, C3), 27.8 (q, C27), 26.6 (t, C7).

IR (cm⁻¹): 2952, 1742, 1700, 1406, 1346, 1032, 1252, 1203, 1143, 1112, 734, 697.

 $[\alpha]_{p}^{24}$ 22.6 (*c* 0.5, MeOH).

LRMS (ESI): $m/z = 635 [M+Na]^{+}$.

HRMS (ESI): $C_{32}H_{40}N_2O_{10}Na$ calculated 635.2575, found 635.2571.

• 1.125b

A mixture of **3.33** (1.11 g, 1.81 mmol), Pd/C (10%, 30 mg) and 10 mL MeOH, under nitrogen, was purged with H_2 (1 atm.). The reaction was left to stir overnight under H_2 (1 atm.), before filtering, and concentrating under vacuum. Purificartion by column chromatography (SiO₂ eluted with $CH_2Cl_2/MeOH$ (98:2)) to yield **1.125b** as a clear oil (0.55 g, 98%).

¹**H NMR** (CDCl₃, 400 MHz): δ (ppm) 5.38 (1H, broad s, NH) 4.43 (1H, d, J = 9.4 Hz, H-9), 3.90 (1H, dd, J = 10.3, 5.5 Hz, H-3), 3.71 (3H, s, H-11), 3.63 (1H, tt, J = 11.3, 3.4 Hz, H-6), 2.42 (1H, m, H-4), 2.19-1.95 (4H, m, H-8, H-7, H-5), 1.79-1.57 (3H, m, H-4, H-5, H-7), 1.43 (9H, s, H-14).

¹³C NMR (CDCl₃, 100 MHz): δ (ppm) 172.1 (s, C10), 168.6 (s, C2), 155.9 (s, C12), 79.7 (s, C13), 60.6 (d, C6), 58.2 (d, C9), 52.2 (q, C11), 52.1 (d, C3), 31.5 (t, C7), 28.6 (t, C8), 28.4 (t, C4), 28.3 (q, C14), 27.7 (t, C5).

IR (cm⁻¹): 3303, 2977, 1748, 1700, 1653, 1532, 1401, 1368, 1255, 1175.

 $[\alpha]_{D}^{24}$ -72.6 (*c* 0.5, MeOH).

LRMS (ESI): $m/z = 335 [M+Na]^{+}$.

HRMS (ESI): Calculated for $C_{15}H_{24}N_2O_5Na$ 335.1577, found 335.1583.

• 3.34

A mixture of **3.32** (1.11 g, 2.17 mmol), Pd/C (10%, 30 mg) and 10 mL MeOH, under nitrogen, was purged with H_2 (1 atm.). The reaction was left to stir overnight under H_2 (1 atm.), before filtering, and concentrating under vacuum. Purification by column chromatography (SiO₂ eluted with $CH_2CI_2/MeOH$ (93:7)) to yield **3.34** as a yellow oil (0.33 g, 72%).

¹**H NMR** (CDCl₃, 400 MHz): δ (ppm) 4.38 (1H, d, J = 9.5 Hz, H-9), 3.71 (3H, s, H-11), 3.56 (1H, tt, J = 10.1, 4.0 Hz, H-6), 3.37 (1H, dd, J = 6.3, 10.9 Hz, H-3), 2.29 (1H, m, H-4), 2.18-2.05 (2H, m, H-5, H-8), 2.04-1.91 (2H, m, H-7, H-8), 1.81-1.50 (5H, m, H-4, H-7, NH₂, H-5).

¹³C NMR (CDCl₃, 100 MHz): δ (ppm) 172.3 (s, C10), 171.8 (s, C2), 60.8 (d, C9), 57.9 (d, C6), 52.2 (q, C11), 52.0 (d, C3), 31.6 (t, C7), 60.6 (t, C4), 29.5 (t, C8), 28.0 (t, C5).

IR (cm⁻¹): 3365, 2952, 1736, 1703, 1629, 1514, 1439, 1365, 1328, 1167.

 $[\alpha]_{D}^{24}$ –107.4 (c 0.5, MeOH).

LRMS (ESI): $m/z = 213 [M+H]^{+}$, 276 $[M+Na+CH_3CN]^{+}$, 447 $[2M+Na]^{+}$.

HRMS (ESI): Calculated for $C_{10}H_{16}N_2O_3Na$ 235.1053, found 235.1057.

nOe experiments (CDCl₃, 400 MHz):

• 1.125c ¹⁰⁷

To a stirred solution of **1.125b** (110 mg, 0.35 mmol) in THF (1.5 mL) was added an aqueous solution of 1N LiOH (0.1 mL) at room temperature. After stirring for 1 h all the starting material was consumed, 1N HCl was added until pH 5. CH_2Cl_2 (10 mL) was used to extract the product, and the combined organic layers were washed with brine (10 mL) and dried over Na_2SO_4 to give the title product quantitatively without further purification.

¹H NMR (D₂O, 300 MHz): δ (ppm) 4.18 (1H, d, J = 9.5 Hz, H-9), 3.90 (1H, m, H-3), 3.63 (1H, m, H-6), 2.35-1.50 (6H, m, H-7, H-8, H-5, H-4), 1.75-1.50 (2H, m, H-5, H-4), 1.39 (9H, s, H-14). There are 1 x OH and 1 x N-H protons missing from the ¹H-spectrum.

¹³C NMR (CDCl₃, 100 MHz): δ (ppm) 174.0 (s, C10), 169.9 (s, C2), 155.9 (s, C12), 79.9 (s, C13), 60.9 (d, C9), 58.8 (d, C6), 52.0 (d, C3), 31.5 (t, C7), 28.5 (t, C8), 28.3 (q, C14), 28.1 (t, C4), 27.8 (t, C5).

IR (cm⁻¹): 3336, 2973, 1703, 1634, 1515, 1445, 1247, 1161.

 $[\alpha]_{D}^{24}$ 20.5 (c 0.8, CHCl₃).

LRMS (ESI): $m/z = 321 [M+Na]^+$, 619 $[2M+Na]^+$.

HRMS (ESI): Calculated for $C_{28}H_{44}N_4O_{10}Na$ 619.2950, found 619.2955.

• 1.138b

A mixture of **1.126b** (1.11 g, 1.82 mmol), Pd/C (10%, 30 mg) and 10 mL MeOH, under nitrogen, was purged with H_2 (1 atm.). The reaction was left to stir overnight under H_2 (1 atm.), before

filtering, and concentrating under vacuum. Purification by column chromatography (SiO_2 eluted with $CH_2Cl_2/MeOH$ (98:2)) gave a mixture of two diastereoisomers **1.125b** (261 mg, 67%) and the title compound **1.138b** (d.r. = 3:1) as a clear oil (130 mg, 23%).

1.138b: ¹**H NMR** (CDCl₃, 400 MHz): δ (ppm) 5.47 (1H, broad s, NH), 4.47 (1H, d, J = 8.0 Hz, H-9), 4.10 (1H, m, H-3), 3.75-3.60 (4H, s+m, H-11, H-6), 2.45-2.39 (1H, m, H-4), 2.19-1.95 (4H, m), 1.73-1.57 (3H, m), 1.40 (9H, s, H-14).

¹³C NMR (CDCl₃, 100 MHz): δ (ppm) 172.1 (s, C10), 169.1 (s, C2), 155.6 (s, C12), 79.4 (s, C13), 58.1 (d, C9), 56.4 (d, C6), 52.2 (d, C3), 49.9 (q, C11), 32.0 (t, C7), 28.9 (t, C8), 28.2 (q, C14), 27.1 (t, C4), 26.7 (t, C5).

IR (cm⁻¹): 3403, 2977, 1748, 1700, 1653, 1506, 1169, 1073.

 $[\alpha]_D^{24}$ –22.5 (c 1.0, MeOH).

HRMS (ESI): Calculated for $C_{15}H_{24}N_2O_5Na$ 335.1577, found 335.1581.

Data according to literature. 108

nOe experiment (CDCl₃, 400 MHz):

Methyl 2-(((benzyloxy)carbonyl)amino)-2-methoxyacetate 3.17

Benzyl carbamate **3.15** (10.0 g, 67.0 mmol) and glyoxylic acid monohydrate **3.14** (6.8 g, 92.0 mmol) were mixed in 90 mL of dry Et_2O and stirred for 16 h. The product was filtered and washed with Et_2O (50 mL) to afford **3.16** (7.57 g, 50% yield) as white crystals. **3.16** (0.69 g, 3.0 mmol) was dissolved in 10 mL methanol and cooled to 0 °C. To this solution 1 mL of concentrated sulphuric acid was added dropwise. The reaction mixture was stirred at room temperature for 2 days. The mixture was poured into 50 mL of ice cooled aqueous saturated

solution of sodium bicarbonate, followed by extraction with EtOAc (3 x 75 mL). All organic layers were combined and dried over $MgSO_4$. After filtration, solvent was removed under reduced pressure to give **3.17** as white solid (0.62 g, 82%) without further purification.

m.p: 75-77 °C (EtOAc/Et₂O).

¹H NMR (CDCl₃, 400 MHz): δ (ppm) 7.45-7.30 (5H, m, H-11, H-10, H-9), 5.93 (1H, d, J = 9.0 Hz, H-5), 5.37 (1H, d, J = 9.0 Hz, H-3), 5.16 (2H, s, H-7), 3.81 (3H, s, H-1), 3.47 (3H, s, H-4).

¹³C NMR (CDCl₃, 100 MHz): δ (ppm) 168.0 (s, C2), 155.7 (s, C6), 135.8 (s, C8), 128.6, 128.2, 128.1 (3 x d, C11, C10, C9), 80.6 (d, C3), 67.4 (t, C7), 56.2 (q, C4), 52.9 (q, C1).

IR (cm⁻¹): 3306, 3036, 2945, 1751, 1712, 1687, 1528, 1455, 1440, 1360, 1258, 1219, 1195, 1099, 1016, 977.

LRMS (ESI): $m/z = 317 [M+Na+CH_3CN]^+$.

Data according to literature. 92

Methyl 2-(benzyloxycarbonyl)-2-(diethoxyphosphoryl)acetate 3.13

3.17 (4.6 g, 18.0 mmol) was dissolved in 20 mL of toluene and stirred at 70 °C for 1 h until a homogeneous solution was acquired. Then PCl₃ (1.95 mL, 18.0 mmol) was added. The reaction mixture was stirred at 70 °C overnight. Triethyl phosphite (3.5 mL, 20.0 mmol) was added dropwise and the reaction mixture stirred at 70 °C for another 2 h. Toluene was removed under reduced pressure to afford an oil which was dissolved in EtOAc (20 mL). The solution was washed with a saturated aqueous solution of NaHCO₃ (15 mL) and dried over MgSO₄. After filtration, the filtrate was concentrated to about 50 mL and hexane (30 mL) was added with vigorous stirring to afford **3.13** (4.3 g, 66%) as a precipitate which was collected by filtration without further purification.

m.p: 79-80 °C (EtOAc/hexane).

¹H NMR (CDCl₃, 400 MHz): δ (ppm) 7.40-7.32 (5H, m, H-11, H-10, H-9), 5.61 (1H, d, J = 6.0 Hz, NH), 5.12 (2H, m, H-7), 4.86 (1H, dd, J = 24.0, 6.0 Hz, H-5), 4.15 (4H, m, H-2), 3.80 (3H, s, H-3), 1.30 (6H, m, H-1).

¹³C NMR (CDCl₃, 100 MHz): δ (ppm) 168.2 (s, C4), 155.6 (s, C6), 135.8 (s, C8), 128.7, 128.5, 128.1 (3 x d, C11, C10, C9), 67.6 (t, C7), 63.9, (t, C2), 53.3 (q, C3), 51.9 (d, C5), 16.3 (q, C1). Additional peaks arise from rotamers at 67.3, 64.0, 63.8, 53.2 and 16.2.

IR (cm⁻¹): 3303, 3220, 3036, 2982, 1749, 1706, 1524, 1328, 1260, 1209, 1176, 1019, 965.

LRMS (ESI): $m/z = 382 [M+Na]^{+}$.

Data according to literature. 92

N-Boc-1.125-Arg(NO₂)Pro-OMe 3.35

1.125b (60 mg, 0.20 mmol) was dissolved in a mixture of THF/LiOH 1N (1:1) (2 mL) and was stirred for 1 h. The solution was acidified with HCl 1N (2 mL) until pH 5. The aqueous layer was extracted with CH_2Cl_2 (5 x 15 mL), and the organic layer was dried over MgSO₄ and concentrated under reduced pressure. The residue **1.125c** was dissolved in DMF (5 mL) and HBTU (110 mg, 0.30 mmol) was added. The resulting mixture was stirred for 15 min. H.Arg(NO₂)Pro-OMe **2.10b** (64 mg, 0.20 mmol) was dissolved in DMF (5 mL) and DIPEA (0.14 mL, 0.80 mL) was added. The resulting solution was added dropwise to the first solution containing **1.125c**. The reaction mixture was stirred overnight at room temperature. Solvents were evaporated under reduced pressure. Purification by column chromatography (SiO₂ eluted with $CH_2Cl_2/MeOH/NH_4OH$ (aq.35% w/v) (95:4:1)) gave the title compound as a white solid (99 mg, 85 %).

m.p.: 109-111 °C (CH₂Cl₂/Et₂O).

¹**H NMR** (CDCl₃, 400 MHz): δ (ppm) 8.05-7.64 (3H, broad s, NH), 7.49-7.35 (1H, broad s, NH), 7.21-6.99 (1H, broad s, NH), 4.74 (1H, m, H-12), 4.51 (1H, dd, J = 5.6, 4.5 Hz, H-24), 4.33 (1H, d, J = 5.5 Hz, H-9), 4.17-3.56 (4H, m, H-3, H-6, H-21), 3.71 (3H, s, H-26), 3.43-3.24 (2H, m, H-15), 2.37-1.54 (16H, m, H-4, H-5, H-7, H-8, H-22, H-23, H-13, H-14), 1.42 (9H, s, H-29).

¹³C NMR (CDCl₃, 100 MHz): δ (ppm) 172.0 (s), 170.8 (s), 169.7 (s), 169.4 (s), 159.6 (s), 155.8 (s), 80.1 (s), 60.7 (d), 60.0 (d), 58.9 (d), 53.4 (d), 52.3 (q), 50.5 (d), 46.9 (t), 40.5 (t), 31.9 (t), 28.8 (t), 28.3 (q), 27.9 (t), 27.7 (t), 27.7 (t), 24.9 (t), 23.4 (t).

IR (cm⁻¹): 3294, 2947, 1620, 1534, 1436, 1366, 1251, 1159.

 $[\alpha]_{D}^{24}$ -77.9 (c 0.5, MeOH).

LRMS (ESI): $m/z = 633 [M+Na]^{+}$.

HRMS (ESI): Calculated for $C_{26}H_{43}N_8O_9611.3148$, found 611.3142.

N-Boc-Arg(NO₂)-1.125-Arg(NO₂)-Pro-OMe 3.37

3.35 (88 mg, 0.14 mmol) was treated with TFA (10 mL of a 20% v/v solution in CH₂Cl₂) at room temperature and the mixture stirred overnight. CH₂Cl₂ was removed under vacuum and the residue washed with toluene (3 x 10 mL), removal of the azetrope with TFA was made under vacuum each time. The crude oil was washed alternately with EtOAc (5 x 10 mL in total) and MeOH (5 x 10 mL in total) until a white solid of consistent weight was obtained **3.35b**. *N*-Boc-Arg(NO₂)-OH **2.5** (46 mg, 0.14 mmol) was dissolved in DMF (2.5 mL) and HBTU (80 mg, 0.22 mmol) was added. The resulting mixture was stirred at room tempearture for 15 min. **3.35b** was dissolved in DMF (2.5 mL) and DIPEA (0.1 mL, 0.58 mmol) was added. The solution was added dropwise to the solution containing *N*-Boc-Arg(NO₂)-OH. The resulting mixture was

stirred overnight at room temperature. Solvents were evaporated under reduced pressure. Purification by column chromatography (SiO₂, CH₂Cl₂/MeOH/NH₄OH (aq.35% w/v) $(94:5:1)\rightarrow (92:7:1)$) gave *N*-Boc-Arg(NO₂)-Pyro-Arg(NO₂)Pro-OMe **3.37** (60 mg, 53%).

m.p.: 120-122 °C (CH₂Cl₂/Et₂O).

¹**H NMR** (CDCl₃, 400 MHz): δ (ppm) 8.58-7.29 (8H, broad s, NH), 5.62 (1H, broad s, NH), 4.76 (1H, m, H-12), 4.62-3.93 (4H, m, H-17, H-9, H-29, H-3), 3.87-3.58 (3H, m, H-6, H-14), 3.71 (3H, s, H-19), 3.41-3.05 (4H, m, H-22, H-40), 2.43-1.53 (20H, m, H-4, H-5, H-7, H-8, H-20, H-21, H-15, H-16, H-39, H-38), 1.42 (9H, s, H-32).

¹³C NMR (CDCl₃, 100 MHz): δ (ppm) 172.2 (s), 171.6 (s), 169.9 (s), 168.8 (s), 167.8 (s), 159.4 (s), 159.4 (s), 155.9 (s), 80.0 (s), 60.4 (d), 59.9 (d), 58.9 (d), 52.4 (q), 50.9 (d), 50.8 (d), 50.5 (d), 47.0 (t), 40.8 (t), 40.8 (t), 31.9 (t), 28.9 (t), 28.7 (t), 28.3 (q), 28.1 (t), 24.9 (t), 24.8 (t). 4 x C (t) are missing due to signals overlapping.

IR (cm⁻¹): 3296, 2949, 1621, 1532, 1438, 1366, 1252, 1158.

 $[\alpha]_{D}^{24}$ -64.9 (c 0.5, MeOH).

LRMS (ESI): $m/z = 834 [M+Na]^{+}$.

HRMS (ESI): Calculated for $C_{32}H_{54}N_{13}O_{12}$ 812.4015, found 812.3978.

N-Ac-Pro-Arg (NO₂)-1.125-Arg(NO₂)-Pro-OMe 3.36

3.37 (50 mg, 0.062 mmol) was treated with TFA (7 mL of a 20% v/v solution in CH_2Cl_2) at room temperature and the mixture stirred overnight. CH_2Cl_2 was removed under vacuum and the residue washed with toluene (3 x 10 mL), removal of the azetrope with TFA was made under vacuum each time. The crude oil was washed alternately with EtOAc (5 x 10 mL in total) and MeOH (5 x 10 mL in total) until a white solid of consistent weight was obtained **3.37b**. *N*-Ac-

Pro-OH **3.38** (10 mg, 0.062 mmol) was dissolved in DMF (2.5 mL) and HBTU (34 mg, 0.093 mmol) was added. The resulting mixture was stirred at room temperature for 15 min. **3.37b** was dissolved in DMF (2.5 mL) and DIPEA (0.1 mL, 0.50 mmol) was added. The solution was added dropwise to the solution containing *N*-Ac-Pro-OH **3.38**. The resulting mixture was stirred overnight at room temperature. Solvents were evaporated under reduced pressure. Purification by column chromatography (SiO₂, CH₂Cl₂/MeOH/NH₄OH (aq.35% w/v) (92:7:1) \rightarrow (89:10:1)) gave the title compound as an off white solid (45 mg, 85%).

m.p: 125-127 °C (CH₂Cl₂/Et₂O).

¹**H NMR** (DMSO- d_6 , 400 MHz, 100 °C): δ (ppm) 8.52 (1H, broad s, NH), 8.36-7.61 (5H, broad s, NH), 7.38-6.93 (2H, broad s, NH), 4.56-3.93 (5H, m, H-12, H-3, H-29, H-9, H-17), 3.61 (3H, s, H-19), 3.77-3.45 (5H, m, H-6, H-14, H-35), 3.15 (4H, m, H-22, H-40), 1.97 (3H, s, H-37), 2.32-1.06 (24 H, m, H-8, H-34, H-16, H-33, H-7, H-4, H-39, H-21, H-38, H-15, H-20, H-5).

¹³C NMR (DMSO-*d*₆, 100 MHz, 80 °C) δ (ppm) 172.2 (s), 171.7 (s), 171.1 (s), 170.0 (s), 169.0 (s), 168.5 (s), 166.8 (s), 159.3 (s), 159.0 (s), 66.0 (d), 59.8 (d), 59.4 (d), 58.5 (d), 54.2 (d), 51.9 (d), 51.7 (q), 49.9 (d), 49.6 (t), 47.7 (t), 46.4 (t), 46.3 (t), 31.7 (t), 31.2 (t), 29.3 (t), 29.1 (t), 28.5 (t), 28.2 (t), 28.0 (t), 27.6 (t), 26.6 (t), 24.3 (t), 22.5 (t), 22.3 (q), 22.0 (t).

IR (cm⁻¹): 3291, 2951, 1742, 1620, 1534, 1435, 1254, 1197, 1126.

 $[\alpha]_{D}^{24}$ - 72.1 (*c* 0.26, MeOH).

LRMS (ESI): $m/z = 873 [M+Na]^{+}$.

HRMS (ESI): Calculated for $C_{34}H_{55}N_{14}O_{12}$ 851.4118, found 851.4128.

LCMS (ESI): 426.3 ([M/2+H]⁺, 100%).

7.4 Compounds appearing in Chapter 4

General procedure for oligomer synthesis:

A] Boc deprotection step

1.125b (0.3 mmol) was treated TFA (10 mL of a 20% v/v solution in CH_2CI_2) at room temperature and the mixture stirred overnight. CH_2CI_2 was removed under vacuum and the residue washed with toluene (3 x 10 mL), removal of the azetrope with TFA was made under vacuum each time. The crude oil was washed alternately with EtOAc (5 x 10 mL in total) and MeOH (5 x 10 mL in total) until a white solid of consistent weight was obtained **4.4.**

B] Hydrolysis step

To a stirred solution of **1.125b** (0.3 mmol) in THF (1 mL) was added LiOH (1 mL of a 1M aqueous solution). The solution was stirred at room temperature for 1 h. The solution was acidified with HCl 1N (2 mL) until pH 5. Aqueous layer was extracted five times with CH_2Cl_2 (5 x 15 mL), and the organic layer was dried over MgSO₄ and concentrated under reduced pressure to afford **1.125c**.

C] Coupling reaction step

To a solution of **1.125c** in DMF (5 mL) were added HOBt (1.2 eq.) and EDC (1.2 eq.). The resulting mixture was stirred at room temperature for 15 min. The solution of **4.4** in DMF (5 mL) with DIPEA (3.0 eq.) was added to the reaction mixture at 0 °C and stirred overnight at room temperature. The solvents were evaporated under reduced pressure. Purification by column chromatography (SiO_2 eluted with $CH_2Cl_2/MeOH/NH_4OH$ (aq. 37%) (95:5:1)) followed by precipitation with Et_2O gave the title compound as a white solid.

Dimer 4.1

Compound **4.4** was prepared from **1.125b** (64 mg, 0.3 mmol) following the general method A. Then, **1.125c** (90 mg, 0.3 mmol) was prepared following general method B. Coupling reaction of **4.4** and **1.125c** was undertaken following method C. The title compound was obtained as a

white solid from column chromatography (SiO₂, CH₂Cl₂/MeOH/NH₄OH (aq. 37%) (93:7:1)) followed by precipitation from Et₂O (119 mg, 81% over 3 steps).

m.p: 87-90 °C.

¹H NMR (CD₃CN, 300 MHz): δ (ppm) 6.80 (1H, broad s, NH), 5.59 (1H, broad s, NH), 4.27 (1H, d, J = 9.6 Hz), 4.19 (1H, d, J = 9.6 Hz), 4.03 (1H, m), 3.85 (1H, m), 3.63 (3H, s, OC H_3), 3.56-3.49 (2H, m, H-6, H-6'), 2.36-1.97 (10H, m), 1.88-1.73 (2H, m), 1.72-1.50 (4H, m), 1.40 (9H, s, C(C H_3)₃).

¹³C NMR (CDCl₃, 100 MHz): δ (ppm) 172.3 (s), 171.1 (s), 169.0 (s), 167.7 (s), 155.8 (s), 79.7 (s), 61.3 (d), 60.3 (d), 59.4 (d), 58.1 (d), 52.4 (d), 52.2 (d), 51.8 (q), 31.8 (t), 31.6 (t), 29.0 (t), 28.4 (t), 28.3 (q), 28.1 (t), 27.8 (t), 27.7 (t), 27.6 (t).

IR (cm⁻¹): 3295, 2949, 2350, 1740, 1631, 1518, 1440, 1364, 1248, 1200, 1166.

 $[\alpha]_{D}^{24}$ –13.8 (*c* 0.25, MeOH).

LRMS (ESI): $m/z = 515 [M+Na]^{+}$.

HRMS (ESI): Calculated for $C_{24}H_{36}N_4O_7Na$ 515.2476, found 515.2480.

LCMS (ESI): 515.2 [M+Na]⁺ (100%).

UV (MeOH, nm): 227 (A = 0.79, c = 0.5 mM, ε = 1580).

Trimer 4.2

Compound **4.5** was prepared from **4.1** (80 mg, 0.16 mmol) following the general method A. Then, **1.125c** (48 mg, 0.16 mmol) was prepared following general method B. Coupling reaction of **4.5** and **1.125c** was undertaken following method C. The title compound was obtained as a white solid from column chromatography (SiO₂, CH₂Cl₂/MeOH/NH₄OH (aq. 37%) (93:7:1)) followed by precipitation from Et₂O (79 mg, 73% over 3 steps).

m.p: 175-178 °C (CH₂Cl₂/Et₂O).

¹H NMR (CD₃CN, 400 MHz): δ (ppm) 7.09 (1H, broad s, NH), 6.94 (1H, d, J = 7.7 Hz, NH), 5.91 (1H, d, J = 6.6 Hz, NH), 4.30 (1H, d, J = 9.5 Hz), 4.26-4.16 (4H, m), 3.82 (1H, m), 3.62 (3H, s, OC H_3), 3.58-3.47 (3H, m, H-6, H-6', H-6''), 2.20-1.45 (24H, m), 1.44 (9H, s, C(C H_3)₃).

¹³C NMR (CD₃CN, 100 MHz): δ (ppm) 173.7 (s), 173.4 (s), 173.1 (s), 170.6 (s), 169.9 (s), 157.9 (s), 80.4 (s), 61.9 (d), 61.9 (d), 61.7 (d), 61.1 (d), 61.0 (d), 59.8 (d), 53.1 (d), 52.5 (q), 51.3 (d), 51.2 (d), 32.9 (t), 32.8 (t), 32.7 (t), 30.2 (t), 30.1 (t), 29.4 (t), 29.3 (t), 29.2 (t), 28.9 (q, 3C), 28.9 (t). 1 x (s) and 3 x C (t) are missing because of the overlapping of peaks in the ¹³C spectrum.

IR (cm⁻¹): 3272, 2949, 2350, 1628, 1532, 1443, 1366, 1326, 1249, 1199, 1168, 1126.

 $[\alpha]_{D}^{24} - 13.9$ (c 0.33, MeOH).

LRMS (ESI): $m/z = 695 [M+Na]^{+}$.

HRMS (ESI): Calculated for C₃₃H₄₈N₆O₉Na 695.3375, found 695.3386.

LCMS (ESI:) 695.3 [M+Na]⁺ (100%).

UV (MeOH, nm): 229 (A = 1.20, c = 0.25 mM, ε = 4800), 281 (A = 0.67, c = 0.25 mM, ε = 2680).

Tetramer 4.3

Compound **4.7** was prepared from **4.2** (48 mg, 0.07 mmol) following the general method A. Then, **1.125c** (21 mg, 0.07 mmol) was prepared following general method B. Coupling reaction of **4.7** and **1.125c** was undertaken following method C. The title compound was obtained as a white solid from column chromatography (SiO_2 , $CH_2Cl_2/MeOH/NH_4OH$ (aq. 37%) (85:15:1)) followed by precipitation from Et_2O (9 mg, 15% over 3 steps).

m.p: 115-118 °C (CH₂Cl₂/Et₂O).

¹H NMR (CD₃CN, 400 MHz): δ (ppm) 6.85 (1H, d, J = 7.6 Hz, NH), 6.79 (2H, d, J = 7.6 Hz, NH), 5.35 (1H, broad s, NH), 4.29 (1H, d, J = 9.6 Hz), 4.22-4.14 (3H, m), 4.12-3.80 (4H, m), 3.64 (3H, s, OCH₃), 3.61-3.47 (4H, m, H-6, H-6', H-6''), 2.22-1.48 (32H, m), 1.40 (9H, s, C(CH₃)₃).

¹³C NMR (CDCl₃, 100 MHz): δ (ppm) 172.3 (s), 171.4 (s), 171.3 (s), 169.1 (s), 168.7 (s), 168.5 (s), 167.9 (s), 155.9 (s), 79.6 (s), 61.2 (d), 60.9 (d), 60.3 (d), 59.5 (d), 59.4 (d), 59.3 (d), 58.2 (d), 52.3 (q), 51.7 (d), 51.6 (d), 51.5 (d), 31.9 (t), 31.8 (t), 31.6 (t), 30.3 (t), 28.4 (t), 28.4 (q, 3C), 28.2 (t), 28.1 (t), 28.1 (t), 27.9 (t), 27.7 (t), 27.6 (t). 1 x (s), 2 x (d) and 4 x C (t) are missing because of the overlapping of peaks in the 13 C spectrum.

IR (cm⁻¹): 3294, 2945, 2358, 1740, 1633, 1520, 1437, 1366, 1204, 1167.

 $[\alpha]_{D}^{24}$ – 17.4 (*c* 0.43, MeOH).

LRMS (ESI): $m/z = 875 [M+Na]^{+} (100 \%)$.

HRMS (ESI): Calculated for $C_{42}H_{60}N_8O_{11}Na$ 875.4274, found 875.4261.

LCMS (ESI): 875.4275 [M+Na]⁺.

UV (MeOH, nm): 228 (A = 1.01, c = 0.125 mM, ϵ = 8080), 276 (A = 0.19, c = 0.125 mM, ϵ = 1520).

7.5 Compounds appearing in Chapter 5

• 1.125d

1.125c (110 mg, 0.35 mmol) was treated with trifluoroacetic acid (10 mL of a 20% v/v solution in CH_2Cl_2) at room temperature and the mixture stirred overnight. CH_2Cl_2 was removed under vacuum and the residue washed with toluene (3 x 15 mL), removal of the azetrope with TFA was made under vacuum each time. The crude oil was washed alternately with EtOAc (5 x 20 mL in total) and MeOH (5 x 20 mL in total) until a white solid of consistent weight was obtained **1.125'**. Then **1.125'** prepared above was dissolved in dioxane (5 mL), Fmoc-OSu (143 mg, 0.42

mmol) and an aqueous saturated solution of Na_2CO_3 (4 mL) were added. The resulting mixture was stirred overnight. Organic solvents were removed under reduced pressure. The aqueous layer was re-acidified to pH 4 with HCl 1M and was extracted with CH_2CI_2 (5 x 15 mL). The combined organic extracts were dried over $MgSO_4$ and concentrated under reduced pressure. Trituration with $Et_2O/hexane$ (1:1) gave **1.125d** as a white solid (104 mg, 71%).

m.p: 92-95 $^{\circ}$ C (hexane/Et₂O).

¹**H NMR** (DMSO- d_6 , 400 MHz): δ (ppm) 12.56 (1H, broad s, OH), 7.89 (2H, d, J = 7.4 Hz, H-19), 7.77-7.49 (2H, m, H-16), 7.47-7.24 (4H, m, H-17, H-18), 5.06 (1H, broad s, NH), 4.41-3.12 (6H, m, H-3, H-9, H-13, H-14, H-6), 2.20-1.03 (8H, m, H-4, H-5, H-7, H-8).

¹³C NMR (DMSO- d_6 , 100 MHz): δ (ppm) 173.1 (s, C10), 167.3 (s, C2), 156.0 (s, C12), 145.2 (s, C15), 140.7 (s, C20), 127.6 (d, C18), 127.0 (d, C17), 125.2 (d, C16), 120.1 (d, C19), 65.5 (t, C13), 59.8 (d, C9), 58.0 (d, C6), 51.1 (d, C3), 46.6 (d, C14), 31.2 (t, C7), 28.3 (t, C8), 28.0 (t, C4), 25.2 (t, C5). Additional peaks arise from rotamers at 143.9 (s), 140.6 (s), 127.1 (s), 126.8 (s), 119.8 (s), 64.9 (t), 50.1 (d).

IR (cm⁻¹): 3300, 3020, 1713, 1611, 1446, 1246, 1188, 759, 739.

 $[\alpha]_D^{24}$ – 38.6 (c 0.5, MeOH).

LRMS (ESI): $m/z = 443 [M+Na]^+$, 863 $[2M+Na]^+$.

HRMS (ESI): Calculated for $C_{24}H_{25}N_2O_5$ 421.1758, found 421.1764.

LCMS (ESI): 421.1764 ([M+H]⁺, 100%).

Data according to literature. 109

Solid phase synthesis methods

1) General techniques

Peptides were synthesised manually using standard Fmoc (fluorenylmethyloxy carbonyl) chemistry performed in three way filtration tubes. The Rink amide resin (Merck) was used for solid support. All Fmoc-protected amino acids were L-confirguration and were purchased from NovaBiochem except for Fmoc-Arg(Pbf)-OH (Aldrich). For L-arginine side chain protection was used 2,2,4,6,7-pentamethyldihydrobenzofuran-sulfonyl (Pbf) groups. General coupling was performed with either HOBt/DIC or HBTU in the presence of DIPEA in DMF. Fmoc deprotection was undertaken with two treatments of 20% v/v piperidine in DMF. The deprotection and coupling step synthesis were monitored with the Kaiser Ninhydrin test (primary L-amino acid residue) or 2,3,5,6-tetrachlorobenzoquinone (chloranil, secondary L-amino acid residue). Acetylation of the *N*-terminus of peptide was undertaken using 50% Ac₂O v/v in pyridine. To cleave the peptide from the support and remove the side chain protecting group, a mixture of TFA/TIS/H₂O (96:2:2) was used. Crude peptides were precipitated from MeOH/Et₂O.

2) General procedure for solid phase peptide synthesis.

a) Deprotection of Fmoc group on resin

Rink amide resin was pre-swollen in CH_2Cl_2 for 15 min. 20% Piperidine in DMF (~20 mL/g of resin) was added to the resin and suspended in the vessel for 20 min. Then the resin was drained and washed alternatively (stand for 1 min before draining) with CH_2Cl_2 (20 mL/g of resin x 3), MeOH (20 mL/g of resin x 3), Et₂O (20 mL/g of resin x 3) and 50% DIPEA/DMF (20 mL/g of resin).

b) Ninhydrin test

Reagent A:

Solution 1: To a stirred solution of phenol (40 g) in 10 mL of hot ethanol was added 4 g of amberlite mix-bed resin MB-3 and stirred for 1 h. The resin was removed by suction filtration.

Solution 2: To a stirred solution of KCN 1.3 mg in 2.0 mL of H_2O was added distilled pyridine to a volume of 100 mL and amberlite mixed bed-resin MB-3 4g was added and was stirred for 1 h. Then the resin was removed by suction filtration. Solution 1 and 2 were mixed together to afford reagent A.

Reagent B: 25 g of Ninhydrin were dissolved in 50 mL of absolute ethanol and stored in the dark.

Method: To a small quantity of resin in a small test tube was added 7 drops of reagent A and 3 drops of reagent B. A control was prepared using the stains without the resin beads. Both test tubes were heated at 100 °C for 5 min. Resin beads and solution became blue (positive result, free amino groups) or stayed pale yellow (negative result, complete coupling).

c) Chloranil test

A few resin beads were placed in a test tube and 2 drops of 2% chloranil in DMF were added. A control was prepared using the stains without the resin beads. Both test tubes were heated at 100 °C for 5 min. The beads contained free amino groups appeared as a deep blue colour (positive result) while completely coupled beads remained colourless (negative result).

d) General coupling of Fmoc-amino acids

The resin with a free amino group (1.0 mmol of resin loading) was pre-swollen in CH_2Cl_2 for 20 min. To a stirred solution of Fmoc-amino acids (3.0 eq., 3.0 mmol) in DMF (2 mL for 3.0 mmol) was added HOBt (3.0 eq., 3.0 mmol) and DIC (3.0 eq., 3.0 mmol), respectively. DIPEA (5.0 eq., 5.0 mmol) was added to the resin and then the activated amino acid solution was added to the resin. The vessel was sealed and shaken for 5 h. All solvents were removed by suction filtration and the resin was washed (stand for one minute before draining) with DMF (20 mL/g of resin x 3), CH_2Cl_2 (20 mL/g of resin x 3), MeOH (20 mL/g of resin x 3) and El_2O (20 mL/g of resin x 3).

e) Coupling of Fmoc-Arg(Pbf)-OH

The resin with a free amino group (1.0 mmol of resin loading) was pre-swollen in CH_2Cl_2 for 20 min. To a stirred solution of Fmoc-Arg(Pbf)-OH (3.0 eq., 3.0 mmol) in DMF (2 mL for 3.0 mmol) was added HBTU (3.0 eq., 3.0 mmol). DIPEA (5.0 eq., 5.0 mmol) was added to the resin and then the activated amino acid solution was added to the resin. The vessel was sealed and shaken for 5 h. All solvents were removed by suction filtration and the resin was washed (stand for one minute before draining) with DMF (20 mL/g of resin x 3), CH_2Cl_2 (20 mL/g of resin x 3), MeOH (20 mL/g of resin x 3) and Et_2O (20 mL/g of resin x 3).

f) Fmoc deprotection

The resin with Fmoc protecting groups was treated with 20% v/v piperidine in DMF (~20 mL/g of resin) and shaken for 30 min. Then the resin was drained and washed alternatively (stand for 1 min before draining) with DMF (20 mL/g of resin x 3), CH_2Cl_2 (20 mL/g of resin x 3), MeOH (20 mL/g of resin x 3), Et_2O (20 mL/g of resin x 3).

g) N-Terminus acylation

Free amine resin (1.0 mmol of resin loading) was treated with 50% Ac_2O v/v in pyridine (3.0 eq., 3.0 mmol) and shaken for 45 min. All solvents were removed by suction filtration and the resin was washed (stand for one minute before draining) with DMF (20 mL/g of resin x 3), CH_2Cl_2 (20 mL/g of resin x 3), MeOH (20 mL/g of resin x 3) and Et_2O (20 mL/g of resin x 3).

h) Peptide cleavage from Rink amide resin

Peptide-resin (1.0 mmol of resin loading) was suspended into a mixture of TFA/TIS/H₂O (96:2:2, 20 mL/g of resin). The vessel was sealed and shaken for 2 h. All solvents were collected by suction filtration. The treatment was repeated one more time with fresh portions of reagents. The resin was washed with CH_2Cl_2 (20 mL/g of resin x 3), MeOH (20 mL/g of resin x 3) and Et_2O (20 mL/g of resin x 3). All solvents were removed by toluene azeotrope *in vacuo*. The desired product was then precipitated from MeOH and Et_2O .

N-Ac-Arg-Pro-Leu-Pro-Val-Ala-Pro-Gly-NH₂ 1.139

The synthesis of compound **1.139** was made following the general procedures (section 7.6, 450 mg of resin loading, 0.28 mmol). Fmoc deprotection on the resin was undertaken first then protected amino acids were subsequently introduced: Fmoc-Gly-OH, Fmoc-Pro-OH, Fmoc-Ala-OH, Fmoc-Val-OH, Fmoc-Pro-OH, Fmoc-Leu-OH, Fmoc-Pro-OH, Fmoc-Arg(Pbf)-OH. Peptide

1.139 was cleaved from the resin and precipitated from MeOH and Et₂O to afford the title compound as a white solid (106 mg, 45%).

m.p: 105-107 °C (MeOH/Et₂O).

¹H NMR (DMSO- d_6 , 400 MHz): δ (ppm) 8.71-6.55 (11H, m, NH), 4.69-3.67 (15H, m, H-10, H-21, H-4, H-17, H-9, H-18, H-26, H-27, H-23, H-14, H-6), 3.26-2.97 (2H, m, H-1), 2.58 (1H, m, H-19), 2.40-0.70 (37H, m, H-8, H-16, H-25, H-3, H-7, H-24, H-15, H-5, H-19, H-11, H-2, H-22, H-20, H-13).

IR (cm⁻¹): 3278, 2958, 1625, 1537, 1440, 1386, 1199, 1045.

 $[\alpha]_{D}^{24}$ -117.6 (c 0.21, MeOH).

LRMS (ESI): $m/z = 847 [M+H]^{+}$.

HRMS (ESI): Calculated for $C_{39}H_{67}N_{12}O_9$ 847.51485, found 847.51512.

LCMS (ESI): 847.5 ([M+H]⁺, 96%).

N-Ac-Arg-Pro-Leu-Pro-Val-1.125-Gly-NH₂ 1.140

The synthesis of compound **1.140** was made following general procedures (section 7.6, 100 mg of resin loading, 0.06 mmol). Fmoc deproetction on the resin was undertaken first then protected amino acids were subsequently introduced: Fmoc-Gly-OH, **1.125d**, Fmoc-Val-OH, Fmoc-Pro-OH, Fmoc-Leu-OH, Fmoc-Pro-OH, Fmoc-Arg(Pbf)-OH. Peptide **1.140** was cleaved from the resin and precipitated from MeOH and Et₂O to afford the title compound as a white solid (21 mg, 40%).

m.p: 110-112 °C (MeOH/Et₂O).

¹**H NMR** (MeOD- d_4 , 400 MHz): δ (ppm) 4.71-4.12 (7H, m, H-9, H-21, H-10, H-4, H-17, H-18, H-27), 3.97-3.59 (7H, m, H-24, H-6, H-28, H-14, H-6), 3.25-3.15 (2H, m, H-1), 1.97 (3H, s, H-5),

2.30-1.51 (23H, m, H-26, H-19, H-8, H-16, H-22, H-25, H-7, H-23, H-15, H-12, H-3, H-11, H-2), 1.13-0.90 (12H, m, H-20, H-13). There are 11 x NH protons missing from the ¹H-spectrum.

IR (cm⁻¹): 3284, 2954, 1628, 1536, 1443, 1200, 1173.

 $[\alpha]_{D}^{24}$ -37 (c 0.1, MeOH).

LRMS (ESI): $m/z = 859 [M+H]^{+}$.

HRMS (ESI): Calculated for $C_{40}H_{67}N_{12}O_9$ 859.51485 found 859.51514.

LCMS (ESI): 859.5 ([M+H]⁺, 96%).

N-Ac-Arg-Pro-1.125-Val-Ala-Pro-Gly-NH₂ 1.141

The synthesis of compound **1.141** was made following general procedures (section 7.6, 100 mg of resin loading, 0.06 mmol). Fmoc deproetction on the resin was undertaken first then protected amino acids were subsequently introduced: Fmoc-Gly-OH, Fmoc-Pro-OH, Fmoc-Ala-OH, Fmoc-Val-OH, **1.125d**, Fmoc-Pro-OH, Fmoc-Arg(Pbf)-OH. Peptide **1.141** was cleaved from the resin and precipitated from MeOH and Et_2O followed by reverse phase HPLC (H_2O / CH_3CN 0-100%) to afford the title compound as a white solid (23 mg, 48%).

m.p: 102-105 °C (MeOH/Et₂O).

¹H NMR (MeOD- d_4 , 400 MHz): δ (ppm) 4.71-3.55 (14H, m, H-6, H-22, H-13, H-26, H-25, H-20, H-10, H-4, H-17, H-9, H-16), 3.26-3.12 (2H, m, H-1), 2.28-1.61 (21H, m, H-8, H-18, H-7, H-11, H-12, H-15, H-24, H-3, H-23, H-14, H-2), 1.97 (3H, s, H-5), 1.34 (3H, d, J = 6.8 Hz, H-21), 0.96 (6H, 2 x d, J = 6.6 Hz, H-19). There are 11 x NH protons missing from ¹H-spectrum.

IR (cm⁻¹): 3272, 2963, 1626, 1537, 1444, 1199, 1177, 1130.

 $[\alpha]_{D}^{24}$ – 46.8 (c 0.25, MeOH).

LRMS (ESI): $m/z = 817 [M+H]^+$, 840 $[M+Na]^+$.

HRMS (ESI): Calculated for $C_{37}H_{61}N_{12}O_9$ 817.46790, found 817.46755.

LCMS (ESI): **817.4** ([M+H]⁺, 99%).

N-Ac-Arg-Pro-1.125-Val-1.125-Gly-NH₂ 1.142

The synthesis of compound **1.142** was made following general procedures (section 7.6, 100 mg of resin loading, 0.06 mmol). Fmoc deprotection on the resin was undertaken first then protected amino acids were subsequently introduced: Fmoc-Gly-OH, **1.125d**, Fmoc-Val-OH, **1.125d**, Fmoc-Pro-OH, Fmoc-Arg(Pbf)-OH. Peptide **1.142** was cleaved from the resin and precipitated from MeOH and Et₂O to afford the title compound as a white solid (20 mg, 41%).

m.p: 117-120 °C (MeOH/Et₂O).

¹H NMR (DMSO d- $_6$, 400 MHz): δ (ppm) 8.51-7.08 (11H, broad s, NH), 4.50-3.41 (13H, m, H-10, H-20, H-9, H-4, H-16, H-26, H-17, H-13, H-23, H-27, H-6), 3.25-3.11 (2H, m, H-1), 2.28-1.61 (25H, m, H-25, H-15, H-8, H-18, H-22, H-11, H-21, H-7, H-3, H-14, H-24, H-12, H-2), 1.97 (3H, s, H-5), 0.97 (6H, app.t, J = 7.1 Hz, H-19).

IR (cm⁻¹): 3287, 2948, 2358, 1665, 1625, 1553, 1446, 1182, 1131.

 $[\alpha]_{D}^{24}$ –58.5 (c 0.1, MeOH).

LRMS (ESI): $m/z = 829 [M+H]^{+}$, 851 $[M+Na]^{+}$.

HRMS (ESI): Calculated for $C_{39}H_{67}N_{12}O_9$ 829.46790, found 829.46894.

LCMS (ESI): 829.5 ([M+H]⁺, 94%).

7.6 Bio-assays mammalian cell culture

General technique materials and culture conditions

Cell culture work and media preparation were performed in a laminar flow hood. All the surfaces were sprayed with 70% ethanol. Sterile pipettes, disposable plasticware and sterile pipette tips were used for cell culture. All culture vessels, test tubes and pipette tip boxes were opened only in the laminar flow hood. Cells were cultured at 37 °C in a humidified atmosphere containing 5% CO₂.

Materials:

From Greiner UK: all tissue cultured plasticware

From Invitrogen Life Technologies UK:

Hank's Balanced Salt Solution (HBSS) Cat. No. 14170088

Dulbecco's Modified Eagle Medium (DMEM) Cat. No. 41966029

From BioWhittaker:

Nutrient Mixture F-12 Medium (Ham's F-12) Cat. No. BE12-615F

From LONZA:

Trypsin-EDTA Cat. No. BE17-161E

Penicillin-Streptomycin Cat. No. DE17-603E (5,000 units/mL Potassium Penicillin and 5,000 μ g/mL Streptomycin Sulfate).

L-Glutamine Cat. No. BE17-605E (200 mM solution in 0.85% NaCl)

From Laboratory stock solution:

Phosphate Buffered Saline (PBS) pH 7.2

(30X) 600 g NaCl, 15 g KCl, 108 g Na₂HPO₄, 18 g KH₂PO₄, and 2.5 L H₂O.

From Autogen Bioclear:

Foetal Calf serum (FCS) Batch 154-161200

From Sigma Diagnostics:

Giemsa solution Cat. No. 080K4365

Preparation of tissue culture mediums:

a) Nutrient mixture Ham's F-12 medium was prepared from 500 mL of Ham's F-12 growth medium, 50 mL of FCS (10% of final volume), 5.0 mL of Penicillin/ Streptomycin (1% of final volume) and 5.0 mL of glutamine (1% of final volume). All of the chemicals above were mixed together at room temperature. The medium was stored in the fridge and warmed up in a water bath (37 $^{\circ}$ C) before use.

b) Dulbecco's Modification of Eagle's (DMEM) medium was prepared from 500 mL of DMEM growth medium, 50 mL of FCS (10% of final volume), 5.0 mL of Penicillin/Streptomycin (1% of final volume) and 5.0 mL of glutamine (1% of final volume). All of chemicals above were mixed together at room temperature. The medium was kept in the fridge and warmed up in water bath (37 $^{\circ}$ C) before use.

Cell lines and normal culture conditions:

a) Bladder transitional cell carcinoma cells (RT112 bladder cancer) were cultured in nutrient mixture Ham's F-12 supplemented with 10% v/v FCS, 1% v/v penicillin/streptomycin and 1% v/v glutamine at 37 $^{\circ}$ C in a humidified incubator containing 5% CO₂.

b) Immortalised normal fibroblasts (MRC5-hTERT fibroblast cells) were cultured in Dulbecco's modification of Eagle's (DMEM) supplemented with 10% v/v FCS, 1% v/v penicillin/streptomycin and 2 mM glutamine at 37 $^{\circ}$ C in a humidified incubator containing 10% $^{\circ}$ CO₂.

General method of tissue culture

Trypsinisation (releasing cells from monolayer surface):

Cell lines that were maintained in tissue culture did not exceed 70% confluence. Trypsin-EDTA, FCS and growth medium were warmed to 37 °C before use and cells were replated in growth medium at 1:10 dilution. The existing tissue culture medium was aspirated from cells; cells were washed with 10.0 mL of HBSS. Trypsin/EDTA solution (1.0 mL) was added to the tissue culture flask and incubated for 5 min at 37 °C until all the cells had become detached from the bottom surface of the flask. Tissue culture medium (9.0 mL) was added to the tissue culture flask.

<u>Determination of total cell counts by using a hemocytometer:</u>

40.0 μ L of trypsinised cell suspension was pipetted and transferred to a hemocytometer. Cells were counted under the microscope and the average number of cells per square (n) was determined from at least three squares. The number of cells in 1 mL was then calculated by the formula: $n \times 10^4$. The appropriate dilutions were made to give different seeding concentrations.

Colony survival assays

Colony survival assay is a cell biology technique for studying the effectiveness of specific agents on the survival and proliferation of cells. This assay is performed to obtain a correlation between the dose of peptide and number of cells dying.

a) Preparation of peptide solution

The exact amount of each peptide was weighed in an eppendorf and dissolved in the tissue culture medium. The solution was sterilised by centrifuge at 11,000 rpm, 3 $^{\circ}$ C for 10 min. Once fully dissolved, the peptide solution was transferred into another fresh eppendorf leaving approximately 50 μ L which might contain bacteria and fungi at the bottom of the first eppendorf. Dilutions of peptide in medium were prepared at two times the required final concentration. The peptide solution was kept in ice all before use.

b) Plating of cells for colonogenic assay

The stock of cell suspension was counted, diluted in tissue culture medium and plated into the well of a 24-well plate (10-250 cells suspension per 250 μ L of medium). 250 μ L were added per plate. Each peptide concentration was prepared and 250 μ L added to each well dish in quadruplicate. Plates were gently agitated to ensure an even cell distribution and incubated in a custom incubator to obtain a humidified atmosphere at 5% CO₂. A custom incubator (**Figure below**) is required to minimise evaporation during the long experiment. The tissue cultures plates are stood at the bottom of the box and kept in a normal incubator. There is a small space left at the top of the incubator which enables CO₂ to easily pass through the cells.

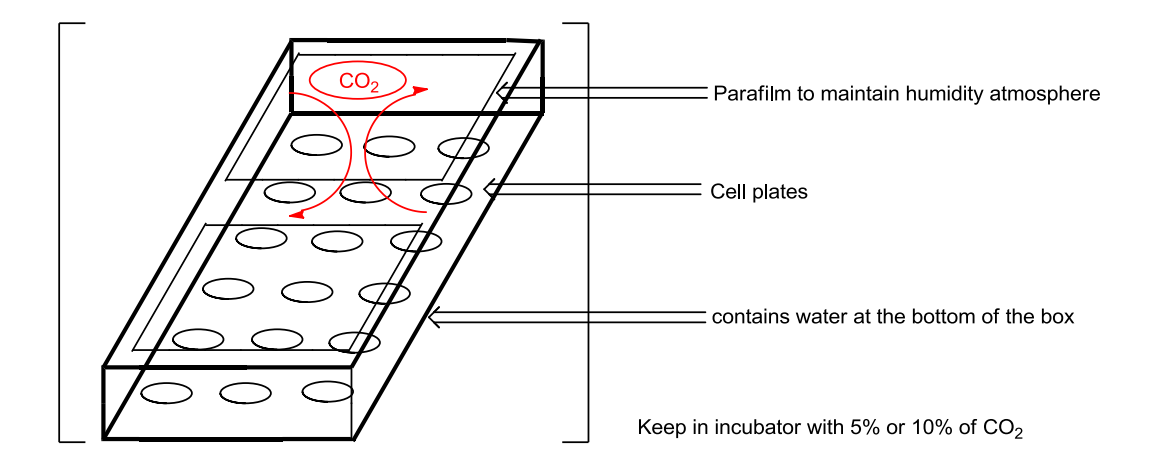


Figure: Custom Incubator

Giemsa's staining protocol

After incubation of cells for up to 29 or 31 days, the tissue culture medium was aspirated from cultures to a waste bottle and cells were carefully washed by 1.0 mL of cold PBS per well. The PBS was aspirated to the waste bottle and the cells were fixed with 0.5 mL of MeOH for 5 minutes. All solvents were removed and the plate was left to air dry. The cells were stained with 0.5 mL of Giemsa solution (1:20 dilution in deionised water) for 30 min on a platform shaker. Giemsa solution was aspirated off and the plate was left to air dry. The cell cultures were then visually examined under a microscope for survival.

7.7 BioNMR experiments

1) Preparation of ¹⁵N/¹³C labelled Fyn-SH3 domain

Methods were based on those of Morton *et al.*⁹, who used the following approach to produce and purify the Fyn SH3 domain. Dr. P. Duriez has undertaken the expression and purification.

Expression:

The Fyn-SH3 domain (residues 82-145) was cloned into the bacterial expression vector pGEX-2T and the derived plasmid was transformed into BL21 CodonPlus RIPL bacteria (Agilent Technologies).

The bacteria were grown in M9 minimal medium in the presence of 1 g/L of 15 N NH₄Cl alone or in combination with 1 g/L of 13 C glucose.

<u>Purification procedure</u>:

The protein expression was induced with 0.3 mM isopropyl-B-D-thiogalactopyranoside at 30 °C overnight, then the cells were harvested by centrifugation at 4 °C, washed once with PBS then stored at -20 °C until processed. Cells were resuspended in TTBS (50 mM Tris-HCl, pH 8.5 +150 mM NaCl and 0.1 % (v/v) Triton X-100) (10 mL per g of cells) in the presence of lysozyme, 10 ug/mL DNase I, 10 mM MgCl₂ and a cocktail of protease inhibitors (Complete from Roche). The suspension was then sonicated (4 x 20 s) to effect lysis of the cells. Samples were maintained on ice during sonication. Cell debris was then pelleted by centrifugation (30 min, 20 000 g) at 4 °C and the pellet discarded. The supernatant was applied onto a column of glutathione-Sepharose beads (GE Healthcare) in TTBS using an AktaPrime FPLC system. After extensive washing of the resin with TBS (without Triton X-100) the bound GST-SH3 fusion was eluted from the column with 15 mM glutathione in TBS. Fractions containing the fusion protein were pooled and applied to a desalting column equilibrated in 50 mM Tris-HCl pH 8.5, 150 mM NaCl to remove the glutathione, prior to thrombin cleavage of the fusion protein. Thrombin (Novagen) was added at a ratio of 1 unit of protease/mg of protein in the presence of 2.5 mM CaCl₂. Cleavage was allowed to proceed at 16 °C overnight and the extent of cleavage of the fusion protein determined by sodium dodecyl sulphate polyacrylamide gel electrophoresis (SDS-PAGE). Cleaved material was applied to glutathione-Sepharose beads to capture free GST and the flow through was passed onto a HiLoad 26/60 Superdex 200 gel filtration column (GE Healthcare) equilibrated in buffer A (20 mM Tris-HCl, pH 8.5 containing 20 mM NaCl). Fyn-SH3

was further purified on a 1 mL Q-trap column (GE Healthcare) equilibrated in buffer A. The protein was eluted with a linear gradient from 0 to 100 % buffer B (20 mM Tris-HCl, pH 8.5 containing 500 mM) over 4 ml. Fractions containing Fyn SH3 domain were pooled and dialysed against 10 mM potassium phosphate pH 6.0, prior to be concentrated in centrifugal concentrator to 0.1 mM for NMR.

2) NMR experiments

NMR spectra of isotope labelled SH3 domain were collected at 25 °C with a 600 MHz four-channel Varian INOVA NMR spectrometer equipped with a room temperature 5 mm triple resonance z-gradient probe. Resonance assignments of the free and peptide bound form of the backbone ¹⁵N and HN nuclei were obtained by a combination of 2D ¹H-¹⁵N-HSQC, 3D ¹⁵N-edited NOESY-HSQC, as well as HNCA, HNCACB and CBCA(CO)NH spectra. All experiments used water flip-back and gradient-enhancement.

NMR data were processed with NMRPipe, applying sine function, zero filling and phasing prior to Fourier Transformation and analysed with NMRView.

The localisation of the peptide binding site was obtained by recording a series of nine 2D ¹H¹⁵N-HSQC spectra at a concentration ratio of peptide:protein of 0:1, 0.25:1, 0.5:, 0.75:1, 1:1,
2:1, 4:1, 8:1, 12:1, 20:1.

Protein concentration (0.1 mM) was kept constant during titrations while ligand concentrations were increased.

The chemical shift perturbation upon peptide addition was calculated by weighting 1HN and ^{15}N chemical shift differences using the following formula: $\Delta\delta_{H,N} = \{(\Delta\delta_H)^2 + 1/6 (\Delta\delta_N)\}^{1/2} (\Delta\delta_H)$ and $\Delta\delta_N$ are the absolute difference between HN and ^{15}N chemical shift of the fully saturated and free protein).

The equilibrium binding constant K_D was obtained for residues in fast exchange by fitting K_D to the fractional shift (Δ/Δ max) using the formula $\frac{\Delta}{\Delta max} = \frac{(K_D + [L] + [P]) - \sqrt{(K_D + [L] + [P])^2 - 4[P][L]}}{2[P]},$ where Δ represents the difference of the measured shift at any(maximal, Δ max) ligand concentration and the shift of the free protein, and [L] and [P] are the ligand and protein concentrations respectively.

Appendix

Contents:

1.0 Purity control (LCMS)	
1.1 N-Ac-Pro-Arg(NO ₂)-Gly-Pro-Arg(NO ₂)-Pro-OMe 2.1	196
1.2 2.14 -Arg(NO ₂)-Gly-Pro-Arg(NO ₂)-Pro-OMe 2.16	197
1.3 <i>N</i> -Ac-Pro-Arg(NO ₂)- 1.125 -Arg(NO ₂)-Pro-OMe 3.36	198
1.4 Dimer 4.1	199
1.5 Trimer 4.2	200
1.6 Tetramer 4.3	201
1.7 Parent-8mer 1.139	202
1.8 Analogue 1.140	203
1.9 Analogue 1.141	204
1.10 Analogue 1.142	205
2.0 UV spectra	
2.1 Dimer 4.1	206
2.2 Trimer 4.2	206
2.3 Tetramer 4.3	207
3.0 CD Spectroscopy	
3.1 Dimer 4.1	208
3.2 Trimer 4.2	209
3.3 Tetramer 4.3	210
3.4 N-Ac-Pro-Arg(NO ₂)-Gly-Pro-Arg(NO ₂)-Pro-OMe 2.1 and	
N-Ac-Pro-Arg(NO ₂)-1.125-Arg(NO ₂)-Pro-OMe 3.36	211
3.5 Parent 8mer 1.139	211
4.0 Pictures clonogenic assays	
4.1 N-Ac-Pro-Arg(NO ₂)-Gly-Pro-Arg(NO ₂)-Pro-OMe 2.1	
4.1.1 RT112 cancer cells	212
4.1.2 MRC5-hTERT cells	213
4.2 2.14 -Arg(NO ₂)-Gly-Pro-Arg(NO ₂)-Pro-OMe 2.16 on RT112 cancer cells	213
4.3 N-Ac-Pro-Arg(NO ₂)- 1.125 -Arg(NO ₂)-Pro-OMe 3.36	214
4.3.1 RT112 cancers cells	
4 3 1.1 Control (no pentide)	215

Appendix

4.3.1.2 Positive control with 2.1 (5 mM)	216
4.3.1.3 Peptide 3.36 , 5 mM	217
4.3.1.4 Peptide 3.36 , 4 mM	218
4.3.1.5 Peptide 3.36 , 3 mM	219
4.3.1.6 Peptide 3.36 , 2 mM	220
4.3.1.7 Peptide 3.36 , 1 mM	221
4.3.2 MRC5-hTERT	
4.3.2.1 Control (no peptide)	223
4.3.2.2 Positive control with 3.36 (5 mM)	224
4.3.2.3 Peptide 3.36 , 5 mM	225
4.3.2.4 Peptide 3.36 , 4 mM	226
4.3.2.5 Peptide 3.36 , 3 mM	227
4.3.2.6 Peptide 3.36 , 2 mM	228
4.3.2.7 Peptide 3.36 , 1 mM	229
5.0 BioNMR data	
5.1 Data SH3 domain	230
5.2 Data Parent 8mer 1.139 /SH3 domain binding	233
5.3 Data Analogue 1.140 /SH3 domain binding	240
5.4 Data Analogue 1.141 /SH3 domain binding	247
5.5 Data Analogue 1.142 /SH3 domain binding	254
5.6 Titration plots	
5.6.1 Parent 8mer 1.139 /SH3 domain	261
5.6.2 Analogue 1.140/ SH3 domain	262
5.6.3 Analogue 1.141/ SH3 domain	263
5.6.4 Analogue 1.142/ SH3 domain	264
6.0 X-ray data	265

1.0 Purity control (LCMS)

General method A

HPLC separations were performed using a Dionex Ultimate® 3000 UHPLC (Thermo Scientific, Hemel Hempstead, UK). Samples were injected (2 μL) directly onto a Kinetex C18 Column (50 mm X 2.1 mm 1.7 μm particle size; Phenomenex, Torrance, CA, USA) thermostatically controlled at 40°C. The separation was achieved using 2% MeOH 0.1% formic acid (hold for 2 minutes followed by a linear gradient to 100% methanol over 7 minutes and returned to 2 % methanol for 2 minutes at a flow rate of 0.3 mL/min. Mass spectra were recorded using a Maxis™ ESI-ToF mass spectrometer (Bruker Daltonics, Bremen, Germany) using positive ion electrospray ionisation (120-1500 m/z)

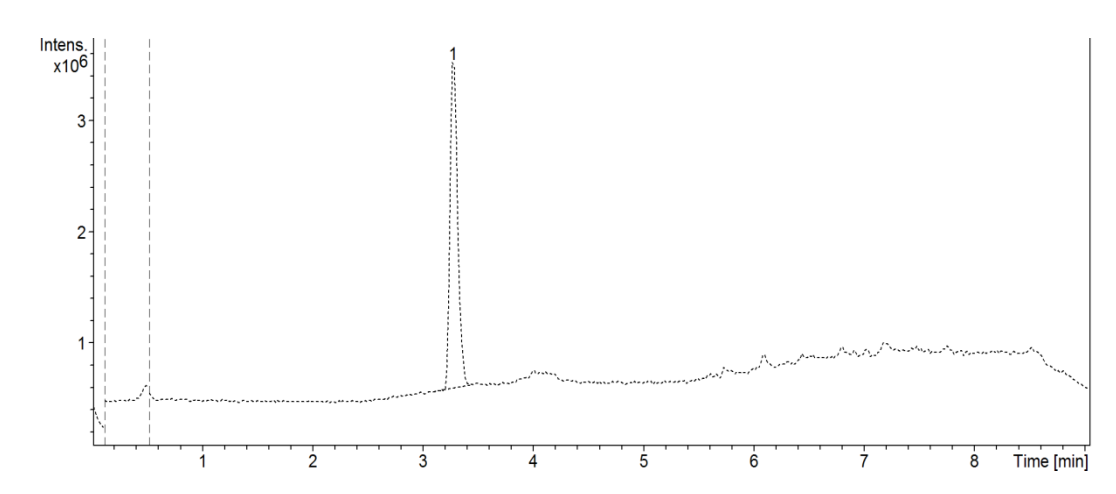
General method B

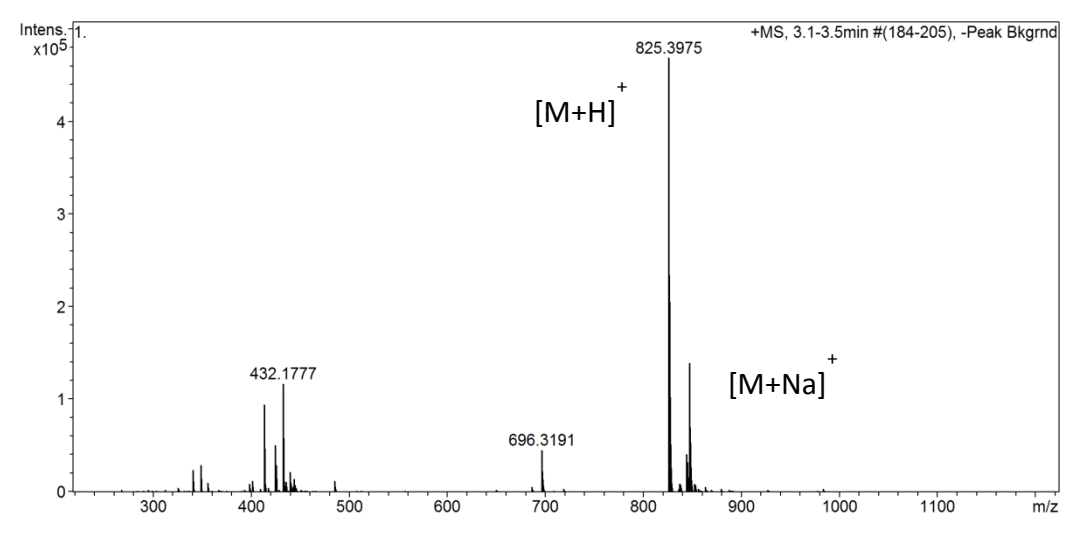
HPLC separations were performed using an Agilent 1200 LCMS. Samples were injected (35 μ L) directly onto a Zorbax SB-C18 Column (4.6 X 150 mm 5 μ m particle size). The separation was achieved following the table conditions.

Time (min)	% water +0.1% formic acid	% MeOH +0.1% formic acid	Flow (mL/min)
0	100	0	1.0
2	98	2	1.0
8	80	20	1.0
10.5	0	100	1.0
12.5	0	100	1.0

1.1 N-Ac-Pro-Arg(NO₂)-Gly-Pro-Arg(NO₂)-Pro-OMe 2.1

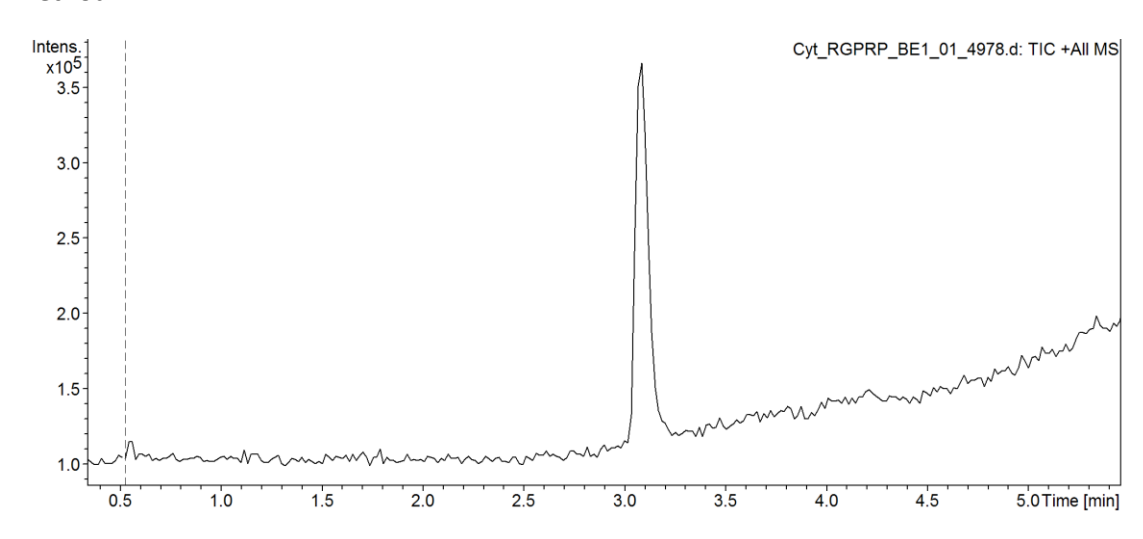
 $C_{32}H_{52}N_{14}O_{12}$: 824.3889

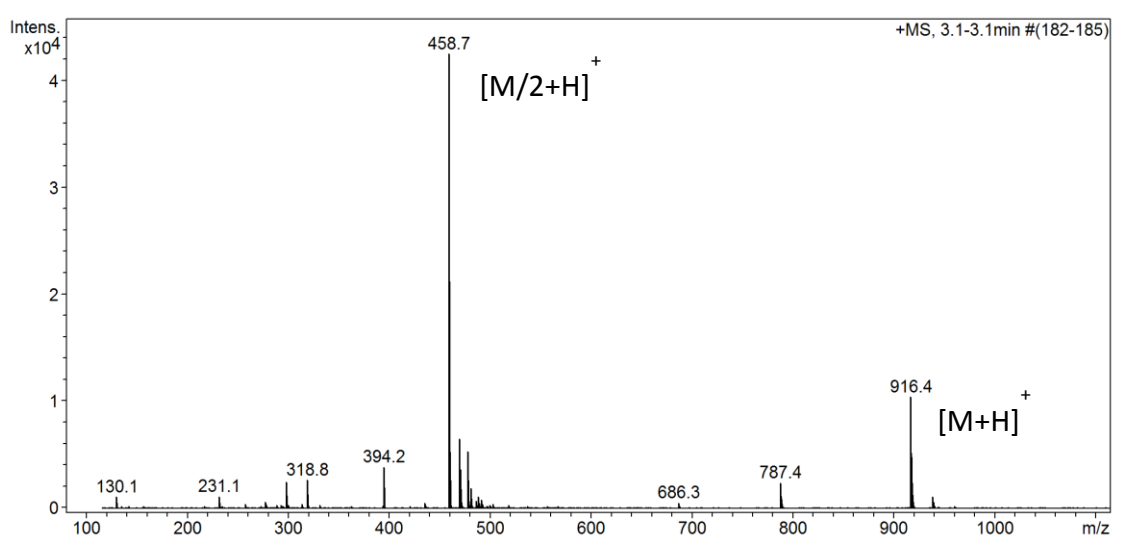




1.2 2.14-Arg(NO₂)Gly-Pro-Arg(NO₂)-Pro-OMe 2.16

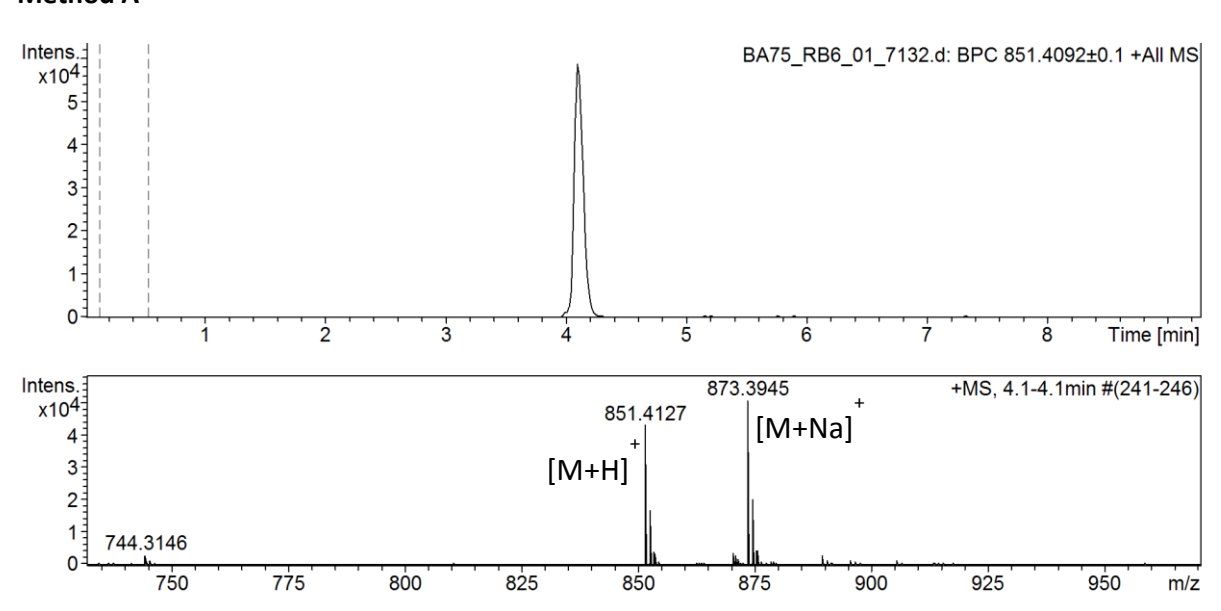
 $C_{38}H_{57}N_{15}O_{12}$: 915.4311





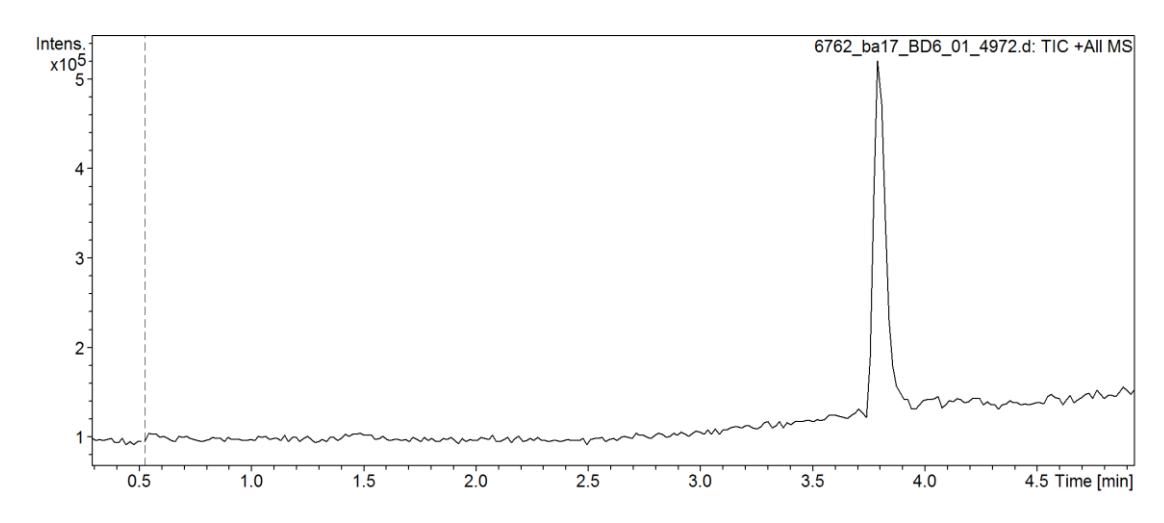
1.3 N-Ac-Pro-Arg(NO₂)-1.125-Arg(NO₂)-Gly-OMe 3.36

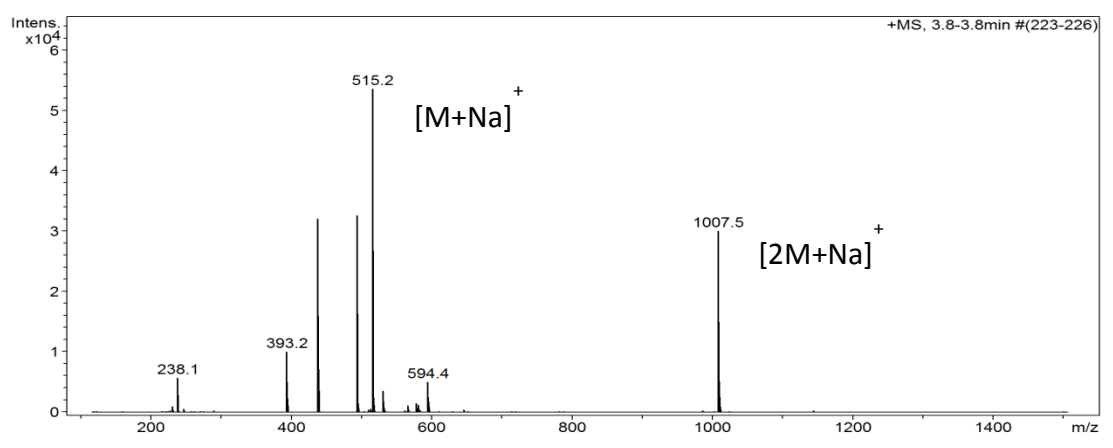
C₃₄H₅₄N₁₄O₁₂: 850.4046



1.4 Dimer 4.1

 $C_{24}H_{36}N_4O_7$: 492.2584

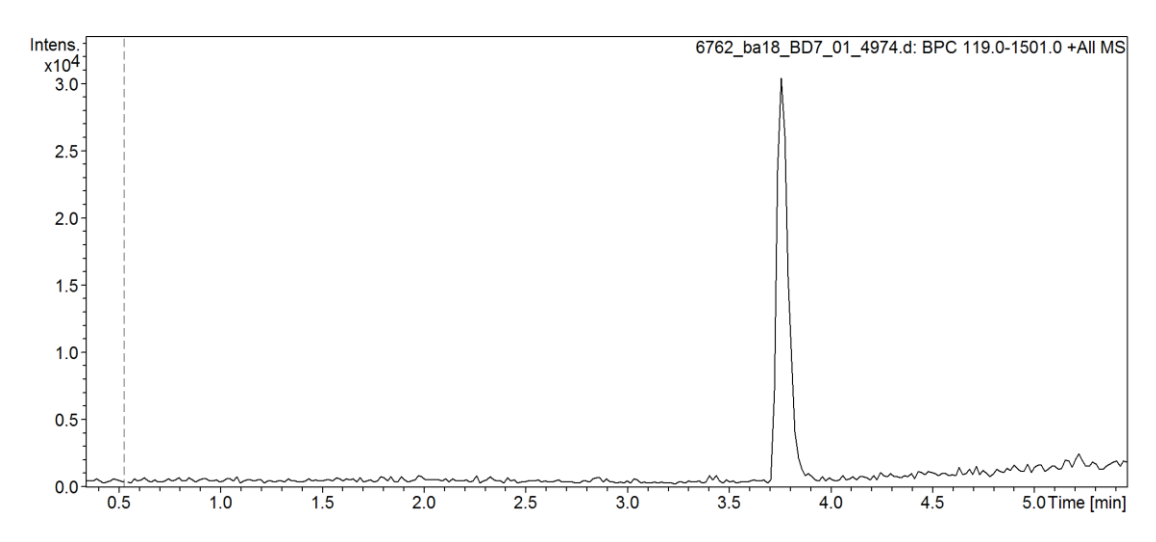


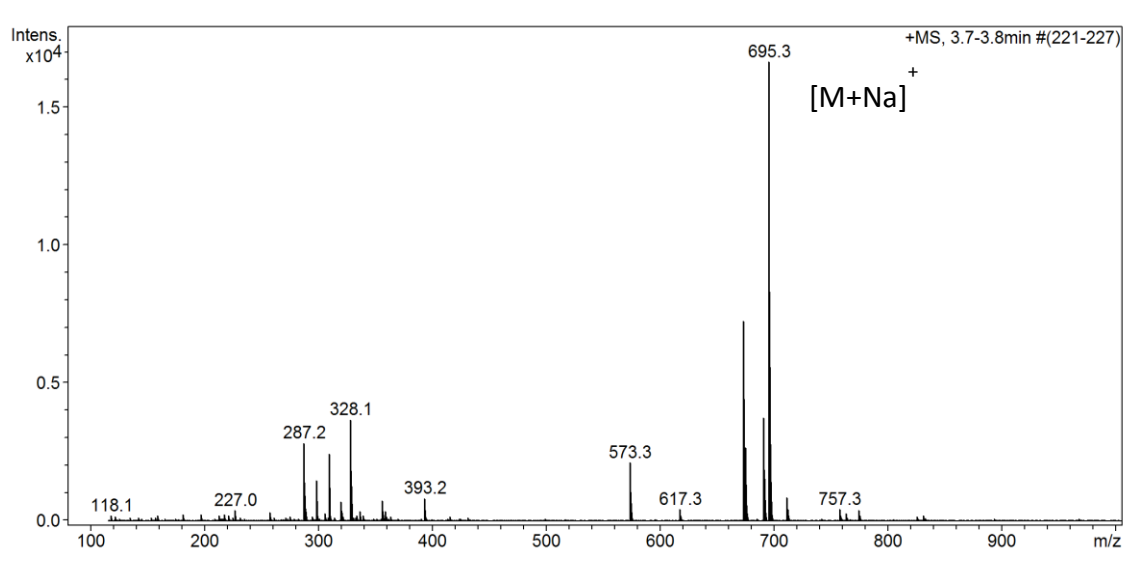


1.5 Trimer 4.2

C₃₃H₄₈N₆O₉: 672.3483

Method A

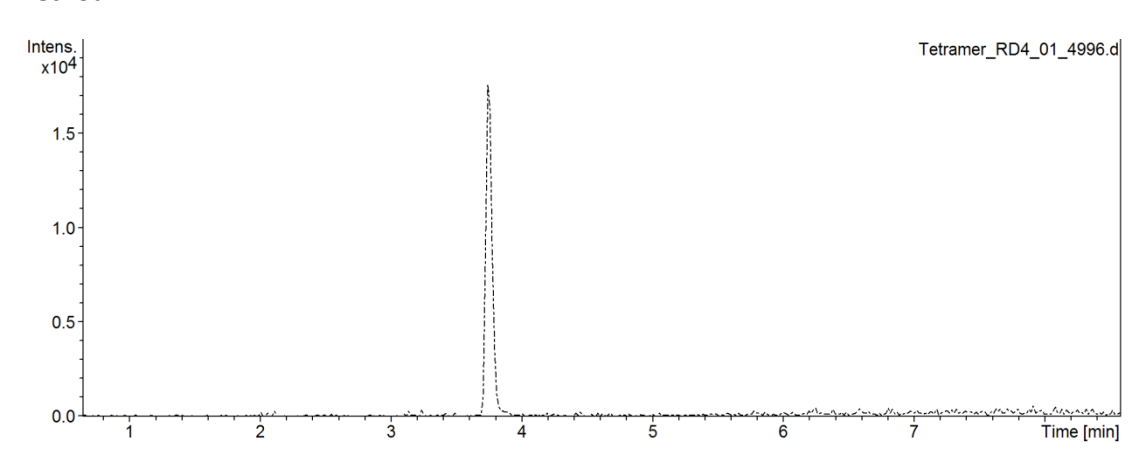


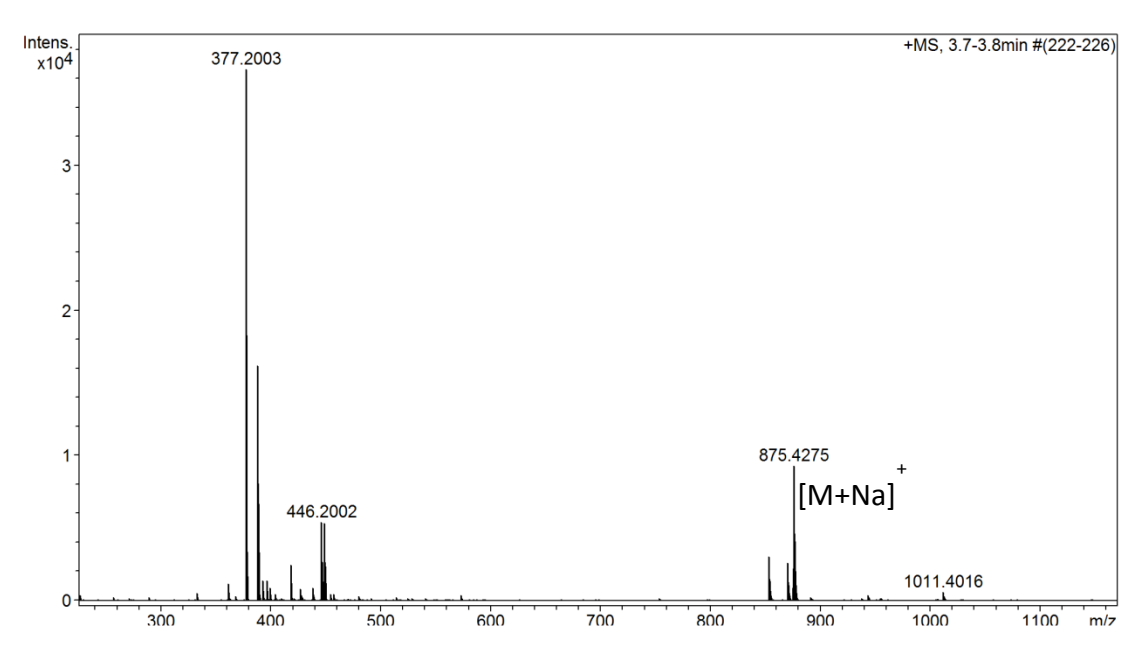


1.6 Tetramer 4.3

 $C_{42}H_{60}N_8O_{11}$: 852.4382

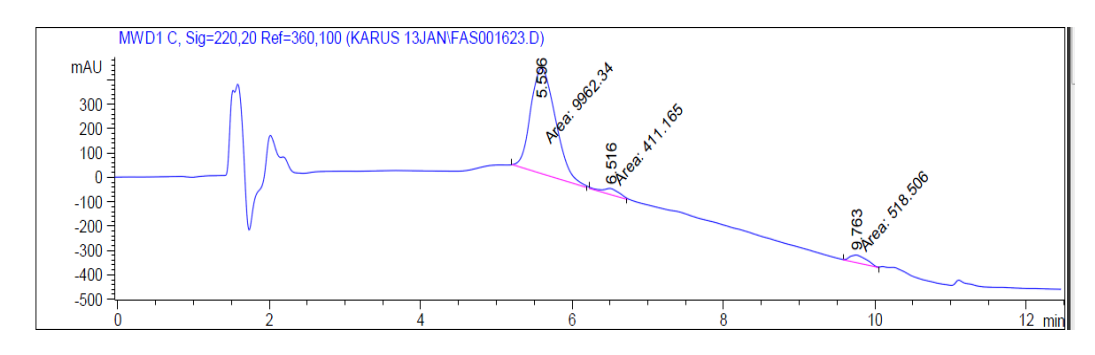
Method A





1.7 Parent 8mer 1.139

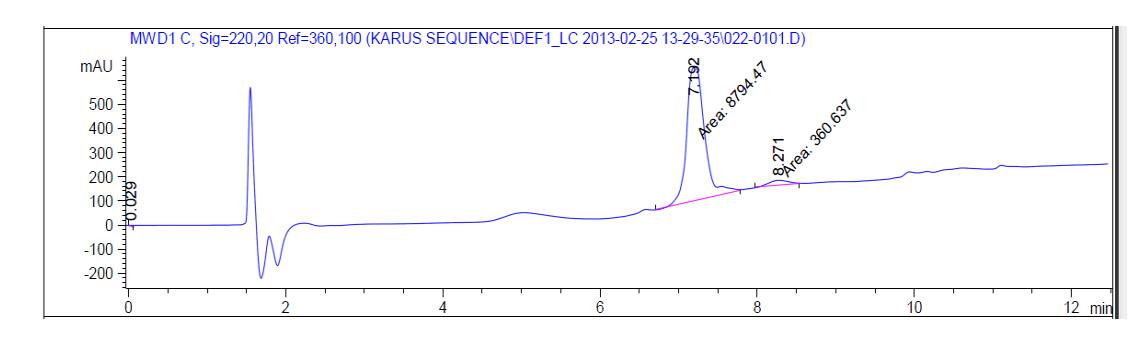
 $C_{39}H_{66}N_{12}O_9$: 846.5076

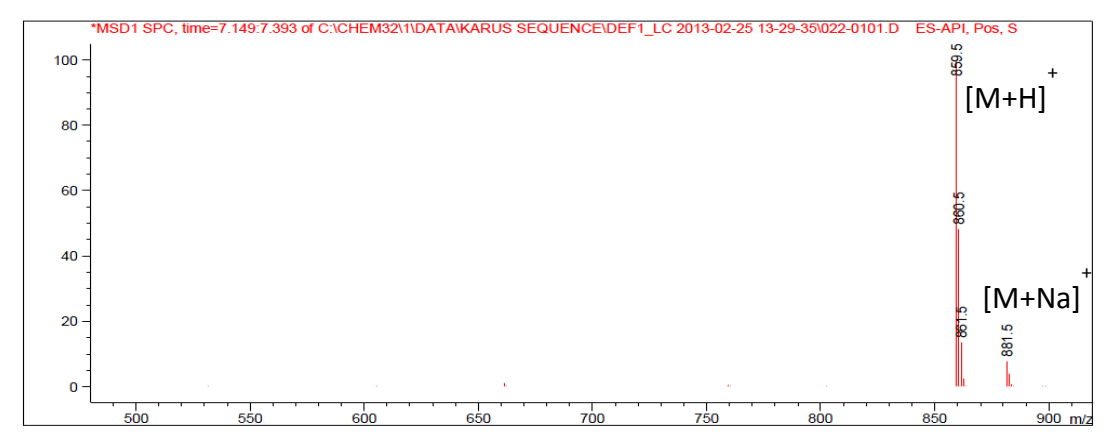




1.8 Analogue 1.140

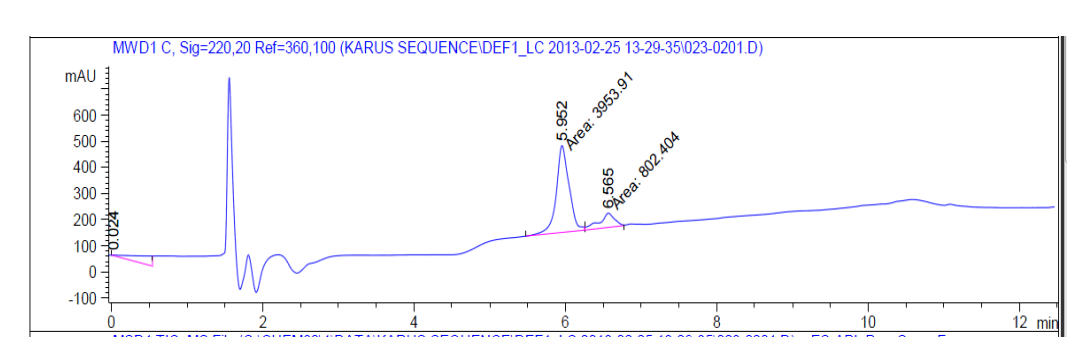
 $C_{40}H_{66}N_{12}O_9$: 858.5076

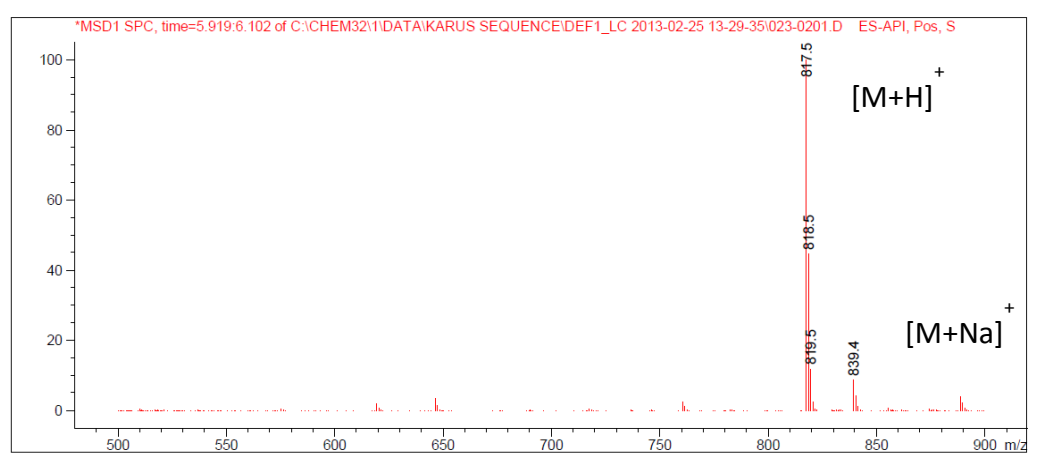




1.9 Analogue 1.141

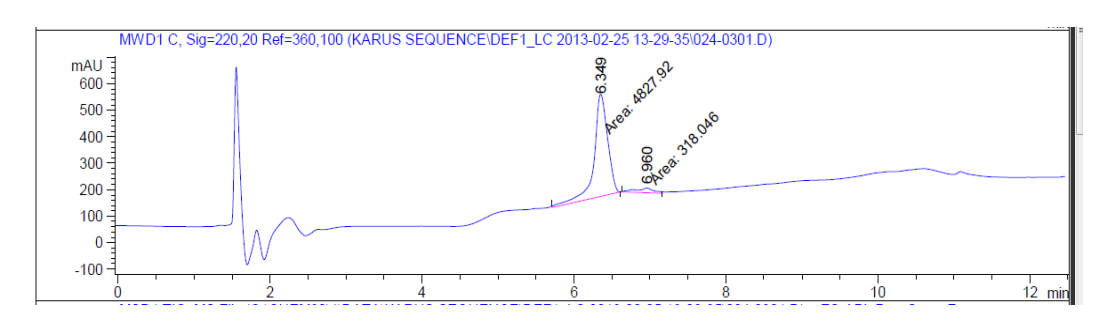
 $C_{37}H_{60}N_{12}O_9$: 816.4606

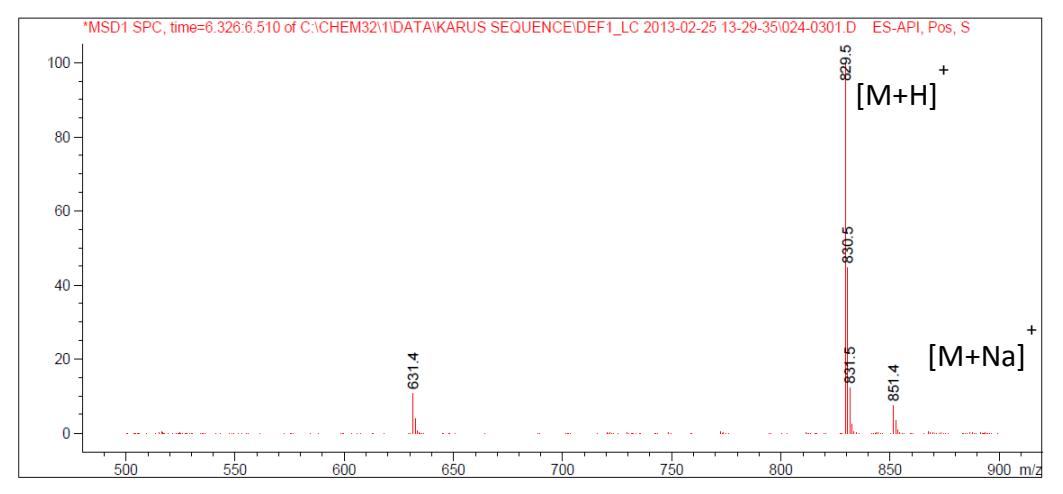




1.10 Analogue 1.142

 $C_{37}H_{60}N_{12}O_9$: 828.4606



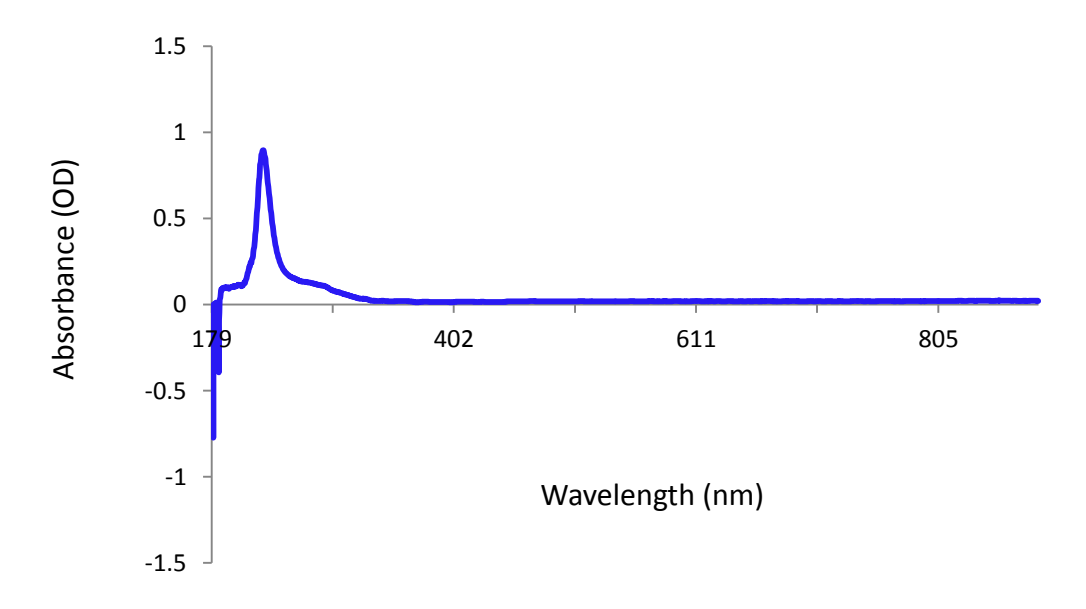


2.0 UV spectra

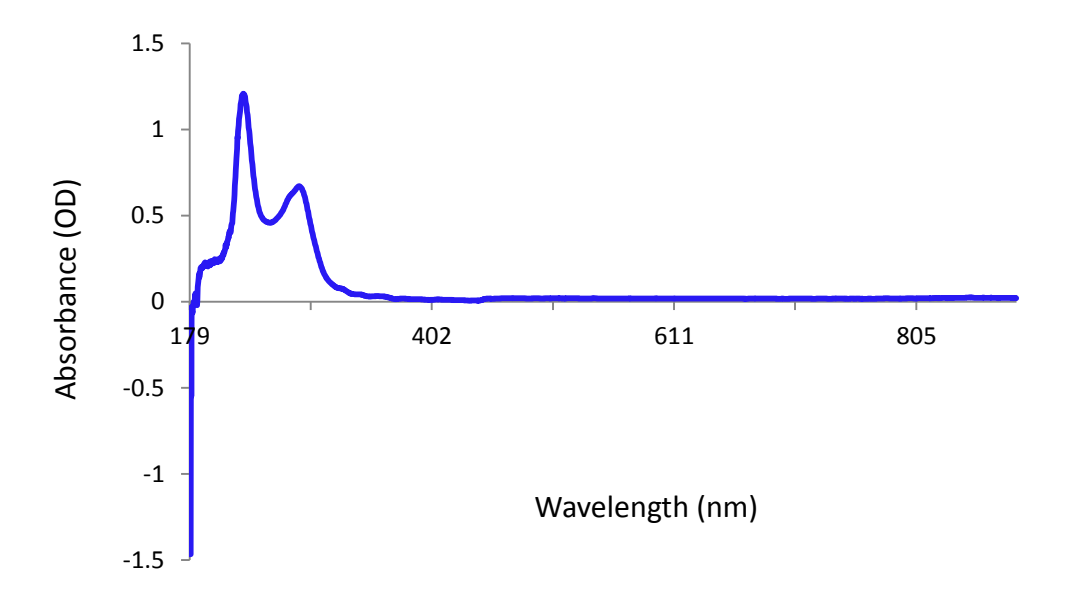
General methods

UV measurements were recorded on an Ocean Optics DH-2000-BAL at room temperature using Spectral suits via a 10 mm path quartz cuvette.

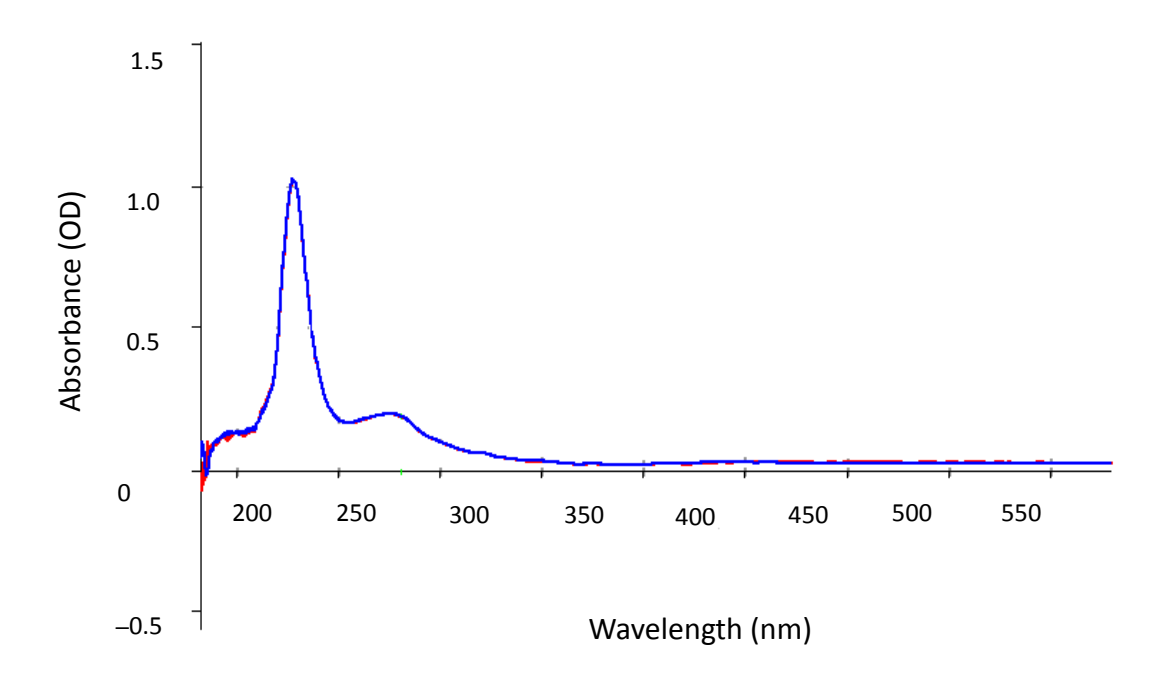
2.1 Dimer 4.1 (c = 0.5 mM)



2.2 Trimer 4.2 (c = 0.25 mM)



2.3 Tetramer 4.3 (c = 0.125 mM)



3.0 CD spectroscopy

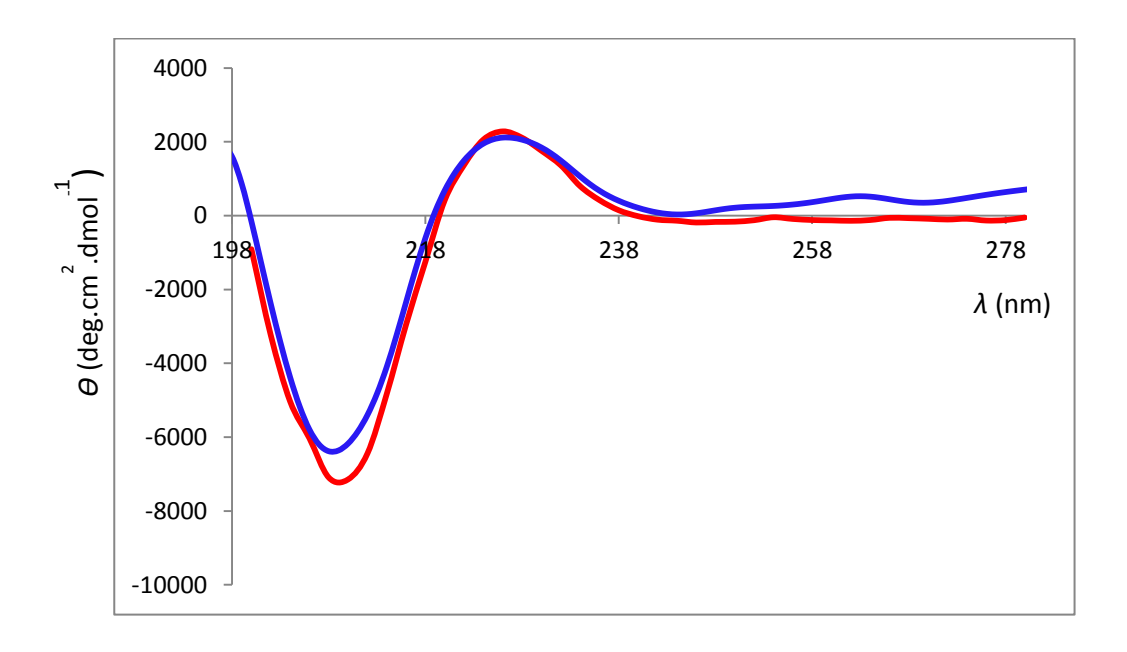
General methods

CD measurements were performed at 25° C with a Jasco J-720 spectropolarimeter at a spectral bandwith of 2 nm with a time constant of 2 sec (scan speed 100 nm/min) and a step resolution of 1 nm. Spectra were recorded as an average of 16 scans. For each spectrum, the background was substrated prior to smoothing and processing. All the measured ellipticities are presented normalised as a function of the concentration of solutions and the number of amide bonds. Machine data units were normalised of millidegrees ellipticity by conversion to mean residue molar ellipticity using the following equation (where n is the number of peptide bonds and *Ellipticity* is the raw data from the instrument).

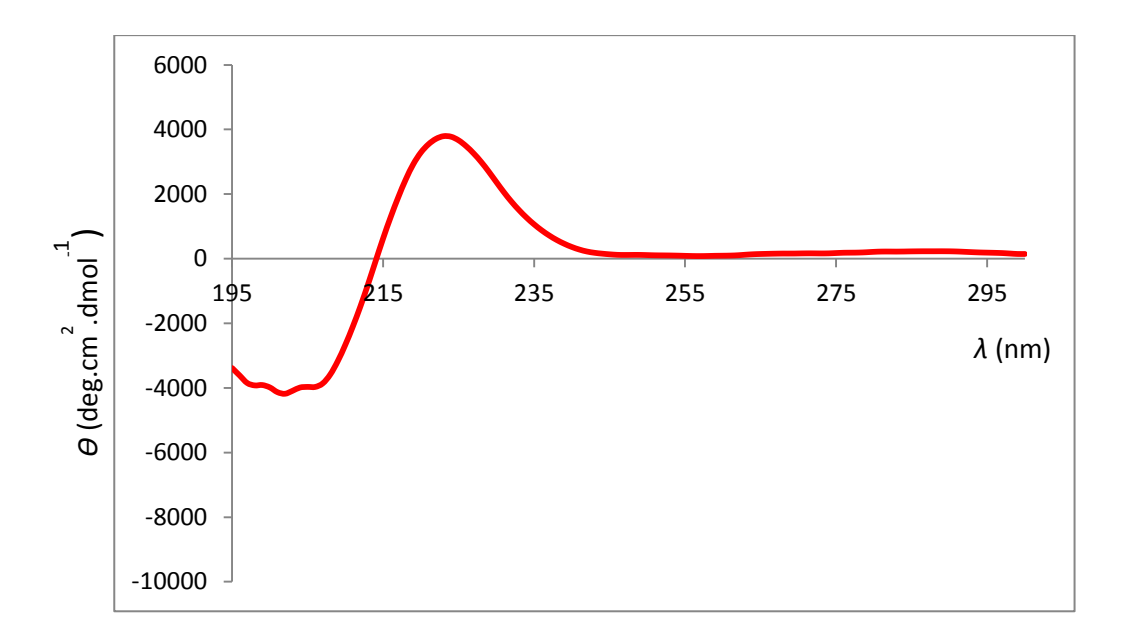
$$\theta (deg.cm^{2}.dmol^{-1}) = \frac{Ellipticity (mdeg).10^{6}}{Pathlenght (mm).[C](\mu M).n}$$

3.1 Dimer 4.1

• MeOH (c = 0.5 mM and c = 0.125 mM)

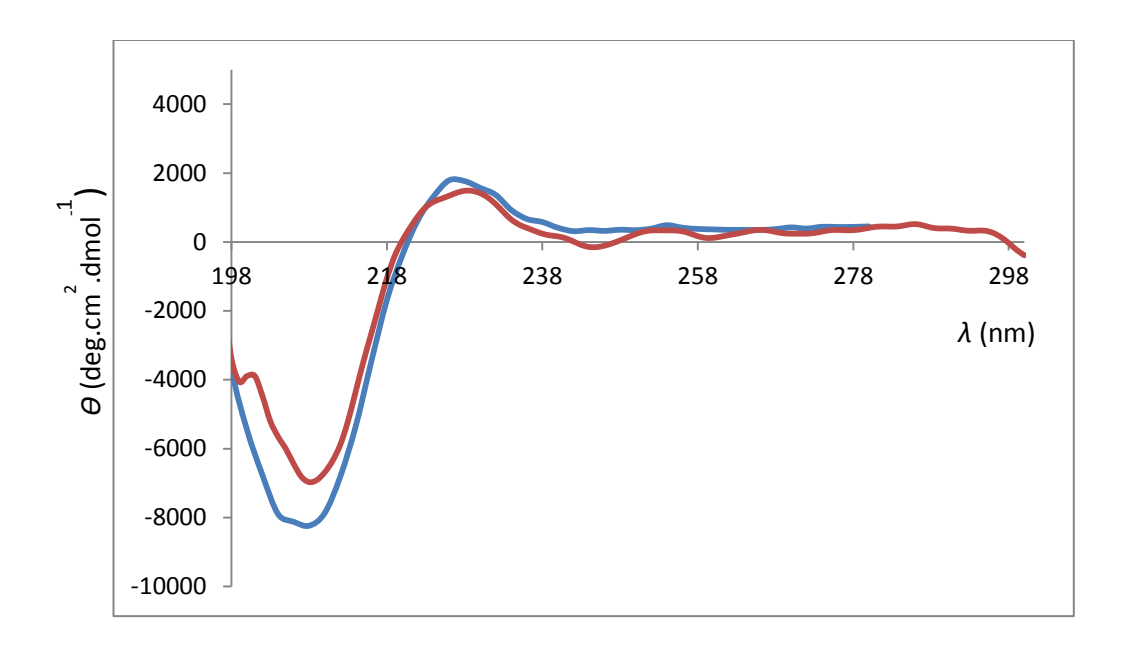


• $H_2O(c = 0.5 \text{ mM})$

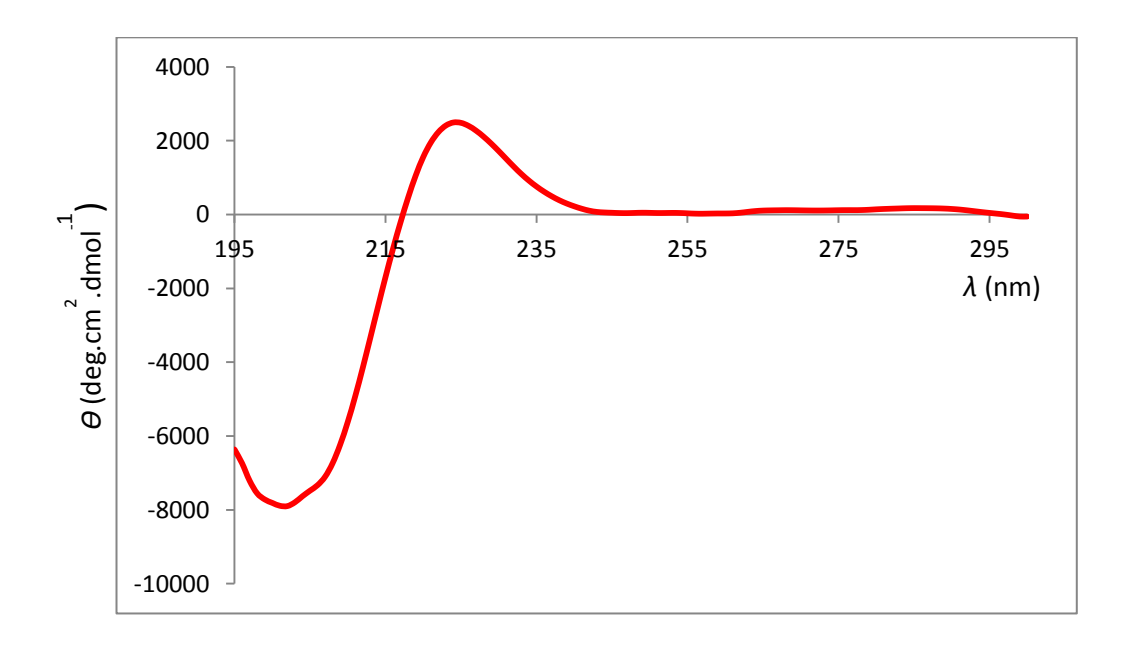


3.2 Trimer 4.2

• MeOH (c = 0.25 mM and c = 0.125 mM)

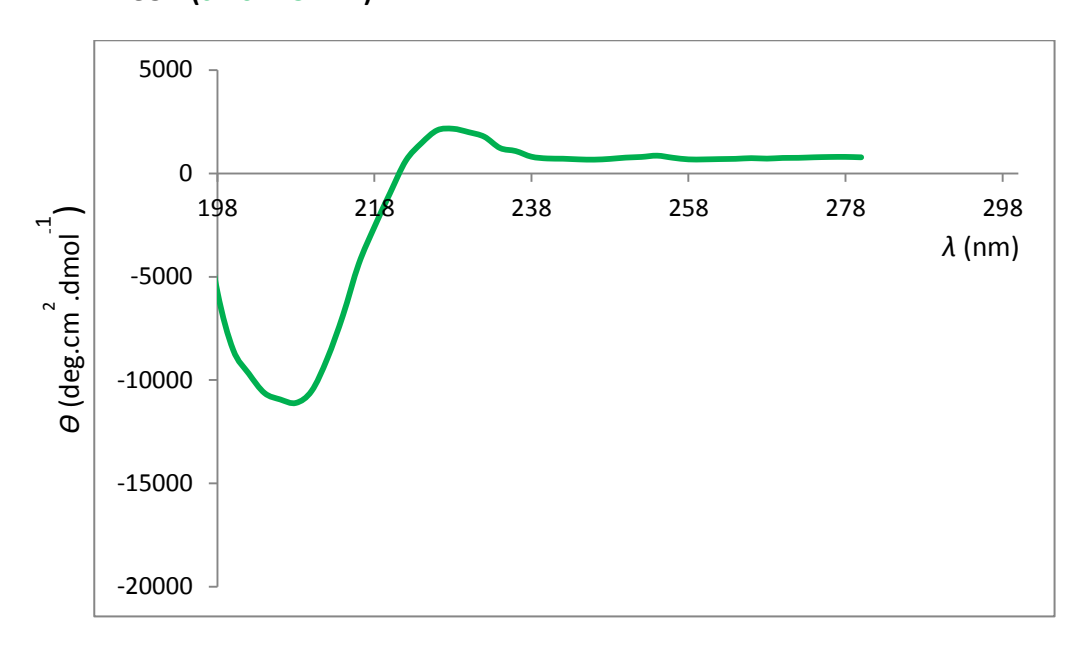


• H₂O (c = 0.25 mM)

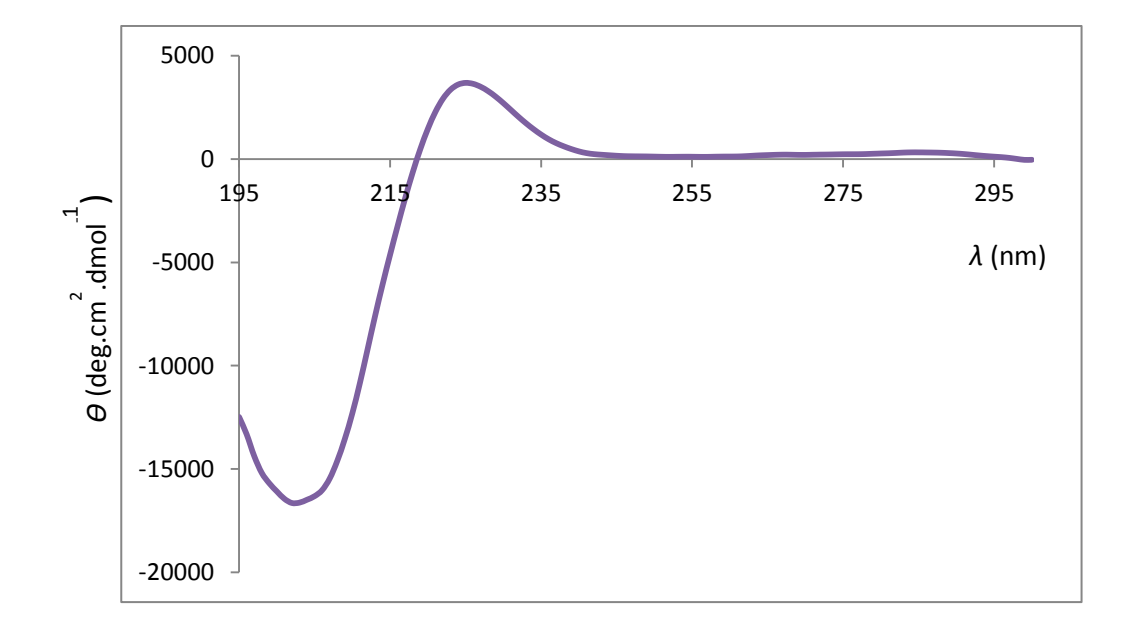


3.3 Tetramer 4.3

• MeOH (c = 0.125 mM)

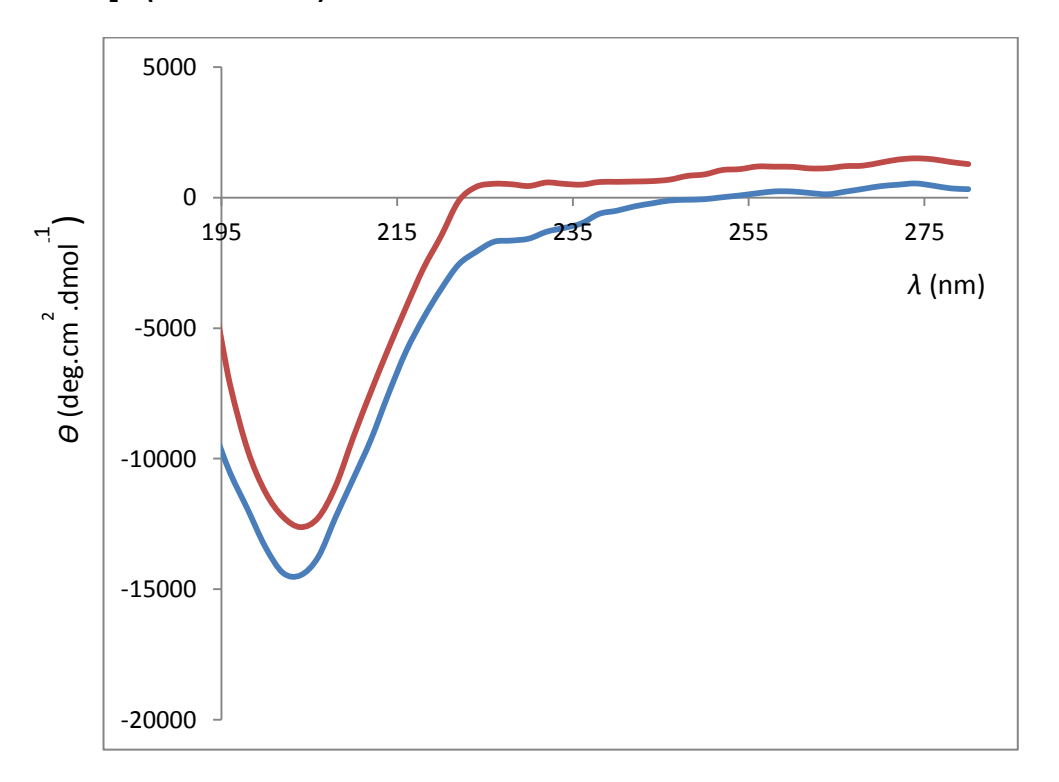


• H₂O (c = 0.125 mM)

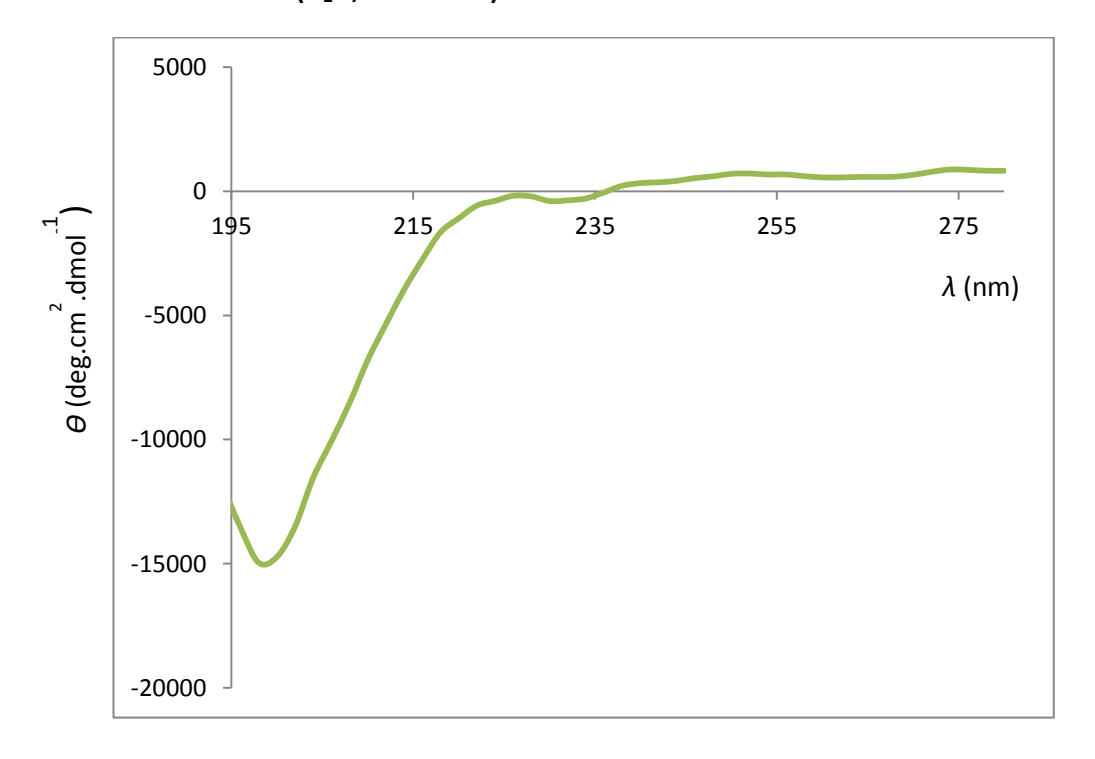


3.4 N-Ac-Pro-Arg(NO₂)-Gly-Pro-Arg(NO₂)-Pro-OMe 2.1 and N-Ac-Pro-Arg(NO₂)-1.125-Arg(NO₂)-Pro-OMe 3.36

• H_2O (c = 0.125 mM)

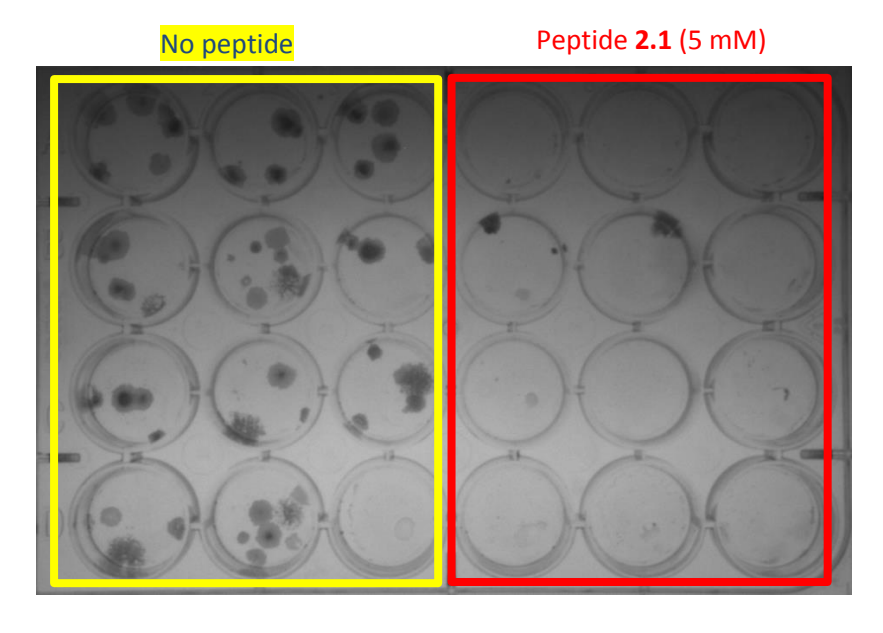


3.5 Parent 8mer 1.139 (H₂O, 0.125 mM)



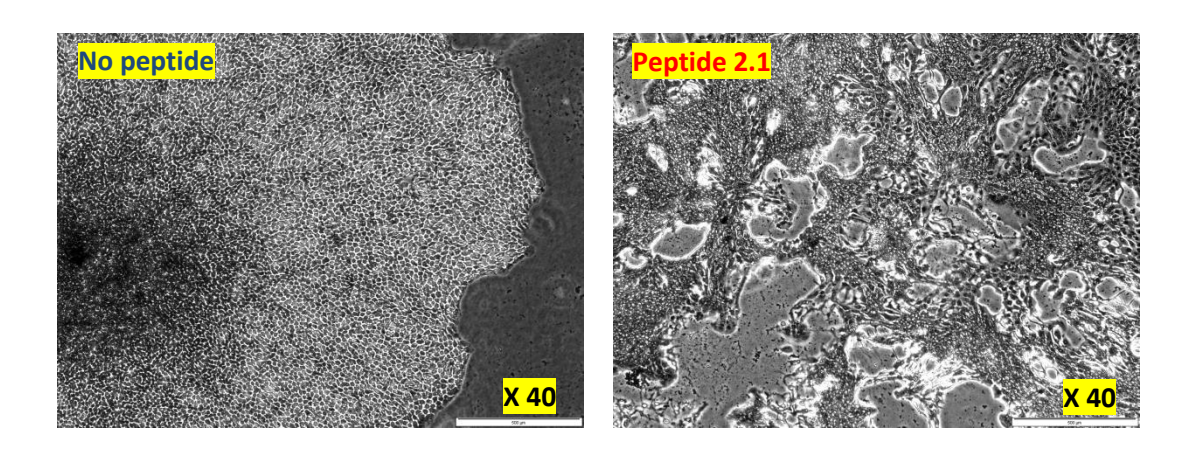
4.0 Clonogenic assays

- 4.1 N-Ac-Pro-Arg(NO₂)-Gly-Pro-Arg(NO₂)-Pro-OMe 2.1
 - 4.1.1 Clonogenic assay on RT112 cancer cells



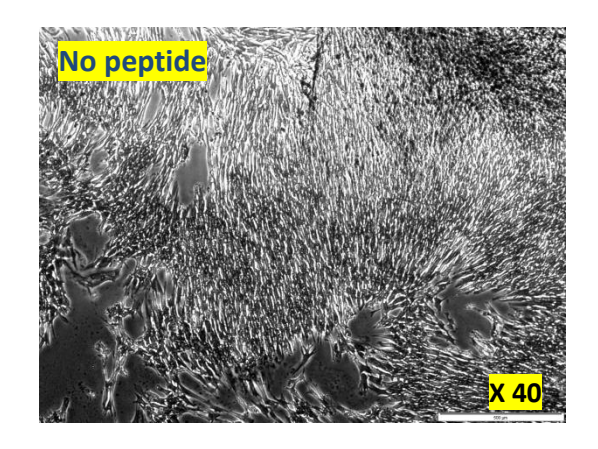
Pictures of colony formation of RT112 bladder cancer cells on day 29.

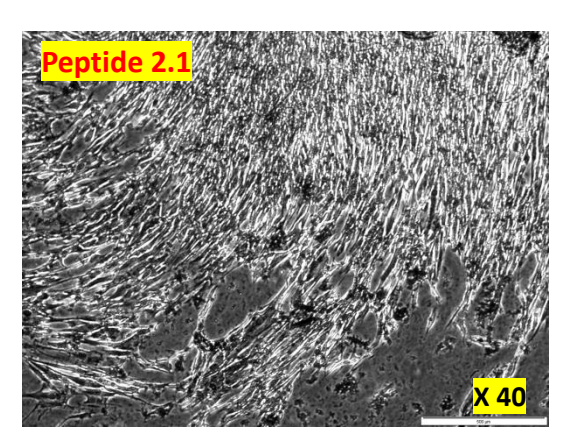
Bladder cells were trypsinised and seeded at 10 cells in each well dish of 24-well plate. The cells were allowed to grow in medium for control experiment (500 μ L of final volume). The anticancer activity was studied was performed when cells were exposed with 5 mM of peptide **2.1**. Plates were kept at 37 °C in 5% CO₂ before staining with Giemsa's stain on day 29.



Morphological appearance of RT112 cells exposure to 5 mM of synthetic peptide **2.1** on day 29. Peptide **2.1** could almost completely kill bladder cancer cells after one month. Picture with a solution of **2.1** (5 mM) showed a survival colony. This picture showed that cells from this survival colony appeared as debris of cells.

4.1.2 Clonogenic assay on MRC5-hTERT

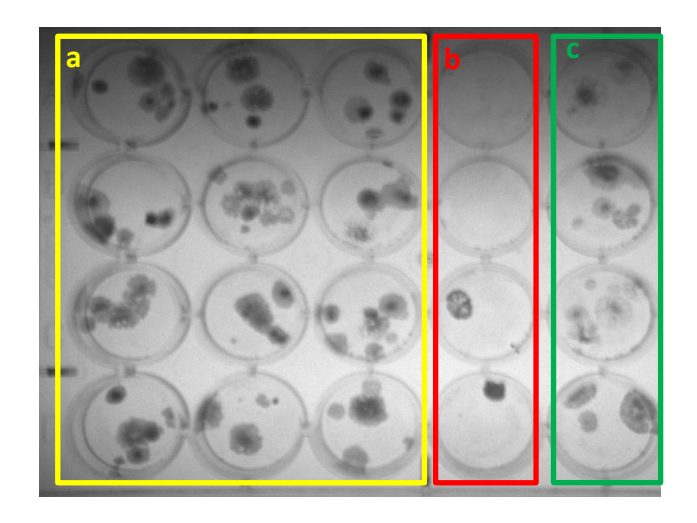




Morphological appearances of MRC5-hTERT cells exposure to 5 mM of synthetic peptide **2.1** on day 29. Normal fibroblasts were trypsinised and seeded at 250 cells in each well dish of 24-well plate. The cells were allowed to grow in DMEM medium for control experiment (500 μ L of final volume). Plates were kept at 37 °C in 5% CO₂ before staining with Giemsa's stain on day 29.

4.2 **2.14**-Arg(NO₂)-Gly-Pro-Arg(NO₂)-Pro-OMe **2.16**

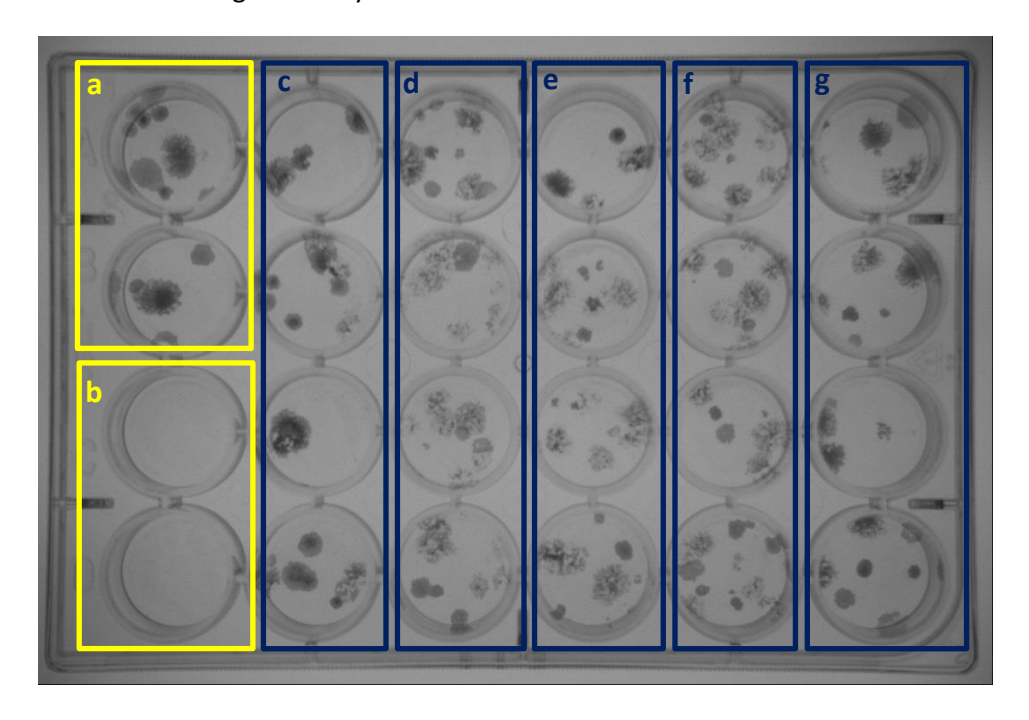
4.2.1 Clonogenic assay on RT112 cancer cells



a) Control wells (no peptide); b) Positive control wells (compound **2.1**, 5 mM); c) Compound **2.16** (5 mM). Pictures of colony forming of RT112 bladder cancer cells on day 29. Bladder cells were trypsinised and seeded at 10 cells in each well dish of 24-well plate. The cells were allowed to grow in medium for control experiment (500 μ L of final volume). The anticancer activity was studied was performed when cells were exposed with 5 mM of peptide **2.16**. Plates were kept at 37 °C in 5% CO_2 before staining with Giemsa's stain on day 29.

4.3 *N*-Ac-Arg(NO₂)-**1.125**-Arg(NO₂)-Pro-OMe **3.36**

4.3.1 Clonogenic assay on RT112 cancer cells

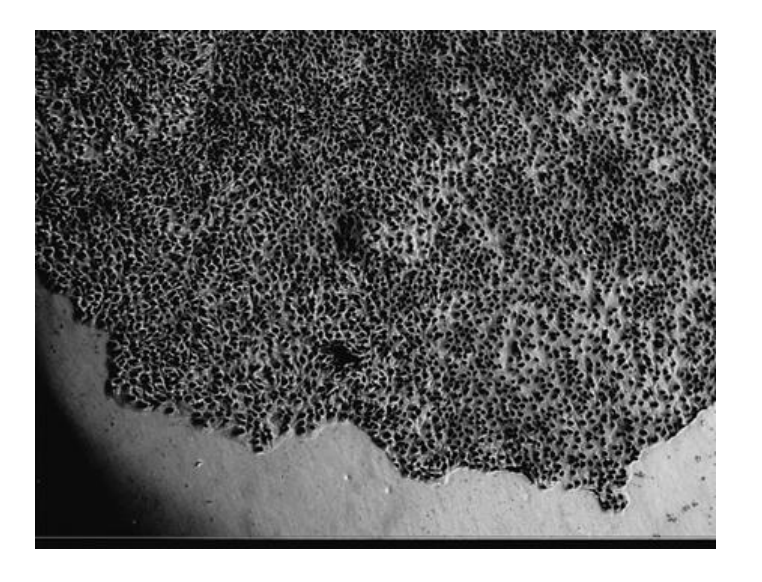


a) Control wells (no peptide); b) Positive control wells (compound **2.1**, 5 mM); c) Compound **3.36** (5 mM); d) Compound **3.36** (4 mM); e) Compound **3.36** (3 mM); f) Compound **3.36** (2 mM); g) Compound **3.36** (1 mM).

Pictures of colony forming of RT112 bladder cancer cells on day 31.

Bladder cells were trypsinised and seeded at 10 cells in each well dish of 24-well plate. The cells were allowed to grow in medium for control experiment (500 μ L of final volume). The anticancer activity was studied was performed when cells were exposed with 5 to 1 mM of peptide **3.36**. Plates were kept at 37 °C in 5% CO₂ before staining with Giemsa's stain on day 31.

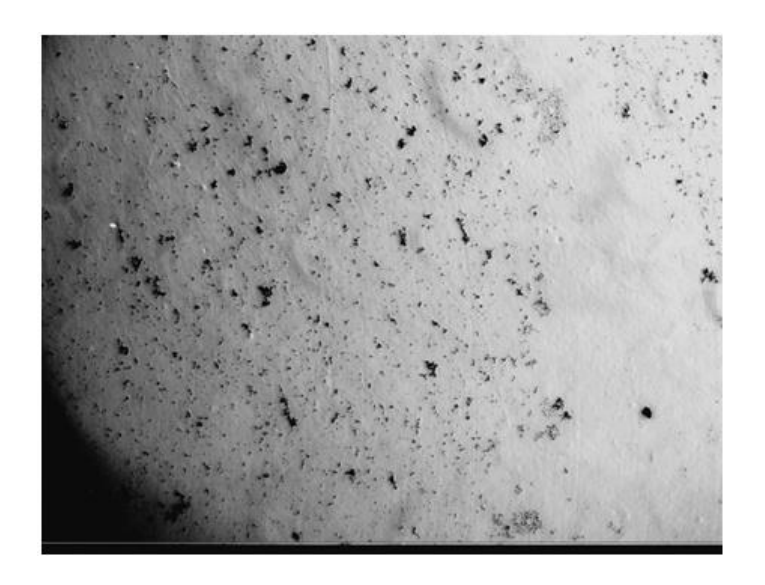
4.3.1.1 Control (no peptide, X 40)

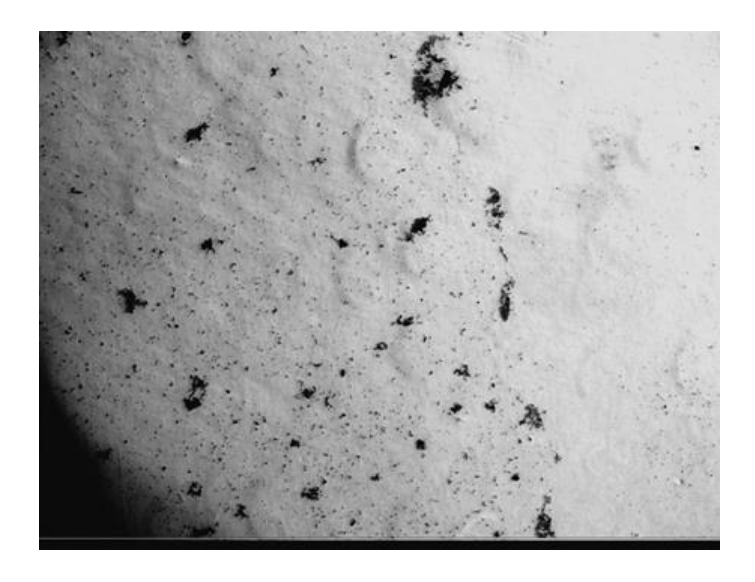




Morphological appearance of RT112 cells on day 31.

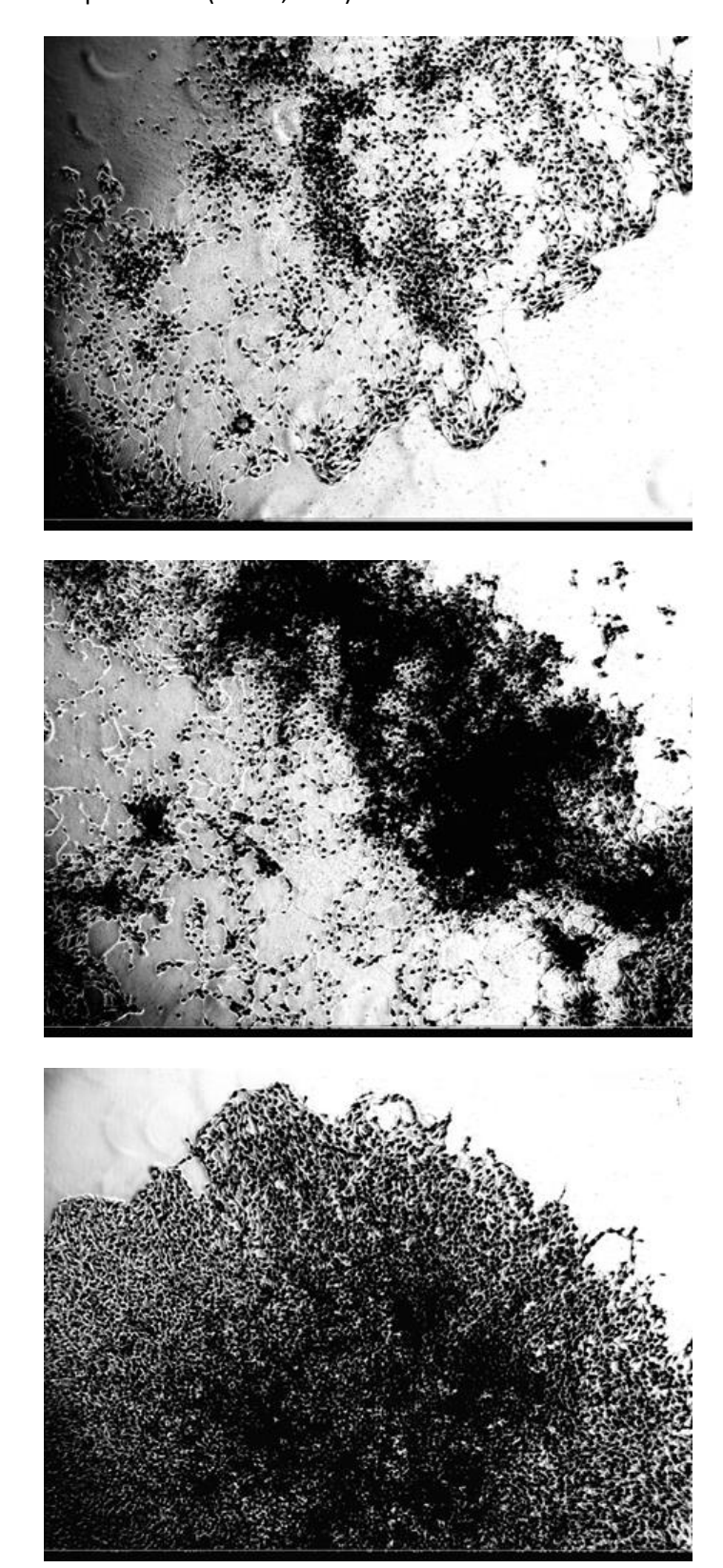
4.2.1.2 Positive control (peptide **2.1**, 5 mM, X 40).





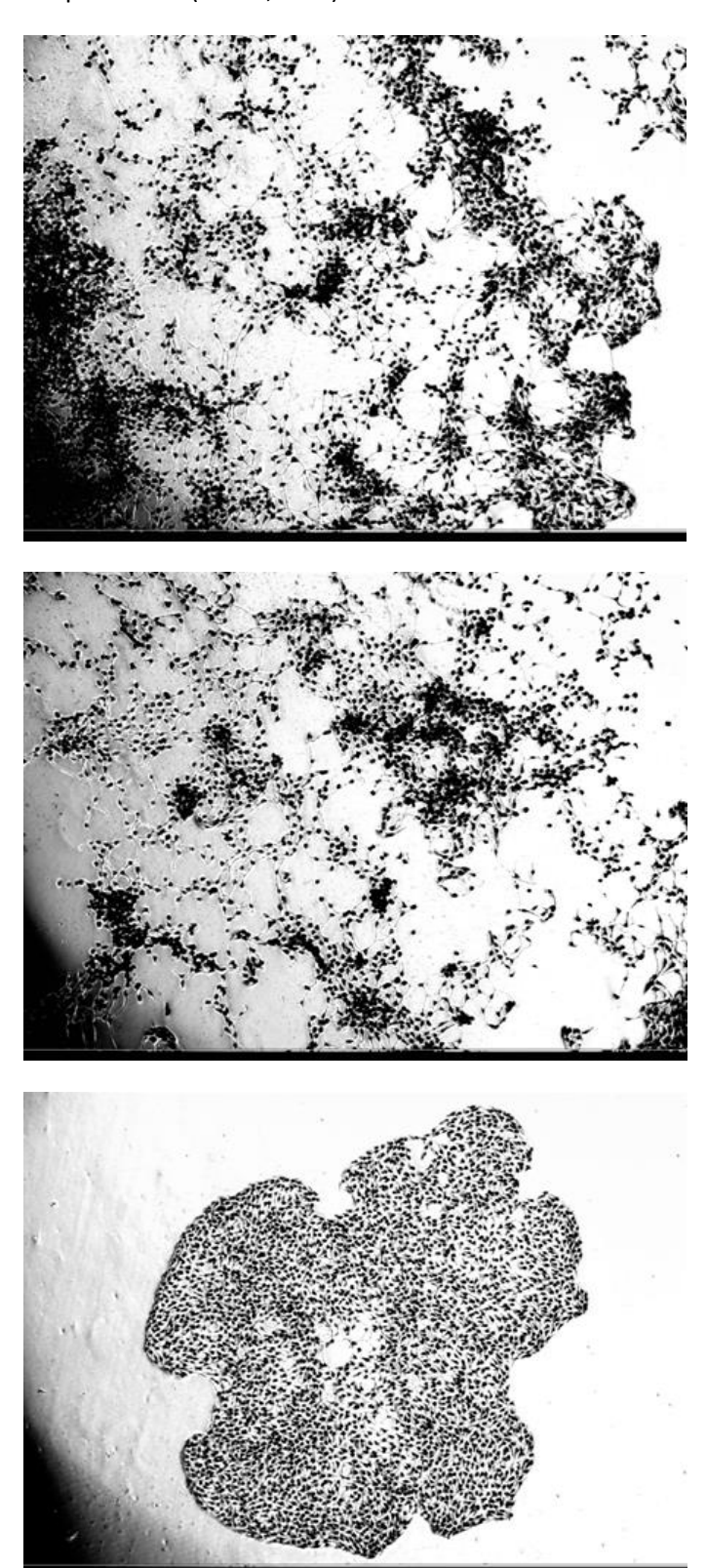
Morphological appearance of RT112 cells exposure to 5 mM of synthetic peptide **2.1** on day 31.

4.2.1.3 Peptide **3.36** (5 mM, X 40)



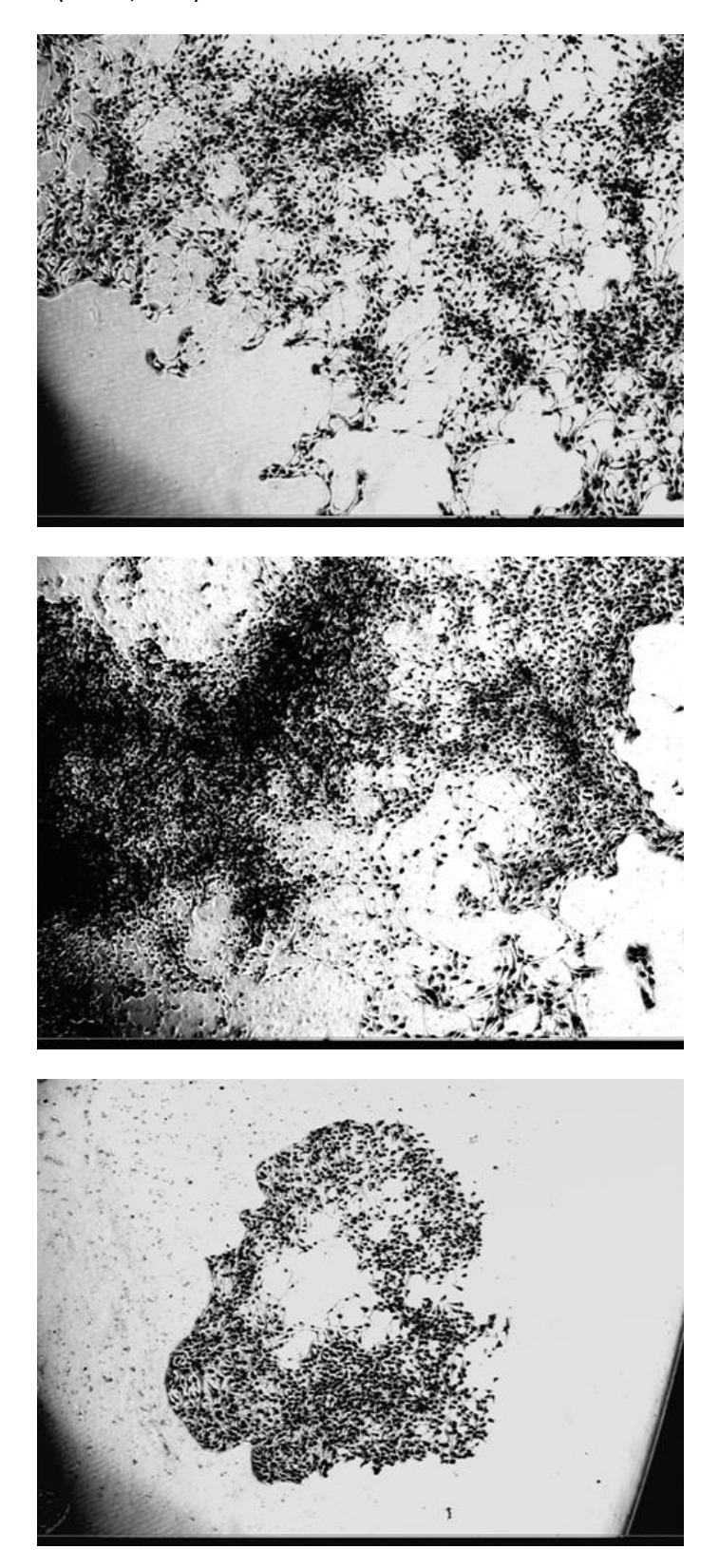
Morphological appearance of RT112 cells exposure to 5 mM of synthetic peptide **3.36** on day 31.

4.3.1.4 Peptide **3.36** (4 mM, X 40)



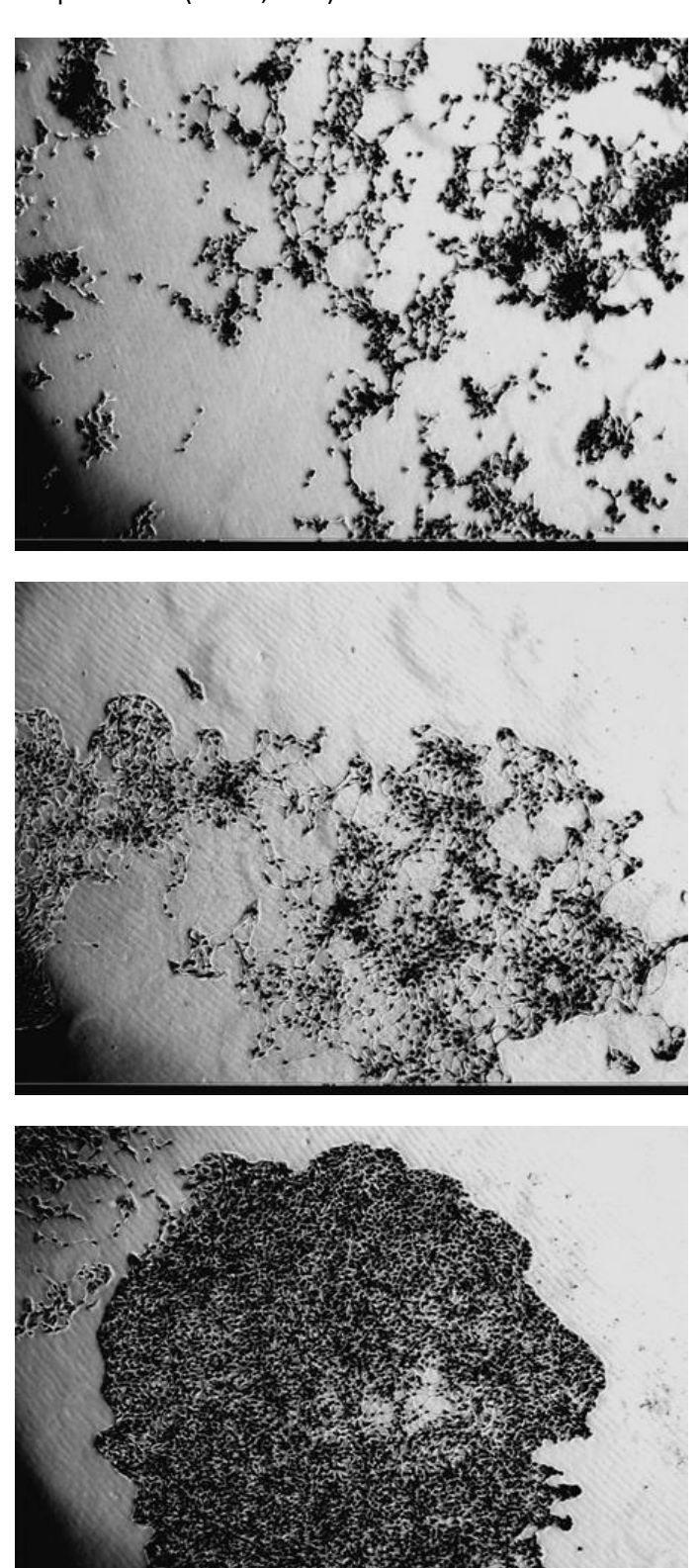
Morphological appearance of RT112 cells exposure to 4 mM of synthetic peptide **3.36** on day 31.

4.3.1.5 Peptide **3.36** (3 mM, X 40)



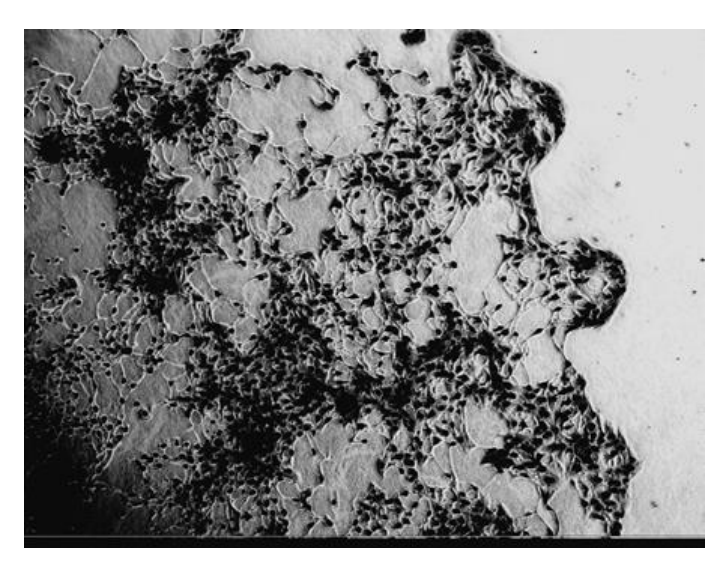
Morphological appearance of RT112 cells exposure to 3 mM of synthetic peptide **3.36** on day 31.

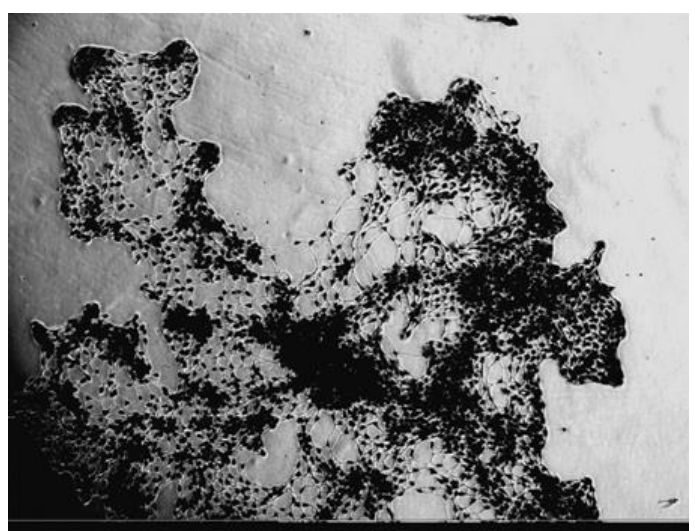
4.3.1.6 Peptide **3.36** (2 mM, X 40)

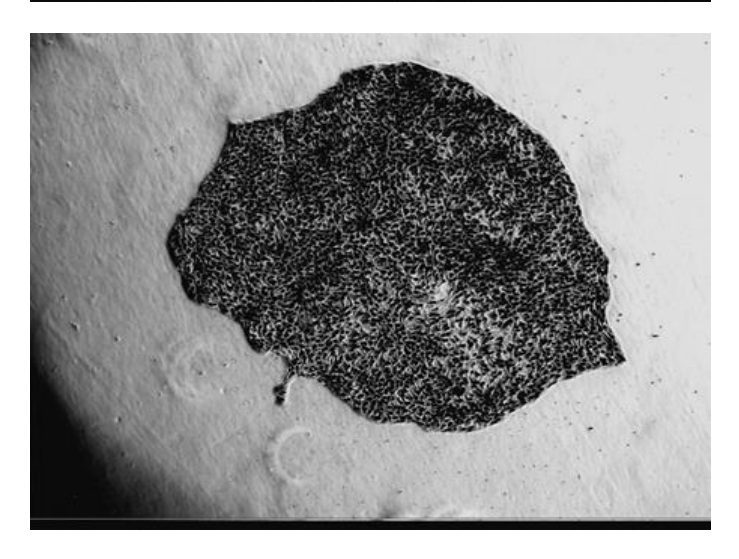


Morphological appearance of RT112 cells exposure to 2 mM of synthetic peptide **3.36** on day 31.

4.3.1.7 Peptide **3.36** (1 mM, X 40)

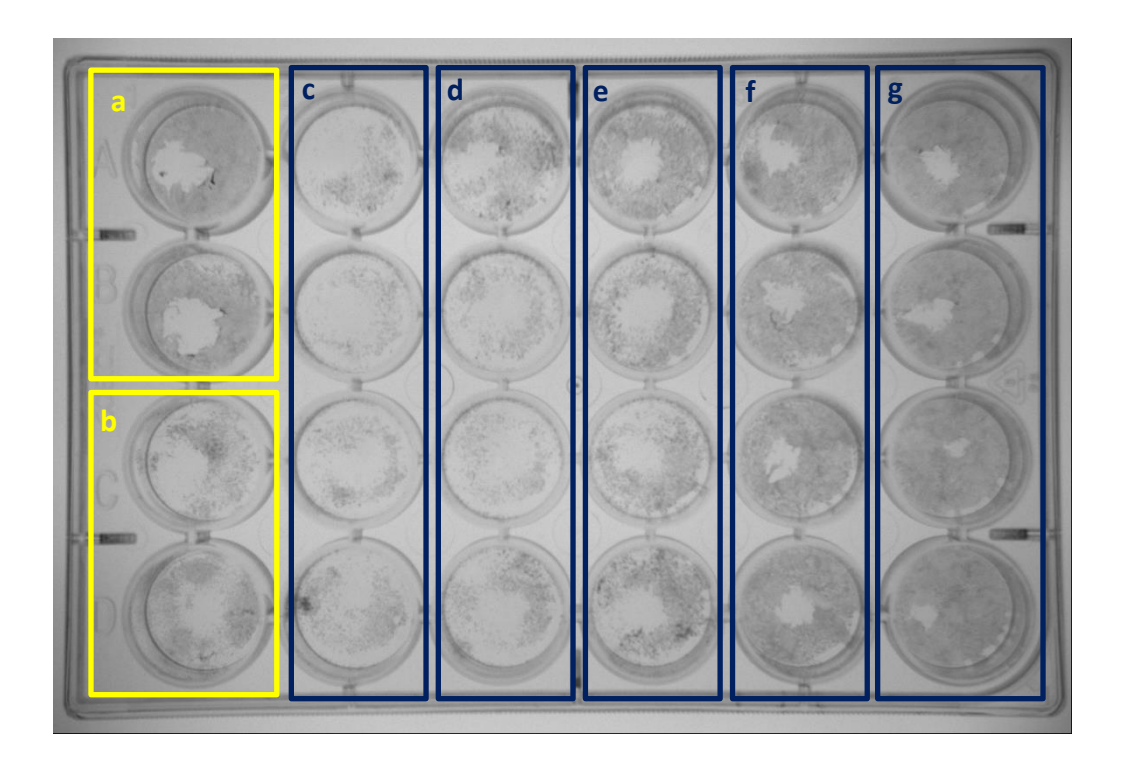






Morphological appearance of RT112 cells exposure to 1 mM of synthetic peptide **3.36** on day 31.

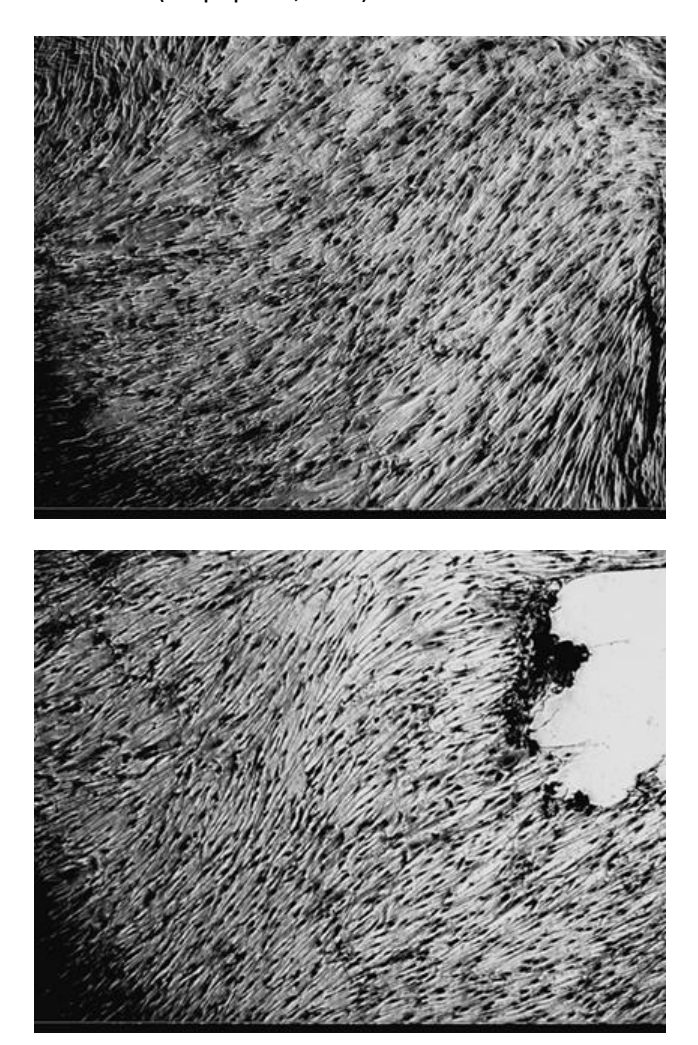
4.3.2 Clonogenic assay on MRC5-hTERT



a) Control wells (no peptide); b) Positive control wells (compound **2.1**, 5 mM); c) Compound **3.36** (5 mM); d) Compound **3.36** (4 mM); e) Compound **3.36** (3 mM); f) Compound **3.36** (2 mM); g) Compound **3.36** (1 mM).

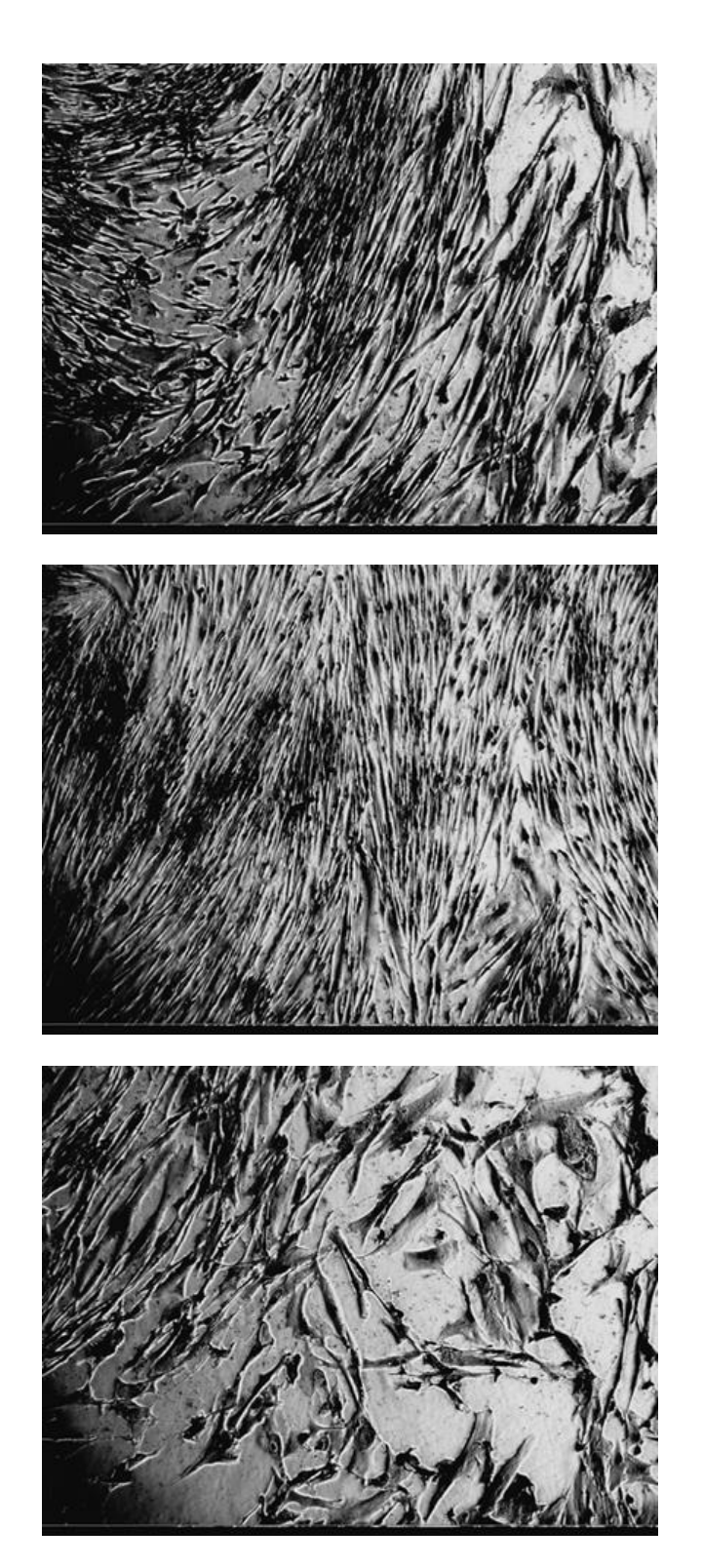
Morphological appearances of MRC5-hTERT cells exposure to synthetic peptide **3.36** at different concentrations (5 to 1 mM) on day 31. Normal fibroblasts were trypsinised and seeded at 250 cells in each well dish of a 24-well plate. The cells were allowed to grow in DMEM medium for the control experiment (500 μ L of final volume). The plates were kept at 37 °C in 5% CO₂ before staining with Giemsa's stain on day 31.

4.3.2.1 Control (no peptide, X 40)



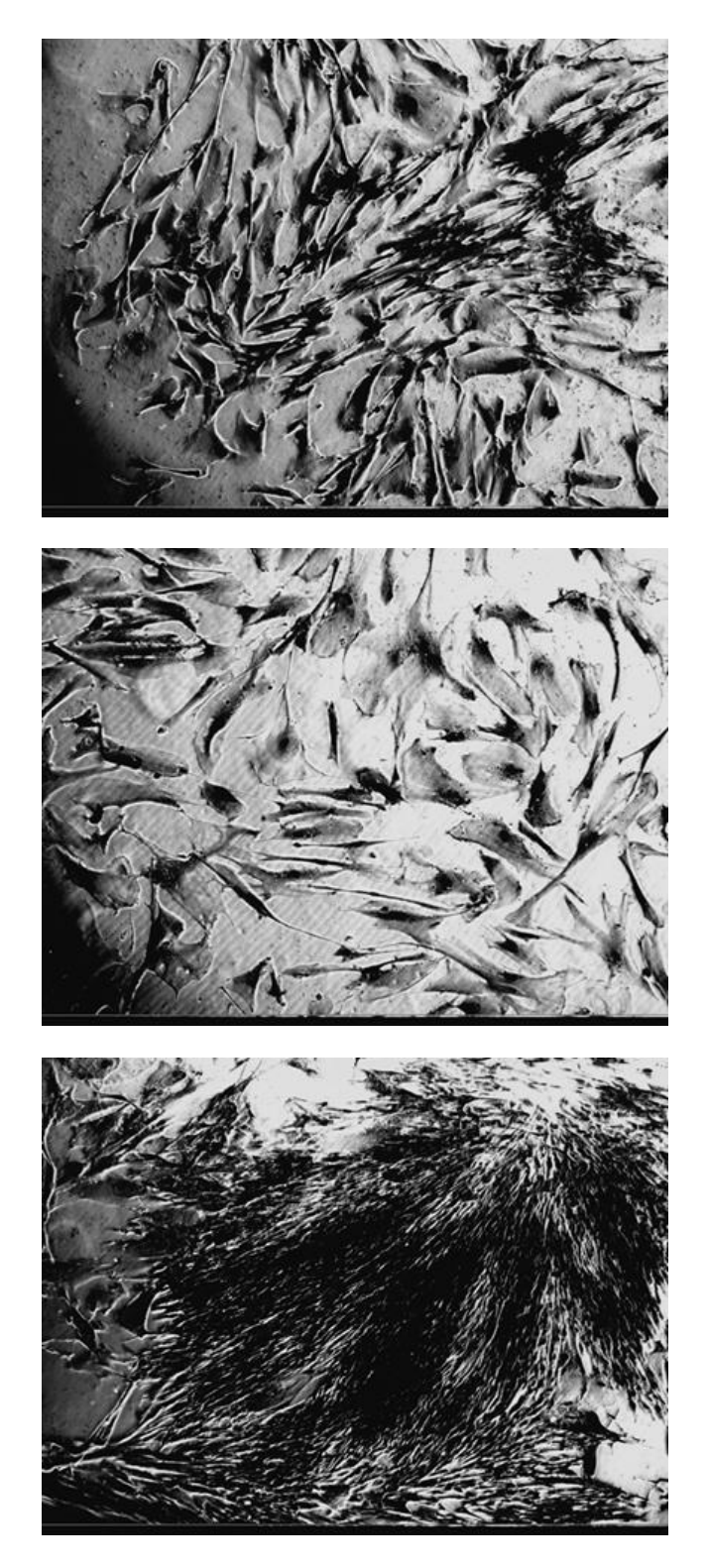
Morphological appearances of MRC5-hTERT cells on day 31.

4.3.2.2 Positive Control (Peptide **2.1**, 5 mM, X 40)



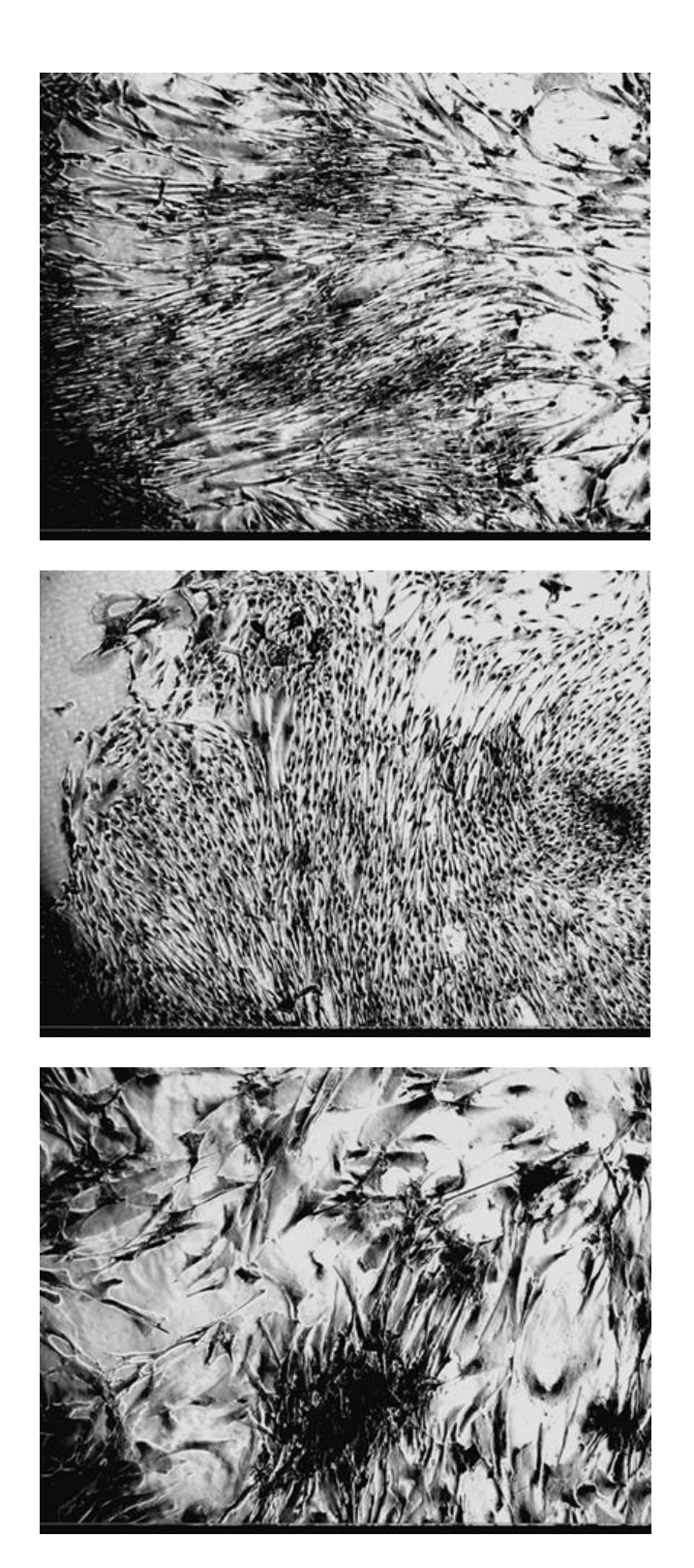
Morphological appearances of MRC5-hTERT cells exposure to 5 mM of synthetic peptide **2.1** on day 31.

4.3.2.3 Peptide **3.36** (5 mM, X 40)

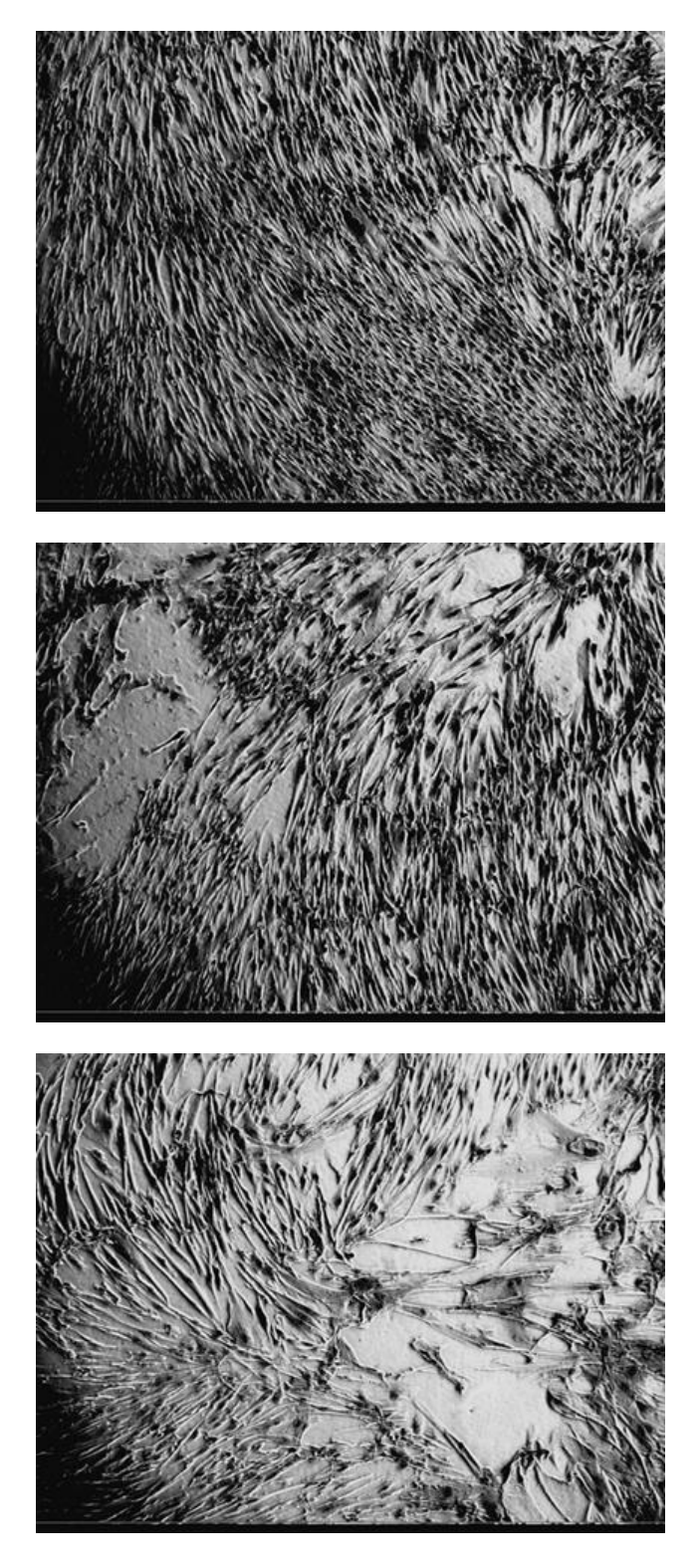


Morphological appearances of MRC5-hTERT cells exposure to 5 mM of synthetic peptide **3.36** on day 31.

4.3.2.4 Peptide **3.36** (4 mM, X 40)

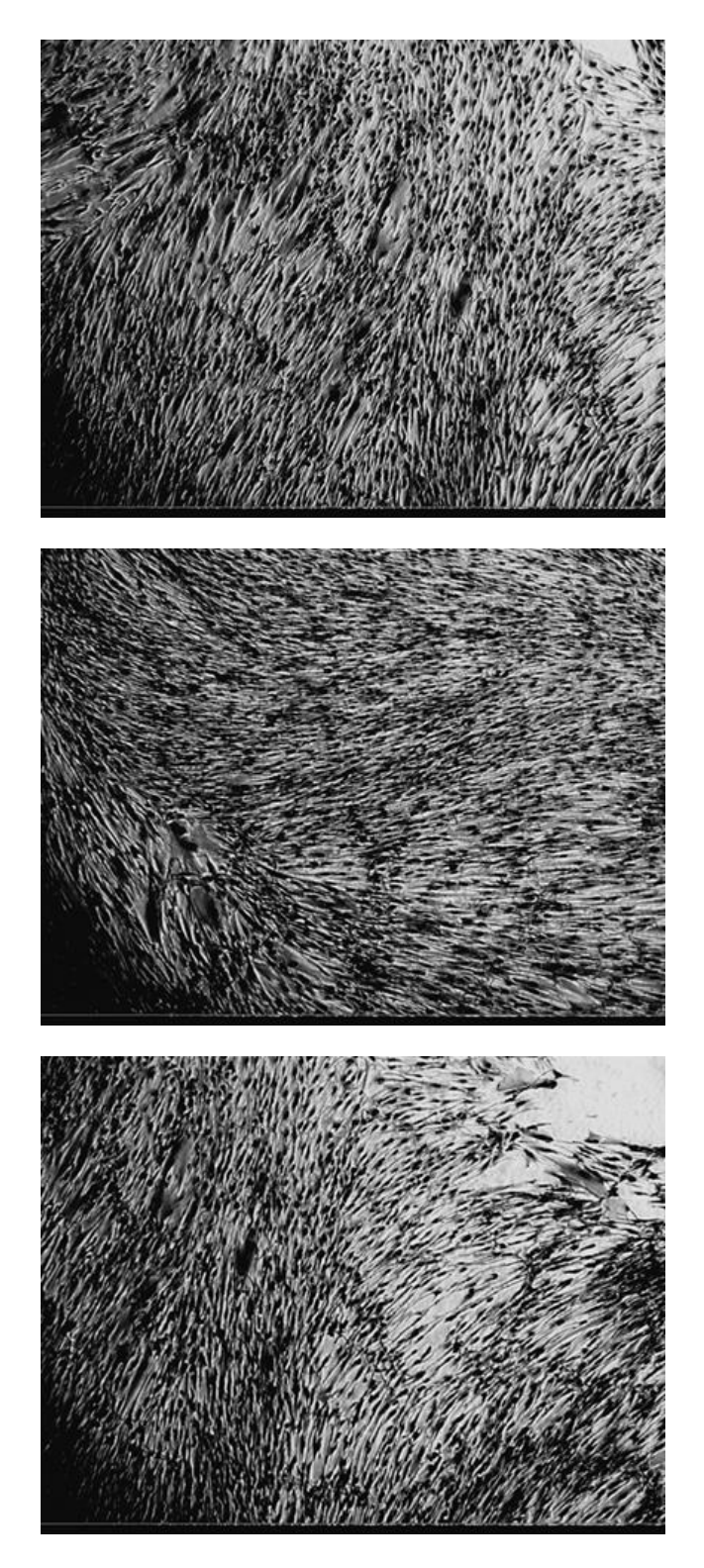


Morphological appearances of MRC5-hTERT cells exposure to 4 mM of synthetic peptide **3.36** on day 31.

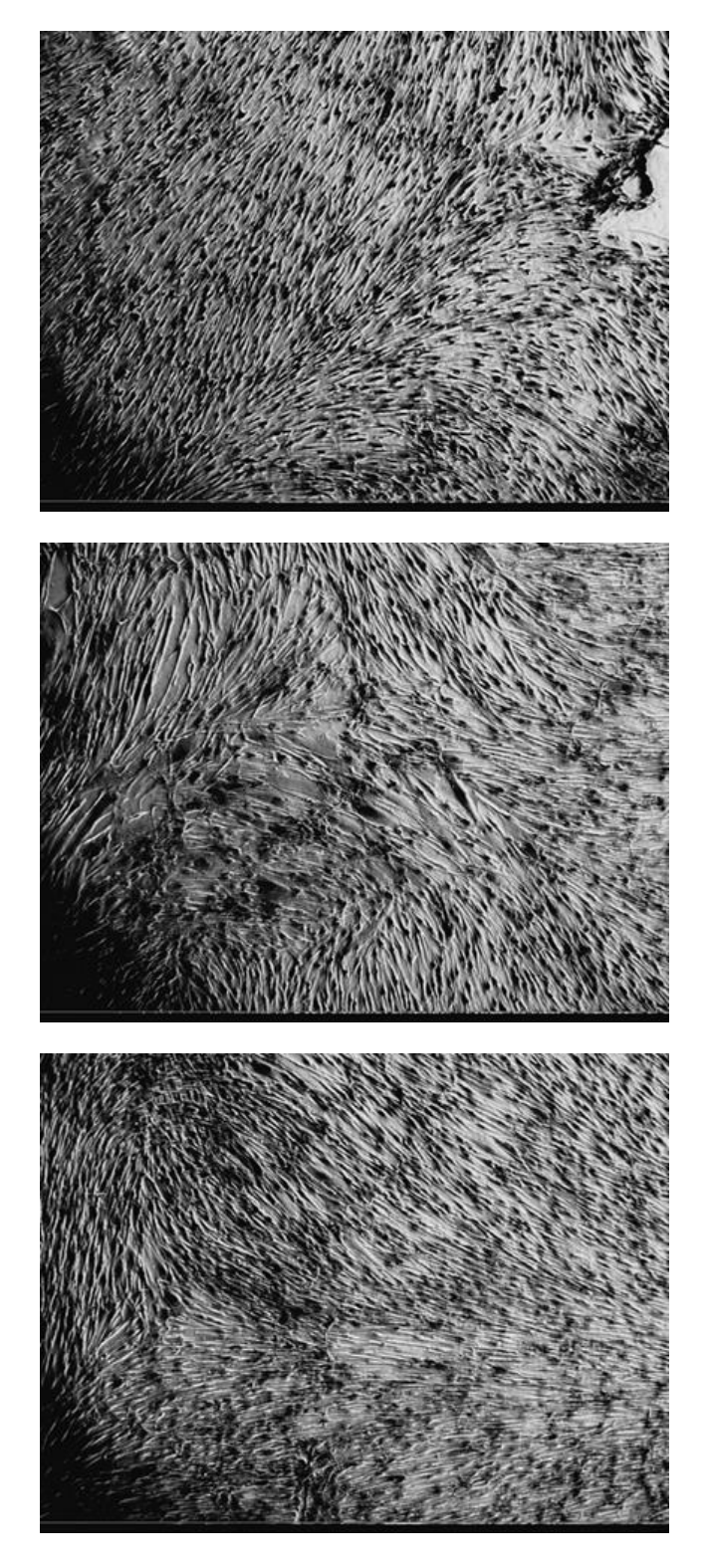


Morphological appearances of MRC5-hTERT cells exposure to 3 mM of synthetic peptide **3.36** on day 31.

4.3.2.6 Peptide **3.36** (2 mM, X 40)



Morphological appearances of MRC5-hTERT cells exposure to 2 mM of synthetic peptide **3.36** on day 31.



Morphological appearances of MRC5-hTERT cells exposure to 1 mM of synthetic peptide **3.36** on day 31.

5.0 BioNMR Data

NMR spectra of isotope labelled SH3 domain were collected at 25 $^{\circ}$ C with a 600 MHz four-channel Varian INOVA NMR spectrometer equipped with a room temperature 5 mm triple resonance z-gradient probe. Resonance assignments of the free and peptide bound form of the backbone 15 N and HN nuclei were obtained by a combination of 2D 1 H- 15 N-HSQC, 3D 15 N-edited NOESY-HSQC, as well as HNCA, HNCACB and CBCA(CO)NH spectra. All experiments used water flip-back and gradient-enhancement. The protein and analogues **1.139**, **1.140**, **1.141** and **1.142** were dissolved in phosphate buffer + 10% DMSO- d_6 .

5.1 Fyn-SH3 domain chemical shifts

Residu	ue number	δ _н (ppm)	δ _N (ppm)	δ _{Cα} (ppm)	δ _{cβ} (ppm)				
Gly	13	8.28	108.63	45.2					
Thr	14	8.15	112.90	45.28	69.71				
Gly	15	8.52	111.22	62.11					
Val	16	7.99	119.55	45.44	32.96				
Thr	17	8.4	119.52	62.13	70.02				
Leu	18	8.25	125.57	54.4	43.94				
Phe	19	8.91	122.13	56.59	43.61				
Val	20	9.77	119.35	58.24	35.62				
Ala	21	9.1	126.72	52.41	21.27				
Leu	22	9.5	125.96	55.56	42.97				
Tyr	23	7.15	111.96	53.88	42.83				
Asp	24	8.31	117.51	54.49	42.13				
Tyr	25	8.34	120.39	58.39	42.41				
Glu	26	7.26	128.05	53.85	30.84				
Ala	27	8.21	125.99	53.05	20.25				
Arg	28	9.61	121.15	56.27	32.39				
Thr	29	8.34	111.99	59.67	71.63				
Glu	30	8.81	118.61	58.14	45.41				
Asp	31	8.02	116.39	54.52	41.93				
Asp	32	7.98	119.95	52.95	42.6				
Leu	33	8.3	120.14	54.21	43.93				
Ser	34	8.04	114.42	58.3	64.59				
Phe	35	8.8	116.35	56.38	41.24				
His	36	8.67	116.44	53.76	31.99				
Lys	37	9.24	121.76	58.63	32.91				
Gly	38	8.96	114.66	45.04					
Glu	39	8.2	124.66	58.33	30.83				
Lys	40	8.13	121.01	54.81	36.01				
Phe	41	9.17	115.68	56.87	44.91				

Gln	42	8.68	119.74	54.3	30.79
Ile	43	9.39	126.59	59.44	34.82
Leu	44	8.94	128.78	55.59	42.27
Asn	45	7.61	115.24	53.68	40.33
Ser	46	8.8	121.11	57.01	62.03
Ser	47	8.02	117.16	60.46	63.88
Glu	48	8.71	121.5	56.08	30.13
Gly	49	8.32	107.86	46.29	
Asp	50	8.55	119.11	55.53	41.14
Trp	51	7.63	120.61	55.88	31.47
Trp	52	9.18	124.26	52.81	32.13
Glu	53	8.71	123.9	56.07	30.85
Ala	54	9.41	131.76	51.06	25.95
Arg	55	8.91	118.63	53.7	34.17
Ser	56	8.8	119.86	57.64	63.33
Leu	57	9.01	130.79	56.68	40.38
Thr	58	8.46	116.43	65.83	69.29
Thr	59	8.07	108.26	61.83	71.04
Gly	60	7.97	111.21	45.78	
Glu	61	8.06	120.81	56.67	31.3
Thr	62	8.4	113.12	60.08	71.19
Gly	63	8.81	111.15	45.4	
Tyr	64	8.76	118.91	58.5	40.28
lle	65	9.24	112.42	57.3	40.14
Ser	67	7.64	121.7	60.67	29.96
Asn	68	8.06	115.04	53.43	36.54
Tyr	69	7.82	119.35	58.53	39.35
Val	70	7.14	108.96	58.28	36.88
Ala	71	8.81	121.87	49.7	21.62
Val	73	8.09	121.86	63.18	32.26
Asp	74	8.28	121.98	54.51	41.02
Ser	75	8.03	115.27	58.41	64.15
lle	76	7.95	122.22	61.17	38.6
Gln	77	7.93	128.89	57.35	30.58
	-				

5.2 Data Parent8mer 1.139/SH3 domain binding

1.139 /SH3	Ratio Ratio		Ratio		Ratio Ratio		atio	Ratio										
	0:1		0.25:1		0.5:1		0.75:1		1:1		2:1		4:1		8:1		12:1	
Residue number	δ _н	δ _N	δ _Η	δ _N	δ _н	δ _N	δ _Η	δ _N	δ _Η	δ _N								
Gly13	8.233	108.554	8.231	108.551	8.232	108.538	8.231	108.570	8.229	108.558	8.229	108.554	8.228	108.575	8.226	108.578	8.225	108.566
Thr14	8.083	112.770	8.082	112.767	8.082	112.754	8.080	112.755	8.078	112.7850	8.078	112.739	8.075	112.719	8.075	112.719	8.074	112.717
Gly15	8.428	111.102	8.429	111.096	8.428	111.090	8.427	111.092	8.426	111.076	8.425	111.075	8.423	111.050	8.421	111.050	8.421	111.050
Val16	7.896	118.790	7.896	118.784	7.898	118.785	7.899	118.779	7.898	118.778	7.901	118.766	7.904	118.743	7.904	118.743	7.906	118.756
Thr17	8.276	118.739	8.272	118.756	8.273	118.782	8.271	118.783	8.266	118.784	8.262	118.823	8.255	118.859	8.251	118.859	8.251	118.881
Leu18	8.145	125.499	8.151	125.470	8.153	125.507	8.156	125.516	8.155	125.489	8.163	125.494	8.171	125.463	8.176	125.463	8.178	125.468
Phe19	8.867	122.355	8.858	122.339	8.853	122.304	8.844	122.300	8.839	122.284	8.823	122.230	8.802	122.084	8.783	122.084	8.779	122.052
Val20	9.703	119.342	9.704	119.349	9.707	119.345	9.712	119.348	9.701	119.349	9.706	119.345	9.709	119.353	9.711	119.353	9.710	119.352

Ala21	9.051	126.857	9.051	126.857	9.051	126.855	9.051	126.857	9.051	126.857	9.050	126.858	9.049	126.845	9.049	126.845	9.049	126.844
Leu22	9.393	125.767	9.393	125.783	9.391	125.808	9.389	125.822	9.388	125.834	9.385	125.894	9.383	125.986	9.377	125.986	9.374	126.011
Tyr23	7.128	112.307	7.118	112.255	7.110	112.226	7.102	112.205	7.095	112.187	7.078	112.096	7.052	111.947	7.031	111.947	7.024	111.898
Asp24	8.245	117.712	8.241	117.703	8.238	117.703	8.234	117.705	8.231	117.680	8.224	117.656	8.213	117.649	8.205	117.623	8.202	117.614
Tyr25	8.249	120.383	8.249	120.342	8.245	120.300	8.244	120.261	8.241	120.229	8.237	120.163	8.307	120.351	8.362	120.473	8.387	120.513
Glu26	7.142	128.143	7.143	128.112	7.138	128.095	7.142	128.107	7.136	128.091	7.142	128.061	7.138	128.035	7.141	127.987	7.142	127.975
Ala27	8.125	126.088	8.133	126.056	8.139	126.007	8.145	125.979	8.149	125.964	8.163	125.930	8.181	125.850	8.197	125.823	8.203	125.805
Arg28	9.702	121.311	9.648	121.158	9.608	120.980	9.603	120.934	9.500	120.815	9.363	120.571	9.212	120.194	9.080	119.866	9.024	119.740
Thr29	8.662	113.323	8.618	113.073	8.668	113.306	8.674	113.270	8.651	113.264	8.681	113.189	8.659	113.229	8.340	112.055	8.244	111.611
Glu30	8.707	118.269	8.727	118.366	8.745	118.461	8.758	118.547	8.770	118.620	8.819	118.771	8.834	118.701	8.842	118.713	8.853	118.727
Asp31	8.016	116.232	7.998	116.221	7.979	116.203	7.965	116.173	7.949	116.156	7.903	116.085	7.855	116.019	7.816	115.960	7.803	115.954
Asp32	8.089	119.919	8.121	119.988	8.146	120.022	8.169	120.057	8.181	120.097	8.173	120.175	8.230	120.044	8.224	119.951	8.219	119.894
Leu33	8.154	119.535	8.097	119.639	8.108	119.826	8.087	120.057	8.090	119.925	7.983	119.909	8.070	120.129	8.044	120.161	8.036	120.175
L		1		l		l		l		l		ı		1		1		

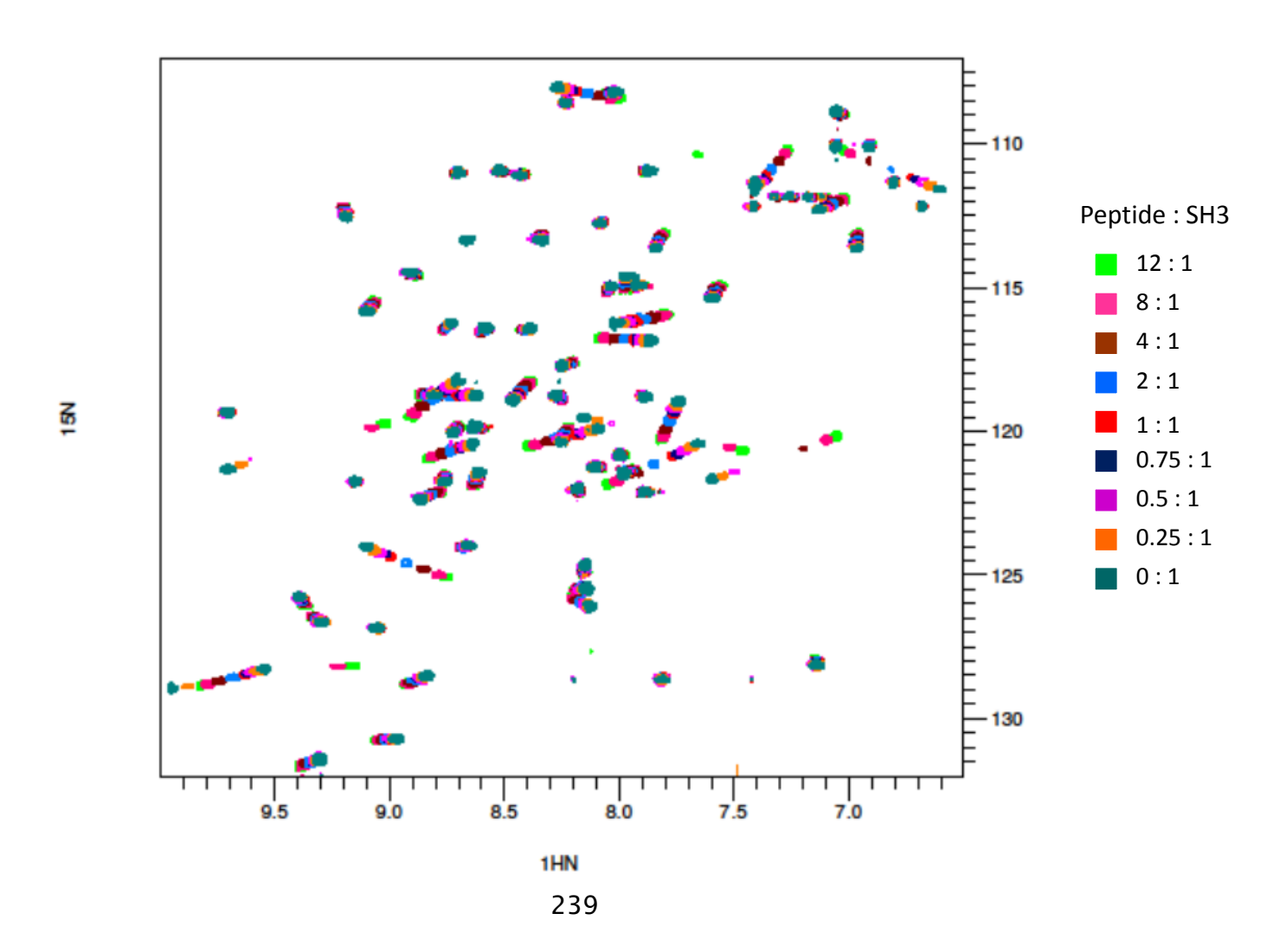
Ser34	7.971	114.593	7.971	114.644	7.970	114.676	7.971	114.718	7.971	114.740	7.969	114.823	7.970	114.928	7.973	115.008	7.974	115.058
Phe35	8.735	116.228	8.739	116.252	8.741	116.267	8.743	116.294	8.744	116.313	8.751	116.346	8.759	116.417	8.765	116.466	8.767	116.490
His36	8.584	116.397	8.584	116.416	8.588	116.429	8.590	116.435	8.589	116.442	8.589	116.473	8.596	116.505	8.597	116.531	8.597	116.525
Lys37	9.153	121.744	9.153	121.751	9.154	121.749	9.155	121.748	9.153	121.755	9.156	121.760	9.156	121.765	9.156	121.773	9.156	121.773
Gly38	8.906	114.467	8.904	114.475	8.902	114.483	8.902	114.496	8.900	114.514	8.895	114.532	8.891	114.559	8.887	114.577	8.886	114.598
Glu39	8.151	124.647	8.151	124.687	8.153	124.719	8.152	124.703	8.151	124.725	8.152	127.779	8.151	124.852	8.152	124.895	8.152	124.913
Lys 40	8.115	121.252	8.106	121.240	8.105	121.262	8.102	121.253	8.098	121.540	8.096	121.248	8.091	121.239	8.083	121.252	8.086	121.242
Phe41	9.097	115.814	9.095	115.799	9.094	115.760	9.094	115.746	9.089	115.721	9.080	115.651	9.077	115.585	9.072	115.519	9.067	115.497
Gln42	8.632	119.863	8.626	119.848	8.625	119.862	8.623	119.865	8.622	119.850	8.618	119.869	8.616	119.895	8.613	119.908	8.607	119.909
Ile43	9.299	126.653	9.305	126.633	9.307	126.623	9.309	126.602	9.309	126.592	9.317	126.535	9.326	126.497	9.333	126.448	9.338	126.431
Leu44	8.835	128.516	8.844	128.534	8.852	128.547	8.858	128.587	8.860	128.605	8.879	128.658	8.899	128.712	8.914	128.770	8.919	128.792
Asn45	7.591	115.372	7.590	115.340	7.589	115.294	7.587	115.271	7.584	115.245	7.581	115.162	7.575	115.080	7.570	114.992	7.565	114.945

Ser46	8.642	120.415	8.659	120.483	8.673	120.516	8.686	120.538	8.694	120.575	8.730	120.683	8.772	120.783	8.811	120.870	8.828	120.932
Ser47	7.870	116.836	7.889	116.829	7.906	116.830	7.920	116.808	7.931	116.805	7.973	116.795	8.020	116.780	8.064	116.781	8.087	116.771
Glu48	8.614	121.434	8.617	121.468	8.620	121.510	8.860	121.540	8.620	121.562	8.625	121.668	8.629	121.759	8.632	821	8.639	121.882
Gly49	8.269	108.050	8.248	108.106	8.225	108.140	8.209	108.159	8.193	108.160	8.144	108.231	8.088	108.313	8.040	108.385	8.050	108.232
Asp50	8.461	118.922	8.454	118.866	8.450	118.811	8.445	118.763	8.439	118.733	8.425	118.585	8.409	118.446	8.395	118.323	8.388	118.296
Trp51	7.685	120.430	7.685	120.567	7.716	120.656	7.744	120.787	7.767	120.861	7.848	121.182	7.833	121.330	7.944	121.356	7.942	121.357
Trp52	9.097	124.022	9.067	124.115	9.040	124.224	9.018	124.273	8.996	124.384	8.930	124.577	8.851	124.785	8.780	125.009	8.752	125.090
Glu53	8.662	123.975	8.664	123.978	8.667	123.994	8.669	123.994	8.669	124.013	8.676	124.009	8.681	124.031	8.689	124.035	8.692	124.018
Ala54	9.306	131.417	9.314	131.444	9.317	131.457	9.327	131.483	9.331	131.480	9.345	131.510	9.363	131.585	9.379	131.643	9.388	131.657
Arg55	8.800	118.745	8.806	118.742	8.810	118.735	8.814	118.730	8.815	118.730	8.823	118.753	8.854	119.112	8.854	118.690	8.900	119.472
Ser56	8.727	120.020	8.724	120.022	8.725	120.018	8.723	119.990	8.721	119.989	8.716	119.925	8.713	199.891	8.709	119.862	8.705	119.823
Leu57	8.964	130.703	8.973	130.687	8.980	130.699	8.985	130.713	8.990	130.704	9.007	130.720	9.025	130.728	9.042	130.756	9.049	130.748
Thr58	8.388	116.434	8.392	116.426	8.395	116.425	8.396	116.427	8.397	116.439	8.402	116.423	8.841	116.428	8.415	116.443	8.417	116.448
	I	1		1		1		1						1				

Thr59	8.021	108.190	8.024	108.202	8.027	108.211	8.029	108.211	8.029	108.204	8.036	108.205	8.042	108.249	8.040	108.354	8.018	108.413
Gly60	7.873	110.944	7.876	110.938	7.878	110.932	7.880	110.932	7.880	110.938	7.886	110.942	7.891	110.938	7.894	110.929	7.894	110.911
Glu61	8.003	120.840	8.002	120.833	8.003	120.844	8.001	120.842	8.000	120.840	7.998	120.840	7.998	120.840	7.994	120.830	7.993	120.792
Thr62	8.333	113.342	8.333	113.328	8.334	113.310	8.336	113.288	8.333	113.277	8.337	113.234	8.336	113.183	8.337	113.179	8.336	113.199
Gly63	8.703	111.011	8.705	111.014	8.706	110.994	8.706	110.998	8.706	110.995	8.709	111.000	8.712	110.994	8.713	111.022	8.718	111.027
Tyr64	8.625	118.756	8.648	118.763	8.664	118.758	8.681	118.754	8.692	118.755	8.739	118.765	8.793	119.762	8.890	119.369	8.856	118.727
Ile65	9.189	112.509	9.191	112.502	9.194	112.473	9.195	112.436	9.238	112.430	9.196	112.347	9.198	112.265	9.203	112.204	9.203	112.186
Ser67	7.594	121.665	7.549	121.561	7.501	121.409	7.467	121.326	7.433	121.250	7.323	120.916	7.197	120.594	7.097	120.296	7.056	120.185
Asn68	8.039	114.944	8.042	114.960	8.043	114.975	8.044	114.996	8.043	115.010	8.046	115.031	8.050	115.081	8.050	115.084	8.053	115.115
Tyr69	7.742	118.962	7.750	119.083	7.756	119.197	7.762	119.296	7.764	119.370	7.780	119.633	7.797	119.938	7.810	120.175	7.816	120.294
Val70	7.052	108.884	7.055	108.882	7.047	108.884	7.045	108.908	7.043	108.913	7.035	108.936	7.030	108.963	7.025	108.976	7.022	108.995
Ala71	8.759	121.766	8.758	121.752	8.761	121.737	8.761	121.720	8.759	121.702	8.760	121.666	8.760	121.609	8.758	121.591	8.757	121.582

Val73	7.983	121.470	7.980	121.465	7.976	121.441	7.973	121.457	7.970	121.436	7.962	121.413	7.952	121.399	8.018	121.708	8.042	121.844
Asp74	8.179	122.007	8.178	122.024	8.178	122.027	8.178	122.027	8.176	122.036	8.175	122.068	8.174	122.081	8.172	122.101	8.172	122.125
Ser75	7.925	114.927	7.926	114.925	7.926	114.922	7.926	114.924	7.925	114.915	7.927	114.928	7.925	114.931	7.926	114.941	7.926	114.932
Ile76	7.893	122.122	7.895	122.110	7.897	122.115	7.895	122.126	7.894	122.117	7.897	122.126	7.897	122.126	7.900	122.124	7.899	122.124
Gln77	7.812	128.624	7.813	128.624	7.813	128.616	7.813	128.622	7.811	128.617	7.811	128.610	7.811	128.606	7.811	128.605	7.810	128.603

Overlay of 2D-¹H-¹⁵N-HSQC spectra obtained for the titration of SH3 with peptide **1.139** with increasing concentration of **1.139**.



5.3 Data Analogue 1.140/SH3 domain binding

1.140 /SH3	R	atio	R	atio	R	atio	R	atio	R	atio	R	atio	F	Ratio	R	atio	Ra	tio
		0:1	0.	25:1	0	.5:1	0.	75:1		1:1	:	2:1		4:1		8:1	17	7:1
Residue number	δ _н	δ _N	δн	δ _N	δн	δ _N	δн	δ _N	δ _н	δ _N	δ _н	δ _N	δн	δ _N	δ _н	δ _N	δн	δ _N
Gly13	8.348	108.564	8.346	108.542	8.345	108.522	8.346	108.526	8.349	108.555	8.347	108.562	8.346	108.559	8.345	108.561	8.351	108.558
Thr14	8.202	112.770	8.199	112.735	8.198	112.735	8.198	112.714	8.198	112.737	8.197	112.732	8.195	112.724	8.194	112.715	8.191	112.699
Gly15	8.546	111.124	8.547	111.097	8.543	111.079	8.543	111.073	8.542	111.074	8.543	111.082	8.540	111.074	8.540	111.061	8.539	111.072
Val16	8.013	118.788	8.012	118.815	8.013	118.757	8.014	118.762	8.013	118.752	8.016	118.762	8.016	118.748	8.021	118.743	8.024	118.760
Thr17	8.393	118.745	8.389	118.785	8.389	118.744	8.388	118.736	8.388	118.760	8.388	118.743	8.384	118.779	8.380	118.808	8.377	118.853
Leu18	8.254	125.476	8.262	125.490	8.265	125.473	8.266	125.478	8.267	125.470	8.270	125.481	8.272	125.463	8.282	125.471	8.290	125.436
Phe19	8.987	122.362	8.977	122.316	8.975	122.332	8.975	122.319	8.970	122.304	8.966	122.280	8.954	122.250	8.942	122.207	8.921	122.152
Val20	9.818	119.329	9.817	119.350	9.818	119.334	9.818	119.334	9.816	119.349	9.821	119.332	9.820	119.331	9.824	119.335	9.823	119.903
Ala21	9.167	126.833	9.165	126.861	9.166	126.839	9.165	126.850	9.165	126.848	9.164	126.850	9.161	126.853	9.159	126.830	9.155	126.828

Leu22	9.517	125.785	9.514	125.758	9.514	125.764	9.513	125.768	9.515	125.778	9.516	125.783	9.520	125.829	9.526	125.888	9.534	125.956
Tyr23	7.243	112.280	7.243	112.288	7.243	112.265	7.243	112.269	7.243	112.269	7.243	112.257	7.246	112.246	7.250	112.220	7.252	112.191
Asp24	8.360	117.697	8.361	117.757	8.359	117.711	8.359	117.708	8.360	117.716	8.362	117.752	8.362	117.758	8.368	117.774	8.374	117.828
Tyr25	8.372	120.383	8.368	120.379	8.369	120.349	8.369	120.345	8.367	120.340	8.366	120.321	8.360	120.282	8.358	120.227	8.435	120.358
Glu26	7.258	128.129	7.255	128.127	7.252	128.127	7.251	128.092	7.248	128.109	7.244	128.088	7.236	128.040	7.228	128.001	7.212	127.927
Ala27	8.240	126.079	8.243	126.026	8.244	126.032	8.246	126.012	8.245	126.019	8.252	125.990	8.259	125.957	8.269	125.893	8.284	125.820
Arg28			9.813	121.294	9.796	121.242	9.782	121.228	9.764	121.183	9.715	121.065					9.327	120.192
Thr29			8.772	113.212	8.755	113.148	8.724	113.082	8.701	113.018					8.631	112.790		
Glu30	8.826	118.253	8.838	118.263	8.840	118.277	8.845	118.308	8.848	118.322	8.867	118.410	8.892	118.582	8.842	118.726	8.891	118.725
Asp31	8.128	116.248	8.126	116.326	8.120	116.285	8.115	116.283	8.112	116.264	8.091	116.255	8.055	116.210	8.008	116.118	7.945	116.008
Asp32			8.251	119.619	8.241	119.647	8.220	119.659	8.431	119.391	8.432	119.408	8.433	119.393	8.430	119.429	8.433	119.463
Leu33			8.227	119.962	8.234	119.994	8.241	120.004	8.246	120.014	8.268	120.068	8.307	120.133	8.166	118.896	8.350	120.158
1		l		L		l .		ı		I		1		l .		1		ı

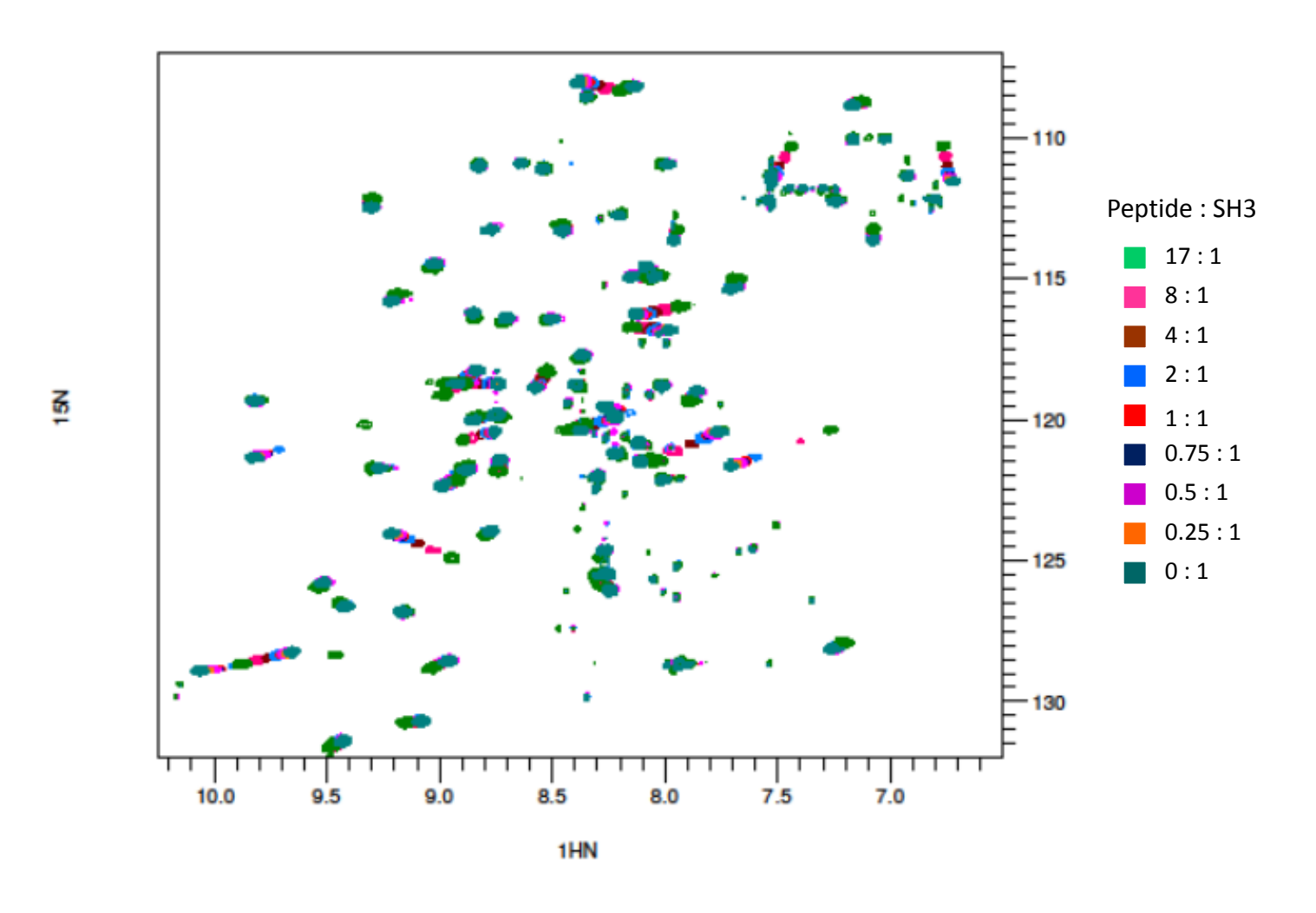
Ser34	8.087	114.574	8.087	114.613	8.084	114.597	8.079	114.617	8.082	114.606	8.080	114.640	8.079	114.672	8.078	114.753	8.075	114.850
Phe35	8.853	116.233	8.858	116.237	8.856	116.235	8.856	116.263	8.853	116.241	8.854	116.266	8.852	116.296	8.850	116.345	8.849	116.415
His36	8.707	116.382	8.707	116.401	8.706	116.422	8.707	116.424	8.707	116.431	8.710	116.448	8.712	116.471	8.720	116.522	8.724	116.554
Lys37	9.271	121.731	9.270	121.735	9.276	121.762	9.272	121.721	9.271	121.716	9.277	121.719	9.282	121.721	9.291	121.734	9.301	121.738
Gly38	9.020	114.484	9.024	114.479	9.022	114.472	9.023	114.468	9.023	114.473	9.024	114.489	9.024	114.511	9.026	114.563	9.029	114.626
Glu39	8.268	124.622	8.271	124.685	8.271	124.666	8.270	124.652	8.271	124.678	8.270	124.696	8.272	124.733	8.275	124.802	8.277	124.887
Lys 40	8.217	121.204	8.221	121.228	8.221	121.221	8.225	121.252	8.221	121.247	8.221	121.252	8.215	121.244	8.211	121.252	8.203	121.254
Phe41	9.214	115.804	9.216	115.805	9.213	115.776	9.213	115.785	9.210	115.756	9.210	115.732	9.204	115.698	9.198	115.637	9.190	115.548
Gln42	8.752	119.844	8.737	119.817	8.747	119.820	8.745	119.833	8.745	119.830	8.745	119.849	8.742	119.869	8.736	119.886	8.737	119.930
Ile43	9.418	126.651	9.422	126.607	9.422	126.616	9.423	126.612	9.424	126.602	9.429	126.600	9.429	126.576	9.437	126.535	9.442	126.503
Leu44	8.954	128.552	8.958	128.511	8.960	128.528	8.963	128.545	8.965	128.549	8.972	128.590	8.984	128.629	9.002	128.707	9.026	128.797
Asn45	7.711	115.378	7.705	115.358	7.707	115.339	7.705	115.337	7.705	115.321	7.704	115.288	7.701	115.228	7.698	115.145	7.695	115.055
Ser46	8.761	120.424	8.771	120.447	8.772	120.448	8.777	120.463	8.793	120.487	8.815	120.533	8.854	120.656	8.897	120.739	8.757	120.425
		l .		l														

Ser47	7.986	116.837	7.992	116.818	7.999	116.818	8.003	116.800	8.007	116.788	8.024	116.784	8.051	116.733	8.092	116.762	8.143	116.715
Glu48	8.728	121.432	8.733	121.452	8.734	121.455	8.735	121.472	8.736	121.489	8.735	121.513	8.736	121.592	8.739	121.712	8.740	121.839
Gly49	8.388	108.062	8.372	108.057	8.369	108.061	8.363	108.086	8.358	108.084	8.336	108.114	8.304	108.162	8.257	108.227	8.200	108.348
Asp50	8.577	118.866	8.575	118.859	8.572	118.839	8.570	118.829	8.568	118.807	8.563	118.743	8.553	118.636	8.541	118.491	8.524	118.296
Trp51	7.761	120.434	7.780	120.483	7.789	120.497	7.795	120.538	7.802	120.560	7.834	120.682	7.882	120.874	7.960	121.125	7.754	120.381
Trp52	9.216	124.049	9.197	124.089	9.188	124.102	9.176	124.123	9.169	124.148	9.147	124.255	9.096	124.408	9.031	124.647	8.946	124.919
Glu53	8.777	123.960	8.784	123.970	8.782	123.973	8.783	123.978	8.783	123.974	8.785	124.005	8.788	124.024	8.792	124.059	8.797	124.107
Ala54	9.427	131.417	9.430	131.390	9.431	131.403	9.433	131.398	9.434	131.103	9.440	131.439	9.448	131.465	9.462	131.508	9.479	131.588
Arg55	8.980	118.730	8.925	118.725	8.923	118.718	8.925	118.728	8.927	118.727	8.931	118.719	8.936	118.708	8.942	118.752	8.955	118.686
Ser56	8.848	120.027	8.842	120.025	8.842	120.11	8.842	120.014	8.839	120.006	8.840	119.987	8.839	119.969	8.834	119.926	8.832	119.876
Leu57	9.078	130.700	9.086	130.686	9.088	130.688	9.090	130.692	9.091	130.694	9.099	130.705	9.112	130.707	9.131	130.721	9.152	130.736
Thr58	8.504	116.442	8.508	116.431	8.506	116.416	8.506	116.419	8.507	116.415	8.511	116.421	8.514	116.421	8.521	116.431	8.526	116.436

Thr59	8.140	108.199	8.139	108.176	8.141	108.176	8.144	108.186	8.142	108.176	8.147	108.187	8.147	108.194	8.155	108.204	8.165	108.244
Gly60	7.994	110.970	7.994	110.962	7.993	110.920	7.996	110.942	7.996	110.941	7.997	110.920	8.001	110.933	8.004	110.942	8.011	110.928
Glu61	8.117	120.830	8.122	120.856	8.122	120.846	8.121	120.848	8.122	120.847	8.121	120.859	8.121	120.851	8.120	861	8.118	120.845
Thr62	8.449	113.308	8.449	113.282	8.445	113.283	8.444	113.279	8.442	113.271	8.444	113.247	8.447	113.215	8.449	113.161	8.454	113.099
Gly63	8.825	111.042	8.826	110.977	8.824	110.974	8.824	110.975	8.825	110.987	8.825	110.972	8.826	110.971	8.827	110.965	8.828	110.959
Tyr64	8.754	118.725	8.755	118.718	8.759	118.727	8.762	118.734	8.776	118.732	8.801	118.722			8.981	119.103	8.741	118.743
Ile65	9.303	112.489	9.309	112.467	9.307	112.457	9.307	112.456	9.306	112.440	9.307	112.410	9.302	112.359	9.300	112.285	9.297	112.185
Ser67	7.708	121.659	7.683	121.571	7.670	121.554	7.656	121.509	7.642	121.484	7.596	121.358	7.520	121.103	7.401	120.760	7.693	121.533
Asn68	8.154	114.963	8.156	114.941	8.153	114.927	8.151	114.924	8.148	114.928	8.139	114.922	8.124	114.919	8.105	114.889	8.062	114.871
Tyr69	7.860	118.991	7.860	119.023	7.862	119.013	7.862	119.018	7.863	119.032	7.866	119.080	7.873	119.146	7.883	119.243	7.893	119.345
Val70	7.173	108.866	7.171	108.876	7.168	108.850	7.166	108.838	7.166	108.860	7.162	108.832	7.154	108.810	7.147	108.789	7.138	108.745
Ala71	8.879	121.791	8.875	121.780	8.876	121.735	8.875	121.723	8.874	121.730	8.876	121.718	8.876	121.708	8.876	121.666	8.877	121.661
Val73	8.105	121.520	8.102	121.467	8.099	121.435	8.099	121.438	8.098	121.416	8.095	121.428	8.088	121.422	8.081	121.399	8.068	121.401

Asp74	8.298	122.024	8.296	122.018	8.296	122.019	8.296	122.021	8.296	122.012	8.297	122.024	8.296	122.031	8.296	122.051	8.296	122.083
Ser75	8.046	114.963	8.044	114.911	8.043	114.906	8.042	114.908	8.042	114.908	8.043	114.912	8.042	114.912	8.042	114.902	8.044	114.928
lle76	8.013	122.147	8.011	122.122	8.011	122.101	8.011	122.098	8.011	122.098	8.012	122.101	8.013	122.105	8.015	122.107	8.016	122.123
Gln77	7.935	128.663	7.931	128.632	7.927	128.644	7.928	128.620	7.928	128.611	7.928	128.607	7.927	128.617	7.928	128.617	7.29	128.616

Overlay of 2D-¹H-¹⁵N-HSQC spectra obtained for the titration of SH3 with peptide **1.140** with increasing concentration of **1.140**.



5.4 Data Analogue 1.141

1.141 /SH3	F	Ratio	R	latio	R	atio	Ra	atio												
		0:1	0.	.25:1	0	.5:1	0.	75:1	:	1:1	2	2:1		4:1	;	3:1	1	2:1	2	5:1
Residue number	δ _н	δ _N																		
Gly13	8.349	108.578	8.347	108.758	8.353	108.740			8.352	108.730	8.346	108.718	8.351	108.700	8.350	108.691	8.348	108.662	8.349	108.609
Thr14	8.202	112.753	8.305	113.110	8.310	113.109	8.305	113.106	8.308	113.117	8.303	113.086	8.306	113.088	8.305	113.050	8.300	113.006	8.294	112.913
Gly15	8.545	111.125	8.531	111.374	8.534	111.342	8.528	111.330	8.532	111.348	8.527	111.318	8.532	111.271	8.526	111.271	8.527	111.248	8.529	111.133
Val16	8.013	118.803	8.075	119.372	8.078	119.354	8.072	119.351	8.015	119.000	8.073	119.332	8.074	119.347	8.070	119.299	8.070	119.251	8.066	119.144
Thr17	8.394	118.741	8.444	119.477	8.448	119.467	8.444	119.454	8.446	119.472	8.442	119.465	8.444	119.467	8.440	119.457	8.441	119.452	8.435	119.247
Leu18	8.253	125.475	8.265	125.617	8.271	125.643	8.268	125.640	8.274	125.624	8.269	125.631	8.275	125.625	8.279	125.607	8.286	125.621	8.306	125.601
Phe19	8.987	122.364	8.967	122.144	8.970	122.156	8.964	122.153	8.966	122.183	8.963	122.151	8.968	122.149	8.963	122.136	8.964	122.127	8.959	122.078

Val20	9.819	119.341	9.808	119.411	9.812	119.391	9.806	119.386	9.813	119.383	9.807	119.395	9.808	119.402	9.813	119.386	9.814	119.397	9.816	119.402
Ala21	9.166	126.834	9.148	126.710	9.152	126.717	9.150	126.706	9.152	126.695	9.149	126.719	9.154	126.737	9.153	126.739	9.156	126.759	9.164	126.830
Leu22	9.517	125.783	9.544	126.031	9.547	126.023	9.545	126.026	9.546	126.024	9.540	126.002	9.542	126.002	9.534	125.960	9.531	125.931	9.518	125.776
Tyr23	7.243	112.279	7.186	112.199	7.191	112.191	7.186	1122.181	7.193	112.203	7.190	112.211	7.205	112.233	7.213	112.247	7.224	112.265	7.242	112.273
Asp24	8.362	117.687	8.349	117.544	8.352	117.568	8.350	117.560	8.354	117.591	8.349	117.574	8.354	117.602	8.353	117.622	8.356	117.650	8.362	117.716
Tyr25	8.371	120.380	8.393	120.568	8.397	120.537	8.389	120.545	8.394	120.540	8.387	120.523	8.388	120.521	8.381	120.480	8.377	120.441	8.370	120.360
Glu26	7.258	128.130	7.292	128.191	7.294	128.192			7.290	128.191	7.282	128.180	7.282	128.175	7.269	128.164	7.267	128.162	7.257	128.132
Ala27	8.241	126.074	8.229	126.028	8.230	126.016	8.227	126.027	8.230	126.013	8.226	126.013	8.231	126.011	8.231	126.015	8.235	126.033	8.246	126.034
Arg28	9.819	121.378	9.776	121.624	9.781	121.624			9.781	121.616	9.783	121.611	9.789	121.583	9.794	121.515	9.811	121.501	9.821	121.349
Thr29	8.773	113.282	8.568	112.644	8.454	113.278	8.576	112.658	8.582	112.691	8.590	112.699	8.613	112.788	8.647	112.901	8.686	113.021	8.772	113.245
Glu30	8.826	118.253	8.828	118.490	8.829	118.493	8.826	118.477	8.830	118.479	8.827	118.478	8.827	118.460	8.823	118.420	8.824	118.376	8.833	118.289
Asp31	8.128	116.264	8.103	116.482	8.104	116.466			8.105	116.472	8.102	116.468	8.105	116.445	8.106	116.424	8.115	116.422	8.138	116.383
Asp32	8.262	119.536	8.151	119.850	8.157	119.837	8.266	120.784	8.161	119.832	8.159	119.809	8.268	120.766	8.194	119.737	8.217	119.714	8.263	119.624

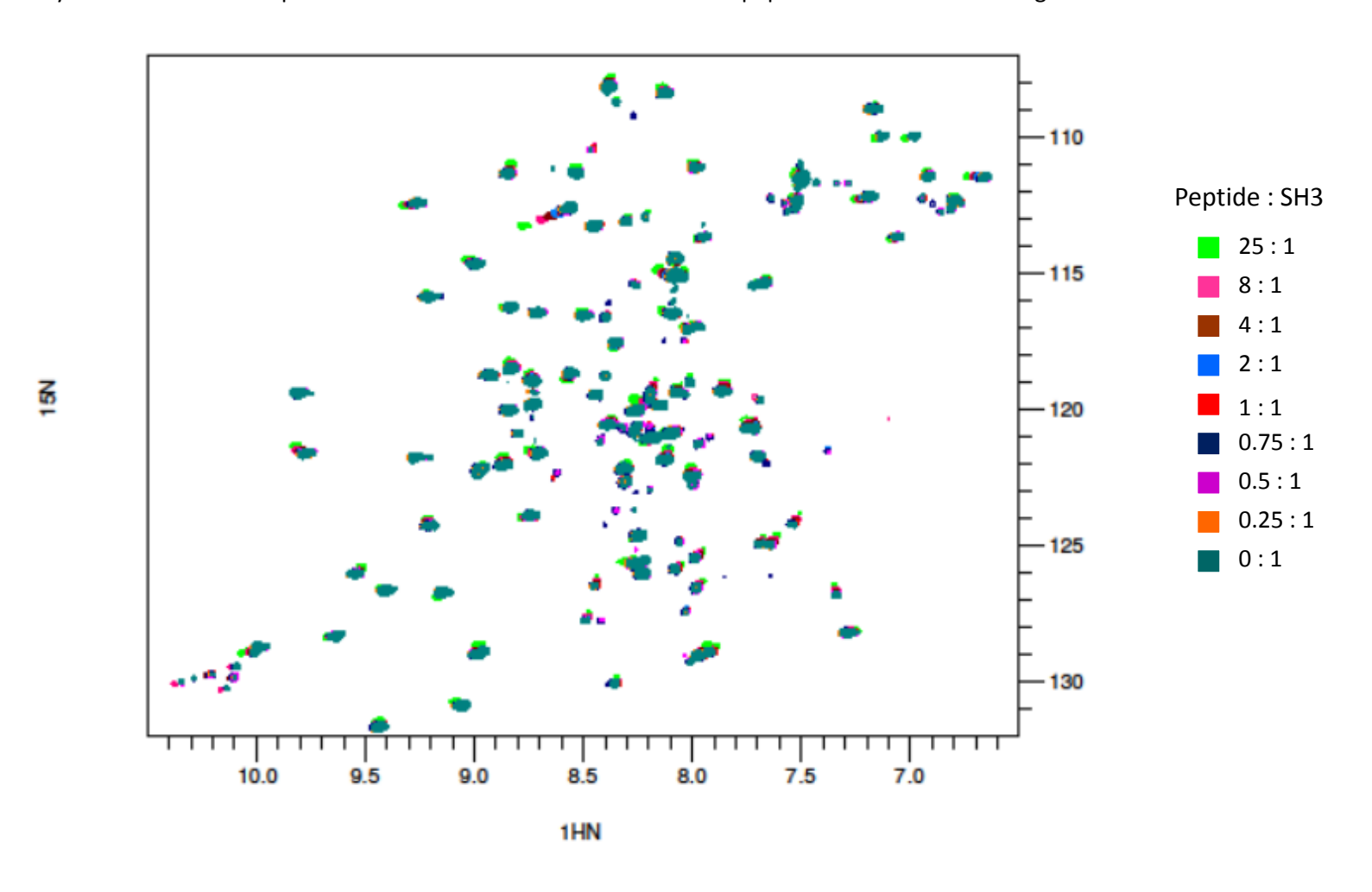
Leu33	8.214	119.936	8.263	120.051	8.267	120.061	8.264	120.061	8.267	120.065	8.260	120.071	8.262	120.083	8.255	120.095	8.255	120.103	8.242	120.021
Ser34	8.087	114.563	8.081	114.471	8.084	114.472	8.078	114.487	8.085	114.478	8.079	114.470	8.083	114.472	8.082	114.489	8.082	114.508	8.083	114.573
Phe35	8.852	116.220	8.836	116.256	8.839	116.262	8.836	116.261	8.840	116.267	8.835	116.266	8.841	116.262	8.840	116.264	8.847	116.266	8.858	116.245
His36	8.707	116.394	8.712	116.460	8.716	116.466	8.710	116.446	8.718	116.447	8.708	116.441	8.711	116.449	8.705	116.441	8.702	116.450	8.705	116.418
Lys37	9.273	121.746	8.276	121.762	9.279	121.767	9.276	121.763	9.278	121.766	9.275	121.762	9.276	121.769	9.273	121.748	9.272	121.747	9.269	121.720
Gly38	9.019	114.473	8.995	114.677	8.997	114.682	8.994	114.650	8.999	114.659	8.996	114.626	9.004	114.645	9.006	114.619	9.012	114.586	9.025	114.476
Glu39	8.267	124.620	8.246	124.644	8.249	124.647			8.248	124.653	8.246	124.650	8.252	124.664	8.254	124.647	8.259	124.674	8.272	124.653
Lys 40	8.217	121.202	8.176	121.046	8.179	121.048	8.172	121.046	8.179	121.048	8.175	121.057	8.182	121.059	8.185	121.100	8.193	121.116	8.218	121.211
Phe41	9.217	115.820	9.217	115.858	9.220	115.878	9.216	115.866	9.222	115.879	9.215	115.864	9.218	115.854	9.217	115.825	9.217	115.815	9.217	115.775
Gln42	8.753	119.840	8.737	119.817	8.736	119.818	8.735	119.827	8.736	119.814	8.730	119.808	8.733	119.813	8.731	119.798	8.729	119.802	8.732	119.786
Ile43	9.417	126.652	9.410	126.642	9.414	126.648	9.410	126.630	9.413	126.637	9.409	126.638	9.415	126.639	9.414	126.616	9.417	126.604	9.428	126.593
Leu44	8.954	128.554	8.984	128.968	8.987	128.970	8.985	128.958	8.990	128.962	8.984	128.925	8.988	128.928	8.987	128.876	8.987	128.817	8.987	128.654

				1		1						1			1					
Asn45	7.711	115.381	7.675	115.382	7.681	115.365	7.676	115.368	7.679	115.340	7.672	115.341	7.674	115.347	7.671	115.314	7.669	115.290	7.663	115.228
Ser46	8.757	120.428	8.797	120.871	8.805	120.891	8.797	120.874	8.805	120.887	8.799	120.876	8.807	120.897	8.807	120.872	8.807	120.866	8.816	120.841
Ser47	7.985	116.841	8.023	117.047	8.026	117.037	8.024	117.039	8.027	117.039	8.024	117.034	8.027	117.023	8.029	117.005	8.030	117.001	8.038	116.956
Glu48	8.727	121.433	8.705	121.583	8.710	121.613	8.707	121.607	8.711	121.604	8.707	121.609	8.715	121.606	8.717	121.563	8.729	121.566	8.750	121.495
Gly49	8.389	108.061	8.389	108.197	8.390	108.162	8.386	108.147	8.389	108.127	8.385	108.126	8.387	108.064	8.382	108.040	8.382	107.999	8.378	107.887
Asp50	8.577	118.864	8.562	118.671	8.566	118.679	8.562	118.681	8.565	118.679	8.561	118.690	8.566	118.733	8.566	118.757	8.570	118.788	8.577	118.891
Trp51	7.761	120.449	7.728	120.721	7.734	120.705			7.733	120.690	7.729	120.649	7.727	120.618	7.728	120.554	7.729	120.484	7.726	120.380
Trp52			9.210	124.274	9.214	124.277			9.214	124.254	9.207	124.251	9.214	124.226	9.215	124.178	9.216	124.131	9.216	124.022
Glu53	8.777	123.964	8.744	123.918	8.747	123.907			8.747	123.915	8.744	123.923	8.751	123.923	8.753	123.936	8.759	123.955	8.778	123.951
Ala54	9.427	131.418	9.437	131.667	9.441	131.673			9.440	131.635	9.436	131.665	9.440	131.618	9.438	131.578	9.440	131.538	9.444	131.474
Arg55	8.920	118.729	8.936	118.752	8.938	118.742	8.932	118.736	8.937	118.736	8.931	118.730	8.937	118.740	8.934	118.734	8.939	118.731	8.943	118.730
Ser56	8.848	120.027	8.842	120.025	8.844	120.042	8.841	120.026	8.843	120.042	8.839	120.030	8.841	120.020	8.839	120.020	8.835	120.020	8.835	120.002
Leu57	9.078	130.703	9.057	130.869	9.061	130.869			9.063	130.860	9.060	130.859	9.064	130.845	9.067	130.816	9.072	130.814	9.087	130.764

Thr58	8.505	116.424	8.500	116.549	8.503	116.559	8.500	116.570	8.504	116.570	8.497	116.550	8.501	116.542	8.500	116.522	8.501	116.493	8.507	116.432
Thr59	8.141	108.202	8.130	108.443	8.133	108.404			8.132	108.399	8.127	108.388	8.135	108.379	8.130	108.326	8.134	108.305	8.139	108.182
Gly60	7.994	110.971	7.985	111.163	7.992	111.133			7.989	111.130	7.988	111.127	7.990	111.113	7.989	111.080	7.992	111.072	7.996	110.965
Glu61	8.115	120.841	8.094	120.883	8.096	120.876	8.094	120.888	8.099	120.890	8.095	120.893	8.100	120.897	8.102	120.894	8.107	120.881	8.121	120.866
Thr62	8.450	113.318	8.449	113.272	8.575	112.642			8.451	113.259	8.446	113.262	8.450	113.263	8.444	113.267	8.441	113.283	8.441	113.280
Gly63	8.825	111.034	8.847	111.385	8.849	111.348	8.845	111.348	8.849	111.339	8.843	111.328	8.846	111.306	8.841	111.252	8.840	111.179	8.832	111.017
Tyr64	8.740	118.746	8.738	118.982	8.743	118.968	8.736	118.960	8.741	118.970	8.737	118.942	8.741	118.921	8.737	118.880	8.738	118.841	8.749	118.740
Ile65	9.304	112.498	9.262	112.444	9.267	112.450	9.265	112.431	9.268	112.436	9.267	112.439	9.278	112.444	9.287	112.459	9.296	112.468	9.320	112.506
Ser67	7.710	121.651	7.699	121.697	7.699	121.713	7.699	121.678	7.699	121.699	7.697	121.675	7.698	121.673	7.697	121.659	7.697	121.663	7.700	121.662
Asn68	8.155	114.958	8.078	115.099	8.086	115.062	8.088	115.071	8.088	115.007	8.094	115.044	8.110	115.014	8.120	114.982	8.132	114.959	8.152	114.842
Tyr69	7.861	118.982	7.866	119.343	7.871	119.351	7.865	119.331	7.869	119.324	7.862	119.299	7.864	119.250	7.858	119.171	7.856	119.121	7.854	119.005
Val70	7.173	108.865	7.177	108.987	7.186	108.969	7.179	108.969	7.186	108.976	7.177	108.966	7.180	108.957	7.176	108.935	7.175	108.917	7.172	108.879

Ala71	8.879	121.790	8.864	122.033	8.867	122.034	8.861	122.026	8.867	121.997	8.863	122.004	8.867	121.977	8.864	121.932	8.865	121.873	8.867	121.732
Val73	8.107	121.519	8.130	121.859	8.131	121.845	8.128	121.835	8.130	121.846	8.125	121.821	8.127	121.800	8.121	121.728	8.123	121.701	8.116	121.501
Asp74	8.298	122.024	8.312	122.213	8.316	122.221	8.313	122.209	8.316	122.216	8.311	122.211	8.313	122.208	8.308	122.167	8.308	122.130	8.303	122.009
Ser75	8.047	114.946	8.067	115.198	8.072	115.159	8.066	115.155	8.070	115.144	8.064	115.152	8.065	115.139	8.058	115.87	8.056	115.057	8.047	114.944
Ile76	8.012	122.156	8.008	122.443	8.014	122.434			8.014	122.427	8.007	122.410	8.011	122.391	8.007	122.340	8.006	122.288	8.007	122.130
Gln77	7.936	128.674	7.975	129.034	7.977	129.032	7.972	129.023	7.977	129.028	7.968	129.015	7.969	128.983	7.959	128.923	7.954	128.870	7.932	128.673

Overlay of 2D-¹H-¹⁵N-HSQC spectra obtained for the titration of SH3 with peptide **1.141** with increasing concentration of **1.141**.



5.5 Data Analogue 1.142/SH3 domain binding

1.142 /SH3		atio 0:1		atio 25:1		atio).5:1		atio .75:1		atio 1:1		atio 2:1		atio 4:1		atio 8:1		atio 1.5:1		Ratio 20:1
Residue number	δн	δ _N	δ _н	δ _N	δ _Η	δ _N	δн	δ _N	δ _н	δ _N										
Gly13	8.346	108.574	8.347	108.570	8.346	108.558	8.345	108.562	8.345	108.571	8.345	108.571	8.345	108.569	8.343	108.575	8.342	108.558	8.346	108.569
Thr14	8.204	112.784	8.201	112.772	8.202	112.769	8.202	112.782	8.200	112.771	8.202	112.753	8.203	112.770	8.202	112.790	8.203	112.803	8.207	112.824
Gly15	8.545	111.122	8.543	11.102	8.543	111.091	8.542	111.112	8.541	111.096	8.543	111.100	8.542	111.079	8.542	111.081	8.540	111.079	8.540	111.062
Val16	8.013	118.796	8.011	118.806	8.011	118.810	8.011	118.807	8.011	118.794	8.008	118.817	8.009	118.839	8.007	118.851	8.007	118.874	8.007	118.891
Thr17	8.393	118.782	8.395	118.740	8.391	118.759	8.392	118.754	8.391	118.780	8.391	118.774	8.394	118.810	8.395	118.854	8.395	118.877	8.400	118.923
Leu18	8.254	125.481	8.257	125.786	8.257	125.477	8.258	125.495	8.256	125.485	8.259	125.488	8.262	125.521	8.264	125.500	8.266	125.514	8.274	125.497
Phe19	8.987	122.364	8.980	122.338	8.984	122.332	8.980	122.330	8.976	122.320	8.975	122.303	8.973	122.277	8.969	122.244	8.963	122.220	8.961	122.187
Val20	9.817	119.348	9.815	119.338	9.815	119.343	9.817	119.349	8.813	119.343	9.817	19.341	9.818	119.347	9.817	119.352	9.814	119.350	9.818	119.359

Ala21	9.166	126.829	9.164	126.835	9.165	126.832	9.165	126.846	9.163	126.829	9.164	126.834	9.164	126.829	9.163	126.827	9.162	126.828	9.164	126.827
Leu22	9.517	125.787	9.515	125.778	9.514	125.776	9.515	125.772	9.514	125.782	9.515	125.774	9.515	125.776	9.513	125.750	9.512	125.752	9.510	125.737
Tyr23	7.242	112.280	7.241	122.283	7.241	112.265	7.241	112.279	7.240	112.283	7.241	112.261	7.241	112.288	7.240	112.275	7.240	112.279	7.242	112.267
Asp24	8.361	117.688	8.360	117.700	8.361	117.696	8.359	117.702	8.358	117.701	8.360	117.699	8.362	117.697	8.362	117.698	8.363	117.703	8.370	117.701
Tyr25	8.371	120.384	8.367	120.375	8.370	120.387	8.369	120.380	8.367	120.378	8.369	120.358	8.368	120.352	8.365	120.335	8.364	120.326	8.357	120.278
Glu26	7.259	128.127	7.256	128.141	7.258	128.142	7.258	128.141	7.261	128.147	7.259	128.144	7.264	128.148	7.267	128.181	7.269	128.166	7.279	128.164
Ala27	8.241	126.069	8.239	126.065	8.241	126.085	8.239	126.062	8.239	126.055	8.241	126.050	8.243	126.037	8.245	126.059	8.247	126.053	8.257	126.090
Arg28			9.827	121.366	9.829	121.364	9.825	121.375	9.826	121.379	9.825	121.375	9.821	121.373	9.810	121.363	9.802	332	9.754	121.197
Thr29	8.779	113.266	8.778	113.255			8.775	113.228	8.771	113.199	8.765	113.138	8.749	113.076	8.736	113.022	8.685	112.923	8.440	113.318
Glu30	8.827	118.257	8.823	118.224	8.823	118.245	8.822	118.240	8.821	118.235	8.820	118.240	8.819	118.241	8.815	118.271	8.815	118.270	8.814	118.396
Asp31	8.127	116.249	8.136	116.350	8.141	116.371	8.140	116.403	8.143	116.445	8.146	116.507	8.160	116.637	8.172	116.778	8.184	116.835	8.196	116.875
Asp32			8.266	119.570	8.266	119.590	8.266	119.606	8.265	119.603	8.266	119.643	8.263	119.680	8.258	119.763	8.253	119.768	8.232	119.728

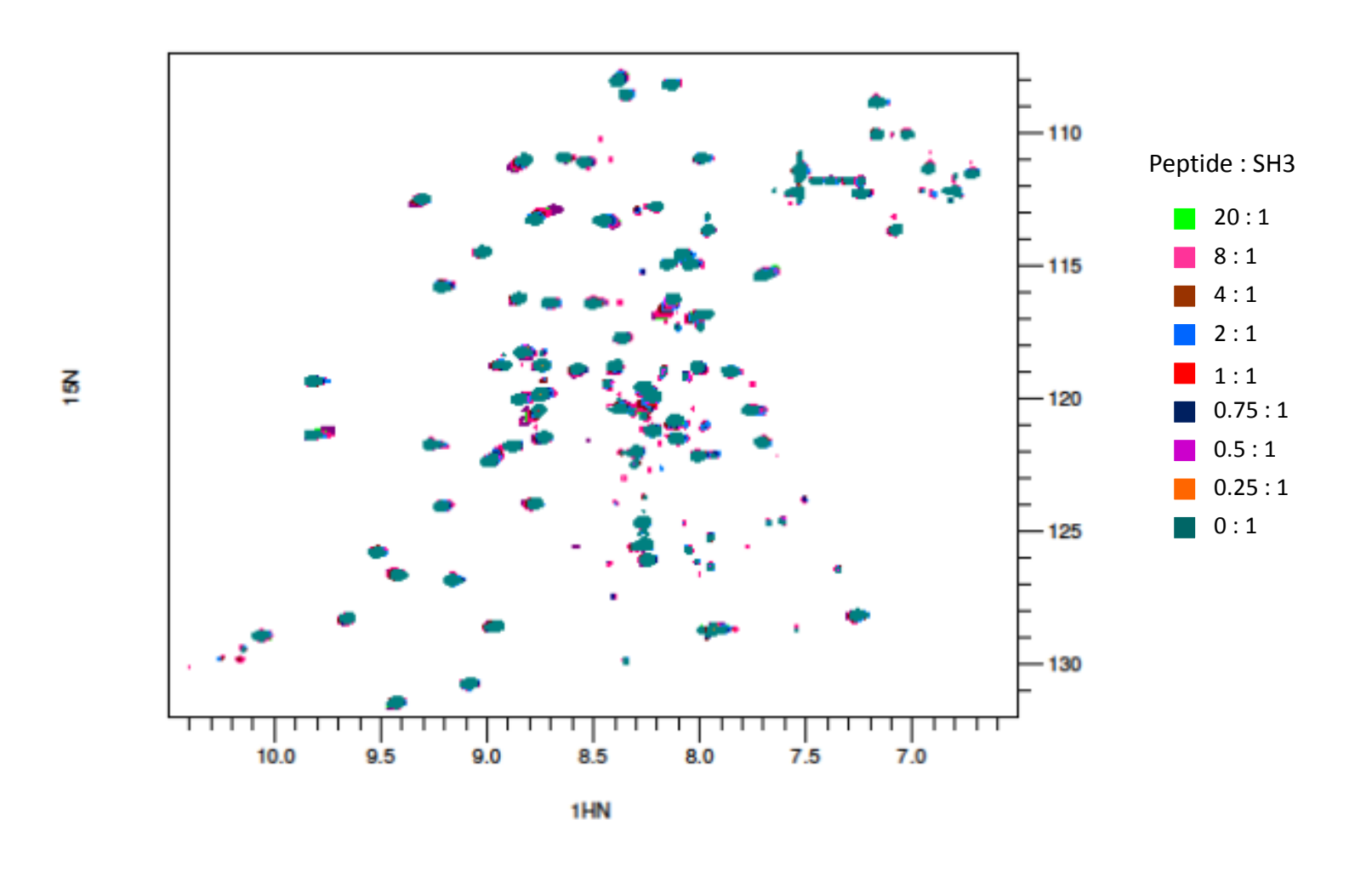
Leu33	8.220	119.976	8.22	120.008	8.225	120.019	8.228	120.032	8.230	120.071	8.242	120.123	8.258	120.206	8.267	120.271	8.278	120.347	8.241	119.932
Ser34	8.088	114.553	8.083	114.576	8.082	114.578	8.081	114.593	8.080	114.583	8.078	114.593	8.082	114.630	8.074	114.621	8.073	114.636	8.075	114.686
Phe35	8.852	116.220	8.852	116.219	8.854	116.239	8.856	116.238	8.855	116.240	8.857	116.236	8.859	116.263	8.862	116.266	8.865	116.287	8.869	116.323
His36	8.707	116.399	8.702	116.402	8.703	116.415	8.703	116.404	8.699	116.418	8.701	116.400	8.702	116.406	8.699	116.403	8.696	116.423	8.697	116.364
Lys37	9.274	121.724	9.269	121.727	9.268	121.728	9.268	121.716	9.268	121.722	9.268	121.725	9.268	121.735	9.266	121.732	9.263	121.752	9.266	121.758
Gly38	9.020	114.489	9.019	114.474	9.021	114.483	9.019	114.484	9.019	114.482	9.021	114.496	9.021	114.484	8.021	114.486	9.024	114.492	9.025	114.513
Glu39	8.267	124.620	8.267	124.645	8.268	124.646	8.267	124.653	8.266	124.650	8.268	124.664	8.269	124.673	8.270	124.697	8.269	124.689	8.269	124.713
Lys 40	8.217	121.205	8.218	121.214	8.218	121.210	8.217	121.212	8.216	121.212	8.216	121.219	8.217	121.229	8.218	121.234	8.219	121.226	8.221	121.241
Phe41	9.215	115.810	9.213	115.805	9.217	115.804	9.214	115.804	9.213	115.796	9.213	115.782	9.215	115.776	9.212	115.753	9.211	115.743	9.212	115.700
Gln42	8.752	119.850	8.743	119.833	8.747	119.823	8.742	119.813	8.739	119.822	8.740	119.806	8.737	119.781	8.728	119.765	8.723	119.756	8.723	119.769
Ile43	9.418	126.649	9.420	126.634	9.420	126.627	9.422	126.631	9.421	126.630	9.423	126.623	9.427	126.620	9.431	126.607	9.434	126.594	9.440	126.583
Leu44	8.953	128.549	8.954	128.541	8.957	128.549	8.956	128.542	8.956	128.546	8.958	128.518	8.963	128.541	8.964	128.532	8.966	128.529	8.971	128.508
Asn45	7.711	115.377	7.706	115.362	7.706	115.369	7.706	115.35	7.704	115.354	7.703	115.352	7.701	115.347	7.695	115.319	7.691	115.319	7.678	115.226

Ser46	8.764	120.463	8.764	120.470	8.765	120.466	8.768	120.482	8.772	120.530	8.779	120.583	8.787	120.635	8.794	120.686	8.826	120.837	8.756	120.424
Ser47	7.986	116.833	7.989	116.835	7.991	116.838	7.990	116.849	7.991	116.845	7.996	116.860	8.002	116.879	8.011	116.885	8.018	116.906	8.045	116.962
Glu48	8.729	121.432	8.731	121.430	8.733	121.455	8.733	121.445	8.734	121.458	8.737	121.458	8.739	121.458	8.743	121.457	8.746	121.477	8.755	121.492
Gly49	8.387	108.073	8.382	108.017	8.386	108.040	8.384	108.024	8.382	108.14	8.383	108.011	8.380	107.981	8.378	107.961	8.376	107.929	8.371	107.881
Asp50	8.579	118.887	8.577	118.888	8.578	118.895	8.577	118.903	8.577	118.899	8.580	118.901	8.581	118.917	8.584	118.947	8.584	118.962	8.586	119.020
Trp51	7.762	120.433	7.756	120.427	7.758	120.425	7.756	120.418	7.750	120.429	7.751	120.422	7.752	120.428	7.743	120.430	7.742	120.426	7.739	120.431
Trp52	9.217	124.047	9.212	124.036	9.214	124.034	9.211	124.031	9.206	120.031	9.209	124.035	9.206	124.030	9.207	124.013	9.207	124.029	9.207	124.004
Glu53	8.778	123.951	8.778	123.958	8.780	123.975	8.780	12.960	8.779	123.957	8.782	123.956	8.787	123.954	8.791	123.951	8.791	123.970	8.803	123.943
Ala54	9.428	131.417	9.427	131.428	9.427	131.419	9.425	131.432	9.425	131.415	9.425	131.425	9.429	131.426	9.431	131.428	9.430	131.436	9.440	131.523
Arg55	8.921	118.734	8.923	118.732	8.924	118.730	8.926	118.735	8.924	118.735	8.926	118.750	8.930	118.741	8.933	118.740	8.936	118.753	8.945	118.766
Ser56	8.847	120.035	8.841	120.024	8.842	120.20	8.841	120.12	8.836	120.019	8.837	120.006	8.833	120.005	8.827	120.009	8.823	119.967	8.814	119.995
Leu57	9.079	130.712	9.079	130.706	9.080	130.706	9.079	130.712	9.078	130.712	9.081	130.706	9.082	130.717	9.082	130.730	9.084	130.730	9.089	130.740

Thr58	8.504	116.429	8.502	116.415	8.503	116.427	8.502	116.417	8.501	116.411	8.501	116.417	8.505	116.398	8.502	116.403	8.500	116.383	8.501	116.358
Thr59	8.139	108.182	8.139	108.193	8.138	108.192	8.137	108.184	8.135	108.181	8.136	108.187	8.137	108.183	8.136	108.151	8.135	108.148	8.135	108.135
Gly60	7.994	110.978	7.994	110.954	7.993	110.970	7.993	110.965	7.994	110.975	7.993	110.966	7.996	110.964	7.996	110.995	7.997	110.982	8.002	110.988
Glu61	8.117	120.823	8.118	120.858	8.119	120.865	8.120	120.862	8.119	120.882	8.121	120.889	8.124	120.929	8.126	120.965	8.129	120.987	8.127	120.981
Thr62	8.450	113.305	8.441	113.285	8.442	113.308			8.437	113.302	8.434	113.297	8.430	113.310			8.412	113.335	8.412	113.428
Gly63	8.826	111.039	8.827	111.044	8.830	111.053	8.831	111.065	8.832	111.072	8.838	111.082	8.844	111.123	8.853	111.186	8.857	111.210	8.871	111.300
Tyr64	8.738	118.717	8.739	118.742	8.739	118.737	8.739	118.731	8.741	118.736	7.743	118.719	8.748	118.765	7.850	118.769	8.763	118.762	8.740	118.746
Ile65	9.304	112.489	9.305	112.502	9.305	112.504	9.307	112.502	9.308	112.501	9.307	112.511	9.315	112.533	9.316	112.545	9.319	112.584	9.329	112.647
Ser67	7.708	121.656	7.705	121.660	7.707	121.664	7.705	121.659	7.704	121.663	7.705	121.660	7.704	121.660	7.702	121.663	7.700	121.648	7.698	121.644
Asn68	8.155	114.955	8.150	114.933	8.150	114.934	8.153	114.937	8.151	114.939	8.149	114.936	9.152	114.920	8.151	114.920	8.152	114.929	8.154	114.934
Tyr69	7.861	118.989	7.858	118.988	7.857	118.976	7.858	118.987	7.855	118.986	7.856	118.984	7.857	118.991	7.855	118.984	7.854	118.985	7.854	118.966
Val70	7.174	108.867	7.171	108.865	7.171	108.863	7.169	108.866	7.170	108.856	7.170	108.861	7.170	108.866	7.169	108.870	7.170	108.866	7.169	108.863
Ala71	8.878	121.785	8.875	121.774	8.877	121.773	8.873	121.775	8.873	121.776	8.874	121.775	8.875	121.772	8.873	121.777	8.871	121.768	8.874	121.749

Val73	8.106	121.513	8.106	121.506	8.106	121.503	8.106	121.506	8.106	121.510	8.104	121.480	8.106	121.476	8.106	121.462	8.107	121.458	8.108	121.451
Asp74	8.298	122.026	8.297	122.017	8.298	122.024	8.298	122.025	8.297	122.034	8.296	122.026	8.298	122.028	8.297	122.025	8.297	122.020	8.297	122.024
Ser75	8.048	114.949	8.045	114.933	8.045	114.939	8.044	114.937	8.044	114.932	8.045	114.941	8.045	114.947	8.044	114.931	8.045	114.932	8.045	114.938
lle76	8.012	122.134	8.010	122.129	8.011	122.139	8.011	122.138	8.010	122.131	8.010	122.130	8.013	122.136	8.013	122.130	8.013	122.122	8.016	122.104
Gln77	7.936	128.675	7.932	128.660	7.932	128.658	7.932	128.659	7.932	128.654	7.931	128.658	7.933	128.659	7.933	128.659	7.931	128.631	7.933	128.603

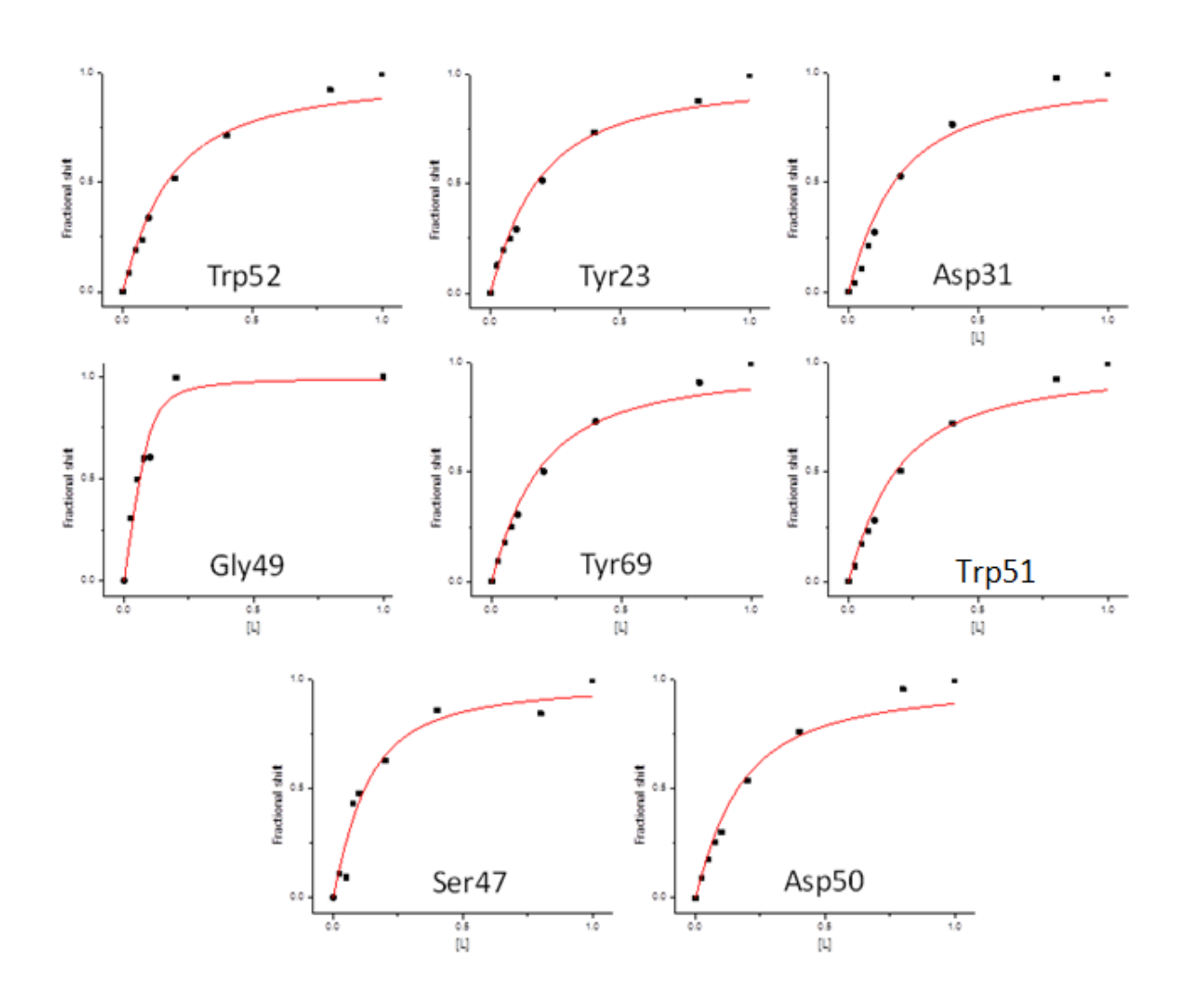
Overlay of 2D-¹H-¹⁵N-HSQC spectra obtained for the titration of SH3 with peptide **1.142** with increasing concentration of **1.142**.



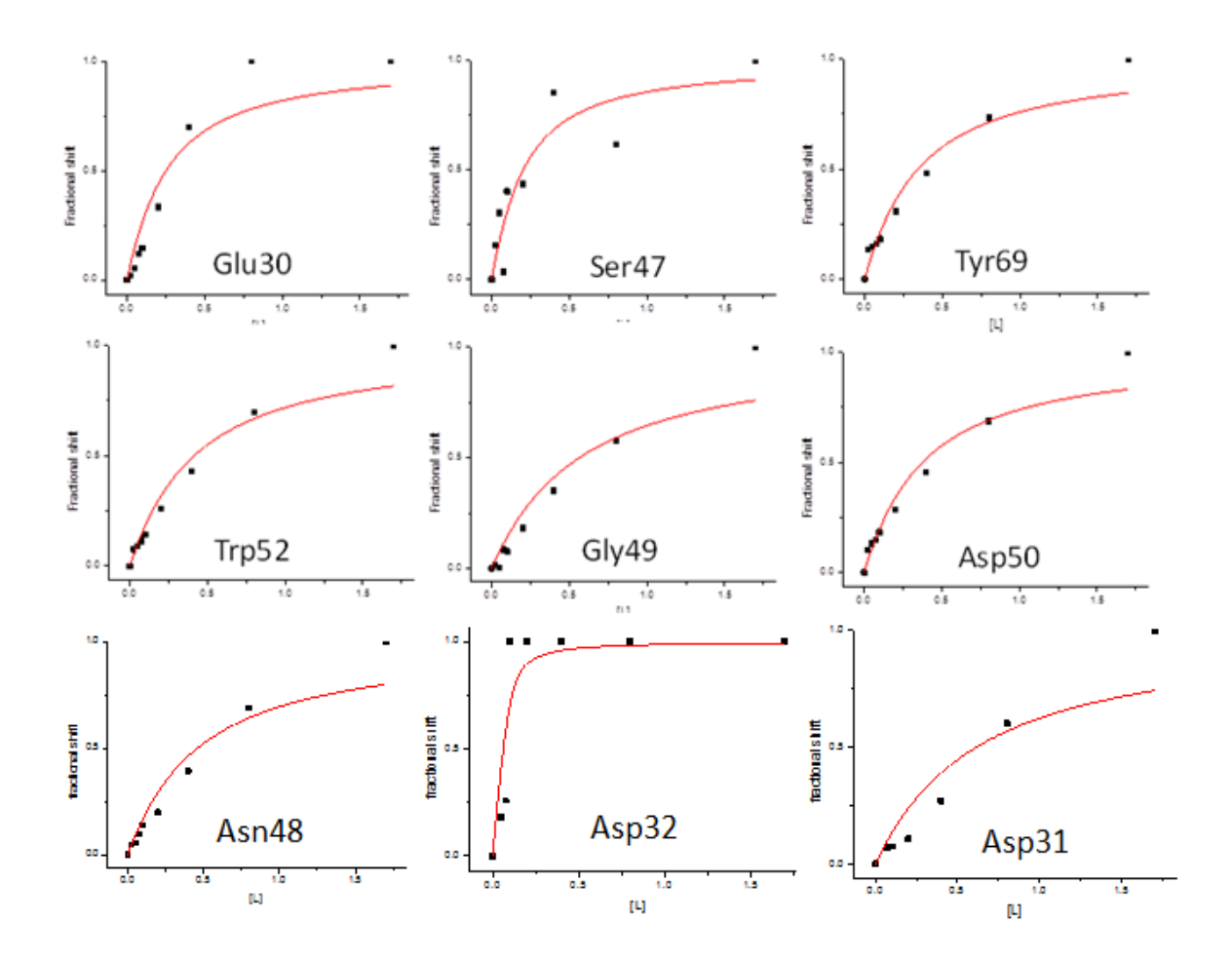
5.6 Titration plots

The equilibrium binding constant K_D was obtained for residues in fast exchange by fitting K_D to the fractional shift (Δ/Δ max) using the formula $\frac{\Delta}{\Delta max} = \frac{(K_D + [L] + [P]) - \sqrt{(K_D + [L] + [P])^2 - 4[P][L]}}{2[P]},$ where Δ represents the difference of the measured shift at any (maximal, Δ max) ligand concentration and the shift of the free protein, and [L] and [P] are the ligand and protein concentrations respectively.

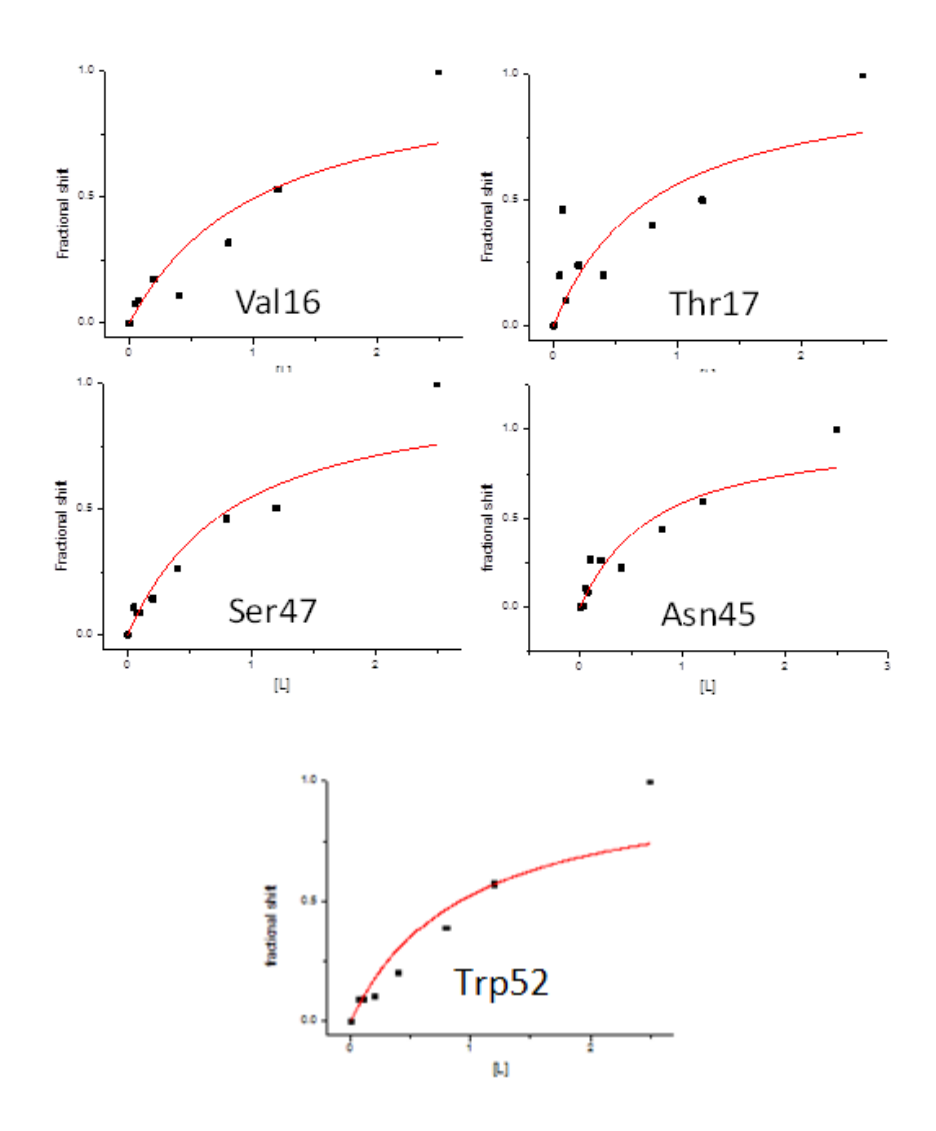
5.6.1 Parent 8 mer 1.139/SH3 domain



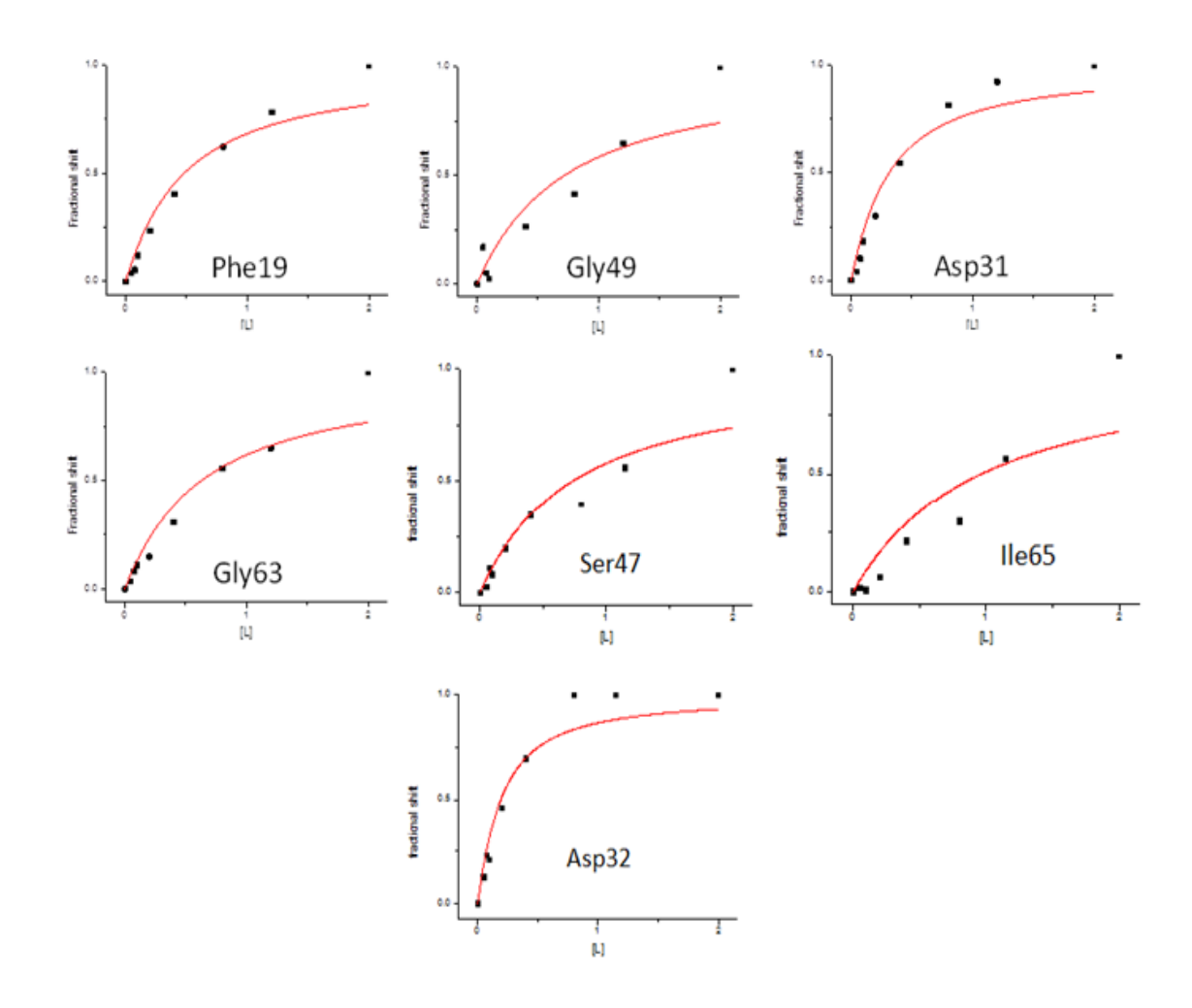
5.6.2 Analogue 1.140/SH3 domain



5.6.3 Analogue 1.141/SH3 domain



5.6.4 Analogue 1.142/SH3 domain



6.0 X-ray data for 1.125 and dimer 4.1

Table 1. Crystal data and structure refinement details.

Identification code	2013ncs0778dlsa	
Empirical formula	$C_{34}H_{55}CIN_6O_{11}$	
Formula weight	759.29	
Temperature	100.15 K	
Wavelength	0.6889 Å	
Crystal system	Monoclinic	
Space group	P21	
Unit cell dimensions	a = 13.568(15) Å	α = 90°
	b = 7.443(7) Å	eta = 105.441(9)°
	c = 19.72(2) Å	γ = 90°
Volume	1920(3) Å ³	
Z	2	
Density (calculated)	$1.314 \text{Mg} / \text{m}^3$	
Absorption coefficient	0.159 mm ⁻¹	
F(000)	812	
Crystal	Colourless; lath	
Crystal size	$0.10 \times 0.05 \times 0.01 \text{ mm}^3$	
heta range for data collection	2.047 – 24.290°	
Index ranges	$-16 \le h \le 16, -6 \le k \le 8, -3$	23 ≤ <i>l</i> ≤ 23
Reflections collected	15867	
Independent reflections	$5852 [R_{int} = 0.1905]$	
Completeness to θ = 25.000°	91.5 %	
Refinement method	Full-matrix least-squares o	n <i>F</i> ²
Data / restraints / parameters	5852 / 1 / 478	
Goodness-of-fit on F ²	0.955	
Final R indices $[F^2 > 2\sigma(F^2)]$	R1 = 0.0837, $wR2 = 0.1702$	
R indices (all data)	R1 = 0.1529, $wR2 = 0.2107$	
Absolute structure parameter	-0.06(17)	
Extinction coefficient	n/a	
Largest diff. peak and hole	0.348 and –0.306 e Å ⁻³	

Diffractometer: Beamline I19 situated on an undulator insertion device with a combination of double crystal monochromator, vertical and horizontal focussing mirrors and a series of beam slits (primary white beam and either side of the focussing mirrors). The experimental hutch (EH1) is equipped with a Crystal Logic 4-circle kappa geometry goniometer with a Rigaku

Saturn 724 CCD detector and an Oxford Cryosystems Cryostream plus cryostat (80-500K). For conventional service crystallography the beamline operates at a typical energy of 18 keV (Zr K absorption edge) and a Rigaku ACTOR robotic sample changing system is available. **Cell determination and data collection**: *CrystalClear-SM Expert 2.0 r5* (Rigaku, 2010). **Data reduction**, **cell refinement and absorption correction**: *CrystalClear-SM Expert 2.0 r5* (Rigaku, 2010). **Structure solution**: *SHELXD-2014* (Sheldrick, G.M. (2008). Acta Cryst. A64, 112-122). **Structure refinement**: *SHELXL-2014* (Sheldrick, G.M. (2008). Acta Cryst. A64, 112-122). **Graphics**: *OLEX2* (Dolomanov, O. V., Bourhis, L. J., Gildea, R. J., Howard, J. A. K. & Puschmann, H. (2009). J. Appl. Cryst. 42, 339-341).

Table 2. Atomic coordinates [× 10^4], equivalent isotropic displacement parameters [Å² × 10^3] and site occupancy factors. U_{eq} is defined as one third of the trace of the orthogonalized U^{ij} tensor.

O1 5346(5) 7879(8) 6777(3) 57(2) 1 O2 3670(5) 4869(9) 7001(3) 52(2) 1 O3 6480(5) 3695(11) 8058(4) 71(2) 1 O4 5547(6) 10781(10) 5367(4) 75(2) 1 O5 4912(5) 11896(9) 6218(4) 59(2) 1 O6 8821(6) 5370(14) 8954(5) 89(3) 1 O7 9510(5) 2583(10) 8977(4) 71(2) 1 N1 3810(6) 8957(11) 6256(4) 54(2) 1 N2 4536(6) 6611(11) 7887(4) 49(2) 1 N3 5319(5) 3589(10) 8680(4) 45(2) 1 N4 8045(6) 2908(12) 9240(5) 67(3) 1 C1 4108(8) 9308(14) 5609(5) 60(3) 1 C2 3105(8) 9991(17) 5115(6) 70(3) 1 C3 2465(8) 10646(16) 5585(5) 67(3) 1	Atom					C o f
O2 3670(5) 4869(9) 7001(3) 52(2) 1 O3 6480(5) 3695(11) 8058(4) 71(2) 1 O4 5547(6) 10781(10) 5367(4) 75(2) 1 O5 4912(5) 11896(9) 6218(4) 59(2) 1 O6 8821(6) 5370(14) 8954(5) 89(3) 1 O7 9510(5) 2583(10) 8977(4) 71(2) 1 N1 3810(6) 8957(11) 6256(4) 54(2) 1 N1 3810(6) 8957(11) 6256(4) 54(2) 1 N2 4536(6) 6611(11) 7887(4) 49(2) 1 N3 5319(5) 3589(10) 8680(4) 45(2) 1 N4 8045(6) 2908(12) 9240(5) 67(3) 1 C1 4108(8) 9308(14) 5609(5) 60(3) 1 C2 3105(8) 9991(17) 5115(6) 70(3) 1 C3 2465(8) 10646(16) 5585(5) 67(3) 1	Atom	Х	У	Z	U_{eq}	S.o.f.
O2 3670(5) 4869(9) 7001(3) 52(2) 1 O3 6480(5) 3695(11) 8058(4) 71(2) 1 O4 5547(6) 10781(10) 5367(4) 75(2) 1 O5 4912(5) 11896(9) 6218(4) 59(2) 1 O6 8821(6) 5370(14) 8954(5) 89(3) 1 O7 9510(5) 2583(10) 8977(4) 71(2) 1 N1 3810(6) 8957(11) 6256(4) 54(2) 1 N1 3810(6) 8957(11) 6256(4) 54(2) 1 N2 4536(6) 6611(11) 7887(4) 49(2) 1 N3 5319(5) 3589(10) 8680(4) 45(2) 1 N4 8045(6) 2908(12) 9240(5) 67(3) 1 C1 4108(8) 9308(14) 5609(5) 60(3) 1 C2 3105(8) 9991(17) 5115(6) 70(3) 1 C3 2465(8) 10646(16) 5585(5) 67(3) 1	Ω1	5346(5)	7879(8)	6777(3)	57(2)	1
O3 6480(5) 3695(11) 8058(4) 71(2) 1 O4 5547(6) 10781(10) 5367(4) 75(2) 1 O5 4912(5) 11896(9) 6218(4) 59(2) 1 O6 8821(6) 5370(14) 8954(5) 89(3) 1 O7 9510(5) 2583(10) 8977(4) 71(2) 1 N1 3810(6) 8957(11) 6256(4) 54(2) 1 N2 4536(6) 6611(11) 7887(4) 49(2) 1 N3 5319(5) 3589(10) 8680(4) 45(2) 1 N4 8045(6) 2908(12) 9240(5) 67(3) 1 C1 4108(8) 9308(14) 5609(5) 60(3) 1 C2 3105(8) 9991(17) 5115(6) 70(3) 1 C3 2465(8) 10646(16) 5585(5) 67(3) 1 C4 2726(7) 9355(14) 6204(5) 57(3) 1 C5 2610(7) 10002(15) 6893(5) 59(3) 1		٠,		• •		
O4 5547(6) 10781(10) 5367(4) 75(2) 1 O5 4912(5) 11896(9) 6218(4) 59(2) 1 O6 8821(6) 5370(14) 8954(5) 89(3) 1 O7 9510(5) 2583(10) 8977(4) 71(2) 1 N1 3810(6) 8957(11) 6256(4) 54(2) 1 N2 4536(6) 6611(11) 7887(4) 49(2) 1 N3 5319(5) 3589(10) 8680(4) 45(2) 1 N4 8045(6) 2908(12) 9240(5) 67(3) 1 C1 4108(8) 9308(14) 5609(5) 60(3) 1 C2 3105(8) 9991(17) 5115(6) 70(3) 1 C3 2465(8) 10646(16) 5585(5) 67(3) 1 C4 2726(7) 9355(14) 6204(5) 57(3) 1 C5 2610(7) 10002(15) 6893(5) 59(3) 1 C6 3064(7) 8613(15) 7449(5) 56(3) 1						
O5 4912(5) 11896(9) 6218(4) 59(2) 1 O6 8821(6) 5370(14) 8954(5) 89(3) 1 O7 9510(5) 2583(10) 8977(4) 71(2) 1 N1 3810(6) 8957(11) 6256(4) 54(2) 1 N2 4536(6) 6611(11) 7887(4) 49(2) 1 N3 5319(5) 3589(10) 8680(4) 45(2) 1 N4 8045(6) 2908(12) 9240(5) 67(3) 1 C1 4108(8) 9308(14) 5609(5) 60(3) 1 C2 3105(8) 9991(17) 5115(6) 70(3) 1 C3 2465(8) 10646(16) 5585(5) 67(3) 1 C4 2726(7) 9355(14) 6204(5) 57(3) 1 C5 2610(7) 10002(15) 6893(5) 59(3) 1 C6 3064(7) 8613(15) 7449(5) 56(3) 1		٠,		• •		
O6 8821(6) 5370(14) 8954(5) 89(3) 1 O7 9510(5) 2583(10) 8977(4) 71(2) 1 N1 3810(6) 8957(11) 6256(4) 54(2) 1 N2 4536(6) 6611(11) 7887(4) 49(2) 1 N3 5319(5) 3589(10) 8680(4) 45(2) 1 N4 8045(6) 2908(12) 9240(5) 67(3) 1 C1 4108(8) 9308(14) 5609(5) 60(3) 1 C2 3105(8) 9991(17) 5115(6) 70(3) 1 C3 2465(8) 10646(16) 5585(5) 67(3) 1 C4 2726(7) 9355(14) 6204(5) 57(3) 1 C5 2610(7) 10002(15) 6893(5) 59(3) 1 C6 3064(7) 8613(15) 7449(5) 56(3) 1 C7 4181(7) 8239(13) 7508(4) 46(2) 1 C8 4477(7) 8273(12) 6818(5) 50(2) 1		٠,		• •		
O7 9510(5) 2583(10) 8977(4) 71(2) 1 N1 3810(6) 8957(11) 6256(4) 54(2) 1 N2 4536(6) 6611(11) 7887(4) 49(2) 1 N3 5319(5) 3589(10) 8680(4) 45(2) 1 N4 8045(6) 2908(12) 9240(5) 67(3) 1 C1 4108(8) 9308(14) 5609(5) 60(3) 1 C2 3105(8) 9991(17) 5115(6) 70(3) 1 C3 2465(8) 10646(16) 5585(5) 67(3) 1 C4 2726(7) 9355(14) 6204(5) 57(3) 1 C5 2610(7) 10002(15) 6893(5) 59(3) 1 C6 3064(7) 8613(15) 7449(5) 56(3) 1 C7 4181(7) 8239(13) 7508(4) 46(2) 1 C8 4477(7) 8273(12) 6818(5) 50(2) 1 C10 4439(7) 3410(12) 8069(5) 47(2) 1						
N1 3810(6) 8957(11) 6256(4) 54(2) 1 N2 4536(6) 6611(11) 7887(4) 49(2) 1 N3 5319(5) 3589(10) 8680(4) 45(2) 1 N4 8045(6) 2908(12) 9240(5) 67(3) 1 C1 4108(8) 9308(14) 5609(5) 60(3) 1 C2 3105(8) 9991(17) 5115(6) 70(3) 1 C3 2465(8) 10646(16) 5585(5) 67(3) 1 C4 2726(7) 9355(14) 6204(5) 57(3) 1 C5 2610(7) 10002(15) 6893(5) 59(3) 1 C6 3064(7) 8613(15) 7449(5) 56(3) 1 C7 4181(7) 8239(13) 7508(4) 46(2) 1 C8 4477(7) 8273(12) 6818(5) 50(2) 1 C9 4223(7) 5026(15) 7602(5) 49(2) 1 C10 4439(7) 3410(12) 8069(5) 47(2) 1 C11 3556(7) 3037(14) 8400(5) 56(3) 1 C12 3927(7) 3803(16) 9143(5) 61(3) 1 C13 5039(7) 3314(19) 9328(5) 67(3) 1 C14 5787(7) 3990(14) 9946(5) 60(3) 1 C15 6824(7) 3232(14) 9948(5) 55(3) 1 C16 7129(7) 3848(14) 9297(5) 53(2) 1		٠,				
N2						
N3 5319(5) 3589(10) 8680(4) 45(2) 1 N4 8045(6) 2908(12) 9240(5) 67(3) 1 C1 4108(8) 9308(14) 5609(5) 60(3) 1 C2 3105(8) 9991(17) 5115(6) 70(3) 1 C3 2465(8) 10646(16) 5585(5) 67(3) 1 C4 2726(7) 9355(14) 6204(5) 57(3) 1 C5 2610(7) 10002(15) 6893(5) 59(3) 1 C6 3064(7) 8613(15) 7449(5) 56(3) 1 C7 4181(7) 8239(13) 7508(4) 46(2) 1 C8 4477(7) 8273(12) 6818(5) 50(2) 1 C9 4223(7) 5026(15) 7602(5) 49(2) 1 C10 4439(7) 3410(12) 8069(5) 47(2) 1 C11 3556(7) 3037(14) 8400(5) 56(3) 1 C12 3927(7) 3803(16) 9143(5) 61(3) 1 C13 5039(7) 3314(19) 9328(5) 67(3) 1 C14 5787(7) 3990(14) 9946(5) 60(3) 1 C15 6824(7) 3232(14) 9948(5) 55(3) 1 C16 7129(7) 3848(14) 9297(5) 53(2) 1						
N4 8045(6) 2908(12) 9240(5) 67(3) 1 C1 4108(8) 9308(14) 5609(5) 60(3) 1 C2 3105(8) 9991(17) 5115(6) 70(3) 1 C3 2465(8) 10646(16) 5585(5) 67(3) 1 C4 2726(7) 9355(14) 6204(5) 57(3) 1 C5 2610(7) 10002(15) 6893(5) 59(3) 1 C6 3064(7) 8613(15) 7449(5) 56(3) 1 C7 4181(7) 8239(13) 7508(4) 46(2) 1 C8 4477(7) 8273(12) 6818(5) 50(2) 1 C9 4223(7) 5026(15) 7602(5) 49(2) 1 C10 4439(7) 3410(12) 8069(5) 47(2) 1 C11 3556(7) 3037(14) 8400(5) 56(3) 1 C12 3927(7) 3803(16) 9143(5) 61(3) 1 C13 5039(7) 3314(19) 9328(5) 67(3) 1 C14 5787(7) 3990(14) 9946(5) 60(3) 1 C15 6824(7) 3232(14) 9948(5) 55(3) 1 C16 7129(7) 3848(14) 9297(5) 53(2) 1			• •	• •		
C1 4108(8) 9308(14) 5609(5) 60(3) 1 C2 3105(8) 9991(17) 5115(6) 70(3) 1 C3 2465(8) 10646(16) 5585(5) 67(3) 1 C4 2726(7) 9355(14) 6204(5) 57(3) 1 C5 2610(7) 10002(15) 6893(5) 59(3) 1 C6 3064(7) 8613(15) 7449(5) 56(3) 1 C7 4181(7) 8239(13) 7508(4) 46(2) 1 C8 4477(7) 8273(12) 6818(5) 50(2) 1 C9 4223(7) 5026(15) 7602(5) 49(2) 1 C10 4439(7) 3410(12) 8069(5) 47(2) 1 C11 3556(7) 3037(14) 8400(5) 56(3) 1 C12 3927(7) 3803(16) 9143(5) 61(3) 1 C13 5039(7) 3314(19) 9328(5) 67(3) 1 C14 5787(7) 3990(14) 9946(5) 60(3) 1 <td></td> <td></td> <td></td> <td></td> <td></td> <td></td>						
C2 3105(8) 9991(17) 5115(6) 70(3) 1 C3 2465(8) 10646(16) 5585(5) 67(3) 1 C4 2726(7) 9355(14) 6204(5) 57(3) 1 C5 2610(7) 10002(15) 6893(5) 59(3) 1 C6 3064(7) 8613(15) 7449(5) 56(3) 1 C7 4181(7) 8239(13) 7508(4) 46(2) 1 C8 4477(7) 8273(12) 6818(5) 50(2) 1 C9 4223(7) 5026(15) 7602(5) 49(2) 1 C10 4439(7) 3410(12) 8069(5) 47(2) 1 C11 3556(7) 3037(14) 8400(5) 56(3) 1 C12 3927(7) 3803(16) 9143(5) 61(3) 1 C13 5039(7) 3314(19) 9328(5) 67(3) 1 C14 5787(7) 3990(14) 9946(5) 60(3) 1 C15 6824(7) 3232(14) 9948(5) 55(3) 1 </td <td></td> <td></td> <td></td> <td></td> <td></td> <td></td>						
C3		٠,		• •		
C4 2726(7) 9355(14) 6204(5) 57(3) 1 C5 2610(7) 10002(15) 6893(5) 59(3) 1 C6 3064(7) 8613(15) 7449(5) 56(3) 1 C7 4181(7) 8239(13) 7508(4) 46(2) 1 C8 4477(7) 8273(12) 6818(5) 50(2) 1 C9 4223(7) 5026(15) 7602(5) 49(2) 1 C10 4439(7) 3410(12) 8069(5) 47(2) 1 C11 3556(7) 3037(14) 8400(5) 56(3) 1 C12 3927(7) 3803(16) 9143(5) 61(3) 1 C13 5039(7) 3314(19) 9328(5) 67(3) 1 C14 5787(7) 3990(14) 9946(5) 60(3) 1 C15 6824(7) 3232(14) 9948(5) 55(3) 1 C16 7129(7) 3848(14) 9297(5) 53(2) 1						
C5 2610(7) 10002(15) 6893(5) 59(3) 1 C6 3064(7) 8613(15) 7449(5) 56(3) 1 C7 4181(7) 8239(13) 7508(4) 46(2) 1 C8 4477(7) 8273(12) 6818(5) 50(2) 1 C9 4223(7) 5026(15) 7602(5) 49(2) 1 C10 4439(7) 3410(12) 8069(5) 47(2) 1 C11 3556(7) 3037(14) 8400(5) 56(3) 1 C12 3927(7) 3803(16) 9143(5) 61(3) 1 C13 5039(7) 3314(19) 9328(5) 67(3) 1 C14 5787(7) 3990(14) 9946(5) 60(3) 1 C15 6824(7) 3232(14) 9948(5) 55(3) 1 C16 7129(7) 3848(14) 9297(5) 53(2) 1						
C6 3064(7) 8613(15) 7449(5) 56(3) 1 C7 4181(7) 8239(13) 7508(4) 46(2) 1 C8 4477(7) 8273(12) 6818(5) 50(2) 1 C9 4223(7) 5026(15) 7602(5) 49(2) 1 C10 4439(7) 3410(12) 8069(5) 47(2) 1 C11 3556(7) 3037(14) 8400(5) 56(3) 1 C12 3927(7) 3803(16) 9143(5) 61(3) 1 C13 5039(7) 3314(19) 9328(5) 67(3) 1 C14 5787(7) 3990(14) 9946(5) 60(3) 1 C15 6824(7) 3232(14) 9948(5) 55(3) 1 C16 7129(7) 3848(14) 9297(5) 53(2) 1						
C7 4181(7) 8239(13) 7508(4) 46(2) 1 C8 4477(7) 8273(12) 6818(5) 50(2) 1 C9 4223(7) 5026(15) 7602(5) 49(2) 1 C10 4439(7) 3410(12) 8069(5) 47(2) 1 C11 3556(7) 3037(14) 8400(5) 56(3) 1 C12 3927(7) 3803(16) 9143(5) 61(3) 1 C13 5039(7) 3314(19) 9328(5) 67(3) 1 C14 5787(7) 3990(14) 9946(5) 60(3) 1 C15 6824(7) 3232(14) 9948(5) 55(3) 1 C16 7129(7) 3848(14) 9297(5) 53(2) 1						
C8 4477(7) 8273(12) 6818(5) 50(2) 1 C9 4223(7) 5026(15) 7602(5) 49(2) 1 C10 4439(7) 3410(12) 8069(5) 47(2) 1 C11 3556(7) 3037(14) 8400(5) 56(3) 1 C12 3927(7) 3803(16) 9143(5) 61(3) 1 C13 5039(7) 3314(19) 9328(5) 67(3) 1 C14 5787(7) 3990(14) 9946(5) 60(3) 1 C15 6824(7) 3232(14) 9948(5) 55(3) 1 C16 7129(7) 3848(14) 9297(5) 53(2) 1						
C9 4223(7) 5026(15) 7602(5) 49(2) 1 C10 4439(7) 3410(12) 8069(5) 47(2) 1 C11 3556(7) 3037(14) 8400(5) 56(3) 1 C12 3927(7) 3803(16) 9143(5) 61(3) 1 C13 5039(7) 3314(19) 9328(5) 67(3) 1 C14 5787(7) 3990(14) 9946(5) 60(3) 1 C15 6824(7) 3232(14) 9948(5) 55(3) 1 C16 7129(7) 3848(14) 9297(5) 53(2) 1						
C10 4439(7) 3410(12) 8069(5) 47(2) 1 C11 3556(7) 3037(14) 8400(5) 56(3) 1 C12 3927(7) 3803(16) 9143(5) 61(3) 1 C13 5039(7) 3314(19) 9328(5) 67(3) 1 C14 5787(7) 3990(14) 9946(5) 60(3) 1 C15 6824(7) 3232(14) 9948(5) 55(3) 1 C16 7129(7) 3848(14) 9297(5) 53(2) 1						
C11 3556(7) 3037(14) 8400(5) 56(3) 1 C12 3927(7) 3803(16) 9143(5) 61(3) 1 C13 5039(7) 3314(19) 9328(5) 67(3) 1 C14 5787(7) 3990(14) 9946(5) 60(3) 1 C15 6824(7) 3232(14) 9948(5) 55(3) 1 C16 7129(7) 3848(14) 9297(5) 53(2) 1				• •		
C12 3927(7) 3803(16) 9143(5) 61(3) 1 C13 5039(7) 3314(19) 9328(5) 67(3) 1 C14 5787(7) 3990(14) 9946(5) 60(3) 1 C15 6824(7) 3232(14) 9948(5) 55(3) 1 C16 7129(7) 3848(14) 9297(5) 53(2) 1						
C13 5039(7) 3314(19) 9328(5) 67(3) 1 C14 5787(7) 3990(14) 9946(5) 60(3) 1 C15 6824(7) 3232(14) 9948(5) 55(3) 1 C16 7129(7) 3848(14) 9297(5) 53(2) 1						
C14 5787(7) 3990(14) 9946(5) 60(3) 1 C15 6824(7) 3232(14) 9948(5) 55(3) 1 C16 7129(7) 3848(14) 9297(5) 53(2) 1						
C15 6824(7) 3232(14) 9948(5) 55(3) 1 C16 7129(7) 3848(14) 9297(5) 53(2) 1						
C16 7129(7) 3848(14) 9297(5) 53(2) 1						
	C17	6280(7)	3611(16)	8617(5)	57(3)	1

C18	4937(8)	10718(16)	5723(5)	60(3)	1
C19	5639(7)	13381(14)	6311(5)	59(3)	1
C20	8785(8)	3720(20)	9046(6)	68(3)	1
C21	10553(8)	3190(20)	8996(7)	88(4)	1
C22	10561(9)	4292(19)	8371(7)	98(5)	1
C23	11101(10)	1454(18)	8975(9)	108(5)	1
C24	10982(10)	4060(20)	9714(9)	123(6)	1
031	1755(6)	762(13)	3048(4)	79(2)	1
032	-557(6)	2283(11)	3041(5)	81(2)	1
033	-154(6)	487(12)	3980(4)	85(2)	1
N31	1485(6)	3491(13)	3430(4)	59(2)	1
N32	2853(6)	2157(11)	2182(4)	62(2)	1
C31	1782(8)	2415(19)	2995(6)	63(3)	1
C32	2058(8)	3269(16)	2373(6)	65(3)	1
C33	2378(10)	5176(18)	2480(7)	86(4)	1
C34	1616(11)	6212(19)	2749(9)	101(5)	1
C35	1600(8)	5524(17)	3461(7)	75(3)	1
C36	758(10)	6010(20)	3798(10)	115(6)	1
C37	764(11)	4510(30)	4315(8)	115(6)	1
C38	1000(8)	2875(19)	3956(6)	76(4)	1
C39	12(8)	1849(16)	3574(6)	59(3)	1
C40	-1114(9)	-448(17)	3672(8)	94(4)	1
Cl61	3713(2)	3672(5)	961(1)	74(1)	1
091	3047(6)	5161(12)	5483(4)	78(2)	1

Table 3. Bond lengths [Å] and angles [°].

O1-C8	1.237(10)
O2-C9	1.228(11)
O3-C17	1.207(11)
O4-C18	1.220(11)
O5-C18	1.320(12)
O5-C19	1.460(11)
O6-C20	1.241(16)
O7-C20	1.334(13)
O7-C21	1.476(13)
N1-C1	1.461(11)
N1-C4	1.477(12)
N1-C8	1.330(11)
N2-H2	0.8800
N2-C7	1.437(11)
N2-C9	1.327(12)

N3-C10	1.460(10)
N3-C13	1.440(11)
N3-C17	1.342(11)
N4-H4	0.8800
N4-C16	1.457(12)
N4-C20	1.315(14)
C1-H1	1.0000
C1-C2	1.534(14)
C1-C18	1.511(14)
C2-H2A	0.9900
C2-H2B	0.9900
C2-C3	1.510(15)
C3-H3A	0.9900
C3-H3B	0.9900
C3-C4	1.520(14)
C4-H4A	1.0000
C4-C5	1.489(13)
C5-H5A	0.9900
C5-H5B	0.9900
C5-C6	1.513(14)
C6-H6A	0.9900
C6-H6B	0.9900
C6-C7	1.515(12)
C7-H7	1.0000
C7-C8	1.519(12)
C9-C10	1.496(13)
C10-H10	1.0000
C10-C11	1.535(12)
C11-H11A	0.9900
C11-H11B	0.9900
C11-C12	1.526(13)
C12-H12A	0.9900
C12-H12B	0.9900
C12-C13	1.500(13)
C13-H13	1.0000
C13-C14	1.453(13)
C14-H14A	0.9900
C14-H14B	0.9900
C14-C15	1.515(13)
C15-H15A	0.9900
C15-H15B	0.9900
C15-C16	1.521(13)
C16-H16	1.0000
C16-C17	1.527(13)
C19-H19A	0.9800
C19-H19B	0.9800
C19-H19C	0.9800
C21-C22	1.484(17)
C21-C23	1.495(18)
	()

C21-C24	1.527(18)
C22-H22A	0.9800
C22-H22B	0.9800
C22-H22C	0.9800
C23-H23A	0.9800
C23-H23B	0.9800
C23-H23C	0.9800
C24-H24A	0.9800
C24-H24B	0.9800
C24-H24C	0.9800
O31-C31	1.236(13)
O32-C39	1.171(11)
O33-C39	1.348(13)
O33-C40	1.459(14)
N31-C31	1.313(14)
N31-C35	1.520(16)
N31-C38	1.442(13)
N32-H32A	0.9100
N32-H32B	0.9100
N32-H32C	0.9100
N32-C32	1.485(12)
C31-C32	1.515(15)
C32-H32	1.0000
C32-C33	1.482(17)
C33-H33A	0.9900
C33-H33B	0.9900
C33-C34	1.496(17)
C34-H34A	0.9900
C34-H34B	0.9900
C34-C35	1.500(18)
C35-H35	1.0000
C35-C36	1.510(17)
C36-H36A	0.9900
C36-H36B	0.9900
C36-C37	1.51(2)
C37-H37A	0.9900
C37-H37B	0.9900
C37-C38	1.485(18)
C38-H38	1.0000
C38-C39	1.553(16)
C40-H40A	0.9800
C40-H40B	0.9800
C40-H40C	0.9800
O91-H91A	0.8505
O91-H91B	0.8502

C18-O5-C19	116.5(8)
C20-O7-C21	122.1(10)
C1-N1-C4	113.9(8)
C8-N1-C1	120.7(8)
C8-N1-C4	125.4(8)
C7-N2-H2	119.9
C9-N2-H2	119.9
C9-N2-C7	120.2(8)
C13-N3-C10	111.6(7)
C17-N3-C10	121.8(8)
C17-N3-C13	125.1(8)
C16-N4-H4	118.9
C20-N4-H4	118.9
C20-N4-C16	122.3(10)
N1-C1-H1	110.6
N1-C1-C2	102.1(8)
N1-C1-C18	111.2(8)
C2-C1-H1	110.6
C18-C1-H1	110.6
C18-C1-C2	111.3(9)
C1-C2-H2A	110.5
C1–C2–H2B	110.5
H2A-C2-H2B	108.7
C3-C2-C1	105.9(8)
C3-C2-H2A	110.5
C3-C2-H2B	110.5
C2-C3-H3A	111.0
C2-C3-H3B	111.0
C2-C3-C4	103.9(9)
H3A-C3-H3B	109.0
C4-C3-H3A	111.0
C4-C3-H3B	111.0
N1-C4-C3	101.4(8)
N1-C4-H4A	108.9
N1-C4-C5	110.3(8)
C3-C4-H4A	108.9
C5-C4-C3	118.0(9)
C5-C4-H4A	108.9
C4-C5-H5A	110.0
C4-C5-H5B	110.0
C4-C5-C6	108.6(9)
H5A-C5-H5B	108.4
C6-C5-H5A	110.0
C6-C5-H5B	110.0
C5-C6-H6A	109.0
C5-C6-H6B	109.0
C5-C6-C7	112.8(8)
H6A-C6-H6B	107.8

C7-C6-H6A	109.0
C7-C6-H6B	109.0
N2-C7-C6	112.6(8)
N2-C7-H7	105.9
N2-C7-C8	110.4(7)
C6-C7-H7	105.9
C6-C7-C8	115.2(8)
C8-C7-H7	105.9
O1-C8-N1	119.1(9)
O1-C8-C7	122.5(9)
N1-C8-C7	117.9(8)
O2-C9-N2	122.6(10)
O2-C9-C10	119.1(9)
N2-C9-C10	117.8(8)
N3-C10-C9	114.7(8)
N3-C10-H10	109.3
N3-C10-C11	103.0(7)
C9-C10-H10	109.3
C9-C10-C11	111.1(8)
C11-C10-H10	109.3
C10-C11-H11A	110.9
C10-C11-H11B	110.9
H11A-C11-H11B	108.9
C12-C11-C10	104.2(7)
C12-C11-H11A	110.9
C12-C11-H11B	110.9
C11-C12-H12A	111.5
C11-C12-H12B	111.5
H12A-C12-H12B	109.3
C13-C12-C11	101.3(8)
C13-C12-H12A	111.5
C13-C12-H12B	111.5
N3-C13-C12	103.7(8)
N3-C13-H13	104.7
N3-C13-C14	113.8(8)
C12-C13-H13	104.7
C14-C13-C12	123.6(9)
C14-C13-H13	104.7
C13-C14-H14A	110.0
C13-C14-H14B	110.0
C13-C14-C15	108.3(8)
H14A-C14-H14B	108.4
C15-C14-H14A	110.0
C15-C14-H14B	110.0
C14-C15-H15A	109.6

C14-C15-H15B	109.6
C14-C15-C16	110.3(8)
H15A-C15-H15B	108.1
C16-C15-H15A	109.6
C16-C15-H15B	109.6
N4-C16-C15	110.5(8)
N4-C16-H16	107.7
N4-C16-C17	109.7(8)
C15-C16-H16	107.7
C15-C16-C17	113.2(8)
C17-C16-H16	107.7
03-C17-N3	123.1(9)
O3-C17-C16	119.7(9)
N3-C17-C16	116.4(8)
04-C18-O5	123.7(11)
04-C18-C1	122.2(10)
05-C18-C1	114.0(9)
O5-C19-H19A	109.5
O5-C19-H19B	109.5
O5-C19-H19C	109.5
H19A-C19-H19B	109.5
H19A-C19-H19C	109.5
H19B-C19-H19C	109.5
06-C20-O7	123.7(12)
06-C20-N4	124.2(11)
N4-C20-O7	112.1(13)
07-C21-C22	111.5(10)
07-C21-C23	102.5(11)
07-C21-C24	106.2(10)
C22-C21-C23	110.0(11)
C22-C21-C24	116.7(13)
C23-C21-C24	108.9(13)
C21-C22-H22A	109.5
C21-C22-H22B	109.5
C21-C22-H22C	109.5
H22A-C22-H22B	109.5
H22A-C22-H22C	109.5
H22B-C22-H22C	109.5
C21-C23-H23A	109.5
C21-C23-H23B	109.5
C21-C23-H23C	109.5
H23A-C23-H23B	109.5
H23A-C23-H23C	109.5
H23B-C23-H23C	109.5
C21-C24-H24A	109.5
C21-C24-H24B	109.5
C21-C24-H24C	109.5
H24A-C24-H24B	109.5
H24A-C24-H24C	109.5
11247-024-11240	109.3

H24B-C24-H24C	109.5
C39-O33-C40	112.5(9)
C31-N31-C35	125.9(11)
C31-N31-C38	123.6(11)
C38-N31-C35	110.5(10)
H32A-N32-H32B	109.5
H32A-N32-H32C	109.5
H32B-N32-H32C	109.5
C32-N32-H32A	109.5
C32-N32-H32B	109.5
C32-N32-H32C	109.5
O31-C31-N31	122.1(12)
031-C31-C32	120.3(11)
N31-C31-C32	117.3(12)
N32-C32-C31	108.9(9)
N32-C32-H32	107.3
C31-C32-H32	107.3
C33-C32-N32	111.4(9)
C33-C32-N32	114.4(10)
C33-C32-H32	107.3
C32-C33-H33A	107.3
C32-C33-H33B	109.7
C32-C33-C34	109.7
H33A-C33-H33B	109.9(11)
C34-C33-H33A	108.2
C34-C33-H33B	109.7
C33-C34-H34A	109.7
C33-C34-H34B	109.7
C33-C34-C35	109.7
H34A-C34-H34B	109.8(12)
C35-C34-H34A	108.2
C35-C34-H34B	109.7
N31–C35–H35	109.7
C34-C35-N31	108.3
C34-C35-H35	109.3(10)
C34-C35-C36	122.1(13)
C36-C35-N31	99.9(10)
C36-C35-N31	108.3
C35-C36-H36A	110.8
C35-C36-H36B	
H36A-C36-H36B	110.8
	108.9
C37-C36-C35	104.6(13)
C37_C36_H36A	110.8
C37_C36_H36B	110.8
C36-C37-H37A	110.9

C36-C37-H37B	110.9
H37A-C37-H37B	108.9
C38-C37-C36	104.2(12)
C38-C37-H37A	110.9
C38-C37-H37B	110.9
N31-C38-C37	106.2(12)
N31-C38-H38	110.4
N31-C38-C39	107.9(9)
C37-C38-H38	110.4
C37-C38-C39	111.5(10)
C39-C38-H38	110.4
O32-C39-O33	124.5(11)
O32-C39-C38	125.3(11)
O33-C39-C38	109.9(9)
O33-C40-H40A	109.5
O33-C40-H40B	109.5
O33-C40-H40C	109.5
H40A-C40-H40B	109.5
H40A-C40-H40C	109.5
H40B-C40-H40C	109.5
H91A-O91-H91B	109.5

Symmetry transformations used to generate equivalent atoms

Table 4. Anisotropic displacement parameters [$\mathring{A}^2 \times 10^3$]. The anisotropic displacement factor exponent takes the form: $-2\pi^2[h^2a^{*2}U^{11} + \cdots + 2\ h\ k\ a^*\ b^*\ U^{12}]$.

Atom	U^{11}	U^{22}	U^{33}	U^{23}	U^{13}	U^{12}	
01	57(4)	59(5)	58(4)	14(3)	19(3)	12(3)	
	• •					· ·	
02	57(4)	49(4)	48(4)	-7(3)	12(3)	3(3)	
03	58(4)	83(5)	74(5)	6(5)	22(4)	5(4)	
04	101(6)	65(5)	78(5)	-1(4)	56(5)	2(4)	
O 5	72(5)	55(5)	61(4)	-9(4)	37(4)	1(4)	
06	75(6)	94(7)	110(7)	6(6)	43(5)	-10(5)	
07	55(4)	89(6)	71(5)	11(4)	19(4)	7(4)	
N1	52(5)	56(6)	57(5)	4(4)	21(4)	13(4)	
N2	49(5)	49(6)	49(5)	5(5)	13(4)	1(4)	
N3	50(4)	41(5)	48(4)	-2(4)	21(4)	-2(4)	
N4	58(6)	72(7)	73(6)	18(5)	23(5)	3(5)	
C1	71(7)	70(8)	48(6)	3(5)	32(6)	3(6)	
C2	78(7)	80(8)	52(6)	8(6)	16(6)	8(6)	
C3	67(7)	80(8)	54(7)	20(6)	14(6)	19(6)	
C4	50(6)	67(8)	53(6)	-9(5)	12(5)	3(5)	
C5	48(6)	67(7)	64(7)	8(6)	17(5)	7(5)	
C6	60(6)	61(7)	51(6)	-10(6)	23(5)	7(6)	
C7	52(5)	48(7)	39(5)	-1(5)	14(4)	1(5)	
C8	48(5)	37(6)	66(6)	8(5)	18(5)	6(5)	
C 9	51(6)	55(8)	45(6)	-8(5)	18(5)	-2(5)	

C10 68(6) 31(6) 42(5) -6(5) 13(5) -4(5) C11 50(5) 65(7) 59(6) -5(5) 25(5) -7(5) C12 62(6) 79(8) 48(6) 4(6) 26(5) -4(6) C13 48(5) 110(10) 49(6) -16(6) 24(5) -6(6) C14 71(7) 55(7) 62(6) -9(5) 31(6) -6(5) C15 58(6) 67(7) 37(5) 0(5) 9(5) 2(5) C16 49(5) 53(7) 60(6) -1(5) 20(5) 2(5) C16 49(5) 53(7) 60(6) -1(5) 20(5) 2(5) C17 61(6) 69(7) 47(6) 9(6) 24(5) 20(6) C18 73(7) 71(8) 43(6) 15(6) 28(6) 8(6) C19 73(7) 50(7) 62(6) 0(5) 31(5) 4(6) C20 47(6) 89(10) 63(7								
$\begin{array}{cccccccccccccccccccccccccccccccccccc$	C10	68(6)	31(6)	42(5)	-6(5)	13(5)	-4(5)	
C13	C11	50(5)	65(7)	59(6)	-5(5)	25(5)	-7(5)	
C14 71(7) 55(7) 62(6) -9(5) 31(6) -6(5) C15 58(6) 67(7) 37(5) 0(5) 9(5) 2(5) C16 49(5) 53(7) 60(6) -1(5) 20(5) 2(5) C17 61(6) 69(7) 47(6) 9(6) 24(5) 20(6) C18 73(7) 71(8) 43(6) 15(6) 28(6) 8(6) C19 73(7) 50(7) 62(6) 0(5) 31(5) 4(6) C20 47(6) 89(10) 63(7) -9(7) 8(5) 4(7) C21 57(7) 116(12) 97(10) -8(9) 33(7) -7(8) C22 72(8) 121(13) 114(11) 30(9) 50(8) -7(7) C23 84(10) 91(11) 157(15) 12(10) 46(10) 17(8) C24 56(8) 149(15) 152(15) -24(12) 5(9) -22(8) O31 7(5) 78(7)	C12	62(6)	79(8)	48(6)	4(6)	26(5)	-4(6)	
C15 58(6) 67(7) 37(5) 0(5) 9(5) 2(5) C16 49(5) 53(7) 60(6) -1(5) 20(5) 2(5) C17 61(6) 69(7) 47(6) 9(6) 24(5) 20(6) C18 73(7) 71(8) 43(6) 15(6) 28(6) 8(6) C19 73(7) 50(7) 62(6) 0(5) 31(5) 4(6) C20 47(6) 89(10) 63(7) -9(7) 8(5) 4(7) C21 57(7) 116(12) 97(10) -8(9) 33(7) -7(8) C22 72(8) 121(13) 114(11) 30(9) 50(8) -7(7) C23 84(10) 91(11) 157(15) 12(10) 46(10) 17(8) C24 56(8) 149(15) 152(15) -24(12) 5(9) -22(8) O31 77(5) 78(7) 92(6) -2(5) 39(5) -4(5) O32 62(5) 95(6)	C13	48(5)	110(10)	49(6)	-16(6)	24(5)	-6(6)	
C16 49(5) 53(7) 60(6) -1(5) 20(5) 2(5) C17 61(6) 69(7) 47(6) 9(6) 24(5) 20(6) C18 73(7) 71(8) 43(6) 15(6) 28(6) 8(6) C19 73(7) 50(7) 62(6) 0(5) 31(5) 4(6) C20 47(6) 89(10) 63(7) -9(7) 8(5) 4(7) C21 57(7) 116(12) 97(10) -8(9) 33(7) -7(8) C22 72(8) 121(13) 114(11) 30(9) 50(8) -7(7) C23 84(10) 91(11) 157(15) 12(10) 46(10) 17(8) C24 56(8) 149(15) 152(15) -24(12) 5(9) -22(8) O31 77(5) 78(7) 92(6) -2(5) 39(5) -4(5) O32 62(5) 95(6) 85(6) 4(5) 18(5) -3(4) N31 58(5) 62(7) <td>C14</td> <td>71(7)</td> <td>55(7)</td> <td>62(6)</td> <td>-9(5)</td> <td>31(6)</td> <td>-6(5)</td> <td></td>	C14	71(7)	55(7)	62(6)	-9(5)	31(6)	-6(5)	
C17 61(6) 69(7) 47(6) 9(6) 24(5) 20(6) C18 73(7) 71(8) 43(6) 15(6) 28(6) 8(6) C19 73(7) 50(7) 62(6) 0(5) 31(5) 4(6) C20 47(6) 89(10) 63(7) -9(7) 8(5) 4(7) C21 57(7) 116(12) 97(10) -8(9) 33(7) -7(8) C22 72(8) 121(13) 114(11) 30(9) 50(8) -7(7) C23 84(10) 91(11) 157(15) 12(10) 46(10) 17(8) C24 56(8) 149(15) 152(15) -24(12) 5(9) -22(8) O31 77(5) 78(7) 92(6) -2(5) 39(5) -4(5) O32 62(5) 95(6) 85(6) 4(5) 18(5) -3(4) O33 78(5) 103(7) 82(6) 22(5) 35(5) 9(5) N31 58(5) 62(7) <td>C15</td> <td>58(6)</td> <td>67(7)</td> <td>37(5)</td> <td>0(5)</td> <td>9(5)</td> <td>2(5)</td> <td></td>	C15	58(6)	67(7)	37(5)	0(5)	9(5)	2(5)	
C18 73(7) 71(8) 43(6) 15(6) 28(6) 8(6) C19 73(7) 50(7) 62(6) 0(5) 31(5) 4(6) C20 47(6) 89(10) 63(7) -9(7) 8(5) 4(7) C21 57(7) 116(12) 97(10) -8(9) 33(7) -7(8) C22 72(8) 121(13) 114(11) 30(9) 50(8) -7(7) C23 84(10) 91(11) 157(15) 12(10) 46(10) 17(8) C24 56(8) 149(15) 152(15) -24(12) 5(9) -22(8) O31 77(5) 78(7) 92(6) -2(5) 39(5) -4(5) O32 62(5) 95(6) 85(6) 4(5) 18(5) -3(4) O33 78(5) 103(7) 82(6) 22(5) 35(5) 9(5) N31 58(5) 62(7) 57(5) -3(4) 17(5) -9(4) C31 56(7) 54(8) </td <td>C16</td> <td>49(5)</td> <td>53(7)</td> <td>60(6)</td> <td>-1(5)</td> <td>20(5)</td> <td>2(5)</td> <td></td>	C16	49(5)	53(7)	60(6)	-1(5)	20(5)	2(5)	
C19 73(7) 50(7) 62(6) 0(5) 31(5) 4(6) C20 47(6) 89(10) 63(7) -9(7) 8(5) 4(7) C21 57(7) 116(12) 97(10) -8(9) 33(7) -7(8) C22 72(8) 121(13) 114(11) 30(9) 50(8) -7(7) C23 84(10) 91(11) 157(15) 12(10) 46(10) 17(8) C24 56(8) 149(15) 152(15) -24(12) 5(9) -22(8) O31 77(5) 78(7) 92(6) -2(5) 39(5) -4(5) O32 62(5) 95(6) 85(6) 4(5) 18(5) -3(4) O33 78(5) 103(7) 82(6) 22(5) 35(5) 9(5) N31 58(5) 62(7) 57(5) -3(5) 16(4) -1(5) N32 66(6) 61(6) 59(5) -3(4) 17(5) -9(4) C31 56(7) 54(8)<	C17	61(6)	69(7)	47(6)	9(6)	24(5)	20(6)	
C20 47(6) 89(10) 63(7) -9(7) 8(5) 4(7) C21 57(7) 116(12) 97(10) -8(9) 33(7) -7(8) C22 72(8) 121(13) 114(11) 30(9) 50(8) -7(7) C23 84(10) 91(11) 157(15) 12(10) 46(10) 17(8) C24 56(8) 149(15) 152(15) -24(12) 5(9) -22(8) O31 77(5) 78(7) 92(6) -2(5) 39(5) -4(5) O32 62(5) 95(6) 85(6) 4(5) 18(5) -3(4) O33 78(5) 103(7) 82(6) 22(5) 35(5) 9(5) N31 58(5) 62(7) 57(5) -3(5) 16(4) -1(5) N32 66(6) 61(6) 59(5) -3(4) 17(5) -9(4) C31 56(7) 54(8) 80(8) -3(7) 18(6) 3(6) C32 65(6) 73(9)	C18	73(7)	71(8)	43(6)	15(6)	28(6)	8(6)	
C21 57(7) 116(12) 97(10) -8(9) 33(7) -7(8) C22 72(8) 121(13) 114(11) 30(9) 50(8) -7(7) C23 84(10) 91(11) 157(15) 12(10) 46(10) 17(8) C24 56(8) 149(15) 152(15) -24(12) 5(9) -22(8) O31 77(5) 78(7) 92(6) -2(5) 39(5) -4(5) O32 62(5) 95(6) 85(6) 4(5) 18(5) -3(4) O33 78(5) 103(7) 82(6) 22(5) 35(5) 9(5) N31 58(5) 62(7) 57(5) -3(5) 16(4) -1(5) N32 66(6) 61(6) 59(5) -3(4) 17(5) -9(4) C31 56(7) 54(8) 80(8) -3(7) 18(6) 3(6) C32 65(6) 73(9) 67(7) 3(6) 34(6) 2(6) C33 95(9) 77(10) 88(9) 4(7) 29(8) 1(8) C34 85(10)	C19	73(7)	50(7)	62(6)	0(5)	31(5)	4(6)	
C22 72(8) 121(13) 114(11) 30(9) 50(8) -7(7) C23 84(10) 91(11) 157(15) 12(10) 46(10) 17(8) C24 56(8) 149(15) 152(15) -24(12) 5(9) -22(8) O31 77(5) 78(7) 92(6) -2(5) 39(5) -4(5) O32 62(5) 95(6) 85(6) 4(5) 18(5) -3(4) O33 78(5) 103(7) 82(6) 22(5) 35(5) 9(5) N31 58(5) 62(7) 57(5) -3(5) 16(4) -1(5) N32 66(6) 61(6) 59(5) -3(4) 17(5) -9(4) C31 56(7) 54(8) 80(8) -3(7) 18(6) 3(6) C32 65(6) 73(9) 67(7) 3(6) 34(6) 2(6) C33 95(9) 77(10) 88(9) 4(7) 29(8) 1(8) C34 85(10) 95(11) <td>C20</td> <td>47(6)</td> <td>89(10)</td> <td>63(7)</td> <td>-9(7)</td> <td>8(5)</td> <td>4(7)</td> <td></td>	C20	47(6)	89(10)	63(7)	-9(7)	8(5)	4(7)	
C23 84(10) 91(11) 157(15) 12(10) 46(10) 17(8) C24 56(8) 149(15) 152(15) -24(12) 5(9) -22(8) O31 77(5) 78(7) 92(6) -2(5) 39(5) -4(5) O32 62(5) 95(6) 85(6) 4(5) 18(5) -3(4) O33 78(5) 103(7) 82(6) 22(5) 35(5) 9(5) N31 58(5) 62(7) 57(5) -3(5) 16(4) -1(5) N32 66(6) 61(6) 59(5) -3(4) 17(5) -9(4) C31 56(7) 54(8) 80(8) -3(7) 18(6) 3(6) C32 65(6) 73(9) 67(7) 3(6) 34(6) 2(6) C33 95(9) 77(10) 88(9) 4(7) 29(8) 1(8) C34 85(10) 95(11) 126(14) -6(10) 35(9) 12(8) C35 53(7) 70(9) 96(10) -13(8) 10(7) -6(6) C36 64(9)	C21	57(7)	116(12)	97(10)	-8(9)	33(7)	−7(8)	
C24 56(8) 149(15) 152(15) -24(12) 5(9) -22(8) O31 77(5) 78(7) 92(6) -2(5) 39(5) -4(5) O32 62(5) 95(6) 85(6) 4(5) 18(5) -3(4) O33 78(5) 103(7) 82(6) 22(5) 35(5) 9(5) N31 58(5) 62(7) 57(5) -3(5) 16(4) -1(5) N32 66(6) 61(6) 59(5) -3(4) 17(5) -9(4) C31 56(7) 54(8) 80(8) -3(7) 18(6) 3(6) C32 65(6) 73(9) 67(7) 3(6) 34(6) 2(6) C33 95(9) 77(10) 88(9) 4(7) 29(8) 1(8) C34 85(10) 95(11) 126(14) -6(10) 35(9) 12(8) C35 53(7) 70(9) 96(10) -13(8) 10(7) -6(6) C36 64(9) 128(14)	C22	72(8)	121(13)	114(11)	30(9)	50(8)	-7(7)	
O31 77(5) 78(7) 92(6) -2(5) 39(5) -4(5) O32 62(5) 95(6) 85(6) 4(5) 18(5) -3(4) O33 78(5) 103(7) 82(6) 22(5) 35(5) 9(5) N31 58(5) 62(7) 57(5) -3(5) 16(4) -1(5) N32 66(6) 61(6) 59(5) -3(4) 17(5) -9(4) C31 56(7) 54(8) 80(8) -3(7) 18(6) 3(6) C32 65(6) 73(9) 67(7) 3(6) 34(6) 2(6) C33 95(9) 77(10) 88(9) 4(7) 29(8) 1(8) C34 85(10) 95(11) 126(14) -6(10) 35(9) 12(8) C35 53(7) 70(9) 96(10) -13(8) 10(7) -6(6) C36 64(9) 128(14) 155(16) -80(12) 36(10) 4(9) C37 76(9) 190(19) 80(10) -55(12) 23(8) -24(11) C38 55(7)	C23	84(10)	91(11)	157(15)	12(10)	46(10)	17(8)	
O32 62(5) 95(6) 85(6) 4(5) 18(5) -3(4) O33 78(5) 103(7) 82(6) 22(5) 35(5) 9(5) N31 58(5) 62(7) 57(5) -3(5) 16(4) -1(5) N32 66(6) 61(6) 59(5) -3(4) 17(5) -9(4) C31 56(7) 54(8) 80(8) -3(7) 18(6) 3(6) C32 65(6) 73(9) 67(7) 3(6) 34(6) 2(6) C33 95(9) 77(10) 88(9) 4(7) 29(8) 1(8) C34 85(10) 95(11) 126(14) -6(10) 35(9) 12(8) C35 53(7) 70(9) 96(10) -13(8) 10(7) -6(6) C36 64(9) 128(14) 155(16) -80(12) 36(10) 4(9) C37 76(9) 190(19) 80(10) -55(12) 23(8) -24(11) C38 55(7) 116(11) 56(7) 8(7) 10(6) 14(7) C39 53(7)	C24	56(8)	149(15)	152(15)	-24(12)	5(9)	-22(8)	
O33 78(5) 103(7) 82(6) 22(5) 35(5) 9(5) N31 58(5) 62(7) 57(5) -3(5) 16(4) -1(5) N32 66(6) 61(6) 59(5) -3(4) 17(5) -9(4) C31 56(7) 54(8) 80(8) -3(7) 18(6) 3(6) C32 65(6) 73(9) 67(7) 3(6) 34(6) 2(6) C33 95(9) 77(10) 88(9) 4(7) 29(8) 1(8) C34 85(10) 95(11) 126(14) -6(10) 35(9) 12(8) C35 53(7) 70(9) 96(10) -13(8) 10(7) -6(6) C36 64(9) 128(14) 155(16) -80(12) 36(10) 4(9) C37 76(9) 190(19) 80(10) -55(12) 23(8) -24(11) C38 55(7) 116(11) 56(7) 8(7) 10(6) 14(7) C39 53(7) 80(9) 50(6) 15(6) 26(6) 25(6) C40 70(8)	031	77(5)	78(7)	92(6)	-2(5)	39(5)	-4(5)	
N31 58(5) 62(7) 57(5) -3(5) 16(4) -1(5) N32 66(6) 61(6) 59(5) -3(4) 17(5) -9(4) C31 56(7) 54(8) 80(8) -3(7) 18(6) 3(6) C32 65(6) 73(9) 67(7) 3(6) 34(6) 2(6) C33 95(9) 77(10) 88(9) 4(7) 29(8) 1(8) C34 85(10) 95(11) 126(14) -6(10) 35(9) 12(8) C35 53(7) 70(9) 96(10) -13(8) 10(7) -6(6) C36 64(9) 128(14) 155(16) -80(12) 36(10) 4(9) C37 76(9) 190(19) 80(10) -55(12) 23(8) -24(11) C38 55(7) 116(11) 56(7) 8(7) 10(6) 14(7) C39 53(7) 80(9) 50(6) 15(6) 26(6) 25(6) C40 70(8) 92(10) 128(12) 7(9) 41(8) -4(7) C161 72(2) 96(2) 55(2) 18(2) 19(1) -2(2)	032	62(5)	95(6)	85(6)	4(5)	18(5)	-3(4)	
N32 66(6) 61(6) 59(5) -3(4) 17(5) -9(4) C31 56(7) 54(8) 80(8) -3(7) 18(6) 3(6) C32 65(6) 73(9) 67(7) 3(6) 34(6) 2(6) C33 95(9) 77(10) 88(9) 4(7) 29(8) 1(8) C34 85(10) 95(11) 126(14) -6(10) 35(9) 12(8) C35 53(7) 70(9) 96(10) -13(8) 10(7) -6(6) C36 64(9) 128(14) 155(16) -80(12) 36(10) 4(9) C37 76(9) 190(19) 80(10) -55(12) 23(8) -24(11) C38 55(7) 116(11) 56(7) 8(7) 10(6) 14(7) C39 53(7) 80(9) 50(6) 15(6) 26(6) 25(6) C40 70(8) 92(10) 128(12) 7(9) 41(8) -4(7) C161 72(2) 96(2) 55(2) 18(2) 19(1) -2(2)	033	78(5)	103(7)	82(6)	22(5)	35(5)	9(5)	
C31 56(7) 54(8) 80(8) -3(7) 18(6) 3(6) C32 65(6) 73(9) 67(7) 3(6) 34(6) 2(6) C33 95(9) 77(10) 88(9) 4(7) 29(8) 1(8) C34 85(10) 95(11) 126(14) -6(10) 35(9) 12(8) C35 53(7) 70(9) 96(10) -13(8) 10(7) -6(6) C36 64(9) 128(14) 155(16) -80(12) 36(10) 4(9) C37 76(9) 190(19) 80(10) -55(12) 23(8) -24(11) C38 55(7) 116(11) 56(7) 8(7) 10(6) 14(7) C39 53(7) 80(9) 50(6) 15(6) 26(6) 25(6) C40 70(8) 92(10) 128(12) 7(9) 41(8) -4(7) C161 72(2) 96(2) 55(2) 18(2) 19(1) -2(2)	N31	58(5)	62(7)	57(5)	-3(5)	16(4)	-1(5)	
C32 65(6) 73(9) 67(7) 3(6) 34(6) 2(6) C33 95(9) 77(10) 88(9) 4(7) 29(8) 1(8) C34 85(10) 95(11) 126(14) -6(10) 35(9) 12(8) C35 53(7) 70(9) 96(10) -13(8) 10(7) -6(6) C36 64(9) 128(14) 155(16) -80(12) 36(10) 4(9) C37 76(9) 190(19) 80(10) -55(12) 23(8) -24(11) C38 55(7) 116(11) 56(7) 8(7) 10(6) 14(7) C39 53(7) 80(9) 50(6) 15(6) 26(6) 25(6) C40 70(8) 92(10) 128(12) 7(9) 41(8) -4(7) C161 72(2) 96(2) 55(2) 18(2) 19(1) -2(2)	N32	66(6)	61(6)	59(5)	-3(4)	17(5)	-9(4)	
C33 95(9) 77(10) 88(9) 4(7) 29(8) 1(8) C34 85(10) 95(11) 126(14) -6(10) 35(9) 12(8) C35 53(7) 70(9) 96(10) -13(8) 10(7) -6(6) C36 64(9) 128(14) 155(16) -80(12) 36(10) 4(9) C37 76(9) 190(19) 80(10) -55(12) 23(8) -24(11) C38 55(7) 116(11) 56(7) 8(7) 10(6) 14(7) C39 53(7) 80(9) 50(6) 15(6) 26(6) 25(6) C40 70(8) 92(10) 128(12) 7(9) 41(8) -4(7) C161 72(2) 96(2) 55(2) 18(2) 19(1) -2(2)	C31	56(7)	54(8)	80(8)	-3(7)	18(6)	3(6)	
C34 85(10) 95(11) 126(14) -6(10) 35(9) 12(8) C35 53(7) 70(9) 96(10) -13(8) 10(7) -6(6) C36 64(9) 128(14) 155(16) -80(12) 36(10) 4(9) C37 76(9) 190(19) 80(10) -55(12) 23(8) -24(11) C38 55(7) 116(11) 56(7) 8(7) 10(6) 14(7) C39 53(7) 80(9) 50(6) 15(6) 26(6) 25(6) C40 70(8) 92(10) 128(12) 7(9) 41(8) -4(7) C161 72(2) 96(2) 55(2) 18(2) 19(1) -2(2)	C32	65(6)	73(9)	67(7)	3(6)	34(6)	2(6)	
C35 53(7) 70(9) 96(10) -13(8) 10(7) -6(6) C36 64(9) 128(14) 155(16) -80(12) 36(10) 4(9) C37 76(9) 190(19) 80(10) -55(12) 23(8) -24(11) C38 55(7) 116(11) 56(7) 8(7) 10(6) 14(7) C39 53(7) 80(9) 50(6) 15(6) 26(6) 25(6) C40 70(8) 92(10) 128(12) 7(9) 41(8) -4(7) C161 72(2) 96(2) 55(2) 18(2) 19(1) -2(2)	C33	95(9)	77(10)	88(9)	4(7)	29(8)	1(8)	
C36 64(9) 128(14) 155(16) -80(12) 36(10) 4(9) C37 76(9) 190(19) 80(10) -55(12) 23(8) -24(11) C38 55(7) 116(11) 56(7) 8(7) 10(6) 14(7) C39 53(7) 80(9) 50(6) 15(6) 26(6) 25(6) C40 70(8) 92(10) 128(12) 7(9) 41(8) -4(7) C161 72(2) 96(2) 55(2) 18(2) 19(1) -2(2)	C34	85(10)	95(11)	126(14)	-6(10)	35(9)	12(8)	
C37 76(9) 190(19) 80(10) -55(12) 23(8) -24(11) C38 55(7) 116(11) 56(7) 8(7) 10(6) 14(7) C39 53(7) 80(9) 50(6) 15(6) 26(6) 25(6) C40 70(8) 92(10) 128(12) 7(9) 41(8) -4(7) C161 72(2) 96(2) 55(2) 18(2) 19(1) -2(2)	C35	53(7)	70(9)	96(10)	-13(8)	10(7)	-6(6)	
C38 55(7) 116(11) 56(7) 8(7) 10(6) 14(7) C39 53(7) 80(9) 50(6) 15(6) 26(6) 25(6) C40 70(8) 92(10) 128(12) 7(9) 41(8) -4(7) Cl61 72(2) 96(2) 55(2) 18(2) 19(1) -2(2)	C36	64(9)	128(14)	155(16)	-80(12)	36(10)	4(9)	
C39 53(7) 80(9) 50(6) 15(6) 26(6) 25(6) C40 70(8) 92(10) 128(12) 7(9) 41(8) -4(7) Cl61 72(2) 96(2) 55(2) 18(2) 19(1) -2(2)	C37	76(9)	190(19)	80(10)	-55(12)	23(8)	-24(11)	
C40 70(8) 92(10) 128(12) 7(9) 41(8) -4(7) Cl61 72(2) 96(2) 55(2) 18(2) 19(1) -2(2)	C38	55(7)	116(11)	56(7)	8(7)	10(6)	14(7)	
Cl61 72(2) 96(2) 55(2) 18(2) 19(1) -2(2)	C39	53(7)	80(9)	50(6)	15(6)	26(6)	25(6)	
	C40	70(8)	92(10)	128(12)	7(9)	41(8)	-4(7)	
O91 74(5) 92(6) 73(5) 7(5) 27(4) 3(5)	Cl61	72(2)	96(2)	55(2)	18(2)	19(1)	-2(2)	
	091	74(5)	92(6)	73(5)	7(5)	27(4)	3(5)	

Table 5. Hydrogen coordinates $[\times~10^4]$ and isotropic displacement parameters $[\mathring{A}^2\times10^3]$.

Atom	Х	у	Z	U_{eq}	S.o.f.	
H2	4963	6666	8310	59	1	
п2 Н4					1	
	8105	1753	9338	80 73	1	
H1	4333	8174	5423	72 84		
H2A	3240	10983	4817	84	1	
H2B	2750	9011	4805	84	1	
H3A	1727	10593	5339	81	1	
H3B	2646	11895	5741	81	1	
H4A	2317	8231	6071	68	1	
H5A	1877	10182	6866	71	1	
H5B	2968	11165	7016	71	1	
H6A	2672	7481	7334	67 67	1	
H6B	2994	9039	7910	67 55	1	
H7	4572	9237	7799	55 56	1	
H10	4538	2342	7786	56	1	
H11A	2922	3645	8133	67	1	
H11B	3423	1731	8414	67	1	
H12A	3829	5120	9146	73 - 3	1	
H12B	3574	3232	9467	73	1	
H13	5051	1981	9392	80	1	
H14A	5601	3616	10377	72	1	
H14B	5806	5319	9934	72	1	
H15A	6799	1903	9958	65	1	
H15B	7341	3641	10376	65	1	
H16	7296	5157	9353	63	1	
H19A	5380	14292	5949	89	1	
H19B	6300	12932	6270	89	1	
H19C	5726	13916	6778	89	1	
H22A	10145	3705	7945	147	1	
H22B	11265	4418	8336	147	1	
H22C	10278	5483	8418	147	1	
H23A	11182	813	9421	162	1	
H23B	11776	1700	8904	162	1	
H23C	10704	712	8587	162	1	
H24A	10560	5101	9759	185	1	
H24B	11685	4457	9759	185	1	
H24C	10976	3190	10085	185	1	
H32A	3466	2339	2502	74	1	
H32B	2900	2475	1746	74	1	
H32C	2679	976	2182	74	1	
H32	1434	3228	1967	78	1	
H33A	2429	5699	2029	103	1	
H33B	3059	5253	2821	103	1	
H34A	928	6085	2419	121	1	
H34B	1800	7502	2782	121	1	
H35	2271	5822	3800	90	1	
H36A	896	7179	4042	137	1	
H36B	90	6070	3440	137	1	

H37A	1294	4721	4762	138	1
H37B	90	4401	4416	138	1
H38	1471	2068	4301	92	1
H40A	-1153	-1526	3949	141	1
H40B	-1145	-7 95	3188	141	1
H40C	-1689	348	3673	141	1
H91A	3340	4768	5892	118	1
H91B	3436	5004	5214	118	1

Table 6. Torsion angles [°].

O2-C9-C10-N3	162.6(8)
O2-C9-C10-C11	-81.1(11)
N1-C1-C2-C3	21.6(11)
N1-C1-C18-O4	153.2(9)
N1-C1-C18-O5	-29.3(12)
N1-C4-C5-C6	-55.5(11)
N2-C7-C8-O1	-46.2(12)
N2-C7-C8-N1	141.9(8)
N2-C9-C10-N3	-25.5(12)
N2-C9-C10-C11	90.8(10)
N3-C10-C11-C12	23.0(10)
N3-C13-C14-C15	-51.9(13)
N4-C16-C17-O3	-41.0(14)
N4-C16-C17-N3	148.8(9)
C1-N1-C4-C3	-21.2(11)
C1-N1-C4-C5	-147.1(9)
C1-N1-C8-O1	-2.5(13)
C1-N1-C8-C7	169.7(9)
C1-C2-C3-C4	-35.1(12)
C2-C1-C18-O4	-93.6(12)
C2-C1-C18-O5	83.9(10)
C2-C3-C4-N1	33.4(10)
C2-C3-C4-C5	153.9(9)
C3-C4-C5-C6	-171.3(9)
C4-N1-C1-C2	0.1(11)
C4-N1-C1-C18	119.0(9)
C4-N1-C8-O1	174.8(9)
C4-N1-C8-C7	-13.1(13)
C4-C5-C6-C7	58.3(11)
C5-C6-C7-N2	-164.2(8)
C5-C6-C7-C8	-36.3(12)
C6-C7-C8-O1	-175.2(9)

C6-C7-C8-N1	12.9(13)
C7-N2-C9-O2	3.8(14)
C7-N2-C9-C10	-167.7(8)
C8-N1-C1-C2	177.6(9)
C8-N1-C1-C18	-63.5(12)
C8-N1-C4-C3	161.4(9)
C8-N1-C4-C5	35.5(13)
C9-N2-C7-C6	70.7(11)
C9-N2-C7-C8	-59.7(11)
C9-C10-C11-C12	-100.3(9)
C10-N3-C13-C12	-25.6(12)
C10-N3-C13-C14	-162.5(9)
C10-N3-C17-O3	8.8(17)
C10-N3-C17-C16	178.7(8)
C10-C11-C12-C13	-38.0(11)
C11-C12-C13-N3	38.5(11)
C11-C12-C13-C14	169.8(11)
C12-C13-C14-C15	-179.0(11)
C13-N3-C10-C9	122.3(9)
C13-N3-C10-C11	1.4(11)
C13-N3-C17-O3	173.6(11)
C13-N3-C17-C16	-16.5(16)
C13-C14-C15-C16	61.4(11)
C14-C15-C16-N4	-171.2(8)
C14-C15-C16-C17	-47.7(12)
C15-C16-C17-O3	-164.9(10)
C15-C16-C17-N3	24.8(14)
C16-N4-C20-O6	6.5(17)
C16-N4-C20-O7	-175.1(8)
C17-N3-C10-C9	-71.0(12)
C17-N3-C10-C11	168.1(9)
C17-N3-C13-C12	168.2(10)
C17-N3-C13-C14	31.4(15)
C18-C1-C2-C3	-97.2(10)
C19-O5-C18-O4	2.5(14)
C19-O5-C18-C1	-174.9(8)
C20-07-C21-C22	-68.1(15)
C20-07-C21-C23	174.3(11)
C20-O7-C21-C24	60.0(15)
C20-N4-C16-C15	-139.1(10)
C20-N4-C16-C17	95.4(12)
C21-O7-C20-O6	18.9(17)
C21-O7-C20-N4	-159.5(10)
O31-C31-C32-N32	-36.3(14)
O31-C31-C32-C33	-161.7(11)
N31-C31-C32-N32	149.8(9)
N31-C31-C32-C33	24.4(14)
N31-C35-C36-C37	36.2(13)
N31-C38-C39-O32	-40.3(15)

N31-C38-C39-O33	146.0(9)
N32-C32-C33-C34	-173.7(11)
C31-N31-C35-C34	27.2(14)
C31-N31-C35-C36	156.4(11)
C31-N31-C38-C37	-178.3(10)
C31-N31-C38-C39	-58.7(13)
C31-C32-C33-C34	-49.6(15)
C32-C33-C34-C35	64.1(14)
C33-C34-C35-N31	-50.4(13)
C33-C34-C35-C36	-166.2(11)
C34-C35-C36-C37	156.5(13)
C35-N31-C31-O31	172.6(10)
C35-N31-C31-C32	-13.6(15)
C35-N31-C38-C37	1.9(12)
C35-N31-C38-C39	121.6(10)
C35-C36-C37-C38	-36.8(14)
C36-C37-C38-N31	21.2(14)
C36-C37-C38-C39	-96.1(13)
C37-C38-C39-O32	76.0(15)
C37-C38-C39-O33	-97.7(13)
C38-N31-C31-O31	−7.1(17)
C38-N31-C31-C32	166.7(9)
C38-N31-C35-C34	-153.1(9)
C38-N31-C35-C36	-23.9(12)
C40-O33-C39-O32	2.0(15)
C40-O33-C39-C38	175.7(9)

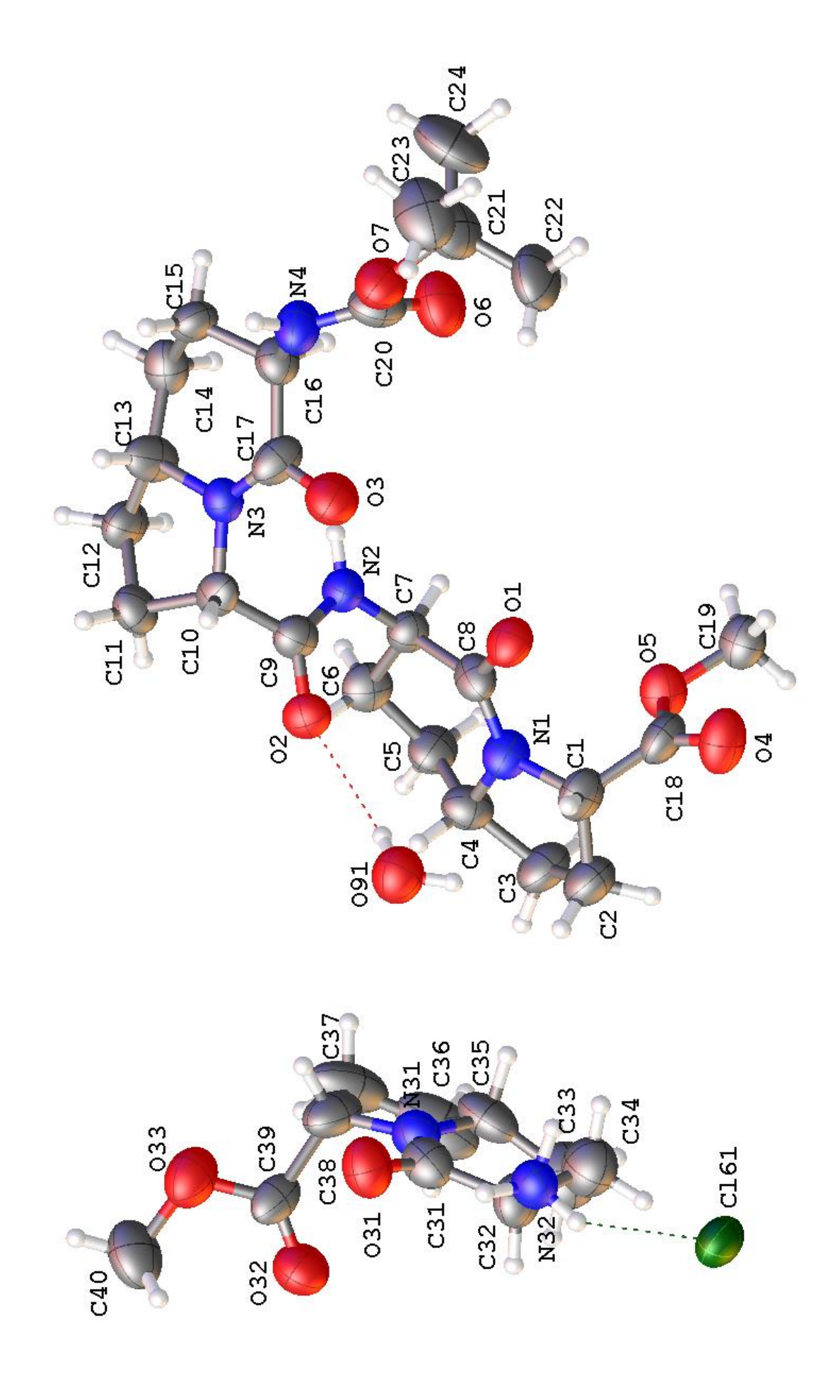
Symmetry transformations used to generate equivalent atoms:

Table 7. Hydrogen bonds [Å and °].

D−H···A	d(D-H)	<i>d</i> (H <i>···A</i>)	$d(D\cdots A)$	∠(DHA)	
N2-H2···Cl61 ⁱ	0.88	2.48	3.206(9)	140.3	
N32-H32A···O1 ⁱⁱ	0.91	1.89	2.793(11)	173.4	
N32-H32BCl61	0.91	2.31	3.151(9)	154.3	
N32-H32C···O3 ⁱⁱ	0.91	2.17	2.813(12)	127.3	
O91-H91A···O2	0.85	2.11	2.893(11)	152.4	
O91–H91B···O4 ⁱⁱ	0.85	2.10	2.892(11)	155.8	

Symmetry transformations used to generate equivalent atoms:

⁽i) -x+1,y+1/2,-z+1 (ii) -x+1,y-1/2,-z+1



References

- 1. R. Mueller, L. Revesz, *Tetrahedron Letters* **1994**, *35*, 4091-4092.
- a) C. J. Andres, T. L. Macdonald, T. D. Ocain, D. Longhi, *The Journal of Organic Chemistry* **1993**, *58*, 6609-6613.
 - b) J. T. Welch, J. Lin, Tetrahedron 1996, 52, 291-304.
- 3. B. Witkop, Y. Fujimoto, F. Irreverre, J. M. Karle, I. L. Karle, *Journal of the American Chemical Society* **1971**, *93*, 3471-3477.
- 4. J. J. Cunningham, R. A. Gatenby, J. S. Brown, *Molecular Pharmaceutics* **2011**, *8*, 2094-2100.
- 5. A. Grauer, B. König, European Journal of Organic Chemistry 2009, 2009, 5099-5111.
- Paolo Ruzza (2012). Peptides and Peptidomimetics in Medicinal Chemistry, Medicinal Chemistry and Drug Design, Prof. Deniz Ekinci (Ed.), ISBN: 978-953-51-0513-8, InTech, DOI: 10.5772/38240.
- 7. J. Gante, Angewandte Chemie International Edition in English 1994, 33, 1699-1720.
- 8. P. W. Schiller, G. Weltrowska, I. Berezowska, T. M. D. Nguyen, B. C. Wilkes, C. Lemieux, N. N. Chung, *Peptide Science* **1999**, *51*, 411-425.
- 9. J. Gante, M. Krug, G. Lauterbach, R. Weitzel, W. Hiller, *Journal of Peptide Science* **1995**, *1*, 201-206.
- Z. Xu, J. Singh, M. D. Schwinden, B. Zheng, T. P. Kissick, B. Patel, M. J. Humora, F. Quiroz, L. Dong, D.-M. Hsieh, J. E. Heikes, M. Pudipeddi, M. D. Lindrud, S. K. Srivastava, D. R. Kronenthal, R. H. Mueller, *Organic Process Research & Development* 2002, 6, 323-328.
- 11. A. S. Verdini, S. Silvestri, C. Becherucci, M. G. Longobardi, L. Parente, S. Peppoloni, M. Perretti, P. Pileri, M. Pinori, *Journal of Medicinal Chemistry* **1991**, *34*, 3372-3379.
- L. Gentilucci, G. Cardillo, F. Squassabia, A. Tolomelli, S. Spampinato, A. Sparta, M. Baiula, *Bioorganic & Medicinal Chemistry Letters* 2007, 17, 2329-2333.

- 13. M. Eguchi, *Medicinal Research Reviews* **2004**, *24*, 182-212.
- 14. C. Gilon, M. A. Dechantsreiter, F. Burkhart, A. Friedler, H. Kessler, *Synthesis of N-Alkylated Peptides*, in: *Methods of Organic Chemistry: Synthesis of Peptides and Peptidomimetics* (Ed.: M. Goodman), Thieme, Stuttgart, New York, **2003**, vol. E22c, p. 215-271.
- 15. A. Rüegger, M. Kuhn, H. Lichti, H.-R. Loosli, R. Huguenin, C. Quiquerez, A. von Wartburg, *Helvetica Chimica Acta* **1976**, *59*, 1075-1092.
- 16. L. Aurelio, R. T. C. Brownlee, A. B. Hughes, *Chemical Reviews* **2004**, *104*, 5823-5846.
- 17. M. Miyoshi, H. Sugano, in: Peptides 1974, (Ed.: Y. Wolman), John Wiley & Sons, New York, 1974, p. 355
- 18. a) M. I. Calaza, C. Cativiela, European Journal of Organic Chemistry 2008, 2008, 3427-3448.
 - b) M. Tanaka, Chemical and Pharmaceutical Bulletin 2007, 55, 349-358.
- 19. S. Sagan, P. Karoyan, O. Lequin, G. Chassaing, S. Lavielle, *Current Medicinal Chemistry* **2004**, *11*, 2799-2822.
- 20. Y. Ohfune, T. Shinada, European Journal of Organic Chemistry 2005, 2005, 5127-5143.
- 21. C. Haskell-Luevano, K. Toth, L. Boteju, C. Job, A. M. d. L. Castrucci, M. E. Hadley, V. J. Hruby, *Journal of Medicinal Chemistry* **1997**, *40*, 2740-2749.
- 22. R. W. Newberry, B. VanVeller, I. A. Guzei, R. T. Raines, *Journal of the American Chemical Society* **2013**, *135*, 7843-7846.
- 23. M. W. MacArthur, J. M. Thornton, Journal of Molecular Biology 1991, 218, 397-412.
- 24. P. Thamm, H. J. Musiol, L. Moroder, Synthesis of Peptides Containing Proline

 Analogues, in: Methods of Organic Chemistry: Synthesis of Peptides and

- Peptidomimetics (Ed.: M. Goodman), Thieme, Stuttgart, New York, **2003**, vol. E22c, p.52-86.
- 25. M. Doi, Y. Nishi, S. Uchiyama, Y. Nishiuchi, H. Nishio, T. Nakazawa, T. Ohkubo, Y. Kobayashi, *Journal of Peptide Science* **2005**, *11*, 609-616.
- 26. Y. Nishi, S. Uchiyama, M. Doi, Y. Nishiuchi, T. Nakazawa, T. Ohkubo, Y. Kobayashi, *Biochemistry* **2005**, *44*, 6034-6042.
- 27. D. Seebach, A. K. Beck, S. Capone, G. Deniau, U. Grošelj, E. Zass, *Synthesis* **2009**, *2009*, 1-32.
- 28. C.-B. Xue, X. He, J. Roderick, R. L. Corbett, C. P. Decicco, *The Journal of Organic Chemistry* **2002**, *67*, 865-870.
- 29. G. Cardillo, L. Gentilucci *, P. Melchiorre, S. Spampinato, *Bioorganic & Medicinal Chemistry Letters* **2000**, *10*, 2755-2758.
- V. Tørfoss, J. Isaksson, D. Ausbacher, B.-O. Brandsdal, G. E. Flaten, T. Anderssen, C. d.
 A. Cavalcanti-Jacobsen, M. Havelkova, L. T. Nguyen, H. J. Vogel, M. B. Strøm, *Journal of Peptide Science* 2012, 18, 609-619.
- 31. S. M. Condon, I. Morize, S. Darnbrough, C. J. Burns, B. E. Miller, J. Uhl, K. Burke, N. Jariwala, K. Locke, P. H. Krolikowski, N. V. Kumar, R. F. Labaudiniere, *Journal of the American Chemical Society* **2000**, *122*, 3007-3014.
- L. D. Walensky, A. L. Kung, I. Escher, T. J. Malia, S. Barbuto, R. D. Wright, G. Wagner, G.
 L. Verdine, S. J. Korsmeyer, *Science* 2004, *305*, 1466-1470
- 33. K. A. Carpenter, P. W. Schiller, R. Schmidt, B. C. Wilkes, *International Journal of Peptide* and *Protein Research* **1996**, *48*, 102-111.
- 34. B. P. Orner, J. T. Ernst, A. D. Hamilton, *Journal of the American Chemical Society* **2001**, *123*, 5382-5383.
- 35. O. Kutzki, H. S. Park, J. T. Ernst, B. P. Orner, H. Yin, A. D. Hamilton, *Journal of the American Chemical Society* **2002**, *124*, 11838-11839.
- 36. J. S. Nowick, M. Pairish, I. Q. Lee, D. L. Holmes, J. W. Ziller, *Journal of the American Chemical Society* **1997**, *119*, 5413-5424.

- 37. a) A. A. Virgilio, J. A. Ellman, *Journal of the American Chemical Society* **1994**, *116*, 11580-11581.
 - b) A. A. Virgilio, A. A. Bray, W. Zhang, T. Lon, M. Snyder, M. M. Morrissey, J. A. Ellman, *Tetrahedron* **1997**, *53*, 6635-6644.
- 38. A. K. Koutras, G. Fountzilas, T. Makatsoris, S. Peroukides, H. P. Kalofonos, *Cancer Treatment Reviews* **2010**, *36*, 75-82.
- 39. H. Warenius, J. Kilburn, J. Essex, R. Maurer, J. Blaydes, U. Agarwala, L. Seabra, *Molecular Cancer* **2011**, *10*, 72.
- T. Honma, T. Yoshizumi, N. Hashimoto, K. Hayashi, N. Kawanishi, K. Fukasawa, T. Takaki,
 C. Ikeura, M. Ikuta, I. Suzuki-Takahashi, T. Hayama, S. Nishimura, H. Morishima, *Journal of Medicinal Chemistry* 2001, 44, 4628-4640.
- 41. T. M. Sielecki, J. F. Boylan, P. A. Benfield, G. L. Trainor, *Journal of Medicinal Chemistry* **2000**, *43*, 1-18.
- 42. M. D. Garrett, A. Fattaey, *Current Opinion in Genetics & amp; Development* **1999**, *9*, 104-111.
- 43. G. M. Cooper, E. R. Hausman, The Cell; A molecular approach: **2004**; Third Edition.
- 44. S. L. Warenius HM, Maw P, Int J Cancer **1996**, *67*, 224-231.
- 45. a) L. Seabra, H. Warenius, *European Journal of Cancer* **2007**, *43*, 1483-1492.
 - b) S. L. Warenius HM, Maw P, Int J Cancer 1996, 67, 224-231.
- P. J. Day, A. Cleasby, I. J. Tickle, M. O'Reilly, J. E. Coyle, F. P. Holding, R. L. McMenamin,
 J. Yon, R. Chopra, C. Lengauer, H. Jhoti, *Proceedings of the National Academy of Sciences of the United States of America* 2009, 106, 4166-4170.
- 47. a) N. J. Leonard,. In The alkaloids; R. H. F. Manske, H. L. Holmes, Eds.; Academic Press: New York, 1953; Vol. 3, pp 119-199.
 - b) E. Marrière, J. Rouden, V. Tadino, M.-C. Lasne, Organic Letters 2000, 2, 1121-1124.

- 48. T. R. Govindachari, S. Rajadurai, M. Subramanian, B. S. Thyagarajan, *Journal of the Chemical Society (Resumed)* **1957**, 3839-3844.
- 49. J. Rouden, A. Ragot, S. Gouault, D. Cahard, J. C. Plaquevent, M. C. Lasne, *Tetrahedron: Asymmetry* **2002**, *13*, 1299-1305.
- 50. P. Imming, P. Klaperski, M. T. Stubbs, G. Seitz, D. Gündisch, *European Journal of Medicinal Chemistry* **2001**, *36*, 375-388.
- 51. M. S. Bernatowicz, Y. Wu, G. R. Matsueda, *Tetrahedron Letters* **1993**, *34*, 3389-3392.
- 52. A. Pechenov, M. E. Stefanova, R. A. Nicholas, S. Peddi, W. G. Gutheil, *Biochemistry* **2002**, 42, 579-588.
- 53. J. De Las Rivas, C. Fontanillo, *PLoS Comput Biol* **2010**, *6*, e1000807.
- 54. E. Klussman, J. Scott, Protein-Protein interactions as New Drug Target 2008, 414.
- 55. A. A. Adzhubei, M. J. E. Sternberg, A. A. Makarov, *Journal of Molecular Biology* **2013**, 425, 2100-2132.
- 56. A. E. Counterman, D. E. Clemmer, *The Journal of Physical Chemistry B* **2004**, *108*, 4885-4898.
- 57. B. Bochicchio, A. M. Tamburro, *Chirality* **2002**, *14*, 782-792.
- 58. K. Ma, L.-s. Kan, K. Wang, *Biochemistry* **2001**, *40*, 3427-3438.
- 59. B. J. Stapley, T. P. Creamer, *Protein Science* **1999**, *8*, 587-595.
- 60. D. J. Witter, S. J. Famiglietti, J. C. Cambier, A. L. Castelhano, *Bioorganic & Medicinal Chemistry Letters* **1998**, *8*, 3137-3142.
- 61. a) P. Tremmel, A. Geyer, Journal of the American Chemical Society **2002**, 124, 8548-8549.
 - b) P. Tremmel, A. Geyer, Angewandte Chemie 2004, 116, 5913-5915.
- J. Zaminer, C. Brockmann, P. Huy, R. Opitz, C. Reuter, M. Beyermann, C. Freund, M. Müller, H. Oschkinat, R. Kühne, H.-G. Schmalz, *Angewandte Chemie International Edition* 2010, 49, 7111-7115.

- 63. B. Raghavan, K. J. Skoblenick, S. Bhagwanth, N. Argintaru, R. K. Mishra, R. L. Johnson, *Journal of Medicinal Chemistry* **2009**, *52*, 2043-2051.
- 64. a) B. K. Kay, M. P. Williamson, M. Sudol, *The FASEB Journal* **2000**, *14*, 231-241.
 - b) B. Zagrovic, J. Lipfert, E. J. Sorin, I. S. Millett, W. F. van Gunsteren, S. Doniach, V. S. Pande, *Proceedings of the National Academy of Sciences of the United States of America* **2005**, *102*, 11698-11703.
- 65. J. S. Petersen, G. Fels, H. Rapoport, *Journal of the American Chemical Society* **1984**, *106*, 4539-4547.
- M. Angiolini, S. Araneo, L. Belvisi, E. Cesarotti, A. Checchia, L. Crippa, L. Manzoni, C. Scolastico, European Journal of Organic Chemistry 2000, 2000, 2571-2581.
- 67. B. J. Mayer, D. Baltimore, *Trends in Cell Biology* **1993**, *3*, 8-13.
- 68. a) P. Cicchetti, B. Mayer, G. Thiel, D. Baltimore, *Science* **1992**, *257*, 803-806.
 - b) R. Ren, B. Mayer, P. Cicchetti, D. Baltimore, *Science* **1993**, *259*, 1157-1161.
 - c) A. Musacchio, M. Saraste, M. Wilsmanns, Nature Structural Biology 1994, 1, 546-551.
 - d) A. Musacchio, M. Noble, R. Pauptit, R. Wierenga, M. Saraste, *Nature*, **1992**, 359, 851-855.
- 69. W. A. Lim, F. M. Richards, R. O. Fox *Nature*, **1994**, 372, 375-379.
- 70. C. J. Morton, D. J. R. Pugh, E. L. J. Brown, J. D. Kahmann, D. A. C. Renzoni, I. D. Campbell, *Structure* **1996**, *4*, 705-714.
- 71. C. J. Morton, I. D. Campbell, *Current Biology* **1994**, *4*, 615-617.
- 72. S. Feng, J. K. Chen, H. Yu, J. A. Simon, S. L. Schreiber, *Science* **1994**, 266, 1241-1247.
- 73. A. A. Di Nardo, S. M. Larson, A. R. Davidson, *Journal of Molecular Biology* **2003**, *333*, 641-655.

- 74. R. J. Rickles, M. C. Botfield, X. M. Zhou, P. A. Henry, J. S. Brugge, M. J. Zoller, *Proceedings of the National Academy of Sciences* **1995**, *92*, 10909-10913.
- 75. R. Alsallaq, H. X. Zhou, *Proteins: Structure, Function, and Bioinformatics* **2008**, *71*, 320-335.
- 76. K. Sugase, H. J. Dyso, P. E. Wright, *Nature* **2007**, 447, 1021-1025.
- 77. A. R. Viguera, J. L. R. Arrondo, A. Musacchio, M. Saraste, L. Serrano, *Biochemistry* **1994**, 33, 10925-10933.
- 78. S. P. Zamora-Leon, G. Lee, P. Davies, B. Shafit-Zagardo, *Journal of Biological Chemistry* **2001**, *276*, 39950-39958.
- 79. O. G. Berg, P. H. von Hippel, *Annual Review of Biophysics and Biophysical Chemistry* **1985**, *14*, 131-158.
- 80. a) S. Y. Han, Y. A. Kim, *Tetrahedron* **2004**, *60*, 2447-2467.
 - b) L. A. Carpino, Journal of the American Chemical Society 1993, 115, 4397-4398.
- 81. G. E. Veitch, K. L. Bridgwood, S. V. Ley, *Organic Letters* **2008**, *10*, 3623-3625.
- 82. H. T. Clarke, H. B. Gillespie, S. Z. Weisshaus, *Journal of the American Chemical Society* **1933**, *55*, 4571-4587.
- 83. J. V. Crivello, *The Journal of Organic Chemistry* **1981**, *46*, 3056-3060.
- 84. A. B. Sheremetev, S. M. Konkina, D. E. Dmitriev, Russ Chem Bull **2007**, *56*, 1575-1579.65.
- 85. S. W. Wright, D. L. Hageman, A. S. Wright, L. D. McClure, *Tetrahedron Letters* **1997**, *38*, 7345-7348.
- P. L. Ornstein, T. J. Bleisch, M. B. Arnold, J. H. Kennedy, R. A. Wright, B. G. Johnson, J. P. Tizzano, D. R. Helton, M. J. Kallman, D. D. Schoepp, M. Hérin, *Journal of Medicinal Chemistry* 1998, 41, 358-378.
- 87. S. R. Hussaini, M. G. Moloney, Synthetic Communications 2005, 35, 1129-1134.
- 88. B. A. D. Neto, A. A. M. Lapis, A. B. Bernd, D. Russowsky, *Tetrahedron* **2009**, *65*, 2484-2496.
- 89. S. Hussaini, G. Hammond, Arkivoc 2008, xiii, 129.

- 90. a) M. Oba, S. Koguchi, K. Nishiyama, D. Kaneno, S. Tomoda, *Angewandte Chemie International Edition* **2004**, *43*, 2412-2415.
 - b) D. Ma, J. Yang, Journal of the American Chemical Society 2001, 123, 9706-9707.
 - c) L. Manzoni, M. Colombo, E. May, C. Scolastico, Tetrahedron 2001, 57, 249-255.
 - d) V. K. Aggarwal, C. J. Astle, M. Rogers-Evans, Organic Letters 2004, 6, 1469-1471.
 - e) P. W. R. Harris, M. A. Brimble, P. D. Gluckman, Organic Letters 2003, 5, 1847-1850.
 - f) Y. Tong, Y. M. Fobian, M. Wu, N. D. Boyd, K. D. Moeller, *The Journal of Organic Chemistry* **2000**, *65*, 2484-2493.
 - g) X. Zhang, A. C. Schmitt, W. Jiang, *Tetrahedron Letters* **2001**, *42*, 5335-5338.
- 91. J. Mulzer, F. Schülzchen, J.-W. Bats, *Tetrahedron* **2000**, *56*, 4289-4298.
- 92. S. Liu, R. N. Ben, *Organic Letters* **2005**, *7*, 2385-2388.
- 93. a) W. Wang, J. Yang, J. Ying, C. Xiong, J. Zhang, C. Cai, V. J. Hruby, *The Journal of Organic Chemistry* **2002**, *67*, 6353-6360.
 - b) T. Imamoto, K. Tamura, Z. Zhang, Y. Horiuchi, M. Sugiya, K. Yoshida, A. Yanagisawa, I. D. Gridnev, *Journal of the American Chemical Society* **2012**, *134*, 1754-1769.
- 94. H. G. Lombart, W. D. Lubell, *The Journal of Organic Chemistry* **1996**, *61*, 9437-9446.
- a) I. Parrot, P. C. Huang, C. Khosla, *Journal of Biological Chemistry* 2002, 277, 45572-45578.
 - b) M. Kuemin, S. Schweizer, C. Ochsenfeld, H. Wennemers, *Journal of the American Chemical Society* **2009**, *131*, 15474-15482.
 - c) C. W. Wu, T. J. Sanborn, R. N. Zuckermann, A. E. Barron, *Journal of the American Chemical Society* **2001**, *123*, 2958-2963.
- 96. a) M. Sattler, J. Schleucher, C. Griesinger, *Progress in Nuclear Magnetic Resonance Spectroscopy* **1999**, *34*, 93-158.

- b) M. P. Williamson, *Progress in Nuclear Magnetic Resonance Spectroscopy* **2013**, *73*, 1-16.
- c) S. B. H. Kent, *Annual Review of Biochemistry* **1988**, *57*, 957-989.
- 97. Arjan H. G. Siebum, Wei S. Woo, J. Raap, J. Lugtenburg, *European Journal of Organic Chemistry* **2004**, *2004*, 2905-2913.
- 98. D. B. Berkowitz, J. M. McFadden, M. K. Sloss, *The Journal of Organic Chemistry* **2000**, *65*, 2907-2918.
- 99. A. Bracci, L. Manzoni, C. Scolastico, *Synthesis* **2003**, *2003*, 2363-2367.
- 100. E. K. Dolence, C. E. Lin, M. J. Miller, S. M. Payne, *Journal of Medicinal Chemistry* **1991**, 34, 956-968.
- 101. M. Miyazaki, H. Naito, Y. Sugimoto, K. Yoshida, H. Kawato, T. Okayama, H. Shimizu, M. Miyazaki, M. Kitagawa, T. Seki, S. Fukutake, Y. Shiose, M. Aonuma, T. Soga, *Bioorganic & Medicinal Chemistry* 2013, 21, 4319-4331.
- 102. C. S. Straub, A. Padwa, Organic Letters 1999, 1, 83-86.
- 103. T. Katoh, Y. Nagata, Y. Kobayashi, K. Arai, J. Minami, S. Terashima, *Tetrahedron* **1994**, *50*, 6221-6238.
- 104. V. K. Aggarwal, C. J. Astle, H. Iding, B. Wirz, M. Rogers-Evans, *Tetrahedron Letters* **2005**, *46*, 945-947.
- 105. L. Colombo, M. Di Giacomo, V. Vinci, M. Colombo, L. Manzoni, C. Scolastico, *Tetrahedron* **2003**, *59*, 4501-4513.
- 106. G. Lesma, A. Colombo, A. Sacchetti, A. Silvani, *The Journal of Organic Chemistry* **2008**, 74, 590-596.
- 107. US2008/269140 A1, 2008.
- 108. L. M. Beal, B. Liu, W. Chu, K. D. Moeller, *Tetrahedron* **2000**, *56*, 10113-10125.
- L. Belvisi, A. Bernardi, A. Checchia, L. Manzoni, D. Potenza, C. Scolastico, M. Castorina,
 A. Cupelli, G. Giannini, P. Carminati, C. Pisano, *Organic Letters* 2001, 3, 1001-1004.